386

386

ONWI-211
Distribution Category UC-70

Systems Study on Engineered Barriers: Barrier Performance Analysis

Technical Report

September 1980

R. T. Stula
T. E. Albert
B. E. Kirstein
D. H. Lester

Science Applications, Inc.
1200 Prospect Street
La Jolla, CA 92037

The content of this report is effective as of September 1980. This report was prepared by Science Applications, Inc. under Subcontract E512-05400 with Battelle Project Management Division, Office of Nuclear Waste Isolation under Contract No. DE-AC06-76-RLO1830-ONWI with the U.S. Department of Energy. This contract was administered by the Battelle Office of Nuclear Waste Isolation.

TABLE OF CONTENTS

TABLE OF CONTENTS
(Continued)

LIST OF FIGURES

LIST OF FIGURES
(Continued)

LIST OF TABLES

LIST OF TABLES
(Continued)

LIST OF TABLES
(Continued)

ABSTRACT

A performance assessment model for multiple barrier packages containing unreprocessed spent fuel has been modified and applied to several package designs. The objective of the study was to develop information to be used in programmatic decision making concerning engineered barrier package design and development. The assessment model, "BARIER", was developed in previous tasks of the System Study on Engineered Barriers (SSEB). The new version discussed in this report contains a refined and expanded corrosion rate data base which includes pitting, crack growth, and graphitization as well as bulk corrosion. Corrosion rates for oxic and anoxic conditions at each of the two temperature ranges are supplied. Other improvements include a rigorous treatment of radionuclide release after package failure which includes resistance of damaged barriers and backfill, refined temperature calculations that account for convection and radiation, a subroutine to calculate nuclear gamma radiation field at each barrier surface, refined stress calculations with reduced conservatism and various coding improvements to improve running time and core usage. This report also contains discussion of alternative scenarios to the assumed flooded repository as well as the impact of water exclusion backfills. The model was used to assess post repository closure performance for several designs which were all variation of basic designs from the Spend Unreprocessed Fuel (SURF) program. Many designs were found to delay the onset of leaching by at least a few hundreds of years in all geologic media. Long delay times for radionuclide release were found for packages with a few inches of sorption backfill. Release of uranium, plutonium, and americium was assessed.

1. EXECUTIVE SUMMARY

This study is concerned with the disposal of unreprocessed fuel elements in salt, shale, basalt, or granite repositories using a system of engineered barriers in addition to the geologic media as containment. In an earlier study, a scoping model of barrier performance was developed and applied to a representative spectrum of barrier designs (Lester, 1979). Results of that work suggested additional designs which were evaluated in a subsequent study (Stula, 1980a). This work represents a continuation of previous studies and includes more refined model development in addition to performance evaluation of many barrier package design variations. "Performance" is related to only a maximum individual dose after repository closure and not to other factors such as waste transportation.

Barrier performance is determined in terms of two main parameters: time of initial release of radionuclides to the geosphere (leach begin time) and duration of radionuclide release. Time is measured from a zero time scenario when the repository is sealed and assumed saturated with water. The performance model treats a barrier package as a series of layers each consisting of a solid wall(s), filler (or backfill), and a gap between barriers. Materials and designs for barrier packages are chosen to give a range of cost and performance. The key concern is to identify where additional barrier cost yields little increased benefit.

The major performance model refinements performed in this study include addition of radionuclide release (transport) and radiation field calculation models, improvement of the temperature gradient and stress calculation models, and expansion of the corrosion rate data base. In addition, the possible effects of alternative repository scenarios and the use of water repellant backfills on performance are discussed. All pertinent performance model theory is provided in this report.

Main barrier package design considerations include the effects of external geologic crushing forces and corrosive behavior of the associated high pressure and high temperature brine/water. Evaluation of various general proposed package design concepts (Stula, 1980a) showed a design with a cast solid lead stabilizer to be the most promising. In this design, corrosion

resistance is the most important factor in determining package life since the voidless package stabilizer is sufficient to withstand geologic crushing forces. Of designs investigated which did not utilize a cast solid stabilizer, a design with a thick corrosion-resistant hole sleeve gave the best performance. Results of this previous study indicated that these two design concepts, or a combination of the two, were most desirable. Thus, performance calculations in this study are limited to design variations of these general concepts. However, evaluation of "best" package designs as determined in previous work is performed in this study with the refined performance model for comparison.

The performance indicates that package lifetimes of at least a few hundreds of years in all geologies can be achieved. Furthermore, judicious use of backfills to sorb radionuclides and or exclude water can reduce radionuclide release after barrier failure as well as delay the onset of radionuclide release. Results indicate that a few inches of backfill thickness are sufficient to supply the necessary barrier to radionuclide release. Large backfill thicknesses are of little advantage as long as sufficient sleeve thicknesses and/or a cast stabilizer are used. The stress defense contribution of the backfill is questionable as it contributes very little and never contributes to stress application if a very "soft" material is used. The key question with regard to backfills remains whether the backfill material will retain its properties or geometry over long periods of time (over 1000 years). There is a serious question that a backfill would be intact in an environment capable of leaching material from a ceramic waste material.

Calculated performance results using the refined BARIER model roughly correspond to those from the previous model. While corrosion rates in the new data base tend to be higher than previous values, the stress calculations for geologic crushing forces are based on real failure rather than ASME code criteria which tend to be very conservative.

2. INTRODUCTION

This report describes the work on engineered barrier performance assessment performed by Science Applications, Inc. (SAI) for Pacific Northwest Laboratories (PNL) during the period January 1, 1980 to September 30, 1980. This effort under Office of Nuclear Waste Isolation (ONWI) sponsorship was a follow-on to previous studies from June through December 1979. The objective of the work was to develop means to evaluate performance of proposed design concepts, assess the sensitivity of the package performance to specific design parameters and support evaluation of the incentives for use of various types of packages. Results of this study are intended to support decisions by ONWI regarding engineered barrier development plans. Additional studies at PNL on the results of releases to the geosphere complement this work and provide additional decision-making inputs.

The code developed as a part of this work provides a good beginning for a detailed near-field model which would be part of an integrated repository risk assessment model. Technology transfer of this work is underway to support efforts to develop such an integrated model.

Efforts under this study were limited to some specific circumstances. Nevertheless, the model was developed in a manner which allows expansion into many other circumstances. A specific list of candidate materials was used (see later section of this report), a limited set of designs was assessed based on previous conceptual studies (Westerman, 1979), four basic water chemistries were used, specific repository designs based on the GEIS (DOE, 1979) were assumed and one specific scenario (flooded repository) was assumed. The study was restricted to PWR spent fuel storage but is easily extended to other waste forms. The parameters considered were not intended to represent an exhaustive list of possibilities but rather to be a wide ranging list of possibilities which provide a representative sample for the purpose of understanding conceptual burial performance parameter sensitivity. Thus, many excellent material choices and design possibilities have likely not been considered due to deliberate scope limitation. Barrier package development activities will provide information for data base expansion as the model is incorporated into integrated risk assessment

models. The code will easily accommodate such changes due to modular design and methods of data entry.

While the code used was written specifically for the DEC-10 system, it is composed of standard FORTRAN IV and will run on most machines with minor changes in input/output and file control statements. A user manual has been prepared and issued under separate cover as an interim report (Stula, 1980b). The report is a condensed version of this report and intended to provide sufficient code documentation for future users. All of the information pertaining to model theory and development in the interim report is contained in this report.

2.1 PREVIOUS STUDIES

The study described in this report represents a follow-on effort to previous studies. The initial work was intended to provide rough assessment to guide further studies. Experience gained in the initial efforts was used to determine where improvements should be made to the model and what additional design concepts should be considered in the follow-on work. The key assumptions, scenario descriptions, and repository designs are the same as reported earlier (Lester, 1979) (Stula, 1980a). The reader is referred to the referenced documents for additional details.

Past assessments focused on some design concepts which appeared to offer lifetimes considerably larger than others. Of particular concern was the problem of package crushing in rock masses where creep was significant (e.g., salt and some shales). Concepts employing heavy-walled bore hole sleeves and/or cast stabilizers around the spent fuel bundle were found to offer good defenses in high creep geologies. These were further evaluated in this study. Other promising concepts from the past studies were also included in this follow-on study.

2.2 THE MODIFIED MODEL-OVERVIEW

The barrier performance model used for the calculation discussed in this report was a modified revision of the model used for previous studies (Lester, 1979) (Stula, 1980a). Extensive modifications have been made. The key changes were

- complete overhaul of corrosion rate data base as a result of expanded literature survey and conversation with various corrosion experts
- addition of a detailed radionuclide release rate model which accounts for resistance from damaged barriers, backfill sorption and diffusion in the backfill
- replacement of ASME code criteria for crushing with a detailed stress model to assess the time of actual plastic yield of a barrier wall under external pressure stress
- refinement of temperature gradient calculation to assess thermal radiation across clearance gaps
- addition of a detailed calculation of nuclear radiation fields at package barriers

Figure 2-1 is a simplified block diagram of the improved model. A more-detailed description and diagram can be found in Section 3.1, General Description.

The current version of the model tends to give failure times which are similar to the old model. This is because the reduction in wall thickness requirement due to less conservative stress treatment is offset by higher corrosion rates in the data base. The higher corrosion rates result from consideration of mechanisms other than bulk corrosion such as pitting, crack growth and graphitization. Radionuclide releases are much more delayed and attenuated than in the old model because sophisticated backfill models are employed which take credit for more sorption and diffusion resistance effects.

Larger time increments are used in the improved code which make running time comparable to the older version. A study of accuracy indicated that large time increments (ten to 100 years) do not significantly affect accuracy within significant figures. Using the DEC-10 computer, it was found that a single package design could be run in one geology and water chemistry (oxic and anoxic) for a few dollars of machine time. This is comparable to experience with the previous version.

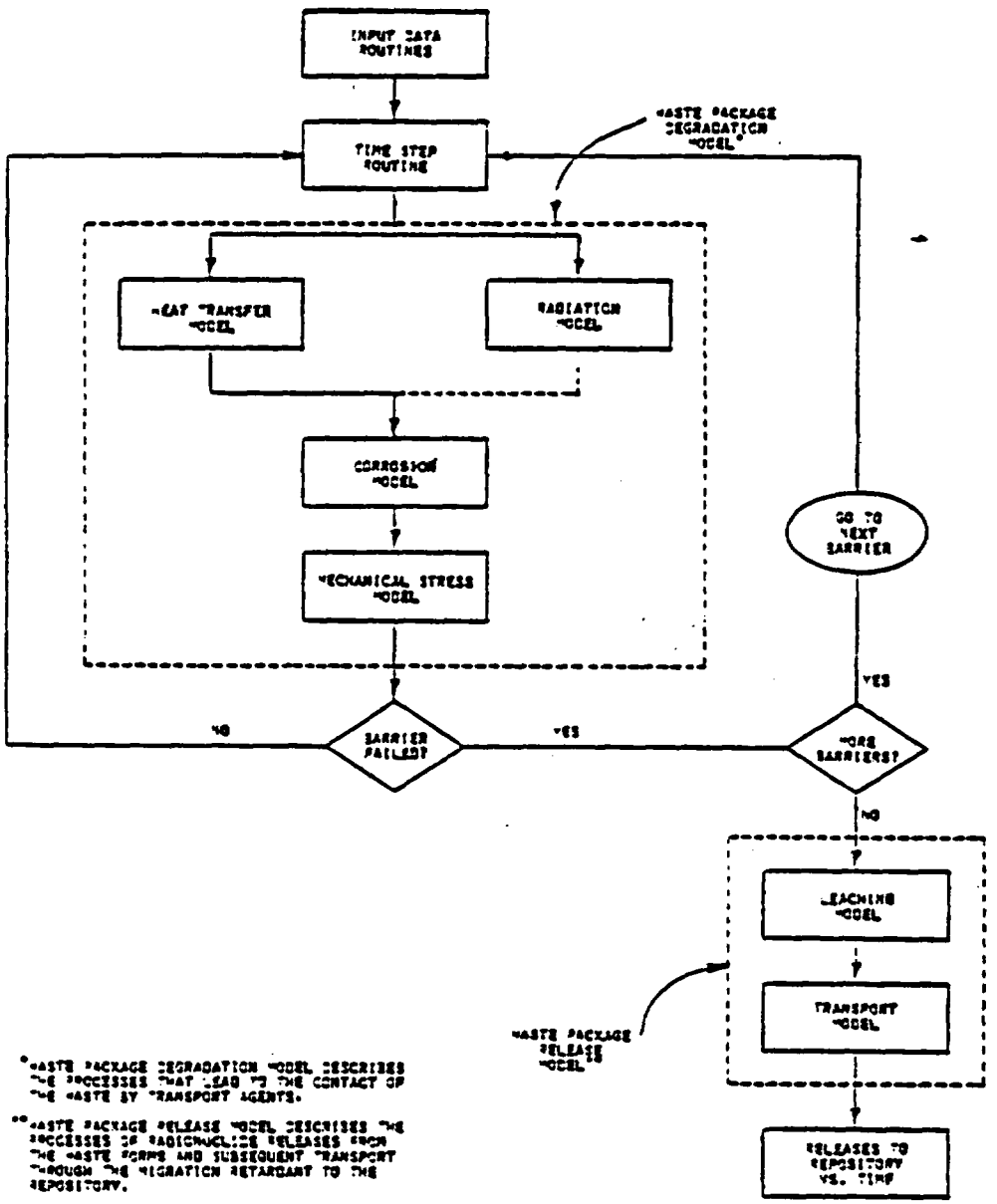

Figure 2-1. Preliminary Waste Package Degradation and Release Model.

2.3 SCENARIOS

The post-repository closure scenario used in this study was the same as that used in previous studies. Like all risk assessment models this one is scenario specific. The scenario considered is a very stringent case for possible package failure and near-field release.

At time zero the package containing one 6.5-year-old, 3.3 percent enriched, 33,000 MWD/MTHM PWR fuel bundle is assumed to be immersed in the geologic medium which is saturated with water of appropriate chemistry for the postulated geologic setting. All calculations are carried out assuming both oxic and anoxic chemistry. The ground water chemistry is described in Section 3.3. Sufficient circulation of water is assumed so that there is no build-up of radionuclides in the near-field. This is a conservative (i.e., highest release) assumption. All packages are assumed to experience the same environment and respond in identical fashion.

The model does not account for upset conditions or sensitization of the package barriers from previous events or manufacturing flaws. Probabilities of such deviation could be included in the model in later risk assessment applications.

Some alternative scenarios are discussed in the next section. While the model does not actually consider these, the effect on the results of calculations if they were to be considered is discussed.

2.4 ALTERNATIVE SCENARIOS

Scenarios other than the saturated near-field scenario could produce similar or greater consequences. The following alternative scenarios are discussed in this section

- moisture in the near-field in limited quantities with package intact at time = 0
- dry environment with later water intrusion (limited and unlimited water available)
- direct package intrusion by humans
- repository flooding with very high velocities and large water availability
- major disruptive natural event such as volcanism or seismic disturbance

2.4.1 Limited Near-Field Moisture

The "BARIER" code is based on some key assumptions which relate to an unlimited moisture supply. These are

- corrosion proceeds in a manner that would be expected in systems with no significant corrosion product build-up or corrosion agent depletion in the water
- radionuclides are carried away from the package at sufficient rate to make a near-zero concentration of radionuclides in the near-field
- corrosion mechanisms are those expected in a liquid/solid system (no vapor or gas phase)
- the mechanical properties of the backfill are those of a medium saturated with water
- radionuclide sorption and water transport in the backfill is characterized by a porous medium saturated with water

In the event that the water supply is limited then a vapor phase would be present, the backfill would not be saturated and the assumptions above would be invalid.

If such a scenario were assessed the effect on corrosion rates would be reduction due to build-up of corrosion products and depletion of corrosion agents and possible increase due to vapor phase reactions. Data are lacking to allow a reliable quantitative assessment. It would be expected that corrosion rates would be equal to or less than those used in the current model since build-up of products and reduced corrosion agents (e.g., oxygen) would probably be a larger influence than influences due to introduction of a vapor phase.

In most instances the backfill mechanical properties are greatly improved when water content is reduced from saturation. Thus, the backfill would offer better defense against crushing in media with high creep.

If the backfill were unsaturated then three effects on radionuclide transport would be expected: (1) reduced sorption because of reduced surface area/moisture contact, (2) reduced flow due to reduction of flow paths and effective moisture conductivity, and (3) reduced discharge rates because of near-field build-up of radionuclide concentration. Effect (1) tends to increase release rate but (2) and (3) greatly reduce release rate. The net effect would likely be reduced release rates, larger release time and longer time to initial release.

The overall result for this scenario would be expected to compare to "BARIER" results in that the package would last longer before initial leaching of the waste and subsequent release would be more delayed and more spread out in time. This is not surprising because water is the key to package failure and radionuclide transport.

2.4.2 Dry Environment with Subsequent Water Intrusion

The same assumptions as mentioned in Section 2.4.1 are affected and similar effects on the results would be expected.

The dry period would introduce a delay time to failure with only the possibility of failure from inadequate design. Experience in archeology shows that ancient, crude metal objects lasted almost indefinitely in a dry environment. If the package is not adequately designed for forces caused by rock creep, such forces could result in crushing of the package. The wet period would then follow and be different from the model only if the water supply is unlimited as discussed in Section 2.4.1.

2.4.3 Direct Intrusion

Direct intrusion may consist of many forms including resource extraction, exploration, or repository exploitation. Direct intrusion introduces mechanisms for damage of the package which are not accounted for in the model. Such intrusion could be considered in package design if reasonable and probabilistic assessment were made of the resultant releases. No relation between this scenario and the one calculated by "BARIER" can be drawn.

2.4.4 High Velocity Flooding - Large Water Availability

Such a scenario could result from a gross breach of the repository under influence of a pressure gradient or could result from "pumping" in the near-field from thermal hydraulic circulation induced by package heat loads. With regard to barrier failure, this would appear no different than the scenario that the "BARIER" code is based on. In terms of radionuclide release, the results would be much different. With large circulation rates the backfill would likely be damaged by erosion and contain flow channels or even disappear from the

system. If such degradation were simulated the results would be greatly reduced or zero release attentuation after the package was breached and leaching had begun. Leaching rates would then be the same as those observed in inversion leach tests previously cited (Katayama, 1980) and the same as those calculated by the old version of BARIER (Lester, 1979).

Frequently, in discussions concerning package leaching, a flow scenario such as depicted in Figure 2-2 is presented. Water flowing past the package in a flood scenario is seen to penetrate on the upstream side, dissolve material, and emerge on the downstream side. Hydrodynamically, this is highly unlikely. If it is assumed that the package backfill is intact then the situation is represented by flow past a transverse cylinder constructed of a porous solid. Figure 2-3 shows the dimensionless pressure distribution around such a transverse cylinder for three flow regimes (Schlichting, 1960): potential flow, subcritical flow, and supercritical flow. In the case of very slow flow (creeping flow) the potential flow profile would be appropriate. As the Reynolds number increases (increasing velocity) the flux would proceed through subcritical to supercritical. In potential flow the backside pressure is precisely equal to the frontside pressure (no drag) and there is a low pressure node at the side shoulder. One would then expect a "backwash" toward the node as depicted in Figure 2-4 if there is any internal circulation. A pure potential flow with no drag will induce no "backwash" but a "near-potential" condition would as described. The other flow regimes are similar with the possibility of some circulation as in Figure 2-2 in the subcritical region because the mode is weak and there is some overall pressure differential. However, the subcritical region will be highly unstable and subject to boundary layer detachment at the slightest perturbation and go toward the supercritical profile. Note that while the supercritical profile shows an overall pressure difference there is a highly pronounced "backwash" node. While the pressure distributions presented are for flow in a large open space around the package (i.e., ignoring the geology) it seems likely that the whole scenario is not plausible unless a large space has opened up (from catastrophic degradation of the repository as in the case of dissolving away the salt).

The BARIER model assumes flow by diffusion only with no "flow through". The foregoing discussion indicates that flow-through models are probably unrealistic.

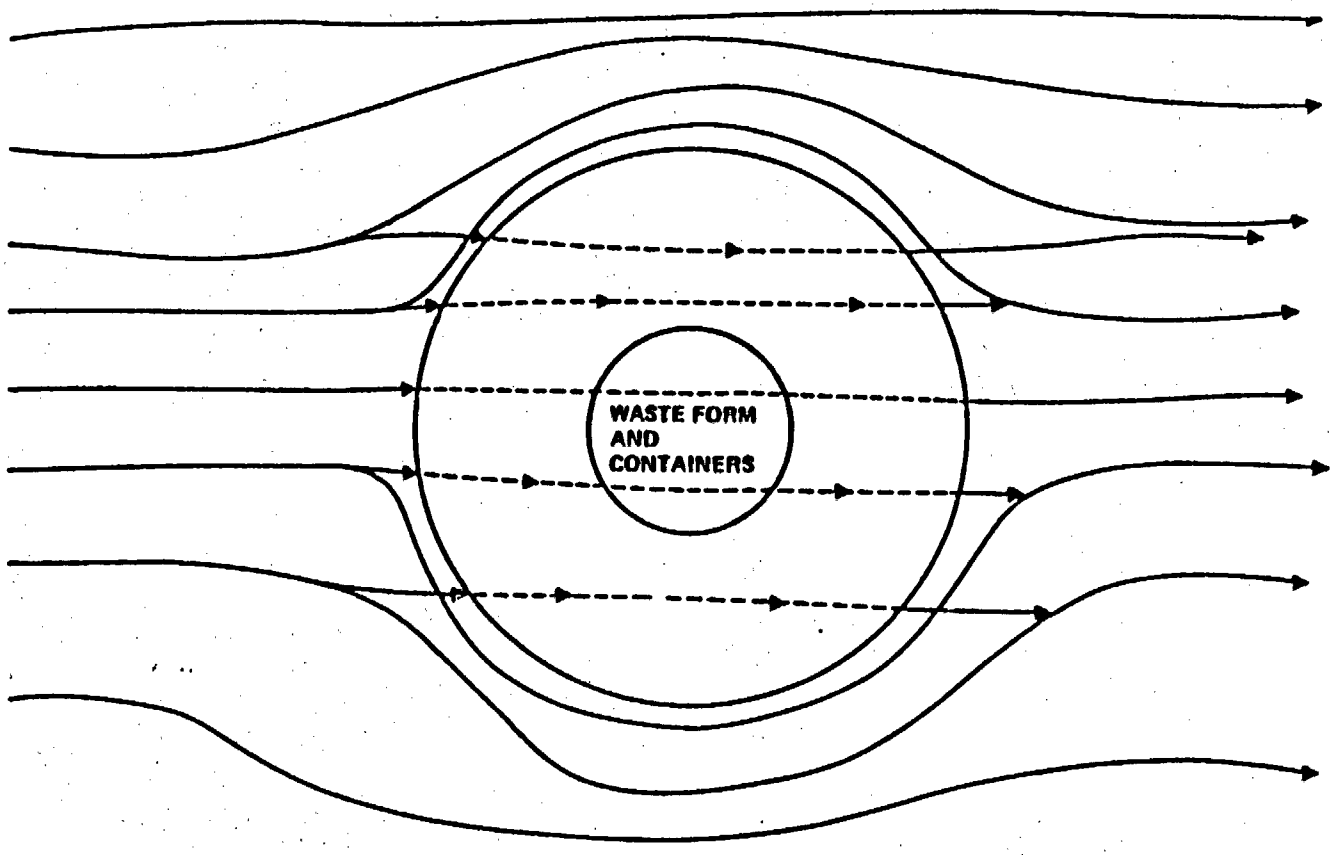

Figure 2-2. Proposed Flow Scenario for Flooded Repository.

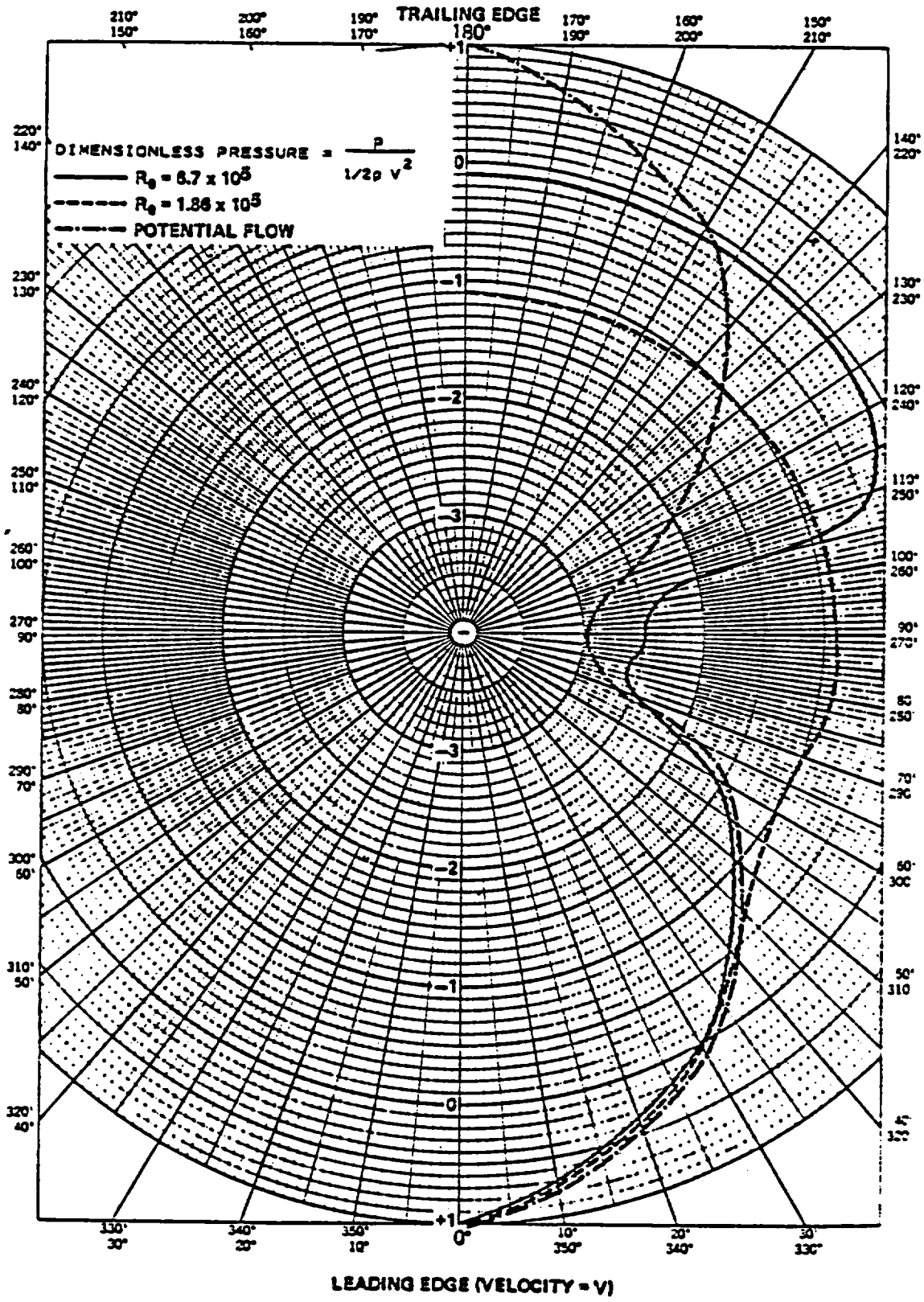

Figure 2-3. Values of Dimensionless Pressure on a Transverse Cylinder.

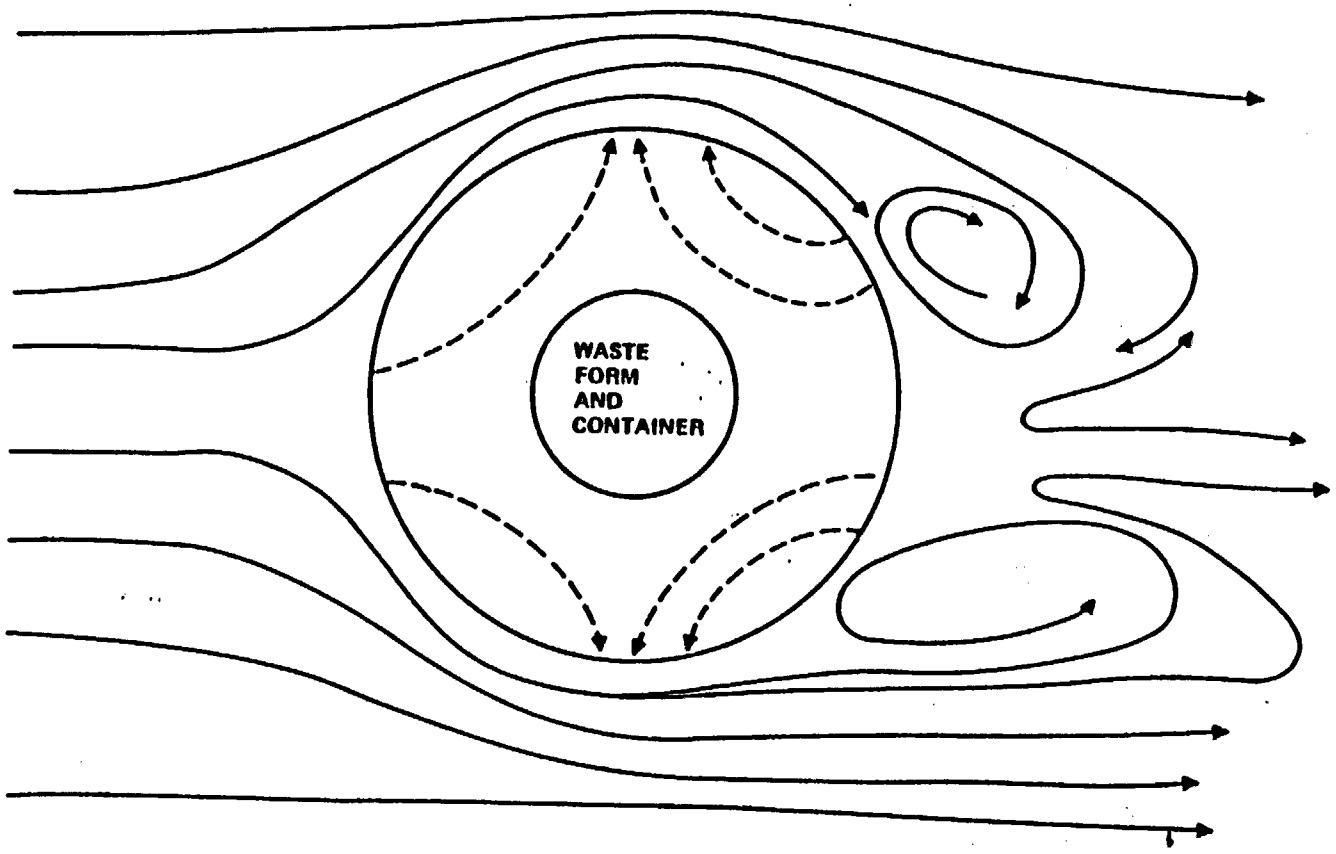

Figure 2-4. Probable Flow Scenario for Flooded Repository.

2.4.5 Major Natural Disruptive Event

The concept of protection through use of an engineered package probably is not compatible with major natural seismic events or repository volcanism. The only relation of such scenarios to the "BARIER" model which can be discussed is the effect of seismic activity some distance away which gives attenuated disturbances to the repository. The near-field effect of such a scenario could be to accelerate degradation by causing vibration damage to the backfill or to the containment vessels. Such damage is only significant if water is also present. Therefore, this is a modification of the scenario considered in the code and is a more severe case. Depending on the severity of the disturbance, the package might be breached at a much earlier time or even immediately. Damage to the backfill (cracks, holes, etc.) could reduce the radionuclide retention properties. The result would be earlier and more sharply peaked release

3. PERFORMANCE MODEL THEORY

In this section details of the physical theory used in the performance assessment model are discussed. The theory subsections generally parallel the subroutines used in the BARIER code. Each subsection is designed to supply sufficient detail for clear understanding of the assumptions, model formulation and contents of the data base.

3.1 GENERAL DESCRIPTION

The package is viewed as a multi-layered (barrier) assembly which undergoes a failure process starting with the outermost barrier and proceeding inward. Each barrier element is envisioned as shown in Figure 3-1 and together the elements form a package concept shown in Figure 3-2. (Note that the number of barriers may be less than or more than that shown in Figure 3-2). The outer material (#2) of a barrier is assumed to possess no structural strength and to act only as a corrosion protector or radiation shield. The existence of solid wall(s), fillers or gaps in a particular design is conveyed to the model by setting the diameters of each barrier layer to the appropriate value. If a particular barrier layer does not exist, then the I. D. of that layer is set equal to the O. D. The inner barriers are protected from corrosive attack and from external forces by the outer barriers. As each barrier fails the next inner barrier is subjected to the water environment and the repository pressure/temperature conditions.

Figure 3-3 shows how the model assesses the successive failure and attack of the barriers which lead to leaching and radionuclide release after failure of the last barrier.

Initially a heat transfer model is used to determine the maximum steady-state temperature that the waste would attain if the package remained intact in a repository at its maximum temperature. If a temperature of 653^{o}K (380^{o}C) is attained in the fuel bundle, the package is rejected and no further calculations are made. If the temperature is within limit, the package is then

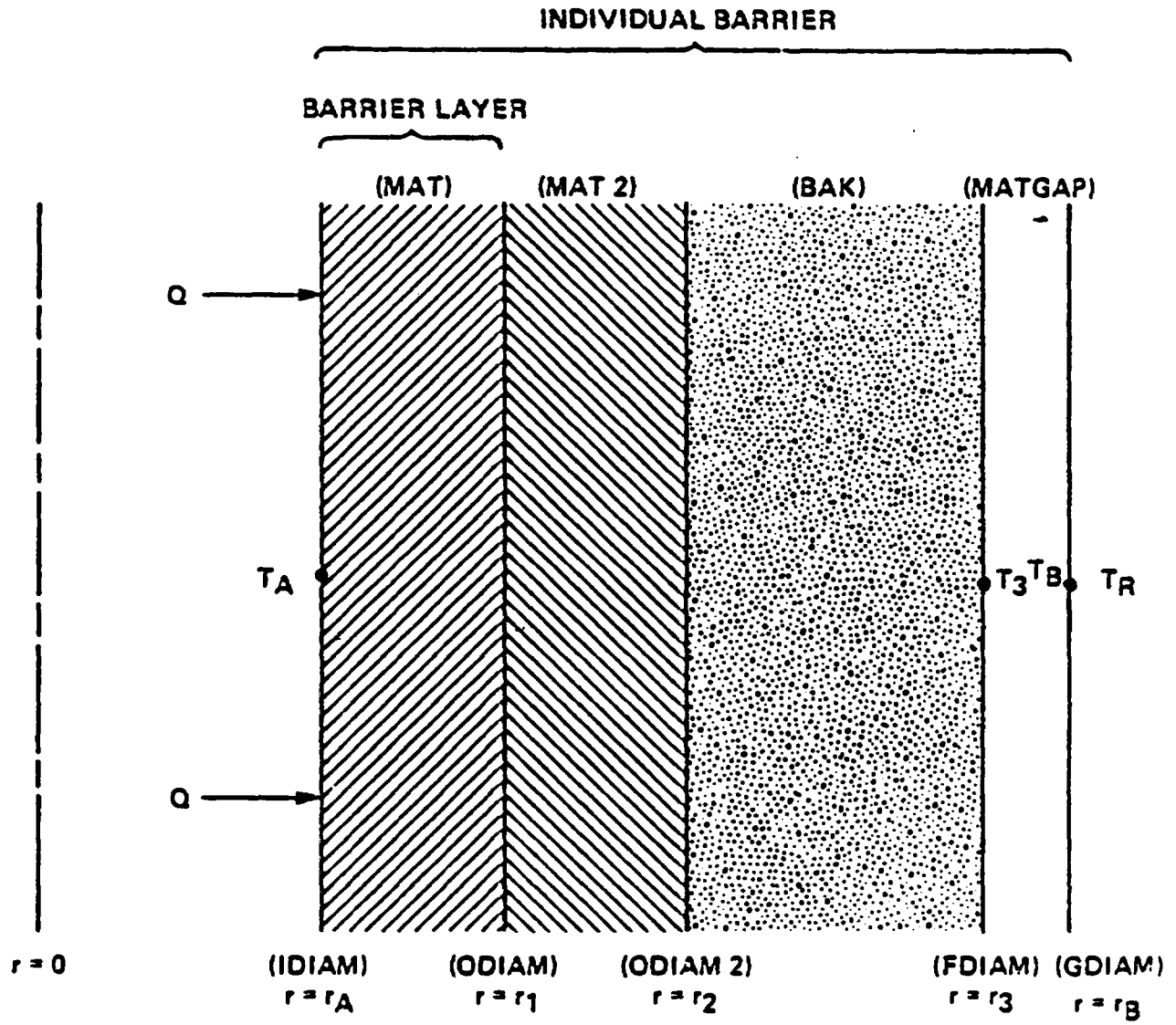

Q = RADIAL WASTE HEAT GENERATION, WATTS

T_A = TEMPERATURE AT INSIDE OF LEFTMOST SOLID WALL (OR WASTE), °K

T_B = TEMPERATURE AT OUTSIDE OF RIGHTMOST SOLID WALL (OR REPOSITORY), °K

WHERE

T_3 = TEMPERATURE AT OUTSIDE OF BACKFILL (OR FILLER), °K

r = RADIUS RELATIVE TO WASTE CENTERLINE (r = o), IN.

( ) = DIMENSIONAL OR MATERIAL VARIABLE NAMES USED IN CODE

T_R = TEMPERATURE OF REPOSITORY, °K

Figure 3-1. PKTEMP Barrier Model.

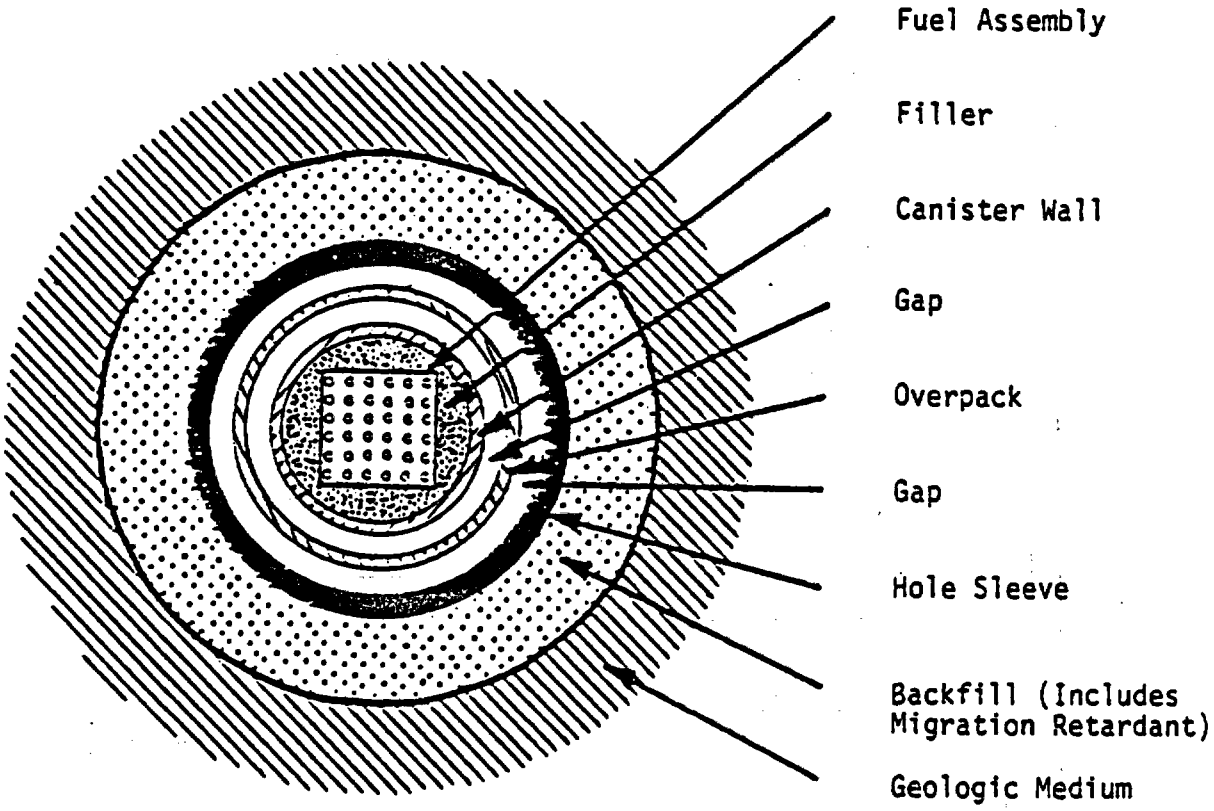

Figure 3-2. Stylized Waste Package Configuration for Fuel Assembly Waste Form.

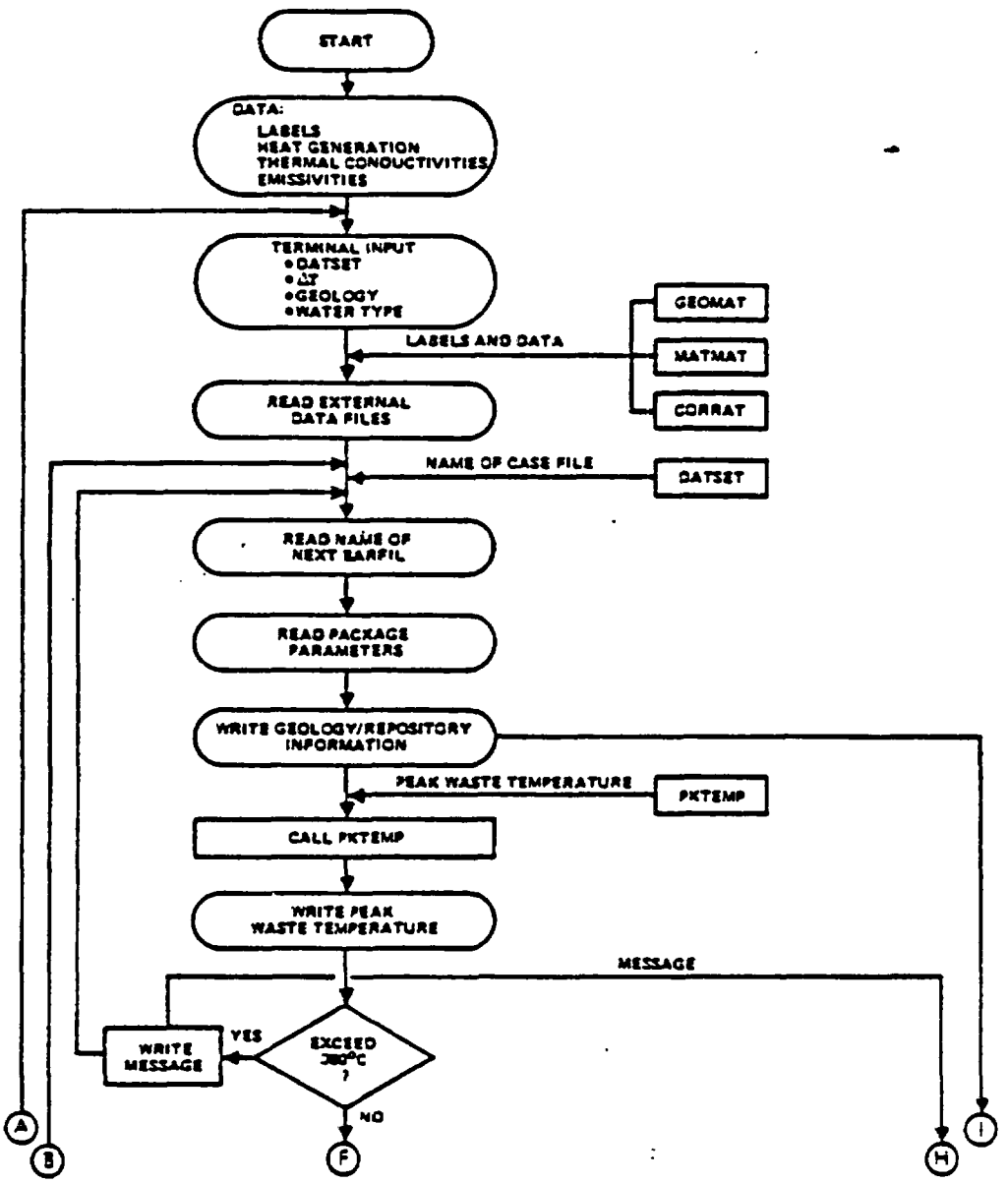

Figure 3-3. BARIER Flowchart.

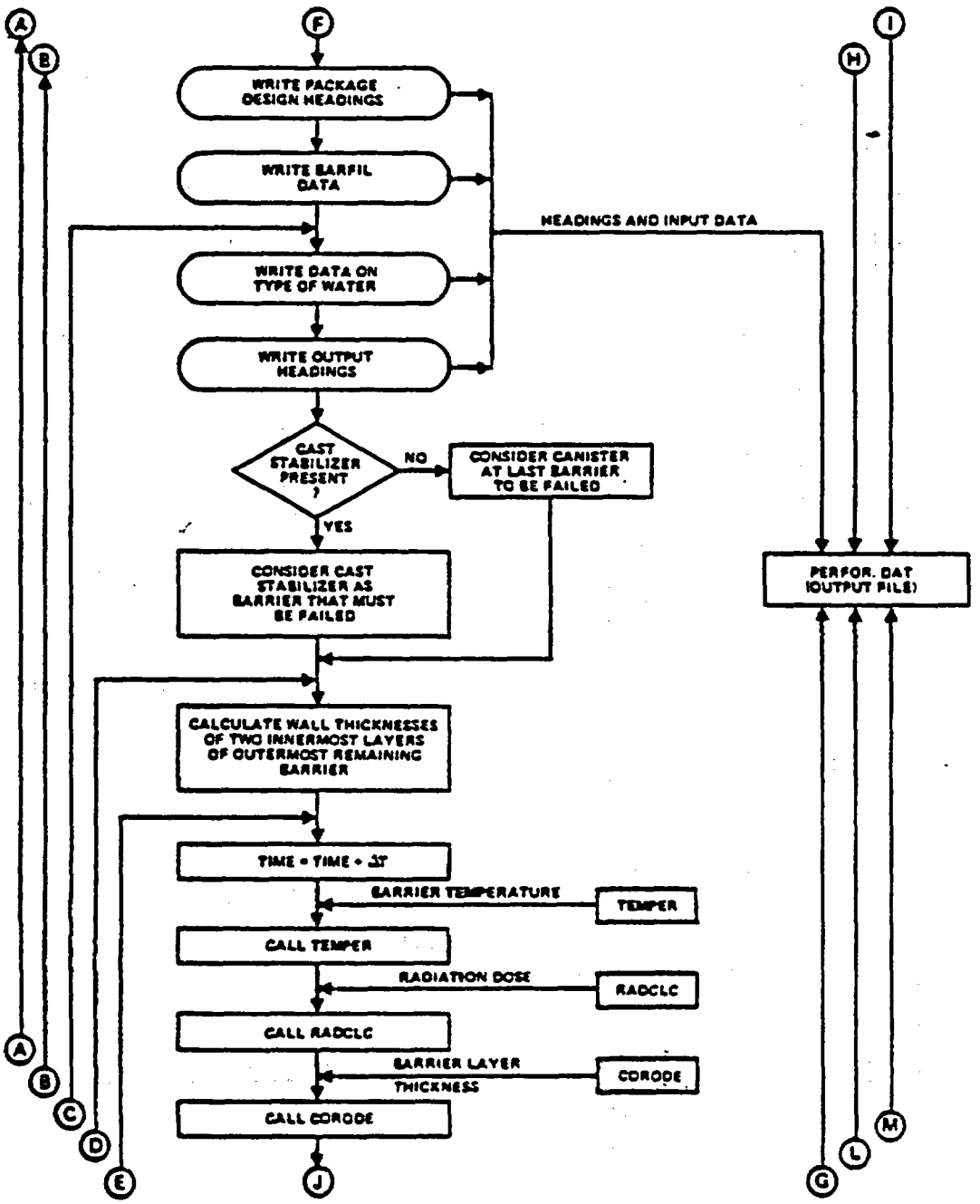

Figure 3-3. BARIER Flowchart (Continued).

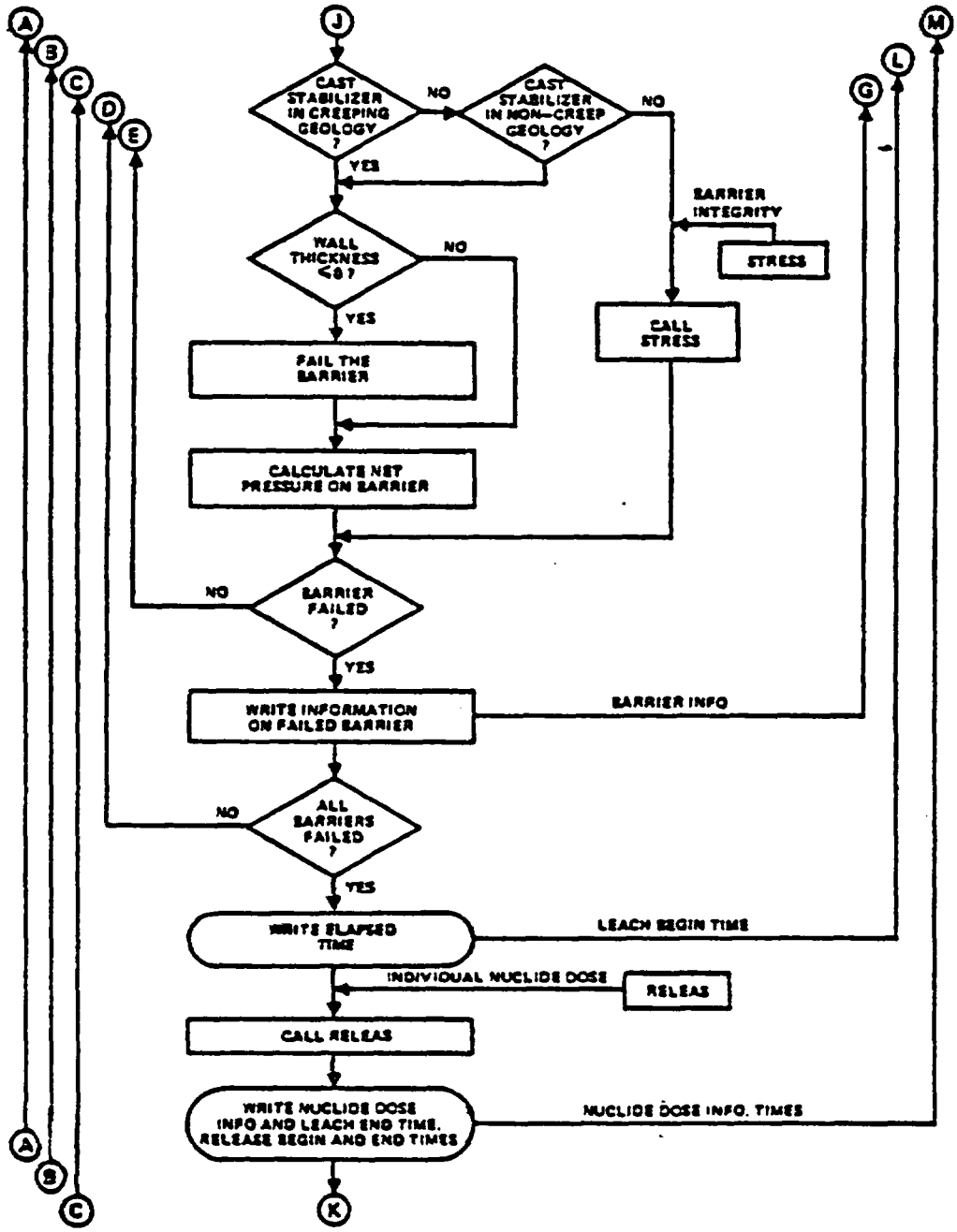

Figure 3-3. BARIER Flowchart (Continued).

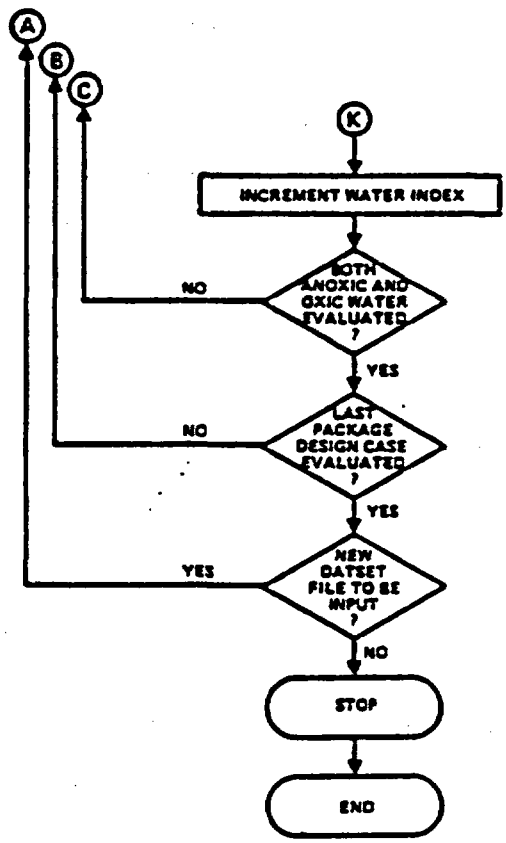

Figure 3-3. BARIER Flowchart (Continued).

taken through time increments as shown in Figure 3-3. The temperature of the outer barrier is assessed in the heat transfer model and the nuclear radiation field is evaluated. Then the corrosion model determines the decrease in barrier wall thickness for that time increment based on the water chemistry, type of material, and temperature range. The revised wall thickness is checked in a mechanical stress model which calculates displacement and stresses and checks the results against failure criteria. If the element does not fail then time is incremented and the process is repeated. Once the barrier fails the next innermost barrier is taken through the process until the last barrier fails. Failure of the last barrier passes control to the waste package release model which includes leaching and transport calculations for specific radionuclides.

Details of the specific models for each of the subroutines identified above are discussed in the following subsections. Specific package designs evaluated are discussed in Section 4.0.

3.2 TEMPERATURE CALCULATIONS

There are three temperature calculations performed by BARIER and its subroutines:

(1) repository surface temperature as a function of time is calculated in the main program

(2) peak waste temperature is calculated in the PKTEMP subroutine

(3) barrier temperature at time of failure is calculated in the TEMPER subroutine

Table 3-1 details the areal heat loadings assumed for the reference waste repository as described in the GEIS (DOE, April 1979). Temperature calculations performed in the GEIS studies are used in the BARIER code. It is conservatively assumed that the bulk temperatures are unchanged by the presence of water from the flooding scenario. An approximate fit to the time-temperature curves in the GEIS is made for each of the four geologic media considered. The repository surface temperature is represented in BARIER by

$$T_R = T1 + T2 \ln t \qquad t \leq T3 \qquad (3.2.1)$$

$$T_R = T4 \qquad t > T3 \qquad (3.2.2)$$

Table 3-1. Thermal Loadings Achieved for the Conceptual Repositories for Once-Through Fuel Cycle.

Thermal Loading at Emplacement	Salt	Granite	Shale	Basalt
PWR				
kW/can	0.72	0.72	0.72	0.72
Near field local kW/acre	50	130	80	130
Far field average kW/acre	40	100	65	100
BWR				
kW/can	0.22	0.22	0.22	0.22
Near field local kW/acre	50	130	55	130
Far field average kW/acre	40	100	44	100

where

T1, T2, T3, T4 = constants for the fit

t = time after emplacement, (yr)

The fit is further conservative in that the temperature is assumed constant beyond time T4 when there is actually a gradual decrease in temperature. Values of constants used are presented in Table 3-2.

The PKTEMP subroutine calculates the peak waste temperature expected during the life of the waste package. A concentric cylinder model is used which accounts for heat transfer by conduction and radiation. Exploratory calculations revealed that free convection effects are small and that coefficients tend to approach pure conduction. When the waste package has gaps between barrier elements, heat radiation effects are significant and are included in the model.

The peak waste temperature is determined by calculating the temperature differential across a series of individual barrier heat transfer resistances while utilizing the maximum repository temperature as the reference temperature. An infinite-length concentric cylinder heat transfer equation is used which assumes individual barrier resistances as depicted in Figure 3-1. Each barrier resistance is modeled as having a maximum of four distinct layers across which heat transfer occurs. These include an inner solid wall, an outer solid wall (e.g., a corrosion-resistant cladding), a filler or backfill material, and a gap between barriers. The variable names corresponding to the inner diameter and material of each of these layers are shown in parentheses in Figure 3-1. These variables are generally subscripted with the variable I to distinguish between individual barriers (I = 1 for the innermost barrier and I = IB for the outermost barrier).

Heat transfer across the first three layers of each barrier (r_A to r_3) is assumed to occur by conduction only. The following conduction equation is used in the code

$$Q/L = \frac{2\pi(T_A - T_3)}{\frac{\ln(r_1/r_A)}{k^{A1}} + \frac{\ln(r_2/r_1)}{k^{12}} + \frac{\ln(r_3/r_2)}{k^{23}}} \qquad (3.2.3)$$

Table 3-2. Constants For Repository Temperature Calculations.

Geology	T1, (°C)	T2, (°C/yr)	T3, (yr)	T4, (°C)
SALT	122.66	23.60	20.00	193.00
BASALT	128.80	31.15	10.00	200.00
GRANITE	129.24	29.97	10.00	198.00
SHALE	100.45	30.00	15.00	182.00

where

Q = waste heat generation, (Watts)

k^{Al}, k^{12}, k^{23} = thermal conductivity of layer, (Watts/in-^{o}K)

L = length of waste heat generation surface, (in)

Values of thermal conductivity are assumed constant and taken at the midpoint of the temperature range considered. Heat transfer across the gap (r_3 to r_3), if present, is assumed to occur by both conduction and radiation. The following equations are used for this situation.

$$Q/L = 2\pi\left[r_3\sigma e(T_3^4 - T_B^4) + \frac{T_3 - T_B}{\frac{\ell n(r_B/r_3)}{k^{3B}}}\right] \qquad (3.2.4)$$

$$e = \frac{1}{\frac{1}{e_3} + \frac{r_3}{r_B}\left(\frac{1}{e_B} - 1\right)} \qquad (3.2.5)$$

where

σ = $3.68\text{x}10^{-11}$, (Watts/in^2-^{o}K^4)

e = effective emissivity, (dimensionless)

e_3 = emissivity at surface 3, (dimensionless)

e_B = emissivity at surface B, (dimensionless)

k^{3B} = thermal conductivity across gap, (Watts/in-^{o}K)

Values of emissivity are assumed constant over the range of temperature considered.

The PKTEMP calculations are performed using the logic depicted in the flowchart shown in Figure 3-4. Initially, the maximum repository temperature is determined. This is followed by determination of the temperature across each barrier starting with the outermost barrier and proceeding inward. For each barrier, the code first determines if a gap is present as defined in the model shown in Figure 3-1. If no gap is present, the code skips over the radiation/conduction heat transfer equation and sets $T_3 = T_B$. The conduction equation calculates T_A for the barrier and sets T_B of the next innermost barrier equal to T_A. This process is repeated until the innermost barrier is reached. If a gap is present in any of the barriers, the code tests for the presence of a filler (backfill) material in that barrier and chooses the appropriate emissivities for use in the radiation/conduction heat transfer equation. A variable $P = f(T_3, T_B)$ is evaluated in an iterative technique to solve for T_3

$$P = 2\pi \left[3.68 \times 10^{-11} \, r_3 e (T_3^4 - T_B^4) + \frac{T_3 - T_B}{\frac{\ell (r_B / r_3)}{k^{38}}} \right] - Q/L \qquad (3.2.6)$$

An initial T_3 is assumed equal to T_B and P is calculated. T_3 is then succesively incremented until P converges giving the desired value of T_3. T_A for the barrier is then solved by the conduction equation. T_A for the innermost barrier is assumed to be the peak waste temperature (MAXTMP) for the waste package. A program listing of PKTEMP is provided in Appendix A.

The TEMPER subroutine calculates the temperature of a barrier at the time of barrier failure. Barrier failure is defined as a breakthrough of the innermost layer (solid wall) of a barrier. TEMPER performs a heat transfer calculation between the repository surface and the outer barrier surface utilizing a calculated repository temperature and an estimated overall heat transfer coefficient. TEMPER calculations are performed using the logic depicted in the flowchart shown in Figure 3-5.

The program first calculates the repository temperature as a function of time. The outermost barrier temperature at failure is then calculated using the following equation

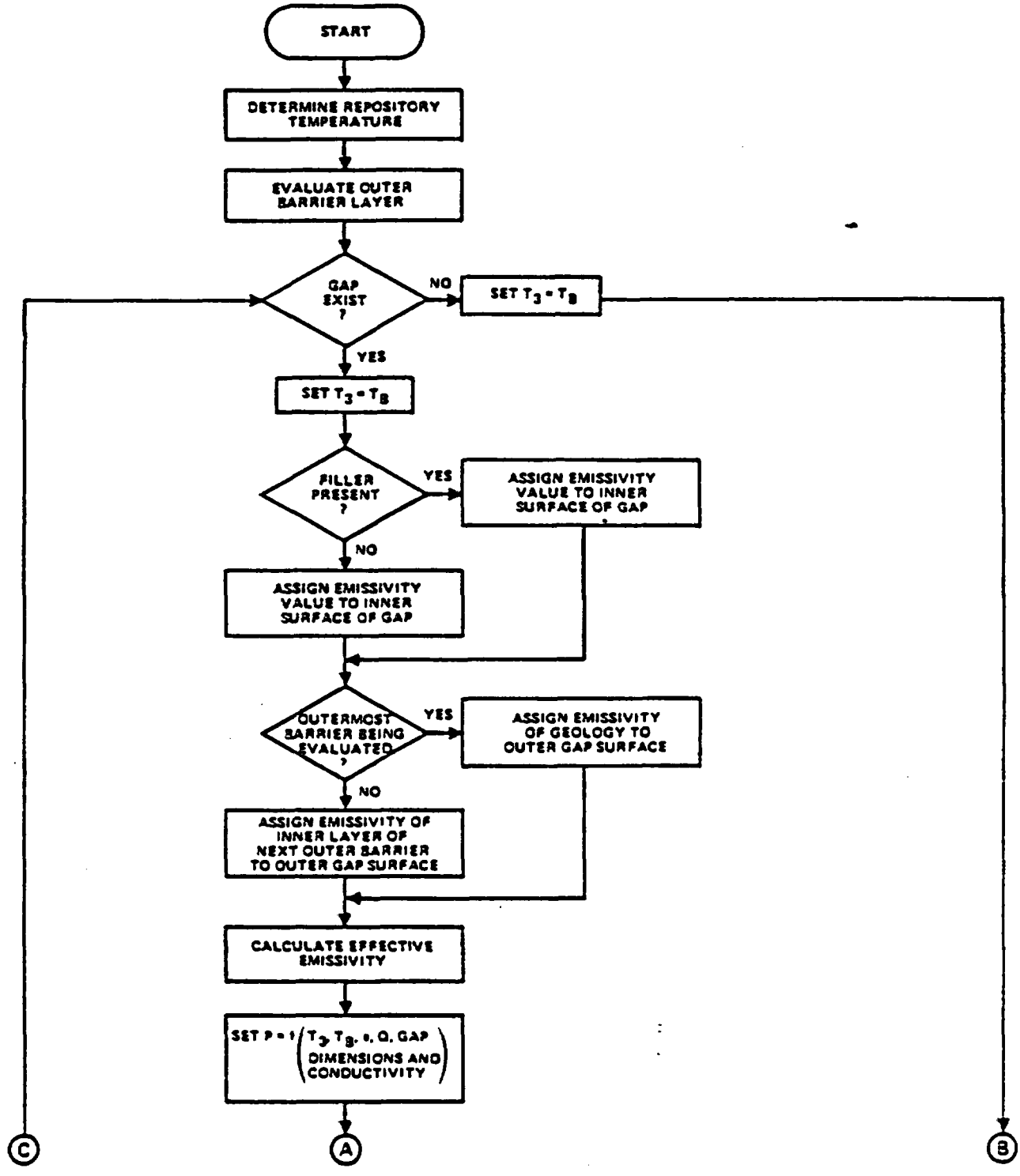

Figure 3-4. PKTEMP Flowchart.

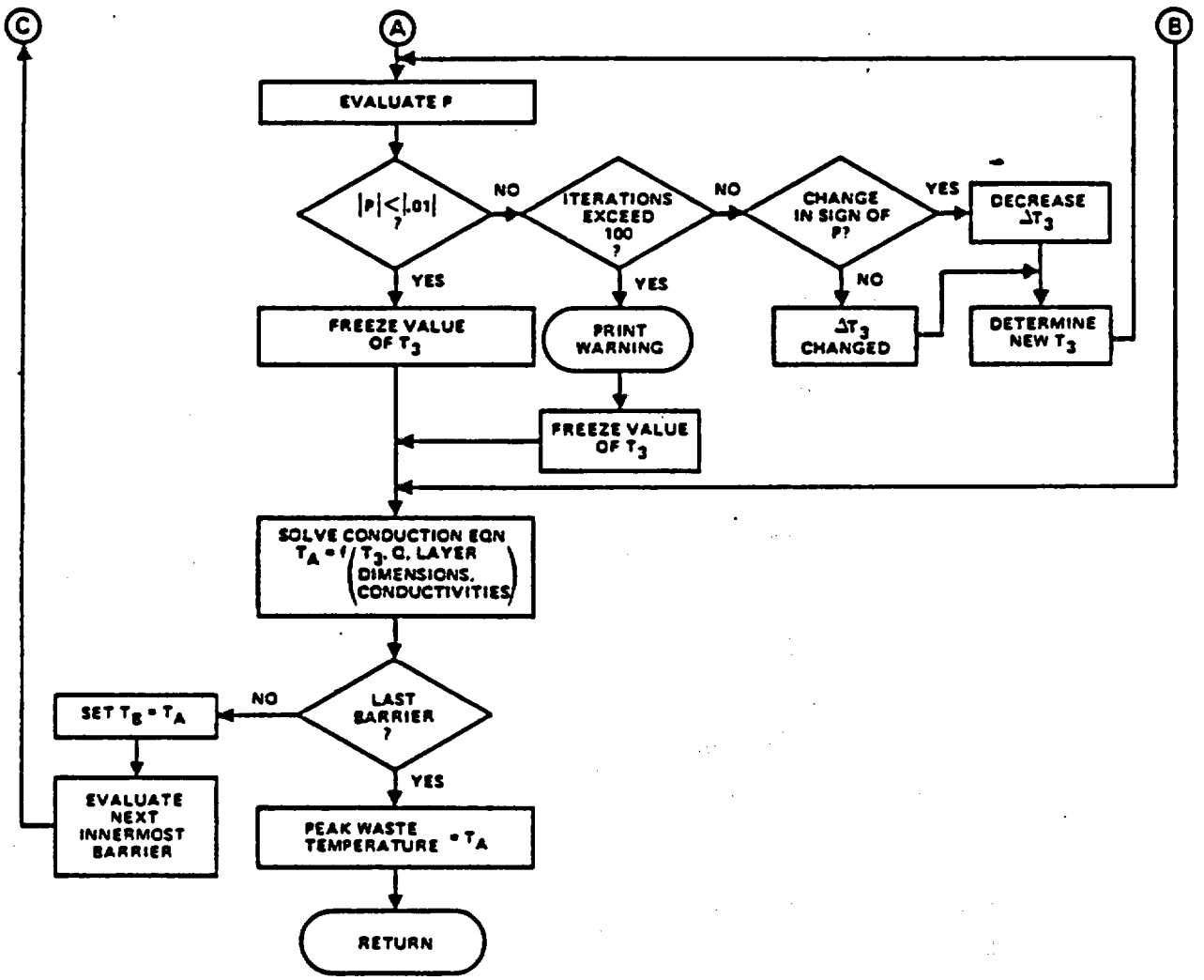

Figure 3-4. PKTEMP Flowchart (Continued).

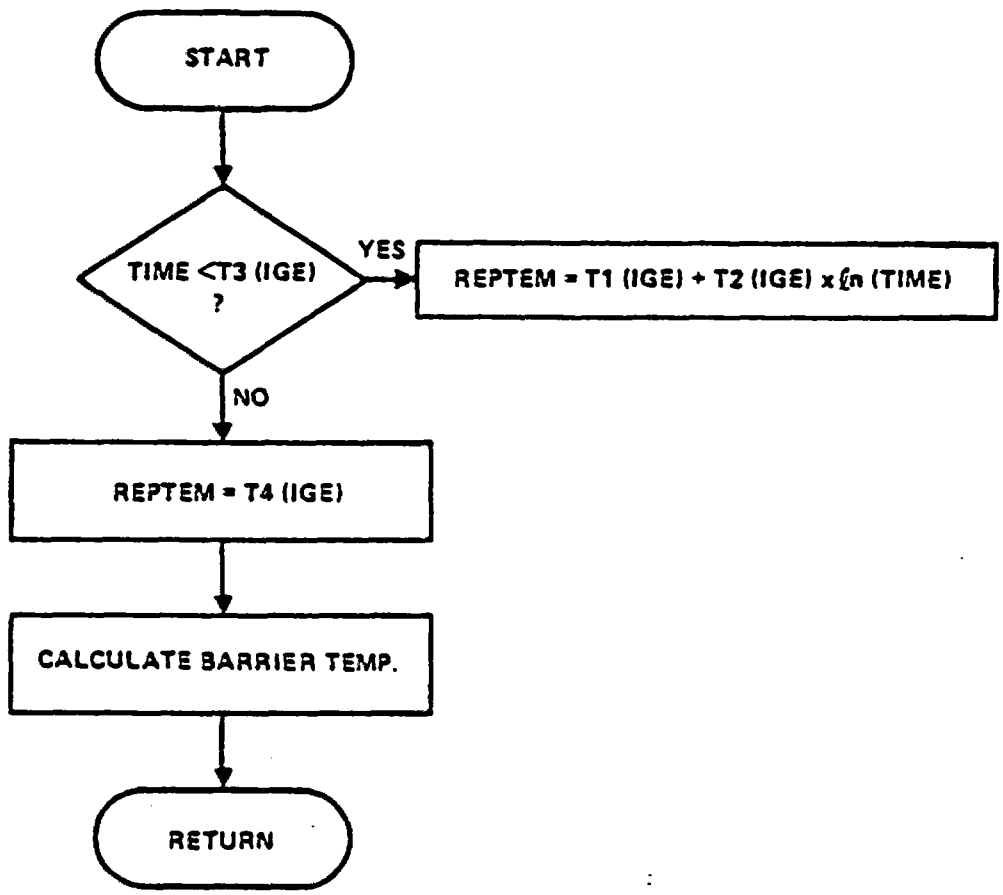

Figure 3-5. TEMPER Flowchart.

$$T_C = \frac{Q/L}{2\pi h_{BR}(r_A + 2\Delta r)} + T_R \qquad (3.2.7)$$

where

T_C = barrier temperature at outer surface, (^oK)

h_{BR} = estimated overall heat transfer coefficient between repository and barrier surface, (Watt/in^2-^oK)

T_R = calculated repository temperature, (^oK)

Δr = thickness of inner barrier layer at time of failure, (in)

For each successive barrier, the repository temperature of the particular geology in question is recalculated and is dependent only upon time. The accuracy of the heat transfer coefficient estimate is relatively unimportant in that typical waste heat generation is such that in the designs studied, calculated barrier temperatures at failure are nearly equal to the repository temperature. A listing of the TEMPER subroutine is provided in Appendix A.

3.3 CORROSION

The CORODE subroutine calculates the thicknesses of the two inner layers (Figure 3-1) of each barrier as a function of time. In each case a corrosion rate is chosen on the basis of temperature and type of repository water and is utilized to calculate the decreasing thickness of a solid barrier wall. The model assumes that the corrosion rate is characteristic of full immersion conditions. The general form of the corrosion equation is as follows

$$x_1 = x_0 - R_c\Delta t \qquad (3.3.1)$$

x_1 = new thickness, (in)

x_0 = previous thickness, (in)

R_c = corrosion rate, (in/yr)

Δt = time increment, (yr)

The CORODE calculations are performed using the logic depicted in the flowchart shown in Figure 3-6. The program first tests for the existence of a corrosion-resistant coating on the outside of the outermost of the two barrier layers in question (Figure 3-1). If present, the coating is defined in terms of time of protection afforded to the surface to be corroded. This length of time is specified in the specific input data files such that the CORODE corrosion calculations do not begin until the specified time period has elapsed. Once corrosion is ready to begin, the program determines the temperature and existing repository water type before choosing the appropriate corrosion rate from the data file CORRAT. For each pass through CORODE, the outer of the two layers in question is decreased in thickness by an amount equal to the corrosion rate times a time increment (specified in input to main program BARIER). Successive calculations occur until terminated by zero cladding layer thickness. After failure of the outer layer, the inner layer is corroded using the appropriate corrosion rate until it fails by either zero thickness of excessive external stress. Once a complete barrier fails, the next innermost barrier is considered to be uniformly flooded and the entire process is repeated. In the event of a barrier with no solid walls to be corroded (e.g., air or helium stabilizer), the two innermost barrier layers are considered to be zero and CORODE is not utilized.

The corrosion rate data contained in CORRAT is comprised of eight separate values for each package material (metals). Four corrosive environments are considered

(1) Anoxic brine B

(2) Oxic brine B

(3) Anoxic water

(4) Oxic water

over two temperature ranges (25^{o}-100^{o}C, 100^{o}-250^{o}C). The chemical compositions of brine B and typical groundwater are summarized in Tables 3-3 and 3-4, respectively. Each corrosion rate is assumed constant over its temperature range and is taken from the maximum of rates corresponding to specific corrosion

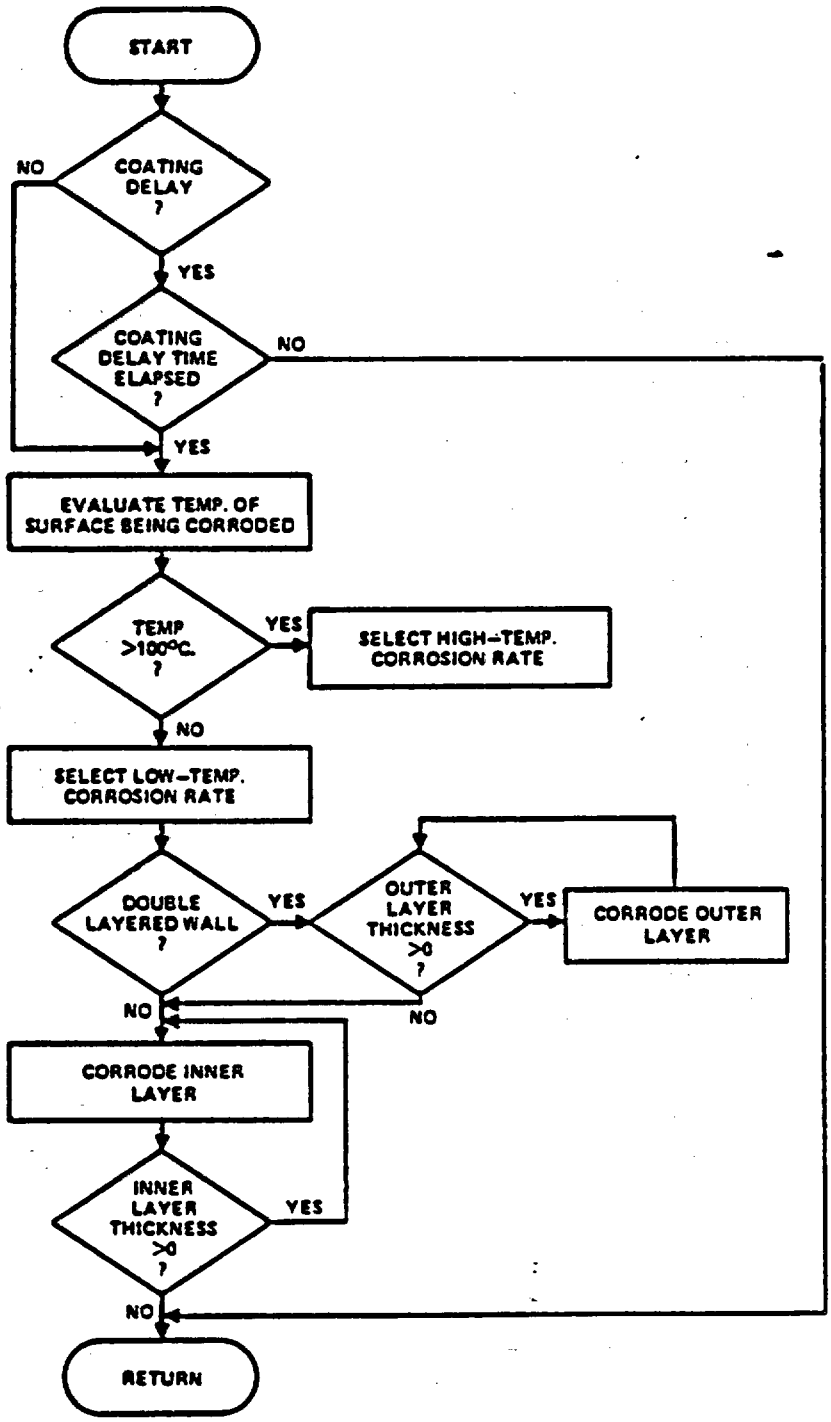

Figure 3-6. CORODE Flowchart.

Table 3-3. Chemical Compostion of WIPP-B Salt Brine*

Compound	Concentration (g/ℓ)
NaCl	287.00
Na_2SO_4	6.20
$Na_2B_4O_7 \cdot 10H_2O$	0.0160
$NaHCO_3$	0.0140
NaBr	0.5200
KCl	0.0290
KI	0.0130
$MgCl_2$	0.0400
$CaCl_2 \cdot 2H_2O$	3.30
$FeCl_3$	0.0060
$SrCl_2 \cdot 2H_2O$	0.0330
Rb_2SO_4	0.0016
CsCl	0.0013
Total Dissolved	297.174 g/ℓ
pH	6.5

*Braithwaite and Molecke, 1979

Table 3-4. Chemical Composition of Typical Arid Ground Water*.

Compound	Concentration (mg/ℓ)	
Sulfate	<50	(1-20)
Chloride	<100	(2-50)
Bicarbonate	<500	(60-400)
Nitrate	<10	(0·1-5)
Sodium	<50	(5-47)
Potassium	<10	(1-5)
Magnesium	<50	(2-20)
pH	7-9	(6·8-8·5)

*Katayama, 1976

mechanisms for a particular environment and temperature range. The corrosion mechanisms considered included uniform corrosion, stress corrosion, pitting, and graphitization (see Appendix B). The general form of CORRAT is shown in Table 3-5 and a listing of CORRAT with current data is provided in Appendix E. A program listing of CORODE is provided in Appendix A. Package materials for which corrosion data are obtained include mild steel, Zircaloy-2, Inconel-600, 304 Stainless Steel, copper, lead, and cast iron.

A degree of uncertainty in the corrosion rate data base exists because of the numerous effects of environmental parameters on package corrosion. Environmental parameters acting upon waste packages vary with the geology of the repository and can have a major impact on resultant corrosion rates. For example, increases in temperature generally increase the corrosion rates of metals (Braithwaite, 1979). Also, increases in temperature in an open system cause a depletion in dissolved oxygen in aqueous solutions. This decreases the corrosion rate of metals whose rate is controlled by diffusion of oxygen.

The restraining pressure which a waste package is subjected to in a repository affects the corrosion rate primarily in that it influences the physical state of intruding water and the concentration of dissolved gaseous species. Waste packages will be exposed to any thermal decomposition products of the geologic isolation formation and any dissolved and gaseous species present. In general, species in solution which increase the oxidizing power of that solution increase the corrosion rate.

The tensile stress present in the barrier wall is one of the essential requirements for stress corrosion cracking. Not all materials are susceptible to stress corrosion cracking in geologic isolation conditions. For susceptible materials, the threshold tensile stress depends strongly on temperature, solution composition, and the presence of an aqueous phase. Alloys containing carbon and chromium can be susceptible to sensitization. For example, sensitization in stainless steels refers to the thermally induced formation of chromium carbide at or near grain boundaries (Molecke, 1979). This increases the susceptibility of the alloy to intergranular attack and intergranular stress corrosion cracking. Welding, because of the high temperatures involved, often leads to sensitization and tensile stress in welded regions.

The corrosion rate data base is generally considered to be conservative in view of the procedure used to choose maximum corrosion rates for each set of temperature and water conditions. In addition, potential effects on corrosion

Table 3-5. General Form of CORRAT.

ENVIRONMENT / MATERIAL	BRINE-ANOXIC		BRINE-OXIC		WATER-ANOXIC		WATER-OXIC	
	25°-100°C	100°-250°C	25°-100°C	100°-250°C	25°-100°C	100°-250°C	25°- 100°C	100°-150°C
Mild Steel								
Zircaloy								
Inconel								
304 SST								
Copper								
Lead								
Cast Iron								

rates caused by radiation levels within the waste package only service to reinforce the use of a conservative "worst-case" approach in performing the corrosion calculations.

3.4 BARRIER FAILURE CRITERIA

The STRESS subroutine determines the time when a particular package barrier fails due to internal or external pressure. Failure of any metal barrier wall due to external pressure is considered to occur when the wall is in plastic strain and there is a uniform pressure across the wall ("hydrostatic"). Failure due to internal pressure is defined as the time when the wall thickness no longer meets the requirements for hoop stress in the AMSE Code, Section VIII, Division 1. The wall thickness is that portion of the original wall not affected by corrosion (including bulk corrosion, pitting, or crack propagation) as determined in the corrosion subroutine. The subroutine updates two binary flags BFAIL and WFAIL. If BFAIL = 0 then the backfill has "failed", which means there is no longer a pressure gradient across the backfill. If WFAIL = 0, then the solid wall has failed. If WFAIL or BFAIL = 1, then they are intact, sustaining a pressure gradient.

In each time increment the wall thickness and temperature of a barrier are revised. Then the STRESS subroutine recalculates the new stress distribution and updates the binary flags BFAIL and WFAIL. The main program acts on the value of WFAIL to determine when the defense shifts to the next inner package barrier. BFAIL is used by STRESS to determine the nature of the pressure distribution.

The barrier is considered as a bimetallic wall adjacent to a porous filler (or backfill as depicted in Figure 3-7. The model is based on assumption of a structural wall, a cladding with no strength attributes, and a structural backfill. Stress-strain properties of the backfill and structural wall determine pressure profiles between R_0 and R_1 and R_2 and R_3. The pressure is assumed uniform between R_1 and R_2.

The mechanical properties of backfill materials vary widely depending on the minerals, particle size and shape distributions, porosity, and moisture content. It is assumed that the backfill is loaded monotonically by creep of the geologic media as it acts to close the borehole.

The yield model used for the backfill is

$$Y = C_o + \beta(P_R - P_{pore}) \qquad (3.4.1)$$

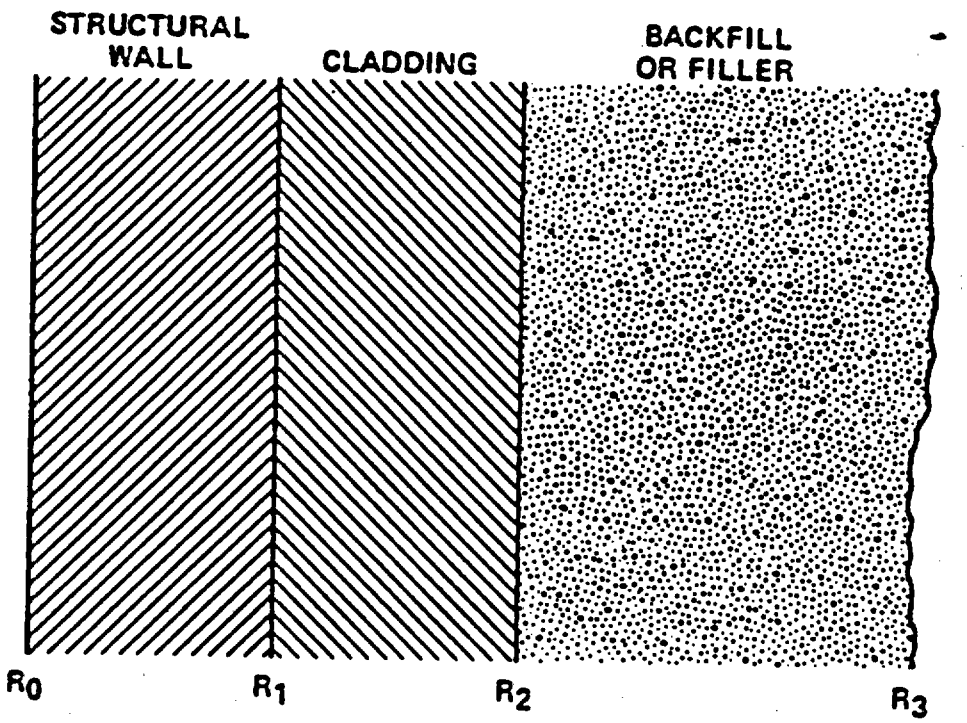

Figure 3-7. Composite Barrier Used in Stress Calculations.

where

C_o = cohesion, (Ksi)

β = constant slope of the Mohr envelope, (dimensionless)

P_R = absolute value of the mean stress (repository pressure), (Ksi)

P_{pore} = pore water pressure, (Ksi)

In this application cohesion is neglected. This could be added later if necessary but is reasonable for most materials in question. For most compacted soils the Mohr slope falls between 0.6 and 1.2. $P_{pore} = 0$ for dry materials and ranges up to about P/2 based on a ratio of the weight of a water column from the repository to surface and the weight of the overburden of typical rock. In the subroutine the yield stress is

$$Y = \beta(P_R - P_{pore}) \tag{3.4.2}$$

Generally, the conservative assumption of $P_{pore} = 0$ is used. Note that this model assumes also that creep is sufficiently rapid that overburden pressure is applied at time = 0.

The pressure-volume relationship for the backfill is a very non-linear and highly variable-based physical characteristic. Any backfill employed must have defined an empirical pressure-volume characteristic. To accommodate the wide range of possibilities, a quadratic data fit is provided in the model using two coefficients. A relation between volume before and after compression is

where

$$V^* = \frac{V_o}{V} - 1 \tag{3.4.3}$$

V_o = original volume, (cm^3)

V = volume after compression by pressure P, (cm^3)

and

$$P_R = AV^* + KV^{*2} \tag{3.4.4}$$

where A and K are empirical coefficients. Thus,

$$V^* = \frac{-A \pm \sqrt{A^2 + 4\,KP_R}}{2K} \tag{3.4.5}$$

In the special case where $K = 0$ or $K \approx 0$

$$V^* = \frac{P_R}{A} \tag{3.4.6}$$

Equation (3.4.5) refers to a "soft" backfill which displays a high degree of volume reduction under small compressive loads. Equation (3.4.6) refers to a "stiff" backfill with low compaction at high pressure. Typical data (Byerlee, 1967) gives a curve for compacted sand

$$P_R = 0.4413V^* + 253V^{*2} \tag{3.4.7}$$

The instantaneous shear modulus, G', was constructed from the instantaneous bulk modulus, B', and Poisson's ratio, ν, according to non-linear elastic theory. The bulk modulus is given by

$$B' = -V \frac{dP_R}{dV} \tag{3.4.8}$$

and shear modulus by

$$G' = \frac{3}{2} B' \frac{(1 - 2\nu)}{(1 + \nu)} \tag{3.4.9}$$

The Lame' constant is given by

$$\lambda' = B' - \frac{2G'}{3} \tag{3.4.10}$$

Differentiating Equation (3.4.4) and substituting into Equation (3.4.8) gives

$$B' = A(V^* + 1) + 2KV^*(V^* + 1) \tag{3.4.11}$$

Then G' and λ' are calculated by Equations (3.4.9) and (3.4.10).

The barrier wall is assumed to be constructed of an elastic material for which the following properties are specified as functions of temperature, T

$$\text{Yield Stress} = Y = Y_1 + Y_2(T) \tag{3.4.12}$$

$$\text{Bulk Modulus} = B = B_1 + B_2(T) \tag{3.4.13}$$

$$\text{Shear Modulus} = G = G_1 + G_2(T) \tag{3.4.14}$$

The Poisson ratio is calculated by

$$\nu = \frac{1}{2}\left(\frac{3B - 2G}{3B + G}\right) \tag{3.4.15}$$

A stress equilibrium calculation is employed to calculate the response of the cylindrical composite at a stressed state as compared with pressures and dimensions in an unstressed state. Because changes occur very slowly, it is reasonable to assume equilibrium.

Consider a single cylinder of outside radius R and length z. In general the stress and strain changes are related by the elastic equations

$$\Delta\sigma_R = (\lambda + 3G)\,\varepsilon_R + \lambda\varepsilon_\theta + \lambda\varepsilon_z \tag{3.4.16}$$

$$\Delta\sigma_\theta = \lambda\varepsilon_R + (\lambda + 2G)\,\varepsilon_\theta + \lambda\varepsilon_z \tag{3.4.17}$$

$$\Delta\sigma_z = \lambda\varepsilon_R + \lambda\varepsilon_\theta + (\lambda + 2G)\,\varepsilon_z \tag{3.4.18}$$

where

σ_R, σ_θ, σ_z = stress components, (Ksi)

ε_R = dU/R = change of radial strain, (in/in)

U = strain, (in)

ε_θ = change of hoop strain, (in/in)

ε_z = change in axial strain, (in/in)

Initial equilibrium stress results in no motion

$$\rho\ddot{R} = \frac{d\sigma^0}{dR} + (\sigma_R^0 - \sigma_\theta^0)\ R = 0 \qquad (3.4.19)$$

$$\rho\ddot{z} = \frac{d\sigma_z^0}{dz} = 0 \qquad (3.4.20)$$

The final equilibrium stresses must produce no motion

$$\rho\ddot{R} = 0 = \frac{d}{dR}(\sigma_R^0 + \Delta\sigma_R) + (\sigma_R^0 + \Delta\sigma_R - \sigma_\theta - \Delta\sigma_\theta^0)/R \qquad (3.4.21)$$

$$\rho\ddot{z} = 0 = \frac{d}{dz}(\sigma_z^0 + \Delta\sigma_z) \qquad (3.4.22)$$

For equilibrium (neglecting rotation)

$$\rho\ddot{R} = 0 = \frac{d}{dR}(\Delta\sigma_R) + (\Delta\sigma_R - \Delta\sigma_\theta)/R \qquad (3.4.23)$$

$$\rho\ddot{z} = 0 = \frac{d}{dz}(\Delta\sigma_z) \qquad (3.4.24)$$

The corresponding equation for rotation was left out as it is assumed that there are no torquing forces. Substituting Equations (3.4.16) - (3.4.18) into Equations (3.4.23) and (3.4.24) and noting that $\varepsilon_R = dU/R$, $\varepsilon_\theta = U/R$ and $\frac{d\varepsilon_z}{dR} = 0$

then

$$(\lambda + 2G)\frac{d^2U}{dR^2} + \frac{d}{dR}(U/R) + \frac{2G}{R}\left(\frac{dU}{dR} + \frac{U}{R}\right) = 0 \qquad (3.4.25)$$

The solution to Equation (3.4.1) is

$$U = fR + \frac{g}{R} \qquad (3.4.26)$$

which gives

$$\varepsilon_R = \frac{dU}{dR} = a - \frac{b}{R^2} \qquad (3.4.27)$$

$$\varepsilon_\theta = \frac{U}{R} = a + \frac{b}{R^2} \qquad (3.4.28)$$

where f and g are constants evaluated from initial conditions. Evaluating a and b from initial conditions

$$a = \frac{R_o^2\,\Delta P_o - R_1^2\,\Delta P_1 - \lambda\varepsilon_z(R_1^2 - R_o^2)}{2(\lambda+G)(R_1^2-R_o^2)} \qquad (3.4.29)$$

$$b = \frac{(\Delta P_o - \Delta P_1)\,R_o^2\,R_1^2}{2G(R_1^2-R_o^2)} \qquad (3.4.30)$$

when

$$\Delta P_o = P_o - P_o^o \qquad (3.4.31)$$

and

$$\Delta P_1 = P_1 - P_1^o \qquad (3.4.32)$$

If the initial condition is unstressed then

$$\Delta P_o = P_o \tag{3.4.33}$$

and

$$\Delta P_1 = P_1 \tag{3.4.34}$$

For the inner cylinder depicted in Figure 3-7

$$U(R_1) = -\frac{P_1 R_1}{2(R_1^2 - R_0^2)}\left[\frac{R_1^2}{\lambda + G} + \frac{R_0^2}{G}\right] - \frac{\lambda \varepsilon_z R_1}{z(\lambda + G)} \tag{3.4.35}$$

and the cladding cylinder

$$U'(R_2) = \frac{P_3 R_2}{2(R_3^2 - R_2^2)}\left[\frac{R_2^2}{\lambda' + G'} + \frac{R_3^2}{G'}\right] - \frac{P_2 R_2}{2(R_3^2 - R_2^2)}\left[\frac{R_3^2}{\lambda' + G'} + \frac{R_3^2}{G'}\right] - \frac{\lambda' \varepsilon_z' R_1}{2(\lambda' + G')} \tag{3.4.36}$$

Since the cladding layer is of zero strength, $P_1 = P_2$. Substituting P_1 for P_2, P for P_3, and letting $\varepsilon_z = \varepsilon'_z = 0$ (constant stress in axial direction), then $U(R_1) = U'(R_2)$ and

$$P_1 = \frac{PR_2R_3\left[\frac{1}{\lambda' + G'} + \frac{1}{G'}\right]}{2(R_3^2 - R_2^2)\left[\frac{R_1}{2(R_1^2 - R_0^2)}\left(\frac{R_1^2}{\lambda + G} + \frac{R_0^2}{G}\right) + \frac{R_2}{2(R_3^2 - R_2^2)}\left(\frac{R_2^2}{\lambda' + G'} + \frac{R_3^2}{G'}\right)\right]} \tag{3.4.37}$$

which gives the interface pressure P_1 as a function of the repository pressure P_R and material properties of backfill and structural wall.

The pressure on the inner boundary of the backfill determines whether or not the backfill will remain as an elastic wall or flow plastically. It is assumed that the outer pressure is the repository pressure. When the inner pressure falls below a threshold value the backfill yields and flows plastically. That is, there is a maximum pressure gradient that the backfill will support. Exceeding this gradient is indicated by a minimum pressure at the inner boundary of the backfill since the outer pressure is maintained constant at repository pressure. Once the minimum is reached yield is triggered, the backfill flows plastically and the interface pressure rises to equal the repository pressure.

The backfield yield triggering is given by

$$P_1 \leq \frac{P_R(1 - \eta)}{\left(1 - \eta \frac{R_2^2}{R_3^2}\right)} \tag{3.4.38}$$

where

$$\eta = \sqrt{\frac{4}{27}\beta^2(1 - \nu)^2 - \frac{1}{3}(1 - 2\nu)^2} \tag{3.4.39}$$

Note that η becomes imaginary if

$$\beta < 1.5 \frac{(1 - 2\nu)}{(1 - \nu)} \tag{3.4.40}$$

If η is imaginary, the backfill will yield plastically for any value of P_1. It is therefore a minimum condition that the backfill have a β and ν such that

$$\beta > 1.5 \frac{(1 - 2\nu)}{(1 - \nu)} \tag{3.4.41}$$

Typical values for β and ν have been found in the literature and range from approximately 0.6-1.2 and 0.25-0.45, respectively.

In the case of wall yield the inside pressure is neglected as it is very small compared to repository pressure. Thus yielding is controlled by the pressure at the outside of the wall. The condition for no yield established for cylindrical shells is

$$Y^2 > 4\left[\frac{P_1}{1 - \frac{R_0^2}{R_1^2}}\right]^2 (1 - \nu + \nu^2) \qquad (3.4.42)$$

Thus yield will occur when

$$P_1 \geq \frac{Y}{2} \frac{1 - \left(R_0^2/R_1^2\right)}{\sqrt{1 - \nu + \nu^2}} \qquad (3.4.43)$$

Internal pressure stress was based on ASME code requirements. Hoop stress criteria from ASME Code, Section VIII, Division 1 (ASME, 1977) give

$$\delta = \frac{P_0 R_0}{(SE - 0.6\, P_0)} \qquad (3.4.44)$$

where

δ = wall thickness, (in)

E = joint efficiency for longitudinal seam
(=1 for seamless or full penetration weld)

S = allowable stress for material, (psi)

P_0 = internal pressure, (psi)

R_0 = inside radius, (in)

The allowable stress tables from the code were used to develop a correlation for S as a function of temperature, T. The subroutine calculates S from

$$S = S1 - S2(T) \qquad T > S3 \qquad (3.4.45)$$

$$S = S4 \qquad T \leq S3 \qquad (3.4.46)$$

Solving Equation (3.4.44) for P_o

$$P_o = \frac{\delta SE}{R_o + 0.6\,\delta} \qquad (3.4.47)$$

When

$$P_o > \frac{\delta SE}{R_o + 0.6\delta} \qquad (3.4.48)$$

then WFAIL is set to 0, meaning the wall has failed.

The STRESS subroutine is called by the main program at each time increment for each barrier layer. The subroutine determines whether the current barrier under consideration remains intact or fails at that time increment. Wall thickness is the current value returned from the corrosion subroutine CORODE.

Figure 3-8 is a flowchart of the subroutine. The subroutine first checks to see if external or internal pressure are of concern. The value of CREEP is then "YES" or "NO". If CREEP = YES then the external routine is used, otherwise internal pressure is checked against the code criteria. If external pressure is of concern then radii are calculated based on the latest value of THICK, the wall thickness. Presence of a backfill is checked. If there is no backfill then the pressure on the outside of the wall ("interfacial" pressure EPRESS) is set equal to repository pressure REPRES. The next step is to check for backfill failure. If the backfill yields then EPRESS = REPRES. If the backfill has not failed then calculations are carried out to determine the status of the backfill. If failure is determined then once again EPRESS = REPRES. Then the subroutine calculates stresses on the wall as interfacial pressure EPRESS and checks for wall yield. WFAIL is set to 1 if the wall is intact or 0 if failure

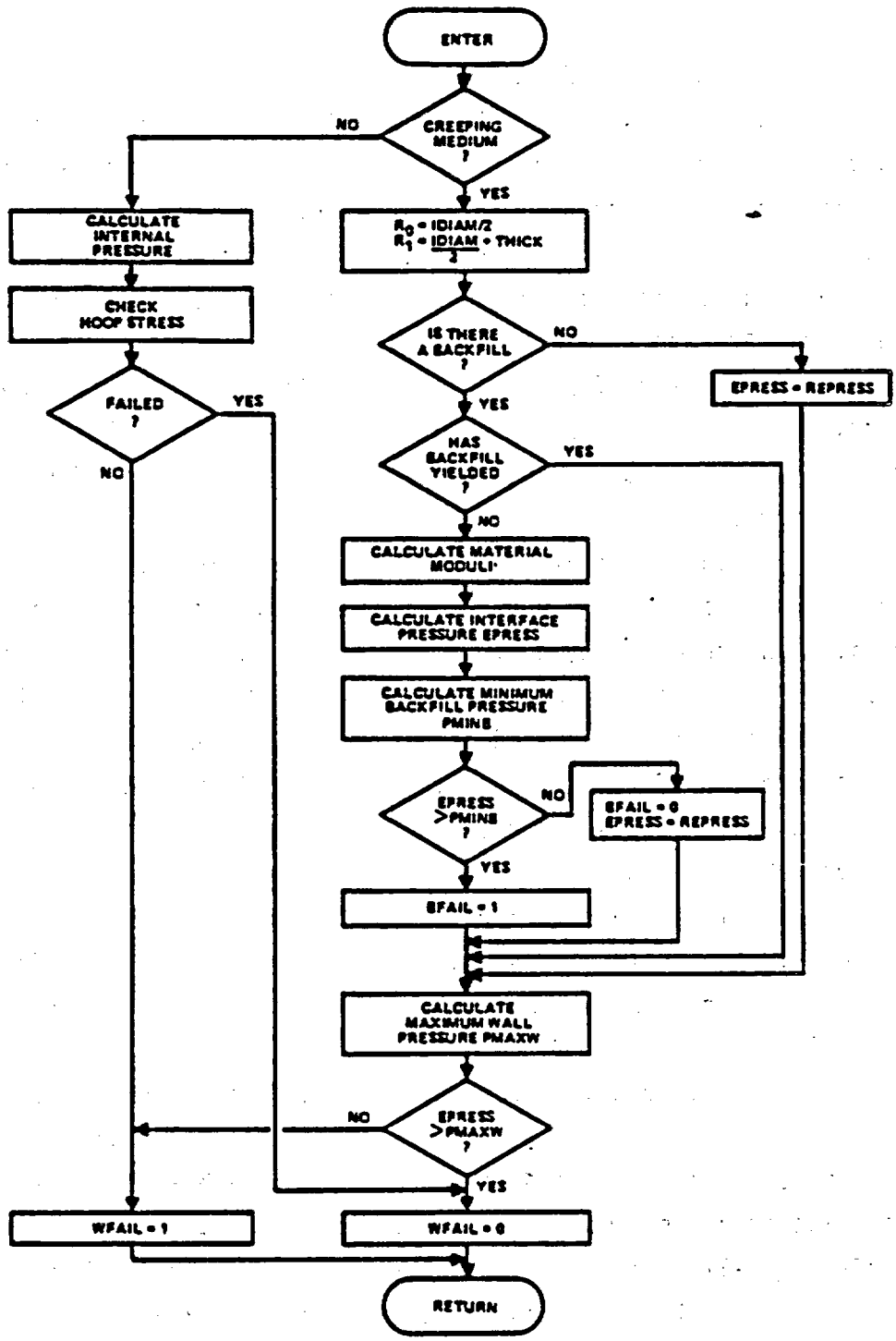

Figure 3-8. STRESS Flowchart.

is determined. Based on the value of WFAIL the main program continues with this barrier or proceeds inward.

3.5 RADIONUCLIDE RELEASE RATES

The radionuclide release model RELEAS calculates the transport rate of specific radionuclides through failed engineered barriers and backfill. The specific rate of interest is the release rate to the geology. The model is based on slab geometry which is a conservative assumption relative to a cylindrical geometry. The engineered barrier package can consist of many layers of different materials. At some time after emplacement in the repository the barriers fail, either by crushing from the lithostatic pressure in the repository or by corrosion. In either case, when the barriers fail, it is assumed that water is available throughout the fuel bundle, barriers, and backfill; and mass transport by diffusion begins.

The objective of the radionuclide release model is to calculate the release rate based on Fick's second law of diffusion, i.e., no countercurrent diffusion and no convection of water. The question of water convection was discussed in Section 2 under the high water flow rate scenario. The backfill is assumed to have capacitance in excess of that of a solution. The capacitance is due to sorption of the species of interest. Resistance to mass transfer is also assumed to exist because of the remains of the failed barriers. This assumption is reasonable because there is a finite distance from the waste to the backfill face, and the failed barriers represent a physical resistance through a void fraction available for transport, i.e., a porous barrier. The failed engineered barrier is assumed to have no capacitance since the capacitance of the backfill is much larger.

In the model description that follows the waste resides next to the backfill slab at $x = \ell$. A zero-capacitance mass transfer resistance is assumed to be present at $x = \ell$, similar in concept to a heat transfer coefficient, and a mass transfer resistance is assumed to be present at the backfill-geology interface ($x=0$) that is 1/10 of that at $x = \ell$. The geology is assumed to sweep away the radionuclides as soon as they arrrive at $x = 0$ so that the boundary condition at $x = 0$ is a zero concentration. Note that the results are relatively insensitive to resistance at the geology face and often insensitive to failed barrier resistance (except for cases with little or no backfill).

Consider a slab of thickness ℓ with the conductance boundary conditions

$$\frac{\partial c}{\partial t} = k \frac{\partial^2 c}{\partial x^2} \qquad 0 < x < \ell \qquad (3.5.1)$$

$$\frac{dc}{dx} + h_\ell (c - c_\ell) = 0 \qquad \text{at } x = \ell \qquad (3.5.2)$$

$$\frac{dc}{dx} - h_o c = 0 \qquad \text{at } x = 0 \qquad (3.5.3)$$

$$\text{and} \quad c(x,0) = 0 \qquad (3.5.4)$$

These equations describe the time-dependent diffusion phenomenon with so-called "radiation" boundary conditions (Carslaw, 1967). Since diffusion is assumed to be occurring through a porous medium, the constant k is not the liquid diffusion coefficient.

In considering diffusion through a porous medium, an effective diffusivity is (Bird, 1965) (Smith, 1970)

$$N_a \equiv - D_e \frac{\partial c}{\partial x} \qquad (3.5.5)$$

where c is the concentration of the species of interest contained in the liquid volume only, not the total unit volume including solid. N_a is the flux per actual unit area and D_e is measured experimentally. The effective diffusivity for a porous medium is estimated to be

$$D_e \equiv \frac{\varepsilon D_\ell}{\delta} \qquad (3.5.6)$$

where ε is the void volume and δ is the tortuosity. Therefore, the effective diffusivity is defined in terms of liquid concentrations.

Transient diffusion is described by

$$D_e \frac{\partial^2 c}{\partial x^2} \equiv \text{Accumulation} \tag{3.5.7}$$

Since the diffusive flux is based on liquid concentration there is accumulation with no adsorption

$$D_e \frac{\partial^2 c}{\partial x^2} \equiv \epsilon \frac{\partial c}{\partial t} \tag{3.5.8}$$

When accumulation by adsorption also occurs, another term must be added to account for it.

The amount of material adsorbed on the solid of the porous medium is obtained from information on the equilibrium constant

$$c_s \equiv k_d c \tag{3.5.9}$$

where c_s = grams of species of interest adsorbed on one gram of solid, so that units are

$$k_d \; [=] \left[\frac{\text{gms on solid}}{\text{gm solid}}\right]\left[\frac{\text{ml of liquid}}{\text{gm in liquid}}\right] \tag{3.5.10}$$

Hence, k_d is reported as ml/gm. Now if ρ is the bulk density of the solid, ρc_s yields the amount of adsorbed material in equilibrium with the liquid concentration c or

$$D_e \frac{\partial^2 c}{\partial x^2} = (\epsilon + k_d \rho) \frac{\partial c}{\partial t} \tag{3.5.11}$$

Therefore,

$$k \equiv \frac{D_\ell}{\delta\left(1 + \frac{k_d \rho}{\varepsilon}\right)} \tag{3.5.12}$$

where

k = constant in Equation (3.5.1), (cm^2/yr)

ρ = bulk density of the solid, (gm/ml)

k_d = distribution constant, (ml/gm)

The boundary condition in Equation (3.5.2) contains the conductance h_ℓ which is derived from

$$D_e \frac{dc}{dx} + H_\ell (c - c_\ell) = 0 \qquad \text{at } x=\ell \tag{3.5.13}$$

where it is seen that

$$h_\ell = \frac{H_e}{D_e} \tag{3.5.14}$$

H_ℓ is called a conductance since it multiplies a gradient rather than a flux and is assumed to be the result of diffusion through a distance Δx with no capacitance. Examining a slab for this assumption yields

$$q(\Delta x) = D(\Delta c) \tag{3.5.15}$$

where q is the flux, Δx is the slab thickness, D is the diffusion coefficient, and Δc is the concentration difference. Therefore, for the problem considered here

$$H_\ell = \frac{D}{\Delta x} \tag{3.5.16}$$

where D is the diffusivity through the medium in Δx which is the corroded barrier.

The solution to Equation (3.5.1) with the prescribed boundary and initial conditions is of the form

$$c(x,t) = w(x,t) + u(x) \tag{3.5.17}$$

where u(x) is the steady state solution and is

$$u(x) = \frac{c_{\ell} h_{\ell}}{1 + h_{\ell}\left(\ell + \frac{1}{h_o}\right)} \left(x + \frac{1}{h_o}\right) \tag{3.5.18}$$

and the transient solution is

$$w(x,t) = \sum_{n=1}^{\infty} A_n X_n \exp(-k\alpha_n^2 t) \tag{3.5.19}$$

and

$$X_n = \cos(\alpha_n x) + \frac{h_o}{\alpha_n} \sin(\alpha_n x) \tag{3.5.20}$$

where α_n is the n-th positive root of

$$\tan(\alpha\ell) = \frac{\alpha(h_o + h_{\ell})}{\alpha^2 - h_{\ell} h_o} \tag{3.5.21}$$

and

$$A_n = \frac{2\alpha_n c_\ell h_\ell \left\{ \frac{h_o \ell}{\alpha_n} \cos(\alpha_n \ell) - \left[\ell + \frac{h_o}{\alpha_n^2} + \frac{1}{h_o} \right] \sin(\alpha_n \ell) \right\}}{\left\{ \left(\alpha_n^2 + h_o^2 \right) \ell + h_\ell \left(\frac{\alpha_n^2 + h_o^2}{\alpha_n^2 + h_\ell^2} \right) + h_o \right\} \left[1 + h_\ell \left(\ell + \frac{1}{h_o} \right) \right]} \qquad (3.5.22)$$

A special case of the conditions described by Equations (3.5.1) - (3.5.4) is considered where the conductances are large, i.e., the resistances are close to zero. This case is illustrated in Figure 3-9 where line A represents the steady state solution for $h_\ell = h_o \to \infty$, and line B represents the steady state solution for h_ℓ and $h_o \ll \infty$ Experience indicates that when "B" approaches "A" the solution described by Equations (3.5.17) - (3.5.22) converges very slowly and is impractical to evaluate. A solution with fixed boundary conditions should be used when

$$\frac{c_1 - c_2}{c_\ell} = A > 0.8 \qquad (3.5.23)$$

is satisfied.

The solution with fixed boundary conditions and zero initial condition is (Carslaw, 1967)

$$c(x,t) = \frac{2c_\ell}{\pi} \sum_{n=1}^{\infty} \frac{(-1)^n}{n} \sin\left(\frac{n\pi x}{\ell}\right) \exp\left[-k\left(\frac{n\pi}{\ell}\right)^2 t\right] + c_\ell \frac{x}{L} \qquad (3.5.24)$$

From the equations described, the quantity of material transported across the boundaries at $x = 0$ and $x = \ell$ can be calculated during the transient period. When steady state is attained, the much simpler steady state solutions yield the quantity transported. The time at which steady state is attained is defined to be when the lead exponential in Equation (3.5.19) has decayed to 0.01, or

$$t_s = \frac{4.6}{k\alpha_1^2} \qquad (3.5.25)$$

or using Equation (3.5.24)

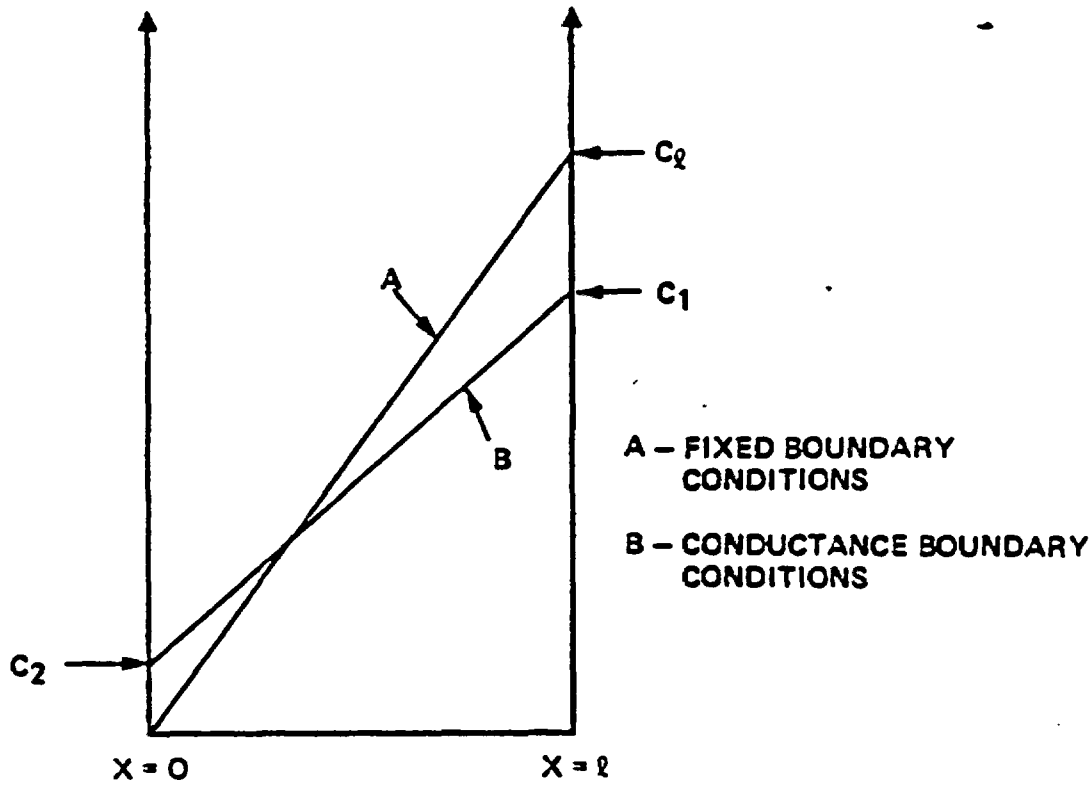

Figure 3-9. Illustration of Steady State Solution.

$$t_s = \frac{4.6}{k(\pi/L)^2} \qquad (3.5.26)$$

The transport of radionuclides occurs only as long as there is material remaining in the waste. A material balance around the waste for a specific radionuclide yields

$$\frac{dy}{dt} = -f(t) - \lambda y \qquad (3.5.27)$$

where y is the quantity of material in the waste at any time t, λ is the decay constant, and f(t) is the rate of transport of material out by diffusion as described by Equations (3.5.17) or (3.5.24). The result for integrating the linear first order differential Equation (3.5.27) where f(t) is described by Equation (3.5.17) is:

$$y(t) = H_\ell^o \sum_{n=1}^{\infty} \frac{B_n}{(\lambda - k\alpha_n^2)} \exp(-k\alpha_n^2 t) + \frac{K_\ell}{\lambda} \qquad (3.5.28)$$

$$+ \exp(-\lambda t)\left[y_o - H_\ell^o \sum_{n=1}^{\infty} \left(\frac{B_n}{\lambda - k\alpha_n^2}\right) - \frac{K_\ell}{\lambda}\right]$$

where

y_o = initial quantity of material

$H_\ell^o = aH_\ell$

a = area available for transport at $x = \ell$

$K_\ell = H_\ell^o [c(\ell)-c_\ell]$

$B_n = A_n x_n \ (x = \ell)$

Likewise for Equation (3.5.24)

$$y(t) = -2K \sum_{n=1}^{\infty} \frac{\exp\left[-k\left(\frac{n\pi}{\ell}\right)^2 t\right]}{\left[\lambda - k\left(\frac{n\pi}{\ell}\right)^2\right]} - \frac{K}{\lambda} \qquad (3.5.29)$$

$$+ \exp(-\lambda t)\left[y_o + 2K \sum_{n=1}^{\infty} \frac{1}{\left[\lambda - k\left(\frac{n\pi}{\ell}\right)^2\right]} + \frac{K}{\lambda}\right] -$$

where

$$K = aD_e c_\ell / \ell.$$

In the event there is sufficient material at $t = 0$ to attain steady state, a material balance on the waste for a specific radionuclide yields

$$\frac{dz}{dt} = -\lambda z - r_{tr} \qquad (3.5.30)$$

where r_{tr} is the constant rate of material transported out by diffusion. Integrating and solving for the time when the quantity of material in the waste is zero yields

$$t_f = \frac{1}{\lambda} \ell n\left[\frac{\lambda z_o + r_{tr}}{r_{tr}}\right] \qquad (3.5.31)$$

where z_o is the quantity of material present when steady state is attained and t_f is the time beyond the steady state time required for $z = 0$.

The transport of radionuclides through an adsorbing medium can be calculated using Equation (3.5.17) for the case when surface conductances are present or Equation (3.5.24) for the case of fixed boundary conditions. The constant k is calculated from Equation (3.5.12) for both Equations (3.5.17) and (3.5.24). The use of Equation (3.5.17) or (3.5.24) is determined by Equation (3.5.23). The steady state times are calculated by Equation (3.5.25) or (3.5.26). The quantity of a specific radionuclide remaining in the waste at any time, t, is calculated from Equation (3.5.28) or (3.5.29). In the event y_o is not large enough to allow steady state transport to be attained, Equation (3.5.28) or (3.5.29) is solved by trial and error to find the time where $y = 0$. If steady state is attained, the additional time required for radionuclides in the waste to attain zero quantity is calculated from Equation (3.5.31). The

calculations essentially stop when y = 0, whether this is before or after steady state. There are no equations derived here for the transport across the x = 0 boundary after y = 0. This "tail" is ignored. Furthermore, radiodecay is not considered for material in the region $0 \leq x \leq \ell$. For the radionuclides considered, such as americium-241, ignoring radiodecay does not result in an appreciable error in predicting transport rates as will be shown in the following discussion. Cases where radiodecay must be considered will be noted. A material balance over a differential thickness in a slab when radiodecay is considered yields

$$D_e \frac{\partial^2 c}{\partial x^2} = (\varepsilon + k_d \rho) \frac{\partial c}{\partial t} + \varepsilon \lambda c \tag{3.5.32}$$

Thus

$$\frac{\partial^2 c}{\partial z^2} - bc - \frac{1}{k} \frac{\partial c}{\partial t} = 0 \tag{3.5.33}$$

where $z = x/\ell$ and

$$b = \frac{\ell^2 \lambda \delta}{D} \tag{3.5.34}$$

A solution is available for the case where the radio-diffusion parameter, b, is zero as described by Equations (3.5.1) - (3.5.4) and Equation (3.5.19). The solution to Equation (3.5.33) is (Danckwerts, 1951)

$$c(x,t) = kb \int_0^t e^{-kbt'} c_0(x,t')dt' + e^{-kbt} c_0(x,t) \tag{3.5.35}$$

where $c_0(x,t)$ is the b = 0 solution.

The above equation is valid for boundary conditions of constant concentration or "radiation", but only with a zero initial condition. Applying Equation (3.5.35) to Equation (3.5.19) yields

$$c(x,t) = \sum_{n=1}^{\infty} A_n \left[\cos \alpha_n x + \frac{h_o}{\alpha_n} \sin (\alpha_n x)\right] \cdot \tag{3.5.36}$$

$$\cdot \left[\frac{b + k\alpha_n^2 \exp\left[-(b + k\alpha_n^2)t\right]}{b + k\alpha_n^2}\right]$$

where A_n and α_n are defined in Equations (3.5.21) and (3.5.22).

The above equation is inconvenient to use in examining the effects of radiodecay, and the same problem examined with fixed boundary conditions rather than "radiation" is more instructive.

Solving Equation (3.5.33) with

$$c(o,t) = 0 \tag{3.5.37}$$

$$c(\ell,t) = 1 \tag{3.5.38}$$

$$c(x,o) = 0 \tag{3.5.39}$$

yields

$$c(z,t) = \frac{2}{\pi} \sum_{n=1}^{\infty} \frac{(-1)^n}{n} \sin \lambda_n Z \left[\frac{b + \lambda_n^2 \exp\left[-(b + \lambda_n^2)t\right]}{b + \lambda_n^2}\right] + z \tag{3.5.40}$$

where $\lambda_n = n\pi$.

The steady state solution can be obtained from the above equation for $t = \infty$, but a simpler form is obtained by solving Equation (3.5.33) with $\partial c/\partial t = 0$. Doing this yields

$$c(z) = \frac{\sinh \sqrt{b}\, z}{\sinh \sqrt{b}} \qquad (3.5.41)$$

which gives the same results as Equation (3.5.40) for $t=\infty$. Equation (3.5.41) is presented in Figure 3.10 for various values of the radio-diffusion parameter, b. Figure 3-10 clearly shows that when $b < 1$ the effect of radiodecay on the diffusion transport rate is negligible. In studying the diffusion transport of isotopes such as americium-241 with a decay constant, λ, of 1.5×10^{-3} year^{-1}, $D = 31.5$ cm^2/year and $\delta = 4$,

$$b = 1.9 \times 10^{-4}\, \ell^2 \qquad (3.5.42)$$

with ℓ in centimeters. Hence, in order for b to be <1, ℓ must be 72.5 cm (28 inches) or less. This value of ℓ is considerably larger than any of those used in the case studies presented in this study and therefore is the justification for ignoring radiodecay in the diffusion transport calculations. Ignoring radiodecay results in a conservatively high computed geological release rate at the $z = 0$ boundary.

If shorter-lived radionuclides are of interest, such as cesium-137 with a $\lambda = 0.023$ year^{-1}, then for $b < 1$, ℓ must be 18.5 cm (7.3 inches) or less in order to use the $b = 0$ diffusion transport equations.

The results presented in Figure 3-10 clearly show how the release rate at $z = 0$ is retarded by the effect of residence time in the slab and radiodecay. The ratio of the transport rate at $z = 0$ to that at $z = 1$ is called the retard factor, R_f, and is calculated from

$$R_f = 1/\cosh \sqrt{b} \qquad (3.5.43)$$

Values of R_f are presented in Table 3-6 for various values of the radio-diffusion parameter, b. Also tabulated is the approximate number of times the transport rate at $z = 0$ is halved relative to that at $z = 1$. Hence, for $b = 100$, the transport rate at $z = 0$ is 2^{-13} of that at $z = 1$. In order to have $b = 100$ for americium-241 with $D = 31.5$ cm^2/year and $\delta = 4$, ℓ must be 725 cm or approximately 24 feet.

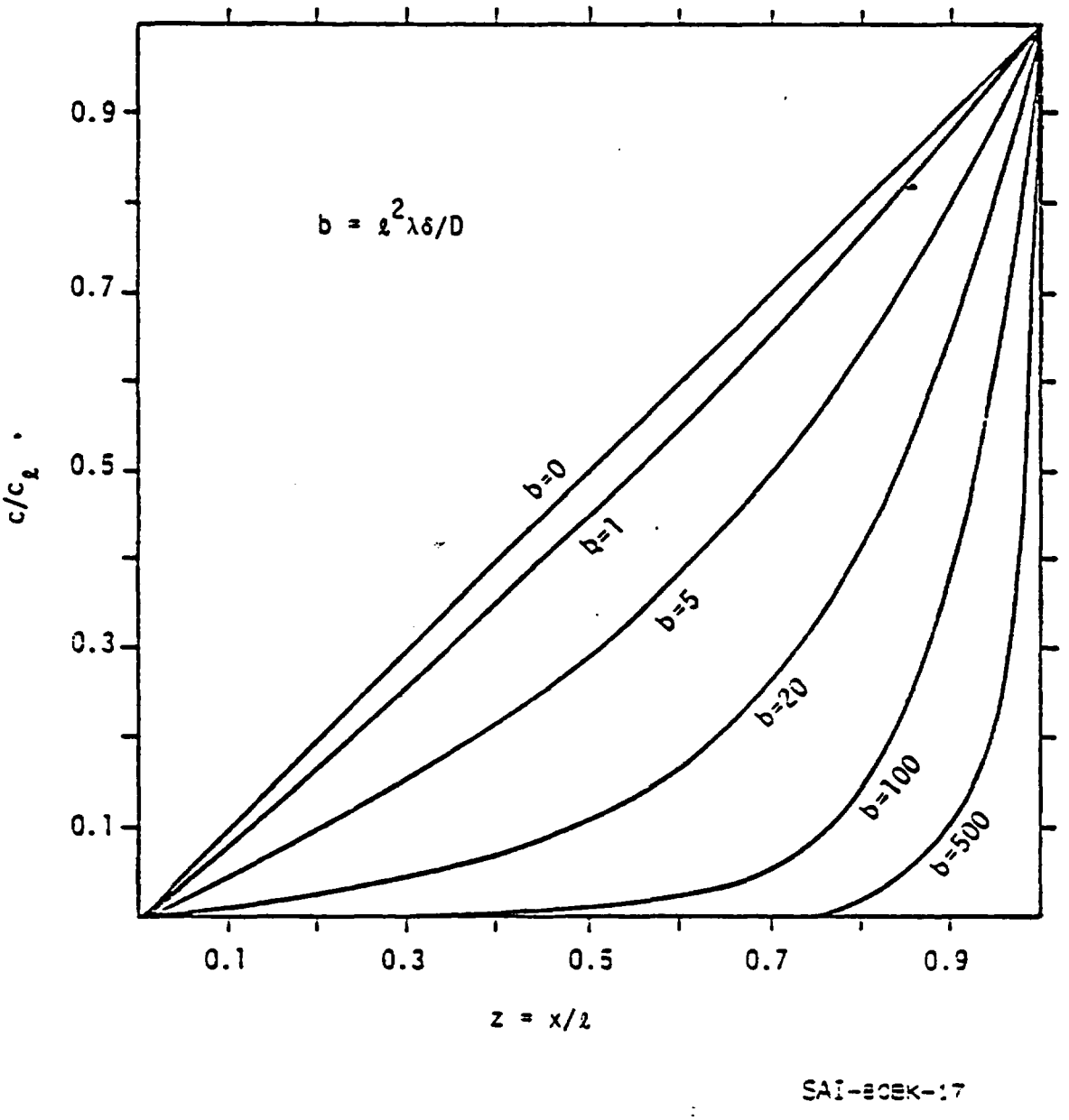

Figure 3-10. Steady State Concentration Profiles in a Slab for Values of the Radio-Diffusion Parameter, b.

Table 3-6. Retardation of the Transport of Radionuclides Through a Slab Barrier at Steady State for Values of the Radio-Diffusion Parameter, b.

Radio-Diffusion Parameter b	Transport Retard Factor R_f	Number of Transport Half-Lives Retarded n
0	1	-
1	0.65	-
5	0.2	2.2
20	0.02	5.4
100	9x10-5	13
500	$4x10^{-10}$	31

The approach to the steady state concentration profiles as a function of the radio-diffusion parameter is described by Equation (3.5.40). Note b always appears with λ_n^2 as $b + \lambda_n^2$. Since $\lambda_n = n\pi$, for large n, $b \ll \lambda_n^2$. For the radionuclides examined in this study b is always $\ll \lambda_1^2$.

In order to justify using Equation (3.5.40), b should be >1 and preferably on the order of 10. The evaluation of the series in Equation (3.5.40) is straightforward with a typical result presented in Figure 3-11 for b = 10. This figure shows that the approach to the steady state concentration profile with respect to time is similar to the results for b = 0, i.e., the high frequency Fourier components decay away very rapidly, and when $\theta > 0.1$, the concentration profile is essentially at steady state.

There are two types of leaching that must be considered when developing a mathematical description for the purpose of obtaining diffusion coefficients from data or for predicting future behavior of leaching systems. The first is the situation where the soluble substance is in solution within the solid matrix at the start of the transport. For a semi-infinite slab containing a dissolved substance in the solution in its pores the defining equations are

$$k_c \frac{\partial^2 c}{\partial x^2} = \frac{\partial c}{\partial t} \qquad 0 < x < \infty \tag{3.5.44}$$

and

$$c(x, 0) = c_0(x) \tag{3.5.45}$$

$$c(0, t) = 0 \tag{3.5.46}$$

$$c(\infty, t) = c_\infty \tag{3.5.47}$$

where

k_c = a constant (mass transfer "conductivity")

In the above case the soluble material is removed as fast as it arrives at the x = 0 face. In the event the solution at the face is not zero or there is an equilibrium condition, the equations are still easily solved.

The second type of leaching is the case where the soluble substance exists in the solid matrix as a solid. The soluble substance must be first dissolved and then diffused out of the solid. Neglecting the transport of

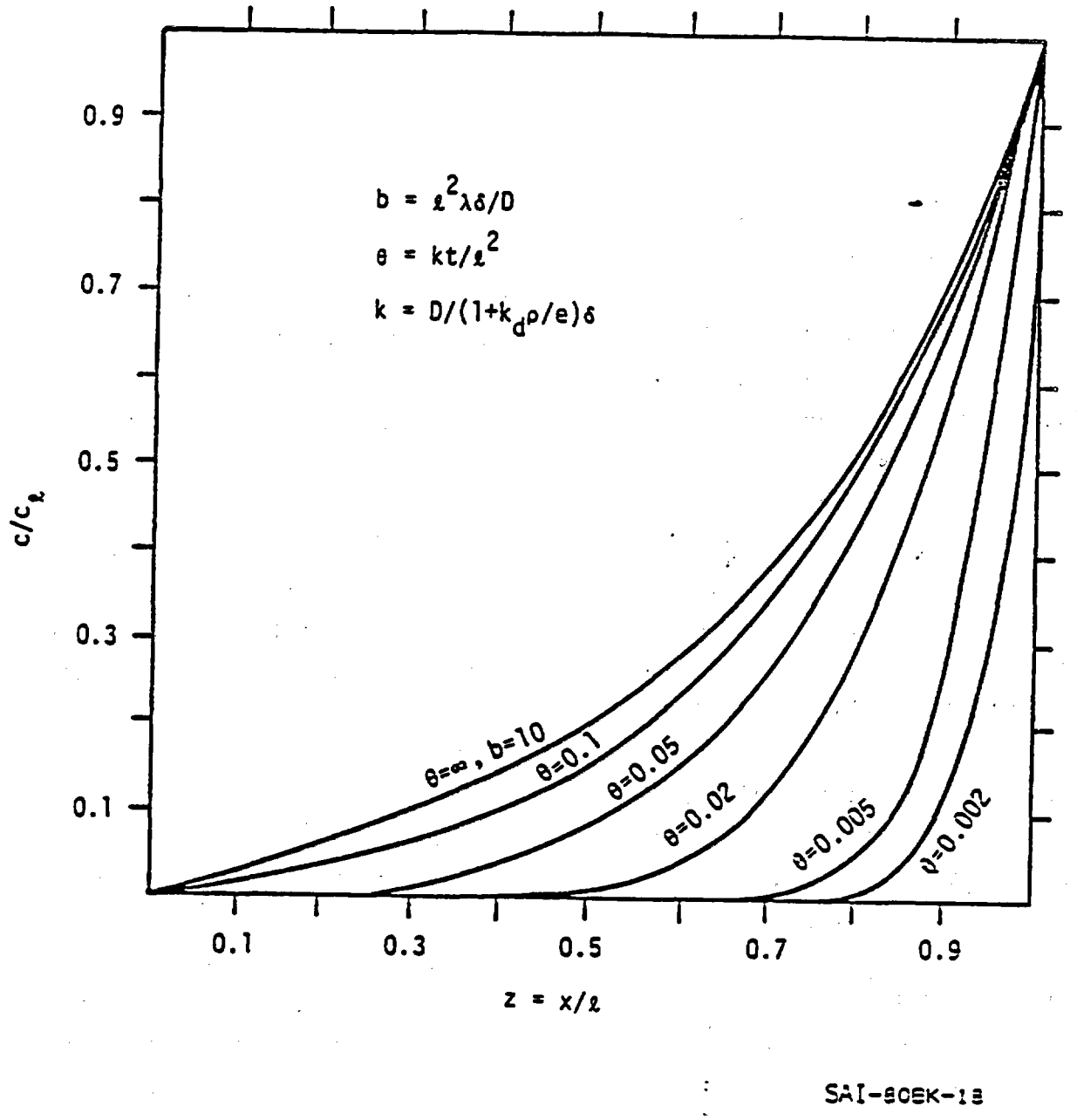

Figure 3-11. Concentration Profiles for the Approach to Steady State in a Slab.

solvent into the matrix, this leads to a condition at the soluble substance-solution interface in the solid that is expressed by

$$D_e \left.\frac{dc}{dx}\right|_{x=z_s} = \rho_s \frac{dz_s}{dt} \quad \text{(at the interface)} \qquad (3.5.48)$$

where z_s is the location of the soluble substance-solution interface and ρ_s is the apparent density of the soluble substance.

The mathematical solution to the latter type of leach problem is similar to the heat transfer problem where a change of state occurs. There are some solutions available for the semi-infinite slab but there appear to be no closed solutions for the important boundary conditions of constant flux. In the case of cylindrical coordinates there is only one simple exact solution for a continuous line source of heat. (Carslaw, 1967).

In examining the available leach data (Katayama, 1976, 1980) for the radionuclides of interest, it is determined that the latter type of leaching is the type occurring. As a result, it was determined that there is not straightforward way to reduce the available data to obtain a diffusivity for the radionuclides of interest. The only practical way the available leach data could be used is to specify a boundary condition either with a flux or a concentration as determined by the available data.

The data are published as a flux based on available spent fuel surface area. Also available in this published data are solution concentrations which were used to obtain the flux data. Therefore, the choice existed to use the data for a flux or a concentration boundary condition. In this study a concentration boundary condition was chosen rather than a flux condition because a flux specification can result in a concentration which is unrealistically large, i.e., the solubility limit is exceeded and unrealistic results can be obtained. The concentration build-up can occur because mass is not transferred away fast enough from the face where the flux is specified. Only after the concentration has increased enough in the immediate vicinity to yield a gradient large enough will the concentration stabilize.

Only one of the published reports (Katayama, 1976) yields sufficient experimental detail to obtain concentration information. These data are used to specify a fixed concentration boundary condition, i.e., not a function of time.

This is in contrast to the published results where the concentration in solution is quite high in the initial experiments. However, the initial effects do not last over very many days of leaching. Since the data are to be used to predict transport rates over hundreds to thousands of years, it is considered justifiable to use a leach concentration that appears more constant after many leaching solution exposures. Also, because of the nature of the adsorption of the backfill in the model, any "front-end" effect in concentration is quickly adsorbed.

It appears that further study of the leaching data, how to use these data to obtain transport coefficients, and the type of model that can use the data is warranted. In examining the leaching data it was found that usually less than one percent of the leachable radionuclides are ever removed from the spent fuel. In this case all the data should be considered as initial phenomena, and extrapolating this information to predict leaching behavior where greater portions are transported is difficult unless the transport process is properly described, i.e., dissolution and diffusion in porous media. Also to be considered is the possibility of adsorption occurring on the UO_2 matrix which would alter the defining mathematics. However, without proper problem definition simple extrapolation of existing data must be used in mathematical models that describe the transport of radionuclides.

In the radionuclide release model the release of radionuclides to the geology is set to zero at the time the inventory of a radionuclide in the canister becomes zero. This is equivalent to deleting the tail-off of the band breakthrough curve as illustrated in Figure 3-12 (shaded area). While it is possible to calculate the tail-off, it is an inordinately time-consuming calculation and is deemed inappropriate for the purposes of the performance model. However, the method of calculation is discussed in this section.

When the inventory of the radionuclide of interest reaches zero in the waste package, the boundary condition at the backfill-can interface is assumed to become insulated. The equations to solve in this case are

$$\frac{\partial c}{\partial t} = k \frac{\partial^2 c}{\partial x^2} \qquad (3.5.49)$$

$$\frac{dc}{dx} - h_o c = 0 \qquad \text{at } x = 0 \qquad (3.5.50)$$

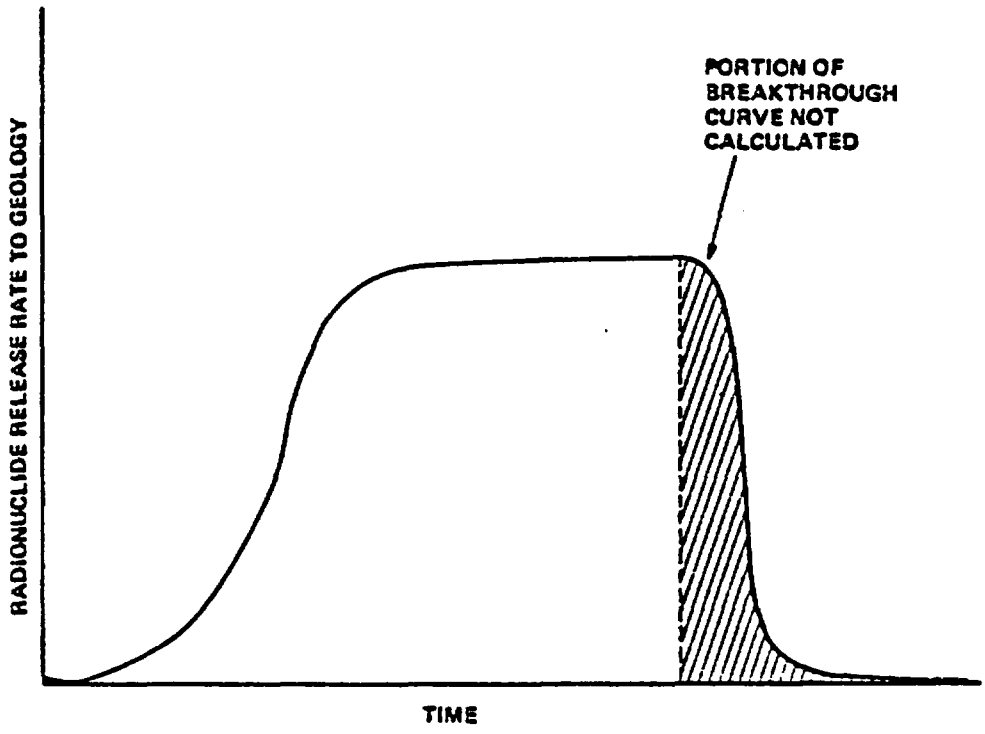

Figure 3-12. Deletion of Breakthrough Tail of Radionuclide Release Rate to Geology.

$$\frac{dc}{dx} = 0 \qquad \text{at } x=\ell \tag{3.5.51}$$

and

$$v(x,0) = f(x) \tag{3.5.52}$$

where f(x) is the concentration profile in the backfill when the zero-inventory condition occurs. Hence, f(x) is Equation (3.5.19) for some value of $t = t_o$. The solution for Equation (3.5.49) is

$$c(x,t) = \sum_{j=1}^{\infty} \left(\frac{2}{\ell(\beta_j^2+h_o^2)+h_o} \right) \exp\left[-k\beta_j^2(t-t_o)\right] \cdot \tag{3.5.53}$$

$$\cdot \left\{ \frac{c_o h_\ell}{1+\ell h_\ell+h_\ell/h_o} \left[\left(\ell + \frac{1}{h_o} + \frac{h_o}{\beta_j^2} \right) \sin \beta_j \ell - \frac{h_o \ell}{\beta_j} \cos \beta_j \ell \right] \right.$$

$$+ \sum_{n=1}^{\infty} \frac{\dfrac{2c_o h_\ell}{1+\ell h_\ell+h_\ell/h_o} \left[\dfrac{h_o \ell}{\alpha_n} \cos \alpha_n \ell - \left(\ell + \dfrac{1}{h_o} + \dfrac{h_o}{\alpha_n^2} \right) \sin \alpha_n \ell \right]}{(\alpha_n^2 + h_o^2)[\ell(\alpha_n^2 + h_\ell^2) + h_\ell] + h_o (\alpha_n^2+h_\ell^2)} \cdot$$

$$\cdot h_\ell (\alpha_n^2 - \beta_j^2) (\alpha_n \cos \alpha_n \ell + h_o \sin \alpha_n \ell) (\beta_j \cos \beta_j \ell + h_o \sin \beta_j \ell) \cdot$$

$$\left. \cdot \exp(-k\alpha_n^2 t_o) \right\} (\beta_j \cos \beta_j x + h_o \sin \beta_j x)$$

where β_j is the n-th positive root of

$$\tan \beta_j \ell = \frac{h_o}{\beta_j} \tag{3.5.54}$$

The above equation does not consider radiodecay and can become slightly more cumbersome if pursued. However, note that Danckwerts' method (Danckwerts, 1951) used previously to examine the effect of radiodecay on diffusion transport is not applicable to Equations (3.5.49) - (3.5.52) because $c(x,o) = 0$.

In order to examine the diffusion transport with radiodecay to the geology from the backfill after inventory depletion, the following equations with a fixed boundary condition at $x = 0$ rather than a "radiation" boundary condition are examined

$$\frac{\partial^2 c}{\partial z^2} - bz - \frac{\partial c}{\partial t} = 0 \tag{3.5.55}$$

$$c(0,t) = 0 \tag{3.5.56}$$

$$\frac{dc}{dz}(1,t) = 0 \tag{3.5.57}$$

$$c(z,0) = f(z) \tag{3.5.58}$$

These equations result in a significantly simpler solution form than the "radiation" case. The solution to the above equations can be obtained by making the substitution

$$c(z,t) = e^{-bt} u(z,t) \tag{3.5.59}$$

which results in the following

$$\frac{\partial^2 u}{\partial t^2} - \frac{\partial u}{\partial t} = 0 \tag{3.5.60}$$

$$u(0,t) = 0 \tag{3.5.61}$$

$$\frac{du}{dt}(1,t) = 0 \tag{3.5.62}$$

and

$$u(z,0) = f(z) \tag{3.5.63}$$

The solution can be obtained by conventional methods, and for the case when steady state is attained in the backfill, f(z) is Equation (3.5.41). The solution is

$$c(z,t) = \frac{2\sqrt{b}\cosh\sqrt{b}}{\sinh\sqrt{b}} \sum_{n=1}^{\infty} \frac{(-1)^{n+1}\sin\lambda_n z}{b+\lambda_n^2} \exp\left[-(b+\lambda_n^2)t\right] \qquad (3.5.64)$$

where $\lambda_n = (2n-1)\,\pi/2$. That the t=0 solution is equal to Equation (3.5.41) can be verified numerically. Also, for b = 0, the solution at t = 0 predicts the concentration profile for the initial condition f(z) = z.

The radio-diffusion parameter, b, appears in Equation (3.5.64) in the same manner as before, i.e., $b + \lambda_n^2$. For the radionuclides studied in this study, $b \ll 1$ which is justification for ignoring b in the calculated results.

The calculated results for the case of b = 10 are presented in Figure 3-13. Note that the concentration profile has essentially attained the $\theta = \infty$ value when $\theta < 0.1$.

In the event the concentration profile has not attained steady state when inventory depletion occurs, the solution form is somewhat more complicated because f(z) in Equation (3.5.58) takes the form of Equation (3.5.40). The solution in this case is

$$c(z,t) = \frac{4}{\pi^2}\sum_{n=1}^{\infty}\left\{\frac{2(-1)^{n+1}}{(2n-1)^2} + (-1)^n \sum_{m=1}^{\infty}\left[\frac{1}{(m-n+1/2)(m+n-1/2)}\right]\right. \cdot \qquad (3.5.65)$$

$$\cdot \left[\frac{b+\lambda_m^2 \exp[-(b+\lambda_m^2)T_o]}{b+\lambda_m^2}\right] \exp\left[-(b+\lambda_n^2)t\right] \cdot$$

$$\left. \cdot \sin\lambda_n z \right\}$$

where $\lambda_m = m\pi$ and T_o is the time at which zero inventory is attained.

Since it appears that essentially zero concentration in the backfill is attained for the dimensionless time $\theta \approx 0.1$, an estimate of "zero" release to the geology can be obtained for the case of americium-241 for a typical backfill.

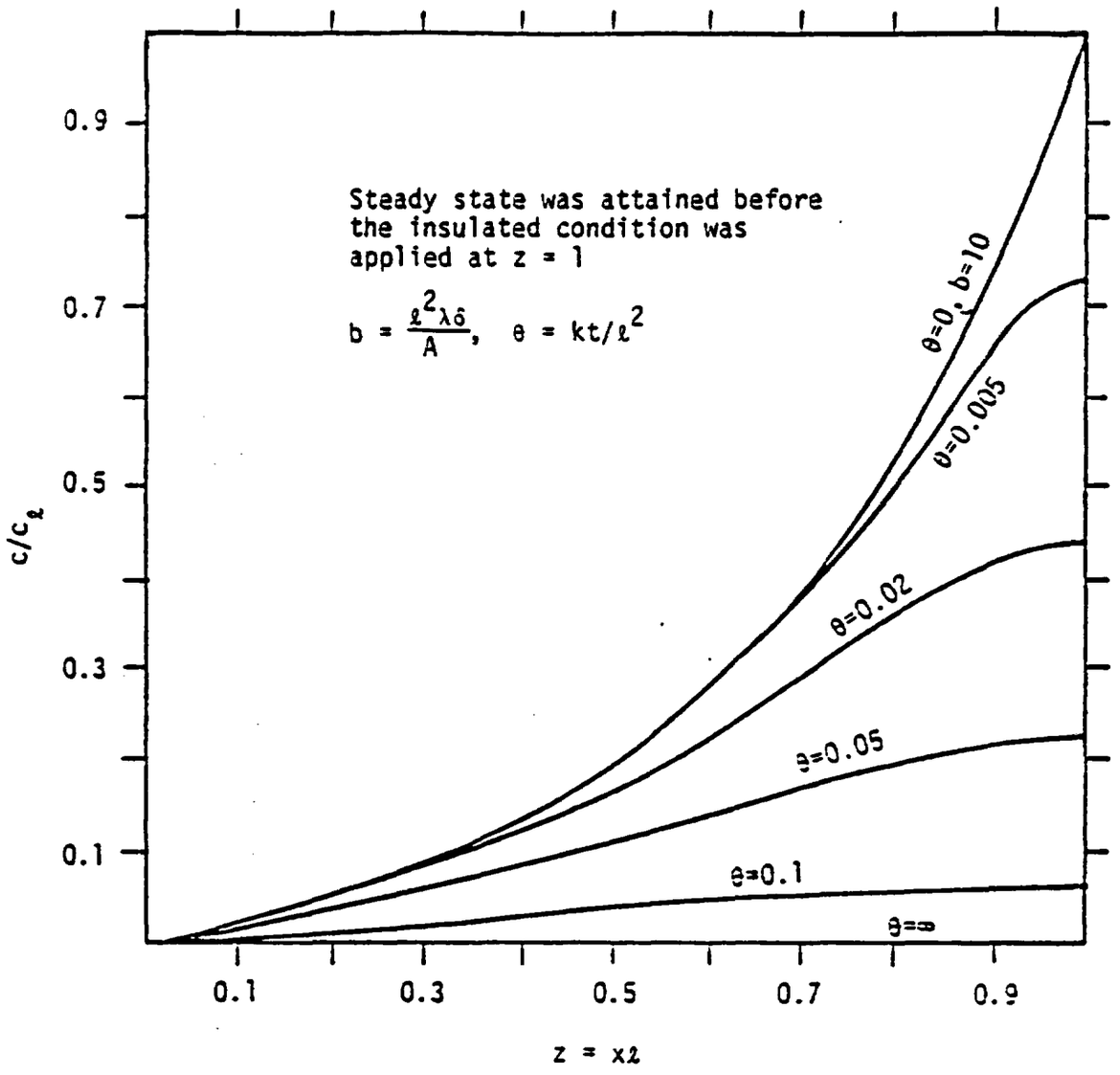

SAI-8CEK-19

Figure 3-13. Concentration Profiles for Zero-Inventory Release to Geology with b = 10.

The parameters used for americium-241 are $k \approx 3.9 \times 10^{-4}$ cm^2/yr and $\ell \approx 30.51$ cm, so that

$$\vartheta \approx 0.1 = kt/\ell^2 \qquad (3.5.66)$$

or $t \approx 2.5 \times 10^5$ years.

A flowchart for the RELEAS subroutine is presented in Figure 3-14. The only input required from the main program are three barrier diameters which are used to calculate h_ℓ as defined in Equation (3.5.2). A listing of RELEAS is provided in Appendix A.

3.6 RADIONUCLIDE RADIATION FIELDS

The objective of the radiation field subroutine RADCLC is to calculate the radiation exposure from gamma rays at the outer surface of each package barrier as a function of time after package emplacement. The radiation source in the model is assumed to be PWR spent fuel with a burnup of 33,000 MWd/MT. The emplacement time is assumed to be 6.5 years after discharge and the burnup is assumed to be constant over 1100 days. The fuel composition assumed (3.3 percent enriched) is given in Table 3-7.

Various materials are chosen for use in the engineered barriers of a package design. Compositions and densities of some of these materials are obtained to estimate the radiation attenuation characteristics. The data for the other materials are estimated or assumed. The following paragraphs identify the compositions used in the radiation analysis.

Bentonite

Bentonite is a naturally occurring clay characterized by the fact that it swells upon absorbing water. The main component is montmorillonite. The chemical composition is

Species	Weight Percent
SiO_2	63.0
Al_2O_3	21.0

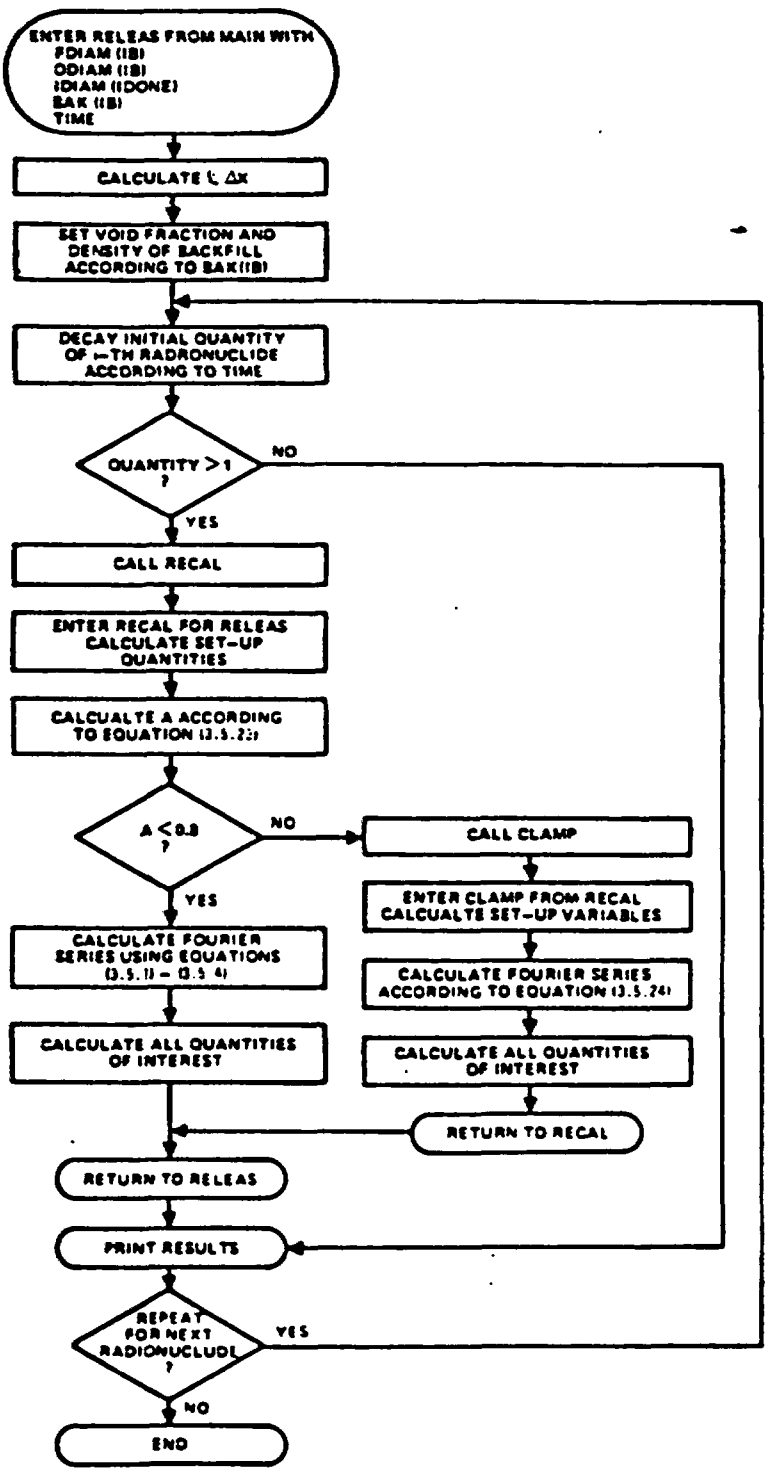

Figure 3-14. RELEAS Flowchart.

Table 3-7. Fuel Composition.

Isotope	Gram-Atoms/MT	Isotope	Gram-Atoms/MT
C^{12}	1.5	Zr^{91}	306.725
Al^{27}	4.0	Zr^{92}	462.239
Si^{28}	.607	Zr^{94}	460.074
Si^{29}	.034	Zr^{96}	72.50
Ti^{46}	.304	Nb^{93}	10.258
Ti^{47}	.277	Mo^{92}	.957
Ti^{48}	2.771	Mo^{94}	.532
Ti^{49}	.204	Mo^{95}	.926
Ti^{50}	.200	Mo^{96}	.958
Cr^{50}	5.040	Mo^{97}	.546
Cr^{52}	57.423	Mo^{98}	1.357
Cr^{53}	6.415	Mo^{100}	.540
Cr^{54}	1.574	Sn^{112}	.321
Mn^{55}	.327	Sn^{114}	.219
Fe^{54}	4.037	Sn^{115}	.113
Fe^{56}	61.018	Sn^{116}	4.681
Fe^{57}	1.439	Sn^{117}	2.470
Fe^{58}	.310	Sn^{118}	7.729
Co^{59}	.915	Sn^{119}	2.739
Ni^{58}	111.862	Sn^{120}	10.392
Ni^{60}	41.783	Sn^{122}	1.467
Ni^{61}	1.869	Sn^{124}	1.823
Ni^{62}	5.645	U^{234}	1.13
Ni^{64}	1.609	U^{235}	140.4
Zr^{90}	1421.122	U^{238}	4062.0

Fe_2O_3	3.2
FeO	0.3
TiO_2	0.1
CaO	0.7
MgO	2.7
Na_2O	2.2
K_2O	0.4
H_2O	5.6
Other	0.8

Density - 2.1 gm/cm^3

Sand

Sand is assumed to be 100 percent SiO_2 with a density of 2.1 gm/cm^3.

Clinoptilolite

Clinoptilolite is assumed to be a clay with a density of 2.2 gm/cm^3.

Mild Steel

Mild steel is assumed to be 100 percent Fe with a density of 7.85 gm/cm^3.

Zircaloy-2

The composition and density used for Zircaloy-2 is

Element	Weight Percent
Zr	98.24
Cr	0.1
Fe	0.21
Sn	1.45

Density - 6.55 gm/cm^3

Inconel-600

The composition and density used for Inconel-600 is

Element	Weight Percent
Ni	75.41
Cr	15.5
C	.08
Si	.25
Fe	8.0
Ca	.25
Mn	.50

Density - 8.43 gm/cm^3

SST-304

The composition and density used for 304 Stainless Steel is

Element	Weight Percent
Fe	68.17
Cr	18.94
Ni	10.51
Mn	1.75
Si	.53
C	.06

Density - 7.93 gm/cm^3

Copper

The density used for copper is 8.92 gm/cm^3.

Lead

The density used for lead is 11.34 gm/cm^3.

Cast Iron

Cast iron is assumed to be 100 percent Fe with a density of 7.85 gm/cm^3.

Helium

The effect of helium as a shielding material is neglected and assumed to be void.

Air

The effect of air as a shielding material is neglected and assumed to be void.

An ORIGEN calculation is performed to obtain the radiation source term for the fuel bundle. In order to confirm that the radiation source term used in the code is consistent with the data in (DOE, 1979), a comparison was made with the radioactivity content and heat generation rate in spent fuel as presented in Table 5.7.2 of that document. This comparison is shown in Table 3-8. With the exception of tritium and C^{14} the calculations in this study agreed with the referenced data. It is concluded that the radiation source term used is consistent with the previous data.

The photon release rate versus time after emplacement is shown in Figure 3-15 for both gamma rays from fission products and from activation products. The photon spectra from fission products and activation products are shown in Figures 3-16 and 3-17, respectively. The photon spectra are shown as photon/sec/MeV normalized to one photon and are shown for one year and 100 years after emplacement. The photon spectra from fission products is seen to be

Table 3-8. Comparison of Radioactivity Content and Heat Generation in Spent Fuel with Prior Data.

	Fission Product Content 6.5 Years after Discharge, Ci	
	Table 5.7.2*	This Work
Fission Product		
H^3	3.1×10^2	5.7×10^{-5}
Kr^{85}	6.5×10^3	6.3×10^3
I^{129}	3.3×10^{-2}	3.3×10^{-2}
$Sr^{90} + Y^{90}$	1.2×10^5	1.3×10^5
$Zr^{95} + Nb^{95}$	3.9×10^{-5}	5.4×10^{-5}
$Ru^{106} + Rh^{106}$	1.1×10^4	1.2×10^4
$Cs^{134} + Cs^{137} + Ba^{137}$	1.8×10^5	2.1×10^5
$Ce^{144} + Pr^{144}$	5.8×10^3	6.7×10^3
Actinide		
Pu^{239}	2.9×10^2	3.2×10^2
Pu^{241}	8.4×10^4	7.7×10^4
$Cm^{242} + Cm^{244}$	1.0×10^3	1.9×10^3
Activation Product		
Fe^{55}	1.0×10^3	3.5×10^2
Co^{60}	2.1×10^3	2.7×10^3
$Zr^{95} + Nb^{95}$	9.0×10^{-7}	9.0×10^{-7}
Heat Generation Rate, W/MTHM	1.4×10^3	1.6×10^3

*Taken from (DOE, 1979)

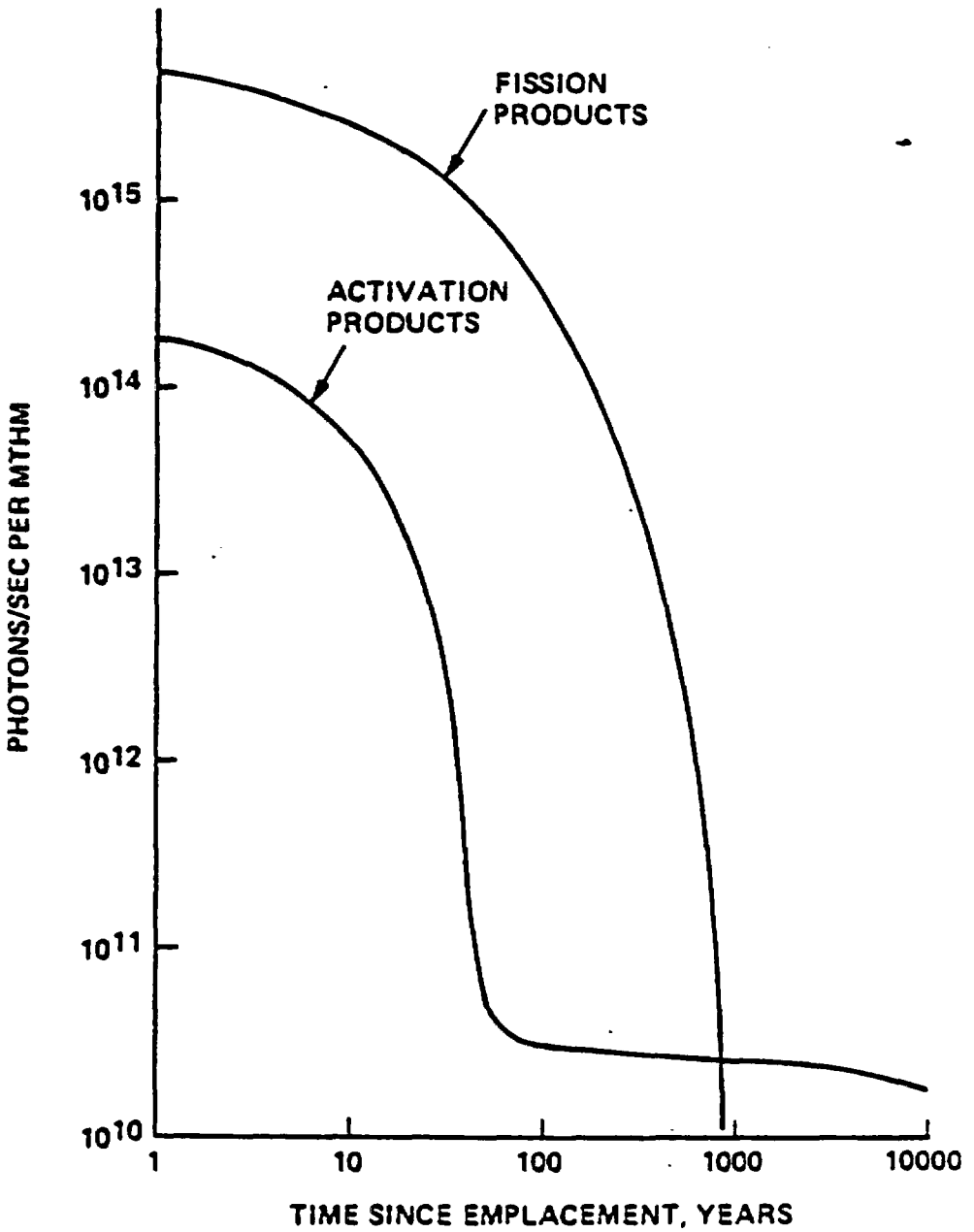

Figure 3-15. Photon Release Rate Vs Time After Emplacement.

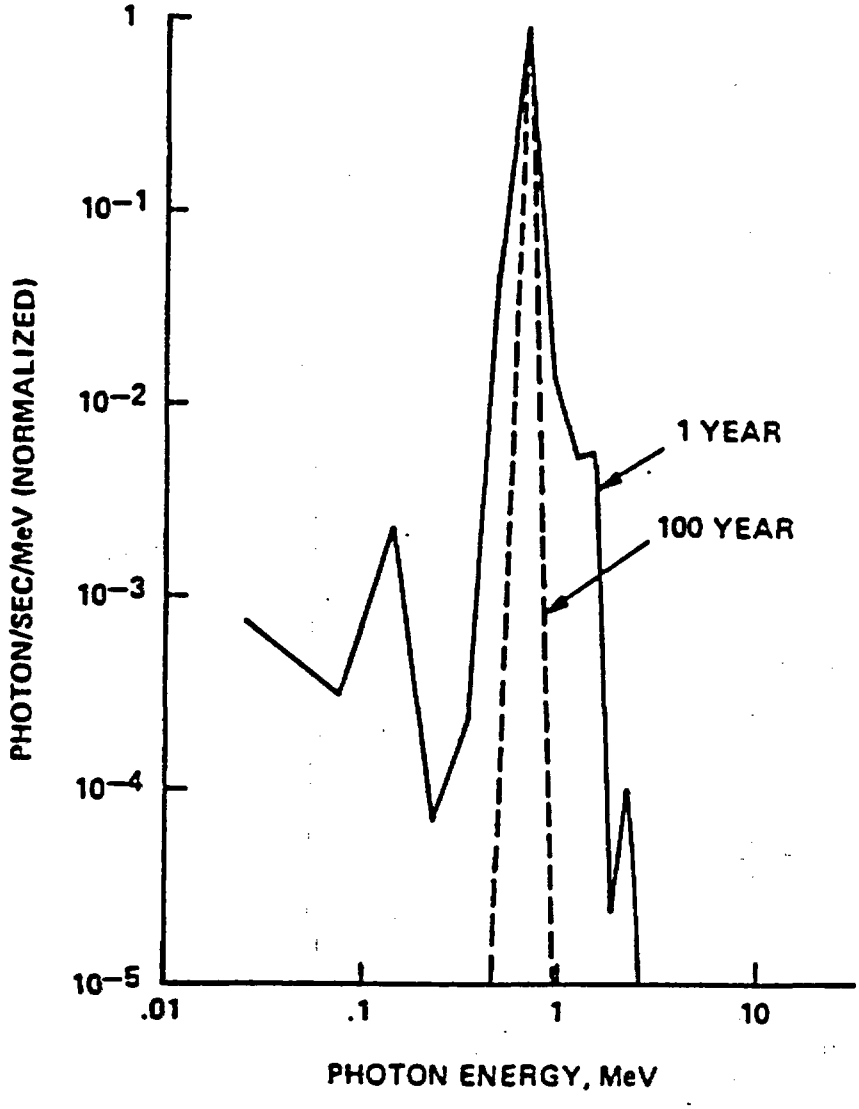

Figure 3-16. Photon Spectrum from Fission Products.

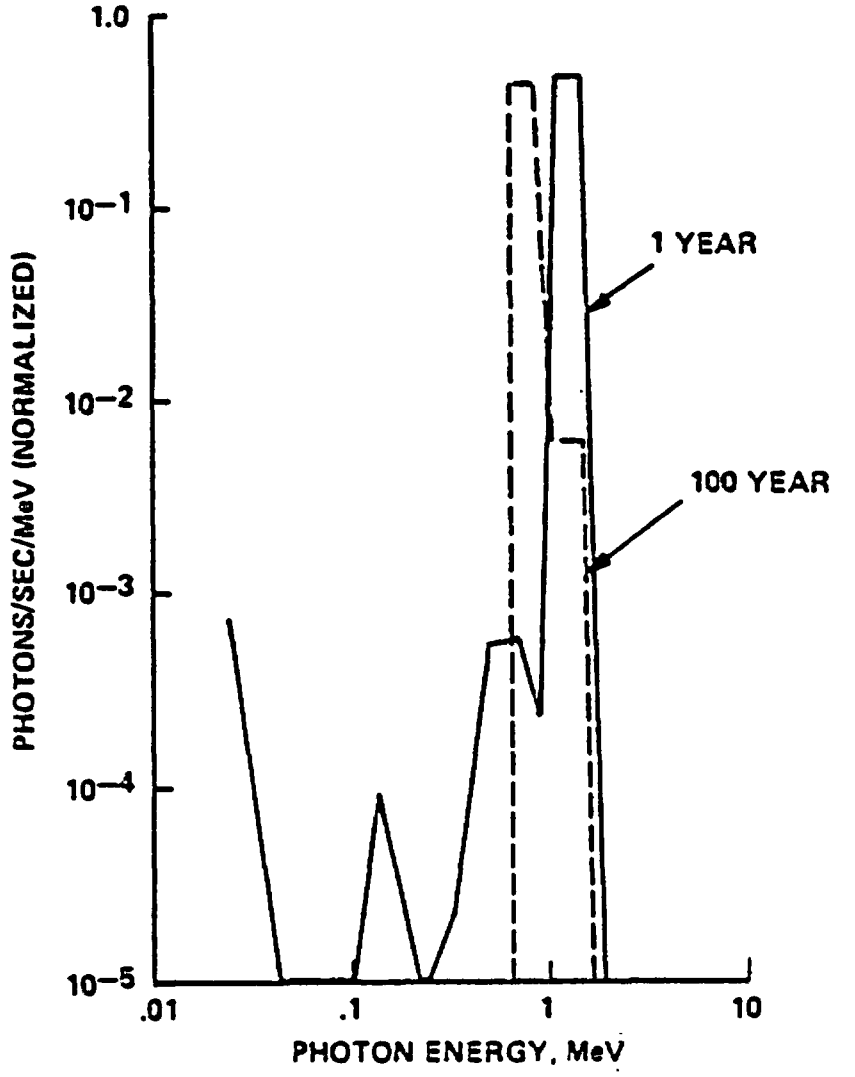

Figure 3-17. Photon Spectrum from Activation Products.

strongly peaked about 0.7 MeV and relatively insensitive to decay time. The spectra for times greater than 100 years are essentially unchanged from 100 years. The photon spectra from activation products shown in Figure 3-17 indicate that there is some time dependence to the spectra. For short times (one to ten years) the spectrum peaks at slightly greater than 1 MeV. However, for time greater than 100 years, the spectrum has softened to about 0.7 MeV. From Figure 3-17, it can be seen that the photons from activation products become important only after about 1000 years and longer. Therefore, the photon spectra for both fission products and activation products are assumed to be about 0.7 MeV since during the time regime that each component is important, the spectra are strongly peaked about 0.7 MeV.

It is fortunate that the photon spectrum is roughly monoenergetic since it allows the use of a monoenergetic cross-section. Table 3-9 lists the linear attenuation coefficient for the materials considered in this study.

The calculation of the gamma ray flux at a particular location in the package employs a simple equation (Rockwell, 1956) for the flux from a cylindrical source

$$\text{Flux} = B \times S_v \times \frac{R_o^2}{a + z} \times F(b_2) \qquad (3.6.1)$$

where

B = buildup factor (dimensionless)

S_v = source intensity, (photons/cm^3/sec)

R_o = radius of the cylinder, (cm)

a = distance to the point of interest from the edge of the cylinder, (cm)

z = self-shielding distance factor, (cm)

b_2 = number of mean free paths to the point of interest, (dimensionless)

F = function defined by

$$F(b_2) = \int_0^{\pi/2} e^{-b_2 \sec\theta} \, d\theta \qquad (3.6.2)$$

Table 3-9. Linear Attenuation Coefficients for Materials

Material	Density, gm/cm^3	Attenuation Coefficient, $\bar{\mu}$, cm^{-1}
Backfill Material		
Bentonite	2.1	.130
Sand & Bentonite	2.1	.140
Clinoptilolite	2.2	.130
Other Materials		
Mild Steel	7.85	.470
Zircaloy-2	6.55	.367
Inconel-600	8.43	.472
SS-304	7.93	.462
Copper	8.92	.500
Lead	11.34	.797
Cast Iron	7.85	.470
Helium	-	8×10^{-5}
Air	-	8×10^{-5}

Buildup data for various materials are available in the form of a parameter fit to the equation (Rockwell, 1956)

$$B(e,b_2) = A_1 e^{-a_1 b_2} + A_2 e^{-a_2 b_2} \qquad (3.6.3)$$

where

A_1, A_2, a_1, and a_2 are a function of energy.

The values for the buildup factor parameters evaluated at 0.7 MeV are shown in Table 3-10. Although buildup factors were not available for all of the specific materials of interest in this work, buildup factors were reasonably approximated by those that were available. Table 3.11 gives the correspondence between the barrier materials and the buildup material used in the analysis.

The RADCLC subroutine was written implementing the procedures described. The output of the subroutine, DOSE, has the units of R/hr.

A flowchart for RADCLC is shown in Figure 3-18 and a program listing is provided in Appendix A.

3.7 WATER REPELLENT BACKFILLS

The model assumes that at time zero the backfill is saturated with water and that water-induced degradation processes proceed from that point. Furthermore, the possible attentuating effects on corrosion of reduced water and/or solute transport through the backfill are not considered. Corrosion is assumed to proceed as if the material is immersed in the water. The action of the backfill to reduce or eliminate water flow to (or from) the package is not considered mainly because there is available no basis on which to evaluate the functional life. This section presents a discussion on the possible effects such a backfill could have on the results of model calculations.

Two modes of backfill behavior would be beneficial in the period prior to package failure

- total exclusion of water from the outer wall of the multiple barrier system for some period of time

Table 3-10. Buildup Factor Parameters at 0.7 MeV.

Material	Parameter Values			
	A_1	A_2	a_1	a_2
Iron	9	-8	-.081	.0255
Lead	2.3	-1.3	-.04	.17
Concrete	10	-9	-.088	.03
Water	11	-10	-.104	.03

Table 3-11. Buildup Factor Material Correspondence.

Material	Buildup Material
Bentonite	Concrete
Sand	Concrete
Clinoptilolite	Concrete
Mild Steel	Iron
Zircaloy-2	Iron
Inconel-600	Iron
SS-304	Iron
Copper	Lead
Lead	Lead
Cast Iron	Iron
Helium	None, B=1
Air	None, B=1

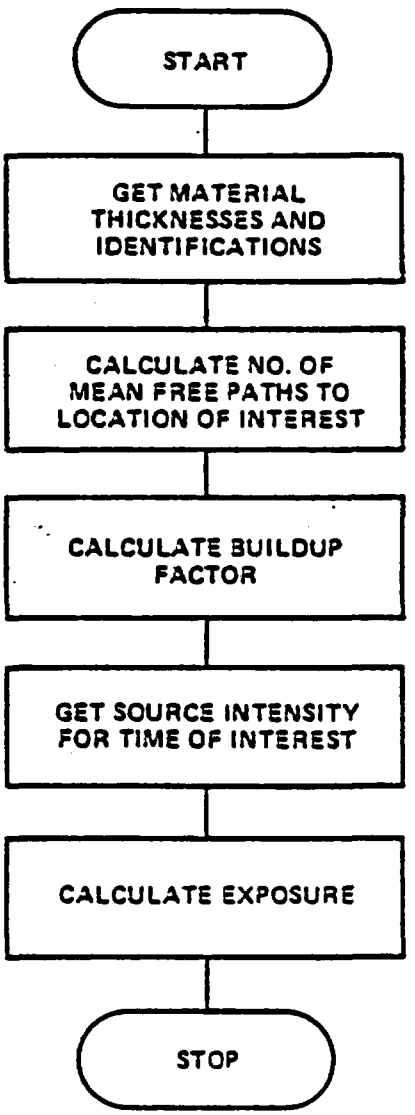

Figure 3-18. RADCLC Flowchart.

- high resistance to water and solute transport through the backfill

Backfills have been proposed which show promise of functioning in these modes. Properly formulated sodium-saturated montmorillonites (bentonites) display enormous swelling pressures when they come in contact with water (Low and Margheim, 1979) (Pusch, 1978a). The effective permeability of such systems becomes essentially zero as characterized in Table 3-12. The swelling phenomenon includes the ability to self-seal and also to seal cracks in the adjacent rock (Pusch, 1978b). Such a material could function as a total exclusion barrier for some time. The key question is how long such a material will retain its properties as a sealant when exposed to repository temperatures, pressures and possibly corrosive water. Evidence on long-term behavior is lacking but predictions based on available data indicate that such materials can be stabilized (for example, use of quartz stabilizes montmorillonite and reduces the tendency for diagenesis to illite) and can last for enormous time periods. In such a case, a pure delay time would be introduced into the results from the BARIER code. This is because there is no mechanism of degradation without water present. The package would last indefinitely in a dry environment as attested to by many ancient artifacts discovered by archeologists in such environments.

The second backfill mode mentioned above pertains to backfills with low permeability. In this case water and solute transport are greatly inhibited over an extended period of time. Studies indicate that degradation rates would be greatly reduced in such cases (Haggblom, 1977). It is likely that corrosion rates used in BARIER were somewnat high and that a reduced corrosion rate would be observed as long as the backfill remained intact. Such effects would require further study if it became desirable to account for them in the performance evaluation.

Note that if a water exclusion backfill is present and its useful life as a barrier is known, then the coating delay feature in BARIER can be used to introduce a delay time before corrosion begins on a particular barrier.

Table 3-12. Permeability of Clays and Sand-Clay Mixtures (Endell, 1938).

	Weight Ratio	Permeability, k_p (cm/min at 65 kg/cm^2)
Quartz sand		1.0×10^{-3}
Quartz sand : mica	9 : 1	4.6×10^{-4}
	7 : 3	4.2×10^{-4}
	1 : 1	5.8×10^{-4}
	0 : 1	4.9×10^{-4}
Quartz sand : kaolin	9 : 1	9.5×10^{-5}
	7 : 3	8.9×10^{-6}
	1 : 1	2.5×10^{-6}
	0 : 1	3.0×10^{-6}
Quartz sand : calcium bentonite	9 : 1	4.3×10^{-5}
	7 : 3	2.1×10^{-6}
	1 : 1	5.5×10^{-7}
	0 : 1	2.0×10^{-7}
Quartz sand : sodium bentonite	9 : 1	1.6×10^{-7}
	7 : 3	3.0×10^{-8}
	1 : 1	impermeable
	0 : 1	impermeable

4. PACKAGE DESIGN DESCRIPTIONS

The package designs evaluated in this study were a subset of a series of designs studied in previous work (Stula, 1980a) (Lester, 1979) with some additional refinements. The designs were restricted to the basic concepts which were described in the SURF program (Westerman, 1979). The philosophy used to choose the design for this study was to pick promising concepts from previous studies which gave a representative spectrum of behavior, complexity and probable cost. Thus, the purposes of the analysis was to provide a basis for programmatic planning and not an optimization of designs or search for the "best" designs.

4.1 PREVIOUS WORK

A large selection of design possibilities was studied in past work using a more simplified version of the "BARIER" code. Four basic SURF program concepts were considered as shown in Figure 4-1 and designated A, B, C, D. An additional concept was studied in which the stabilizer was a cast-in-place solid rather than segmented blocks. This was designated Concept "E". Variation on each of the concepts (i.e., different dimensions and materials) are designated A.1, A.2, or B.1, etc. Table 4-1 is a table of concepts studied in the first series of evaluations in previous work (Lester, 1979) and Table 4-2 is a subsequent series from follow-on studies using the previous version of BARIER (Stula, 1980a).

The results of the past studies yielded a list of concepts which were the best in performance in each of the major concept categories. These concepts and the performance results from the old version of BARIER are summarized in Table 4-3. These concepts were reevaluated in this study using the new version of BARIER and the results are given in this report.

The package designs used in the current study are described in the following sections and summarized in Table 4-4.

4.2 CAST STABILIZERS (Concept E)

The cast stabilizer "E" concept showed promising results in previous work when the geology was a high creep medium (i.e., salt or shale). In effect, the cast stabilizer and the canister act like a solid rod in resisting medium crushing forces. Included in the current group of Concept E cases were concepts E.3, E.4, and E.24, which were analyzed with the old version of BARIER. New variations on this concept in this study were designated with an "N" suffix and included changes in materials and material thickness.

4.3 HEAVY SLEEVE PACKAGES (Concept B1)

Another promising concept from past work was the "B1" design which incorporates a heavy-walled sleeve to line the bore-hole. The sleeve serves as a defense against high crushing forces in a creeping medium. The stabilizer in this design is a segmented solid or a gas filler. The only other barrier element is the canister which contributes very little to long-term defense. Concepts B1.7 and B1.11 were promising designs in the former evaluation using the old version of BARIER. These were reevaluated with the new model. In addition, several variations are introduced as suffix "N" cases such as B1.1N. These package design variations are summarized in Table 4-4.

4.4 COMBINATION SLEEVE/CAST STABILIZERS (Concept BE)

This type of package was a new design analyzed in this study. Designated as "BE" it combines the heavy sleeve and cast stabilizer features. In a creeping medium this package offers a redundant defense against the medium crushing forces. The package design variations studied are summarized in Table 4-4.

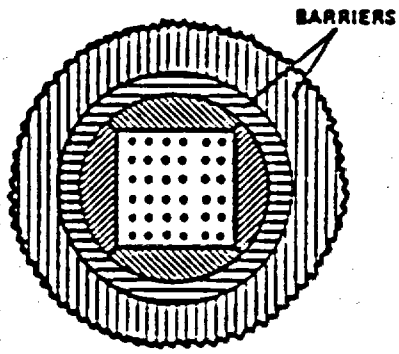

A. CORROSION-RESISTANT METAL CANISTER IN SPECIALLY TAILORED BACKFILL

MAXIMUM NUMBER OF BARRIERS: 2

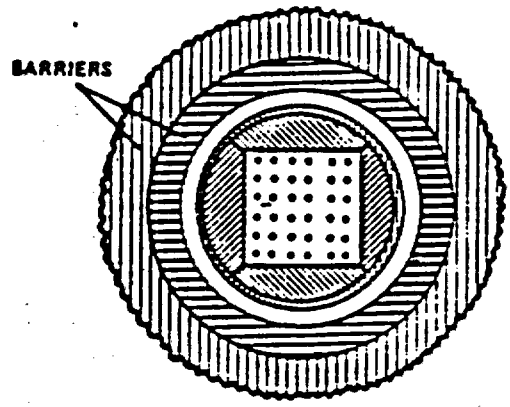

B. MILD STEEL CANISTER WITH CORROSION-RESISTANT OVERPACK OR CORROSION-RESISTANT HOLE SLEEVE, IN SPECIALLY TAILORED BACKFILL

MAXIMUM NUMBER OF BARRIERS: 2

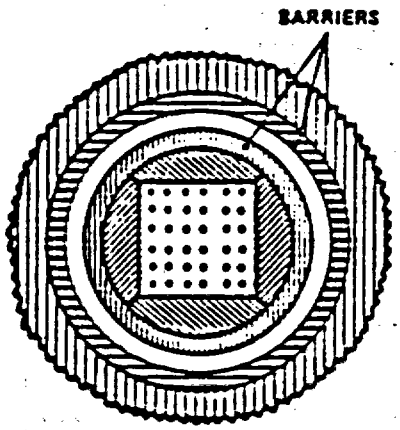

C. CORROSION-RESISTANT CANISTER WITH CORROSION-RESISTANT OVERPACK OR CORROSION-RESISTANT HOLE SLEEVE, IN SPECIALLY TAILORED BACKFILL

MAXIMUM NUMBER OF BARRIERS: 3

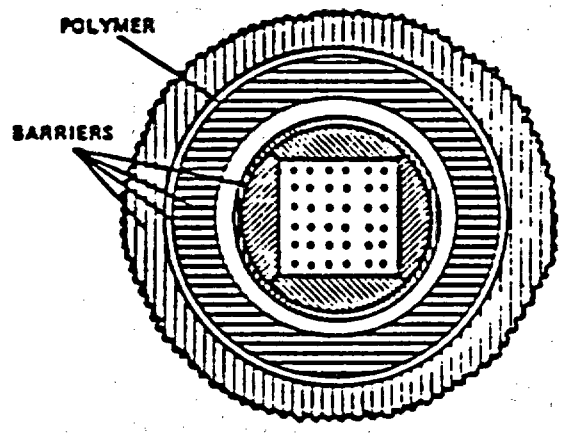

D. MILD STEEL CANISTER IN THICK, CORROSION-RESISTANT BORE SLEEVE WITH SURROUNDING POLYMER LAYER IN SPECIALLY TAILORED BACKFILL

MAXIMUM NUMBER OF BARRIERS: 3
WITH CORROSION-RESISTANT CANISTER: 4

Figure 4-1. Barrier System Conceptual Designs from SURF/SFHP Program.

Table 4-1. Summary of Concepts Studied in FY'79 with Previous Version of "BARIER" Code. (Lester, 1979).

Concept	Element	Inside Material		Outside Material		Filler	Inside Material	Outside Material	Coating Delay (yrs)	Filler
		ID	OD	ID	OD	OD				
A.1	stab	12.0	13.5	13.5	13.5	13.5	304sst	304sst	0.0	none
	can	13.5	14.0	14.0	14.0	40.0	304sst	304sst	0.0	sand-b
A.2	stab	12.0	13.5	13.5	13.5	13.5	304sst	304sst	0.0	none
	can	13.5	15.5	15.5	15.5	40.0	304sst	304sst	0.0	sand-b
A.3	stab	12.0	13.5	13.5	13.5	13.5	304sst	304sst	0.0	none
	can	13.5	14.0	14.0	14.0	20.0	304sst	304sst	0.0	sand-b
A.4	stab	12.0	13.5	13.5	13.5	13.5	304sst	304sst	0.0	none
	can	13.5	15.5	15.5	15.5	20.0	304sst	304sst	0.0	sand-b
A.5	stab	12.0	13.5	13.5	13.5	13.5	helium	helium	0.0	none
	can	13.5	14.0	14.0	14.0	40.0	304sst	304sst	0.0	sand-b
A.6	stab	12.0	13.5	13.5	13.5	13.5	helium	helium	0.0	none
	can	13.5	15.5	15.5	15.5	40.0	304sst	304sst	0.0	sand-b
A.7	stab	12.0	13.5	13.5	13.5	13.5	helium	helium	0.0	none
	can	13.5	14.0	14.0	14.0	20.0	304sst	304sst	0.0	sand-b
A.8	stab	12.0	13.5	13.5	13.5	13.5	helium	helium	0.0	none
	can	13.5	14.0	14.0	14.0	40.0	304sst	304sst	0.0	clino
A.9	stab	12.0	13.5	13.5	13.5	13.5	zirc	zirc	0.0	none
	can	13.5	14.0	14.0	14.0	20.0	zirc	zirc	0.0	sand-b
A.10	stab	12.0	13.5	13.5	13.5	13.5	zirc	zirc	0.0	none
	can	13.5	15.5	15.5	15.5	20.0	zirc	zirc	0.0	sand-b

Note: Unless otherwise noted, all dimensions are in inches.

Table 4-1. (Continued)

Concept	Element	Inside Material		Outside Material		Filler	Inside Material	Outside Material	Coating Delay (yrs)	Filler
		ID	OD	ID	OD	OD				
B.1	stab	12.0	13.5	13.5	13.5	13.5	steel	steel	0.0	none
	can	13.5	14.0	14.0	14.0	14.5	steel	steel	0.0	sand-b
	o pack	14.5	15.0	15.0	15.0	40.0	304sst	304sst	0.0	sand-b
B.2	stab	12.0	13.5	13.5	13.5	13.5	steel	steel	0.0	none
	can	13.5	14.0	14.0	14.0	14.5	steel	steel	0.0	sand-b
	o pack	14.5	16.5	16.5	16.5	40.0	304sst	304sst	0.0	sand-b
B.3	stab	12.0	13.5	13.5	13.5	13.5	steel	steel	0.0	none
	can	13.5	14.0	14.0	14.0	14.5	steel	steel	0.0	sand-b
	o pack	14.5	15.0	15.0	15.0	20.0	304sst	304sst	0.0	sand-b
B.4	stab	12.0	13.5	13.5	13.5	13.5	steel	steel	0.0	none
	can	13.5	14.0	14.0	14.0	14.5	steel	steel	0.0	sand-b
	o pack	14.5	16.5	16.5	16.5	20.0	304sst	304sst	0.0	sand-b
B.5	stab	12.0	13.5	13.5	13.5	13.5	steel	steel	0.0	none
	can	13.5	14.0	14.0	14.0	14.5	steel	steel	0.0	sand-b
	o pack	14.5	15.0	15.0	15.0	20.0	304sst	304sst	0.0	clino
B.6	stab	12.0	13.5	13.5	13.5	13.5	steel	steel	0.0	none
	can	13.5	14.0	14.0	14.0	14.5	steel	steel	0.0	sand-b
	o pack	14.5	16.5	16.5	16.5	20.0	304sst	304sst	0.0	clino
B.7	stab	12.0	13.5	13.5	13.5	13.5	steel	steel	0.0	none
	can	13.5	14.0	14.0	14.0	14.5	steel	steel	0.0	sand-b
	o pack	14.5	15.0	15.0	15.0	20.0	zirc	zirc	0.0	sand-b
B.8	stab	12.0	13.5	13.5	13.5	13.5	steel	steel	0.0	none
	can	13.5	14.0	14.0	14.0	14.5	steel	steel	0.0	sand-b
	o pack	14.5	16.5	16.5	16.5	20.0	zirc	zirc	0.0	sand-b
B.9	stab	12.0	13.5	13.5	13.5	13.5	steel	steel	0.0	none
	can	13.5	14.0	14.0	14.0	14.5	steel	steel	0.0	sand-b
	o pack	14.5	15.0	15.0	15.0	20.0	copper	copper	0.0	sand-b

Table 4-1. (Continued)

Concept	Element	Inside Material		Outside Material		Filler	Inside Material	Outside Material	Coating Delay (yrs)	Filler
		ID	OD	ID	OD	OD				
B.10	stab	12.0	13.5	13.5	13.5	13.5	steel	steel	0.0	none
	can	13.5	14.0	14.0	14.0	14.5	steel	steel	0.0	sand-b
	o pack	14.5	16.5	16.5	16.5	20.0	copper	copper	0.0	sand-b
B.11	stab	12.0	13.5	13.5	13.5	13.5	steel	steel	0.0	none
	can	13.5	14.0	14.0	14.0	14.5	steel	steel	0.0	sand-b
	o pack	14.5	15.0	15.0	15.0	40.0	copper	copper	0.0	sand-b
B.12	stab	12.0	13.5	13.5	13.5	13.5	steel	steel	0.0	none
	can	13.5	14.0	14.0	14.0	14.5	steel	steel	0.0	sand-b
	o pack	14.5	16.5	16.5	16.5	40.0	copper	copper	0.0	sand-b
B.13	stab	12.0	13.5	13.5	13.5	13.5	steel	steel	0.0	none
	can	13.5	14.0	14.0	14.0	14.5	steel	steel	0.0	sand-b
	o pack	14.5	15.0	15.0	19.0	40.0	steel	lead	0.0	sand-b
B.14	stab	12.0	13.5	13.5	13.5	13.5	steel	steel	0.0	none
	can	13.5	14.0	14.0	14.0	14.5	steel	steel	0.0	sand-b
	o pack	14.5	15.0	15.0	27.0	40.0	steel	lead	0.0	sand-b
B.15	stab	12.0	13.5	13.5	13.5	13.5	helium	helium	0.0	none
	can	13.5	14.0	14.0	14.0	14.5	steel	steel	0.0	sand-b
	o pack	14.5	15.0	15.0	27.0	40.0	steel	lead	0.0	sand-b
B1.1	stab	12.0	13.5	13.5	13.5	13.5	steel	steel	0.0	none
	can	13.5	14.0	14.0	14.0	14.5	steel	steel	0.0	sand-b
	sleeve	14.5	21.5	21.5	21.5	48.0	iron	iron	0.0	sand-b
B1.2	stab	12.0	13.5	13.5	13.5	13.5	steel	steel	0.0	none
	can	13.5	14.0	14.0	14.0	14.5	steel	steel	0.0	sand-b
	sleeve	14.5	21.5	21.5	21.5	30.0	iron	iron	0.0	sand-b
B1.3	stab	12.0	13.5	13.5	13.5	13.5	helium	helium	0.0	none
	can	13.5	14.0	14.0	14.0	14.5	steel	steel	0.0	sand-b
	sleeve	14.5	21.5	21.5	21.5	48.0	iron	iron	0.0	sand-b

Table 4-1. (Continued)

Concept	Element	Inside Material		Outside Material		Filler	Inside Material	Outside Material	Coating Delay (yrs)	Filler
		ID	OD	ID	OD	OD				
B1.4	stab	12.0	13.5	13.5	13.5	13.5	air	air	0.0	none
	can	13.5	14.0	14.0	14.0	14.5	steel	steel	0.0	sand-b
	sleeve	14.5	21.5	21.5	21.5	48.0	iron	iron	0.0	sand-b
B1.5	stab	12.0	13.5	13.5	13.5	13.5	steel	steel	0.0	none
	can	13.5	14.0	14.0	14.0	14.5	steel	steel	0.0	sand-b
	sleeve	14.5	15.0	15.0	15.0	40.0	304sst	304sst	0.0	sand-b
B1.6	stab	12.0	13.5	13.5	13.5	13.5	steel	steel	0.0	none
	can	13.5	14.0	14.0	14.0	14.5	steel	steel	0.0	sand-b
	sleeve	14.5	15.0	15.0	15.0	20.0	304sst	304sst	0.0	sand-b
B1.7	stab	12.0	13.5	13.5	13.5	13.5	steel	steel	0.0	none
	can	13.5	14.0	14.0	14.0	14.5	steel	steel	0.0	sand-b
	sleeve	14.5	15.0	15.0	23.0	30.0	steel	lead	0.0	clino
B1.8	stab	12.0	13.5	13.5	13.5	13.5	helium	helium	0.0	none
	can	13.5	14.0	14.0	14.0	14.5	steel	steel	0.0	sand-b
	sleeve	14.5	15.0	15.0	15.0	20.0	304sst	304sst	0.0	clino
B1.9	stab	12.0	13.5	13.5	13.5	13.5	steel	steel	0.0	none
	can	13.5	14.0	14.0	14.0	14.5	steel	steel	0.0	sand-b
	sleeve	14.5	21.5	21.5	21.5	48.0	iron	zirc	0.0	sand-b
B1.10	stab	12.0	13.5	13.5	13.5	13.5	steel	steel	0.0	none
	can	13.5	13.8	13.8	13.8	15.0	steel	steel	0.0	none
	sleeve	15.0	22.0	22.0	22.1	48.0	iron	zirc	0.0	sand-b
B1.11	stab	12.0	13.5	13.5	13.5	13.5	steel	steel	0.0	none
	can	13.5	14.0	14.0	14.0	14.5	steel	steel	0.0	sand-b
	sleeve	14.5	22.5	22.5	22.7	48.0	iron	zirc	0.0	sand-b
C.1	stab	12.0	13.5	13.5	13.5	13.5	304sst	304sst	0.0	none
	can	13.5	14.0	14.0	14.0	14.5	304sst	304sst	0.0	sand-b
	o pack	14.5	15.0	15.0	15.0	40.0	304sst	304sst	0.0	sand-b

Table 4-1. (Continued)

Concept	Element	Inside Material		Outside Material		Filler	Inside Material	Outside Material	Coating Delay (yrs)	Filler
		ID	OD	ID	OD	OD				
C.2	stab	12.0	13.5	13.5	13.5	13.5	304sst	304sst	0.0	none
	can	13.5	15.5	15.5	15.5	16.0	304sst	304sst	0.0	sand-b
	o pack	16.0	18.0	18.0	18.0	40.0	304sst	304sst	0.0	sand-b
C.3	stab	12.0	13.5	13.5	13.5	13.5	304sst	304sst	0.0	none
	can	13.5	15.5	15.5	15.5	16.0	304sst	304sst	0.0	sand-b
	o pack	16.0	18.0	18.0	18.0	20.0	304sst	304sst	0.0	sand-b
C.4	stab	12.0	13.5	13.5	13.5	13.5	zirc	zirc	0.0	none
	can	13.5	14.0	14.0	14.0	14.5	zirc	zirc	0.0	sand-b
	o pack	14.5	15.0	15.0	15.0	20.0	zirc	zirc	0.0	sand-b
C.5	stab	12.0	13.5	13.5	13.5	13.5	zirc	zirc	0.0	none
	can	13.5	15.5	15.5	15.5	16.0	zirc	zirc	0.0	sand-b
	o pack	16.0	18.0	18.0	18.0	20.0	zirc	zirc	0.0	sand-b
C.6	stab	12.0	13.5	13.5	13.5	13.5	304sst	304sst	0.0	none
	can	13.5	15.5	15.5	15.5	16.0	304sst	304sst	0.0	sand-b
	o pack	16.0	16.5	16.5	24.5	30.0	304sst	lead	0.0	sand-b
C.7	stab	12.0	13.5	13.5	13.5	13.5	helium	helium	0.0	none
	can	13.5	15.5	15.5	15.5	16.0	zirc	zirc	0.0	sand-b
	o pack	16.0	18.0	18.0	18.0	40.0	zirc	zirc	0.0	sand-b
C1.1	stab	12.0	13.5	13.5	13.5	13.5	inconel	inconel	0.0	none
	can	13.5	14.0	14.0	14.0	14.5	inconel	inconel	0.0	sand-b
	o pack	14.5	15.0	15.0	15.0	15.5	304sst	304sst	0.0	sand-b
	sleeve	15.5	22.5	22.5	22.5	45.0	iron	iron	0.0	sand-b
C1.2	stab	12.0	13.5	13.5	13.5	13.5	inconel	inconel	0.0	none
	can	13.5	14.0	14.0	14.0	14.5	inconel	inconel	0.0	sand-b
	o pack	14.5	15.0	15.0	15.0	15.5	304sst	304sst	0.0	sand-b
	sleeve	15.5	22.5	22.5	22.5	30.0	iron	iron	0.0	sand-b
C1.3	stab	12.0	13.5	13.5	13.5	13.5	helium	helium	0.0	none

Table 4-1. (Continued)

Concept	Element	Inside Material		Outside Material		Filler	Inside Material	Outside Material	Coating Delay (yrs)	Filler
		ID	OD	ID	OD	OD				
C1.3	can	13.5	14.0	14.0	14.0	14.5	inconel	inconel	0.0	sand-b
	o pack	14.5	15.0	15.0	15.0	15.5	304sst	304sst	0.0	sand-b
	sleeve	15.5	22.5	22.5	22.5	45.0	iron	iron	0.0	sand-b
C1.4	stab	12.0	13.5	13.5	13.5	13.5	304sst	304sst	0.0	none
	can	13.5	14.0	14.0	14.0	14.5	304sst	304sst	0.0	sand-b
	o pack	14.5	15.0	15.0	15.0	15.5	304sst	304sst	0.0	sand-b
	sleeve	15.5	16.5	16.5	16.5	40.0	steel	steel	0.0	sand-b
C1.5	stab	12.0	13.5	13.5	13.5	13.5	304sst	304sst	0.0	none
	can	13.5	14.0	14.0	14.0	14.5	304sst	304sst	0.0	sand-b
	o pack	14.5	15.0	15.0	15.0	15.5	304sst	304sst	0.0	sand-b
	sleeve	15.5	16.5	16.5	16.5	24.0	steel	steel	0.0	sand-b
C1.6	stab	12.0	13.5	13.5	13.5	13.5	zirc	zirc	0.0	none
	can	13.5	14.0	14.0	14.0	14.5	zirc	zirc	0.0	sand-b
	o pack	14.5	15.0	15.0	15.0	15.5	zirc	zirc	0.0	sand-b
	sleeve	15.5	16.5	16.5	16.5	24.0	steel	steel	0.0	sand-b
D.1	stab	12.0	13.5	13.5	13.5	13.5	helium	helium	0.0	none
	can	13.5	14.0	14.0	14.0	14.5	steel	steel	0.0	sand-b
	sleeve	14.5	21.5	21.5	21.5	48.0	iron	iron	10.0	sand-b
D.2	stab	12.0	13.5	13.5	13.5	13.5	steel	steel	0.0	none
	can	13.5	14.0	14.0	14.0	14.5	steel	steel	0.0	sand-b
	sleeve	14.5	21.5	21.5	21.5	48.0	iron	iron	10.0	sand-b
D.3	stab	12.0	13.5	13.5	13.5	13.5	steel	steel	0.0	none
	can	13.5	14.0	14.0	14.0	14.5	steel	steel	0.0	sand-b
	sleeve	14.5	21.5	21.5	21.5	48.0	iron	iron	100.0	sand-b
D.4	stab	12.0	13.5	13.5	13.5	13.5	steel	steel	0.0	none
	can	13.5	14.0	14.0	14.0	14.5	steel	steel	0.0	sand-b
	sleeve	14.5	16.5	16.5	16.5	24.0	zirc	zirc	100.0	sand-b

Table 4-1. (Continued)

Concept	Element	Inside Material		Outside Material		Filler	Inside Material	Outside Material	Coating Delay (yrs)	Filler
		ID	OD	ID	OD	OD				
D.5	stab	12.0	13.5	13.5	13.5	13.5	steel	steel	0.0	none
	can	13.5	14.0	14.0	14.0	14.5	steel	steel	0.0	sand-b
	sleeve	14.5	16.5	16.5	16.5	48.0	zirc	zirc	100.0	sand-b
D1.1	stab	12.0	13.5	13.5	13.5	13.5	304sst	304sst	0.0	none
	can	13.5	14.0	14.0	14.0	14.5	304sst	304sst	0.0	sand-b
	sleeve	14.5	22.5	22.5	22.5	48.0	304sst	304sst	10.0	sand-b
D1.2	stab	12.0	13.5	13.5	13.5	13.5	304sst	304sst	0.0	none
	can	13.5	14.0	14.0	14.0	14.5	304sst	304sst	0.0	sand-b
	sleeve	14.5	22.5	22.5	22.5	48.0	iron	iron	100.0	sand-b
D1.3	stab	12.0	13.5	13.5	13.5	13.5	helium	helium	0.0	none
	can	13.5	14.0	14.0	14.0	14.5	304sst	304sst	0.0	sand-b
	sleeve	14.5	22.5	22.5	22.5	48.0	iron	iron	100.0	sand-b
D1.4	stab	12.0	13.5	13.5	13.5	13.5	zirc	zirc	0.0	none
	can	13.5	14.0	14.0	14.0	14.5	zirc	zirc	0.0	sand-b
	sleeve	14.5	22.5	22.5	22.5	48.0	zirc	zirc	100.0	sand-b
D1.5	stab	12.0	13.5	13.5	13.5	13.5	304sst	304sst	0.0	none
	can	13.5	14.0	14.0	14.0	14.5	304sst	304sst	0.0	sand-b
	sleeve	14.5	15.0	15.0	15.0	20.0	304sst	304sst	100.0	sand-b
D2.1	stab	12.0	13.5	13.5	13.5	13.5	inconel	inconel	0.0	none
	can	13.5	14.0	14.0	14.0	14.5	inconel	inconel	0.0	sand-b
	o pack	14.5	15.0	15.0	15.0	15.5	inconel	inconel	0.0	sand-b
	sleeve	15.5	23.5	23.5	23.5	48.0	iron	iron	100.0	sand-b
D2.2	stab	12.0	13.5	13.5	13.5	13.5	inconel	inconel	0.0	none
	can	13.5	14.0	14.0	14.0	14.5	inconel	inconel	0.0	sand-b
	o pack	14.5	15.0	15.0	15.0	15.5	inconel	inconel	0.0	sand-b
	sleeve	15.5	23.5	23.5	23.5	30.0	iron	iron	100.0	sand-b
D2.3	stab	12.0	13.5	13.5	13.5	13.5	304sst	304sst	0.0	none

Table 4-1. (Continued)

Concept	Element	Inside Material		Outside Material		Filler	Inside Material	Outside Material	Coating Delay (yrs)	Filler
		ID	OD	ID	OD	OD				
D2.3	can	13.5	14.0	14.0	14.0	14.5	304sst	304sst	0.0	sand-b
	o pack	14.5	15.0	15.0	15.0	15.5	304sst	304sst	0.0	sand-b
	sleeve	15.5	23.5	23.5	23.5	30.0	iron	iron	100.0	sand-b
D2.4	stab	12.0	13.5	13.6	13.5	13.5	helium	helium	0.0	none
	can	13.5	14.0	14.0	14.0	14.5	304sst	304sst	0.0	sand-b
	o pack	14.5	15.0	15.0	15.0	15.5	304sst	304sst	0.0	sand-b
	sleeve	15.5	16.0	16.0	16.0	48.0	304sst	304sst	100.0	clino
D2.5	stab	12.0	13.5	13.5	13.5	13.5	helium	helium	0.0	none
	can	13.5	14.0	14.0	14.0	14.5	304sst	304sst	0.0	sand-b
	o pack	14.5	15.0	15.0	23.0	23.5	304sst	lead	0.0	sand-b
	sleeve	23.5	24.0	24.0	24.0	48.0	304sst	304sst	100.0	clino
D2.6	stab	12.0	13.5	13.5	13.5	13.5	helium	helium	0.0	none
	can	13.5	14.0	14.0	14.0	14.5	304sst	304sst	0.0	sand-b
	o pack	14.5	15.0	15.0	27.0	27.5	304sst	lead	0.0	sand-b
	sleeve	27.5	28.0	28.0	28.0	48.0	304sst	304sst	100.0	clino
D2.7	stab	12.0	13.5	13.5	13.5	13.5	304sst	304sst	0.0	none
	can	13.5	14.0	14.0	14.0	14.5	304sst	304sst	0.0	sand-b
	o pack	14.5	15.0	15.0	27.0	27.5	304sst	lead	0.0	sand-b
	sleeve	27.5	28.0	28.0	28.0	48.0	304sst	304sst	100.0	clino
D2.8	stab	12.0	13.5	13.5	13.5	13.5	zirc	zirc	0.0	none
	can	13.5	14.0	14.0	14.0	14.5	zirc	zirc	0.0	sand-b
	o pack	14.5	15.0	15.0	27.0	27.5	zirc	lead	0.0	sand-b
	sleeve	27.5	28.0	28.0	28.0	48.0	zirc	zirc	100.0	clino
E.1	stab	12.0	12.0	12.0	12.0	12.0	lead	lead	0.0	none
	stab	12.0	12.0	12.0	13.5	13.5	lead	lead	0.0	none
	can	13.5	14.0	14.0	14.0	20.0	304sst	304sst	0.0	sand-b
E.2	stab	12.0	12.0	12.0	12.0	12.0	lead	lead	0.0	none
	stab	12.0	12.0	12.0	13.5	13.5	lead	lead	0.0	none
	can	13.5	14.0	14.0	14.2	20.0	steel	zirc	0.0	sand-b

Table 4-1. (Continued)

Concept	Element	Inside Material		Outside Material		Filler	Inside Material	Outside Material	Coating Delay (yrs)	Filler
		ID	OD	ID	OD	OD				
E.3	stab	12.0	12.0	12.0	12.0	12.0	lead	lead	0.0	none
	stab	12.0	12.0	12.0	13.5	13.5	lead	lead	0.0	none
	can	13.5	14.0	14.0	14.2	20.0	304sst	zirc	0.0	sand-b
BASE	stab	12.0	13.5	13.5	13.5	13.5	helium	helium	0.0	none
	can	13.5	13.6	13.6	13.6	13.6	steel	steel	0.0	none

Table 4-2. Summary of Concepts Studied in FY'80 Follow-on Work Using Previous Version of "BARIER" Code. (Stula, 1980a).

Concept	Element	Inside Material ID	Inside Material OD	Outside Material ID	Outside Material OD	Filler OD	Inside Material	Outside Material	Coating Delay (yrs)	Filler
A.11	stab	12.0	13.5	13.5	13.5	13.5	304sst	304sst	0.0	none
	can	13.5	14.0	14.0	14.0	40.0	titaniu	titaniu	0.0	sand-b
A.12	stab	12.0	13.5	13.5	13.5	13.5	304sst	304sst	0.0	none
	can	13.5	14.0	14.0	14.0	40.0	cu-ni	cu-ni	0.0	sand-b
B1.12	stab	12.0	13.5	13.5	13.5	13.5	steel	steel	0.0	none
	can	13.5	14.0	14.0	14.0	14.5	steel	steel	0.0	sand-b
	sleeve	14.5	22.5	22.5	22.6	48.0	iron	zirc	0.0	sand-b
B1.13	stab	12.0	13.5	13.5	13.5	13.5	steel	steel	0.0	none
	can	13.5	14.0	14.0	14.0	14.5	steel	steel	0.0	sand-b
	sleeve	14.5	22.5	22.5	22.8	48.0	iron	zirc	0.0	sand-b
B1.14	stab	12.0	13.5	13.5	13.5	13.5	steel	steel	0.0	none
	can	13.5	14.0	14.0	14.0	14.5	steel	steel	0.0	sand-b
	sleeve	14.5	22.5	22.5	23.0	48.0	iron	zirc	0.0	sand-b
B1.15	stab	12.0	13.5	13.5	13.5	13.5	steel	steel	0.0	none
	can	13.5	14.0	14.0	14.0	14.5	steel	steel	0.0	sand-b
	sleeve	14.5	22.5	22.5	22.7	48.0	304sst	zirc	0.0	sand-b
B1.16	stab	12.0	13.5	13.5	13.5	13.5	steel	steel	0.0	none
	can	13.5	14.0	14.0	14.0	14.5	steel	steel	0.0	sand-b
	sleeve	14.5	22.5	22.5	22.6	48.0	304sst	zirc	0.0	sand-b
B1.17	stab	12.0	13.5	13.5	13.5	13.5	steel	steel	0.0	none
	can	13.5	14.0	14.0	14.0	14.5	steel	steel	0.0	sand-b
	sleeve	14.5	22.5	22.5	23.0	48.0	304sst	zirc	0.0	sand-b
B1.18	stab	12.0	13.5	13.5	13.5	13.5	steel	steel	0.0	none

Table 4-2. Summary of Concepts Studied in FY'80 Follow-on Work Using Previous Version of "BARIER" Code. (Stula, 1980a). (Continued)

Concept	Element	Inside Material ID	Inside Material OD	Outside Material ID	Outside Material OD	Filler OD	Inside Material	Outside Material	Coating Delay (yrs)	Filler
B1.18	can	13.5	14.0	14.0	14.0	14.5	steel	steel	0.0	sand-b
	sleeve	14.5	22.5	22.5	22.7	48.0	iron	304sst	0.0	sand-b
B1.19	stab	12.0	13.5	13.5	13.5	13.5	steel	steel	0.0	none
	can	13.5	14.0	14.0	14.0	14.5	steel	steel	0.0	sand-b
	sleeve	14.5	22.5	22.5	23.0	48.0	iron	304sst	0.0	sand-b
B1.20	stab	12.0	13.5	13.5	13.5	13.5	steel	steel	0.0	none
	can	13.5	14.0	14.0	14.0	14.5	steel	steel	0.0	sand-b
	sleeve	14.5	18.5	18.5	18.7	48.0	iron	zirc	0.0	sand-b
B1.21	stab	12.0	13.5	13.5	13.5	13.5	steel	steel	0.0	none
	can	13.5	14.0	14.0	14.0	14.5	steel	steel	0.0	sand-b
	sleeve	14.5	18.5	18.5	19.0	48.0	iron	zirc	0.0	sand-b
B1.22	stab	12.0	13.5	13.5	13.5	13.5	steel	steel	0.0	none
	can	13.5	14.0	14.0	14.0	14.5	steel	steel	0.0	sand-b
	sleeve	14.5	15.0	15.0	15.1	48.0	iron	zirc	0.0	sand-b
B1.23	stab	12.0	13.5	13.5	13.5	13.5	steel	steel	0.0	none
	can	13.5	14.0	14.0	14.0	14.5	steel	steel	0.0	sand-b
	sleeve	14.5	15.0	15.0	15.1	48.0	iron	304sst	0.0	sand-b
B1.24	stab	12.0	13.5	13.5	13.5	13.5	steel	steel	0.0	none
	can	13.5	14.0	14.0	14.0	14.5	steel	steel	0.0	sand-b
	sleeve	14.5	18.5	18.5	18.5	40.0	304sst	304sst	0.0	sand-b
B1.25	stab	12.0	13.5	13.5	13.5	13.5	steel	steel	0.0	none
	can	13.5	14.0	14.0	14.0	14.5	steel	steel	0.0	sand-b
	sleeve	14.5	21.5	21.5	21.5	48.0	copper	copper	0.0	sand-b
B1.26	stab	12.0	13.5	13.5	13.5	13.5	steel	steel	0.0	none
	can	13.5	14.0	14.0	14.0	14.5	steel	steel	0.0	sand-b
	sleeve	14.5	21.5	21.5	21.5	48.0	inconel	inconel	0.0	sand-b

Table 4-2. Summary of Concepts Studied in FY'80 Follow-on Work Using Previous Version of "BARIER" Code. (Stula, 1980a). (Continued)

Concept	Element	Inside Material ID	Inside Material OD	Outside Material ID	Outside Material OD	Filler OD	Inside Material	Outside Material	Coating Delay (yrs)	Filler
B1.27	stab	12.0	13.5	13.5	13.5	13.5	steel	steel	0.0	none
	can	13.5	14.0	14.0	14.0	14.5	steel	steel	0.0	sand-b
	sleeve	14.5	21.5	21.5	21.5	48.0	304sst	304sst	0.0	sand-b
B1.28	stab	12.0	13.5	13.5	13.5	13.5	steel	steel	0.0	none
	can	13.5	14.0	14.0	14.0	14.5	steel	steel	0.0	sand-b
	sleeve	14.5	15.0	15.0	15.0	40.0	copper	copper	0.0	sand-b
B1.29	stab	12.0	13.5	13.5	13.5	13.5	steel	steel	0.0	none
	can	13.5	14.0	14.0	14.0	14.5	steel	steel	0.0	sand-b
	sleeve	14.5	15.0	15.0	15.0	40.0	inconel	inconel	0.0	sand-b
B1.30	stab	12.0	13.5	13.5	13.5	13.5	steel	steel	0.0	none
	can	13.5	14.0	14.0	14.0	14.5	steel	steel	0.0	sand-b
	sleeve	14.5	15.0	15.0	15.0	40.0	iron	iron	0.0	sand-b
B1.31	stab	12.0	13.5	13.5	13.5	13.5	steel	steel	0.0	none
	can	13.5	14.0	14.0	14.0	14.5	steel	steel	0.0	sand-b
	sleeve	14.5	26.5	26.5	26.5	48.0	304sst	304sst	0.0	sand-b
B1.32	stab	12.0	13.5	13.5	13.5	13.5	steel	steel	0.0	none
	can	13.5	14.0	14.0	14.0	14.5	steel	steel	0.0	sand-b
	sleeve	14.5	20.5	20.5	21.0	48.0	iron	zirc	0.0	sand-b
B1.33	stab	12.0	13.5	13.5	13.5	13.5	steel	steel	0.0	none
	can	13.5	14.0	14.0	14.0	14.5	steel	steel	0.0	sand-b
	sleeve	14.5	20.5	20.5	20.7	48.0	iron	zirc	0.0	sand-b
B1.34	stab	12.0	13.5	13.5	13.5	13.5	steel	steel	0.0	none
	can	13.5	14.0	14.0	14.0	14.5	steel	steel	0.0	sand-b
	sleeve	14.5	26.5	26.5	26.5	48.0	iron	iron	0.0	sand-b
B1.35	stab	12.0	13.5	13.5	13.5	13.5	steel	steel	0.0	none
	can	13.5	14.0	14.0	14.0	14.5	steel	steel	0.0	sand-b
	sleeve	14.5	26.5	26.5	27.0	48.0	304sst	zirc	0.0	sand-b

Table 4-2. Summary of Concepts Studied in FY'80 Follow-on Work Using Previous Version of "BARIER" Code. (Stula, 1980a). (Continued)

Concept	Element	Inside Material ID	Inside Material OD	Outside Material ID	Outside Material OD	Filler OD	Inside Material	Outside Material	Coating Delay (yrs)	Filler
B1.36	stab	12.0	13.5	13.5	13.5	13.5	steel	steel	0.0	none
	can	13.5	14.0	14.0	14.0	14.5	steel	steel	0.0	sand-b
	sleeve	14.5	26.5	26.5	26.6	48.0	304sst	zirc	0.0	sand-b
E.4	stab	12.0	12.0	12.0	12.0	12.0	lead	lead	0.0	none
	stab	12.0	12.0	12.0	13.5	13.5	lead	lead	0.0	none
	can	13.5	14.0	14.0	14.0	20.0	zirc	zirc	0.0	sand-b
E.5	stab	12.0	12.0	12.0	12.0	12.0	lead	lead	0.0	none
	stab	12.0	12.0	12.0	13.5	13.5	lead	lead	0.0	none
	can	13.5	14.0	14.0	14.0	20.0	inconel	inconel	0.0	sand-b
E.6	stab	12.0	12.0	12.0	12.0	12.0	lead	lead	0.0	none
	stab	12.0	12.0	12.0	13.5	13.5	lead	lead	0.0	none
	can	13.5	14.0	14.0	14.0	20.0	steel	steel	0.0	sand-b
E.7	stab	12.0	12.0	12.0	12.0	12.0	304sst	304sst	0.0	none
	stab	12.0	12.0	12.0	13.5	13.5	304sst	304sst	0.0	none
	can	13.5	14.0	14.0	14.0	20.0	304sst	304sst	0.0	sand-b
E.8	stab	12.0	12.0	12.0	12.0	12.0	steel	steel	0.0	none
	stab	12.0	12.0	12.0	13.5	13.5	steel	steel	0.0	none
	can	13.5	14.0	14.0	14.0	20.0	steel	steel	0.0	sand-b
E.9	stab	12.0	12.0	12.0	12.0	12.0	inconel	inconel	0.0	none
	stab	12.0	12.0	12.0	13.5	13.5	inconel	inconel	0.0	none
	can	13.5	14.0	14.0	14.0	20.0	inconel	inconel	0.0	sand-b
E.10	stab	12.0	12.0	12.0	12.0	12.0	lead	lead	0.0	none
	stab	12.0	12.0	12.0	13.5	13.5	lead	lead	0.0	none
	can	13.5	15.5	15.5	15.5	20.0	304sst	304sst	0.0	sand-b
E.11	stab	12.0	12.0	12.0	12.0	12.0	lead	lead	0.0	none
	stab	12.0	12.0	12.0	13.5	13.5	lead	lead	0.0	none
	can	13.5	15.5	15.5	15.5	20.0	steel	steel	0.0	sand-b

Table 4-2. Summary of Concepts Studied in FY'80 Follow-on Work Using Previous Version of "BARIER" Code. (Stula, 1980a). (Continued)

Concept	Element	Inside Material ID	Inside Material OD	Outside Material ID	Outside Material OD	Filler OD	Inside Material	Outside Material	Coating Delay (yrs)	Filler
E.12	stab	12.0	12.0	12.0	12.0	12.0	lead	lead	0.0	none
	stab	12.0	12.0	12.0	13.5	13.5	lead	lead	0.0	none
	can	13.5	14.0	14.0	14.1	20.0	304sst	zirc	0.0	sand-b
E.13	stab	12.0	12.0	12.0	12.0	12.0	lead	lead	0.0	none
	stab	12.0	12.0	12.0	13.5	13.5	lead	lead	0.0	none
	can	13.5	14.0	14.0	14.3	20.0	304sst	zirc	0.0	sand-b
E.15	stab	12.0	12.0	12.0	12.0	12.0	lead	lead	0.0	none
	stab	12.0	12.0	12.0	13.5	13.5	lead	lead	0.0	none
	can	13.5	14.0	14.0	14.0	20.0	304sst	304sst	0.0	clino
E.16	stab	12.0	12.0	12.0	12.0	12.0	lead	lead	0.0	none
	stab	12.0	12.0	12.0	13.5	13.5	lead	lead	0.0	none
	can	13.5	14.0	14.0	14.0	40.0	304sst	304sst	0.0	clino
E.17	stab	12.0	12.0	12.0	12.0	12.0	lead	lead	0.0	none
	stab	12.0	12.0	12.0	13.5	13.5	lead	lead	0.0	none
	can	13.5	14.0	14.0	14.0	20.0	304sst	304sst	0.0	bent
E.18	stab	12.0	12.0	12.0	12.0	12.0	lead	lead	0.0	none
	stab	12.0	12.0	12.0	13.5	13.5	lead	lead	0.0	none
	can	13.5	14.0	14.0	14.0	20.0	copper	copper	0.0	sand-b
E.19	stab	12.0	12.0	12.0	12.0	12.0	lead	lead	0.0	none
	stab	12.0	12.0	12.0	13.5	13.5	lead	lead	0.0	none
	can	13.5	14.0	14.0	14.0	20.0	lead	lead	0.0	sand-b
E.20	stab	12.0	12.0	12.0	12.0	12.0	lead	lead	0.0	none
	stab	12.0	12.0	12.0	13.5	13.5	lead	lead	0.0	none
	can	13.5	14.0	14.0	14.0	20.0	iron	iron	0.0	sand-b
E.21	stab	12.0	12.0	12.0	12.0	12.0	lead	lead	0.0	none
	stab	12.0	12.0	12.0	13.5	13.5	lead	lead	0.0	none
	can	13.5	14.0	14.0	14.0	40.0	304sst	304sst	0.0	sand-b

Table 4-2. Summary of Concepts Studied in FY'80 Follow-on Work Using Previous Version of "BARIER" Code. (Stula, 1980a). (Continued)

Concept	Element	Inside Material		Outside Material		Filler OD	Inside Material	Outside Material	Coating* Delay (yrs)	Filler
		ID	OD	ID	OD					
E.22	stab	12.0	12.0	12.0	12.0	12.0	lead	lead	0.0	none
	stab	12.0	12.0	12.0	13.5	13.5	lead	lead	0.0	none
	can	13.5	14.0	14.0	14.2	40.0	304sst	zirc	0.0	sand-b
E.23	stab	12.0	12.0	12.0	12.0	12.0	lead	lead	0.0	none
	stab	12.0	12.0	12.0	13.5	13.5	lead	lead	0.0	none
	can	13.5	20.5	20.5	20.5	40.0	304sst	304sst	0.0	sand-b
E.24	stab	12.0	12.0	12.0	12.0	12.0	lead	lead	0.0	none
	stab	12.0	12.0	12.0	13.5	13.5	lead	lead	0.0	none
	can	13.5	20.5	20.5	20.7	40.0	304sst	zirc	0.0	sand-b
A.1S**	stab	12.0	12.0	12.0	12.0	12.0	lead	lead	0.0	none
	stab	12.0	12.0	12.0	13.5	13.5	lead	lead	0.0	none
	can	13.5	14.0	14.0	14.0	40.0	304sst	304sst	0.0	sand-b
B1.1S	stab	12.0	12.0	12.0	12.0	12.0	lead	lead	0.0	none
	stab	12.0	12.0	12.0	13.5	13.5	lead	lead	0.0	none
	can	13.5	14.0	14.0	14.0	14.5	steel	steel	0.0	sand-b
	sleeve	14.5	22.5	22.5	22.7	48.0	iron	zirc	0.0	sand-b
C1.1S	stab	12.0	12.0	12.0	12.0	12.0	lead	lead	0.0	none
	stab	12.0	12.0	12.0	13.5	13.5	lead	lead	0.0	none
	can	13.5	14.0	14.0	14.0	14.5	inconel	inconel	0.0	sand-b
	o pack	14.5	15.0	15.0	15.0	15.5	304sst	304sst	0.0	sand-b
	sleeve	15.5	22.5	22.5	22.5	45.0	iron	iron	0.0	sand-b
D.3S	stab	12.0	12.0	12.0	12.0	12.0	lead	lead	0.0	none
	stab	12.0	12.0	12.0	13.5	13.5	lead	lead	0.0	none
	can	13.5	14.0	14.0	14.0	14.5	steel	steel	0.0	sand-b
	sleeve	14.5	21.5	21.5	21.5	48.0	iron	iron	100.0	sand-b
D1.2S	stab	12.0	12.0	12.0	12.0	12.0	lead	lead	0.0	none
	stab	12.0	12.0	12.0	13.5	13.5	lead	lead	0.0	none
	can	13.5	14.0	14.0	14.0	14.5	304sst	304sst	0.0	sand-b
	sleeve	14.5	22.5	22.5	22.5	48.0	iron	iron	100.0	sand-b

*Coating delay represents an assumed length of time after which corrosion of the coated surface would begin

**"S" indicates a concept identical to one in the FY'79 study but with a cast solid lead stabilizer

Table 4-2. Summary of Concepts Studied in FY'80 Follow-on Work Using Previous Version of "BARIER" Code. (Stula, 1980a). (Continued).

Concept	Element	Inside Material ID	Inside Material OD	Outside Material ID	Outside Material OD	Filler OD	Inside Material	Outside Material	Coating Delay (yrs)	Filler
D2.1S	stab	12.0	12.0	12.0	12.0	12.0	lead	lead	0.0	none
	stab	12.0	12.0	12.0	13.5	13.5	lead	lead	0.0	none
	can	13.5	14.0	14.0	14.0	14.5	inconel	inconel	0.0	sand-b
	c pack	14.5	15.0	15.0	15.0	15.5	inconel	inconel	0.0	sand-b
	sleeve	15.5	23.5	23.5	23.5	48.0	iron	iron	100.0	sand-b

Table 4-3. Best Concepts in FY'79 Performance Study (Stula, 1980a).

Concept	Release Begin Time (Yrs) - Oxic Conditions		
	Salt	Shale	Basalt-Granite
A.1, A.5	31	46	
A.10			24,700
B.8			24,700
B1.7			1100
B1.11	1920	1930	
C.7			49,400
C1.1, C1.3	27	41	
C1.6			11,900
D.1		54	
D.3	130		
D.5			24,800
D1.2	140	150	
D1.5			1700
D2.1	140	150	
D2.8			1900
E.3	2600	3500	

Table 4-4. Summary of Concepts Studied With New Version of "BARIER" Code. (Unless Otherwise Noted, Dimensions in Inches).

CONCEPT	ELEMENT	INSIDE MATERIAL ID	INSIDE MATERIAL OD	OUTSIDE MATERIAL OD	FILLER OD	CAP OD	INSIDE MATERIAL	OUTSIDE MATERIAL	COATING DELAY (YRS)	FILLER
A.1	STAB	12.0	13.5	13.5	13.5	13.5	304SST	304SST	0.0	NONE
	CAN	13.5	14.0	14.0	40.0	40.0	304SST	304SST	0.0	SAND-B
A.5	STAB	12.0	13.5	13.5	13.5	13.5	304SST	304SST	0.0	NONE
	CAN	13.5	15.5	15.5	20.0	20.0	304SST	304SST	0.0	SAND-B
A.10	STAB	12.0	13.5	13.5	13.5	13.5	ZIRC	ZIRC	0.0	NONE
	CAN	13.5	15.5	15.5	20.0	20.0	ZIRC	ZIRC	0.0	SAND-B
B.8	STAB	12.0	13.5	13.5	13.5	13.5	STEEL	STEEL	0.0	NONE
	CAN	13.5	14.0	14.0	14.5	14.5	STEEL	STEEL	0.0	SAND-B
	O PACK	14.5	16.5	16.5	20.0	20.0	ZIRC	ZIRC	0.0	SAND-B
B1.7	STAB	12.0	13.5	13.5	13.5	13.5	STEEL	STEEL	0.0	NONE
	CAN	13.5	14.0	14.0	14.5	14.5	STEEL	STEEL	0.0	SAND-B
	SLEEVE	14.5	15.0	23.0	30.0	30.0	STEEL	LEAD	0.0	CLINO
B1.11	STAB	12.0	13.5	13.5	13.5	13.5	STEEL	STEEL	0.0	NONE
	CAN	13.5	14.0	14.0	14.5	14.5	STEEL	STEEL	0.0	SAND-B
	SLEEVE	14.5	22.5	22.7	48.0	48.0	IRON	ZIRC	0.0	SAND-B
B1.1N	STAB	12.0	13.5	13.5	13.5	13.5	STEEL	STEEL	0.0	NONE
	CAN	13.5	14.0	14.0	14.5	14.5	STEEL	STEEL	0.0	SAND-B
	SLEEVE	14.5	15.0	15.0	48.0	48.0	IRON	IRON	0.0	SAND-B
B1.2N	STAB	12.0	13.5	13.5	13.5	13.5	STEEL	STEEL	0.0	NONE
	CAN	13.5	14.0	14.0	14.5	14.5	STEEL	STEEL	0.0	SAND-B
	SLEEVE	14.5	21.5	21.5	48.0	48.0	IRON	IRON	0.0	SAND-B
B1.3N	STAB	12.0	13.5	13.5	13.5	13.5	STEEL	STEEL	0.0	NONE
	CAN	13.5	14.0	14.0	14.5	14.5	STEEL	STEEL	0.0	SAND-B

Table 4-4. (Continued)

CONCEPT	ELEMENT	INSIDE MATERIAL ID	INSIDE MATERIAL OD	OUTSIDE MATERIAL OD	FILLER OD	CAP OD	INSIDE MATERIAL	OUTSIDE MATERIAL	COATING DELAY (YRS)	FILLER
B1.3N	SLEEVE	14.5	26.5	26.5	48.0	48.0	IRON	IRON	0.0	SAND-B
B1.4N	STAB	12.0	13.5	13.5	13.5	13.5	STEEL	STEEL	0.0	NONE
	CAN	13.5	14.0	14.0	14.5	14.5	STEEL	STEEL	0.0	SAND-B
	SLEEVE	14.5	21.5	21.6	48.0	48.0	IRON	ZIRC	0.0	SAND-B
B1.5N	STAB	12.0	13.5	13.5	13.5	13.5	STEEL	STEEL	0.0	NONE
	CAN	13.5	14.0	14.0	14.5	14.5	STEEL	STEEL	0.0	SAND-B
	SLEEVE	14.5	21.5	21.8	48.0	48.0	IRON	ZIRC	0.0	SAND-B
B1.6N	STAB	12.0	13.5	13.5	13.5	13.5	STEEL	STEEL	0.0	NONE
	CAN	13.5	14.0	14.0	14.5	14.5	STEEL	STEEL	0.0	SAND-B
	SLEEVE	14.5	21.5	22.0	48.0	48.0	IRON	ZIRC	0.0	SAND-B
B1.7N	STAB	12.0	13.5	13.5	13.5	13.5	STEEL	STEEL	0.0	NONE
	CAN	13.5	14.0	14.0	14.5	14.5	STEEL	STEEL	0.0	SAND-B
	SLEEVE	14.5	15.0	15.3	48.0	48.0	IRON	ZIRC	0.0	SAND-B
B1.8N	STAB	12.0	13.5	13.5	13.5	13.5	STEEL	STEEL	0.0	NONE
	CAN	13.5	14.0	14.0	14.5	14.5	STEEL	STEEL	0.0	SAND-B
	SLEEVE	14.5	26.5	26.8	48.0	48.0	IRON	ZIRC	0.0	SAND-B
B1.9N	STAB	12.0	13.5	13.5	13.5	13.5	STEEL	STEEL	0.0	NONE
	CAN	13.5	14.0	14.0	14.5	14.5	STEEL	STEEL	0.0	SAND-B
	SLEEVE	14.5	21.5	21.6	48.0	48.0	304SST	ZIRC	0.0	SAND-B
B1.10N	STAB	12.0	13.5	13.5	13.5	13.5	STEEL	STEEL	0.0	NONE
	CAN	13.5	14.0	14.0	14.5	14.5	STEEL	STEEL	0.0	SAND-B
	SLEEVE	14.5	21.5	22.0	48.0	48.0	304SST	ZIRC	0.0	SAND-B
B1.11N	STAB	12.0	13.5	13.5	13.5	13.5	STEEL	STEEL	0.0	NONE
	CAN	13.5	14.0	14.0	14.5	14.5	STEEL	STEEL	0.0	SAND-B
	SLEEVE	14.5	15.0	15.0	48.0	48.0	COPPER	COPPER	0.0	SAND-B

Table 4-4. (Continued)

CONCEPT	ELEMENT	INSIDE MATERIAL ID	INSIDE MATERIAL OD	OUTSIDE MATERIAL OD	FILLER OD	CAP OD	INSIDE MATERIAL	OUTSIDE MATERIAL	COATING DELAY (YRS)	FILLER
B1.12N	STAB	12.0	13.5	13.5	13.5	13.5	STEEL	STEEL	0.0	NONE
	CAN	13.5	14.0	14.0	14.5	14.5	STEEL	STEEL	0.0	SAND-B
	SLEEVE	14.5	21.5	21.5	48.0	48.0	COPPER.	COPPER	0.0	SAND-B
B1.13N	STAB	12.0	13.5	13.5	13.5	13.5	STEEL	STEEL	0.0	NONE
	CAN	13.5	14.0	14.0	14.5	14.5	STEEL	STEEL	0.0	SAND-B
	SLEEVE	14.5	15.0	15.0	48.0	48.0	INCONEL	INCONEL	0.0	SAND-B
B1.14N	STAB	12.0	13.5	13.5	13.5	13.5	STEEL	STEEL	0.0	NONE
	CAN	13.5	14.0	14.0	14.5	14.5	STEEL	STEEL	0.0	SAND-B
	SLEEVE	14.5	21.5	21.5	48.0	48.0	INCONEL	INCONEL	0.0	SAND-B
B1.15N	STAB	12.0	13.5	13.5	13.5	13.5	STEEL	STEEL	0.0	NONE
	CAN	13.5	14.0	14.0	14.5	14.5	STEEL	STEEL	0.0	SAND-B
	SLEEVE	14.5	15.0	15.0	48.0	48.0	304SST	304SST	0.0	SAND-B
B1.16N	STAB	12.0	13.5	13.5	13.5	13.5	STEEL	STEEL	0.0	NONE
	CAN	13.5	14.0	14.0	14.5	14.5	STEEL	STEEL	0.0	SAND-B
	SLEEVE	14.5	21.5	21.5	48.0	48.0	304SST	304SST	0.0	SAND-B
B1.17N	STAB	12.0	13.5	13.5	13.5	13.5	STEEL	STEEL	0.0	NONE
	CAN	13.5	14.0	14.0	14.5	14.5	STEEL	STEEL	0.0	SAND-B
	SLEEVE	14.5	15.0	15.0	48.0	48.0	ZIRC	ZIRC	0.0	SAND-B
B1.18N	STAB	12.0	13.5	13.5	13.5	13.5	STEEL	STEEL	0.0	NONE
	CAN	13.5	14.0	14.0	14.5	14.5	STEEL	STEEL	0.0	SAND-B
	SLEEVE	14.5	21.5	21.5	48.0	48.0	ZIRC	ZIRC	0.0	SAND-B
B1.19N	STAB	12.0	13.5	13.5	13.5	13.5	STEEL	STEEL	0.0	NONE
	CAN	13.5	14.0	14.0	14.5	14.5	STEEL	STEEL	0.0	SAND-B
	SLEEVE	14.5	21.5	21.6	48.0	48.0	IRON	ZIRC	0.0	SAND-B
B1.20N	STAB	12.0	13.5	13.5	13.5	13.5	STEEL	STEEL	0.0	NONE
	CAN	13.5	14.0	14.0	14.5	14.5	STEEL	STEEL	0.0	SAND-B
	SLEEVE	14.5	21.5	21.8	48.0	48.0	IRON	ZIRC	0.0	SAND-B

Table 4-4. (Continued)

CONCEPT	ELEMENT	INSIDE MATERIAL ID	INSIDE MATERIAL OD	OUTSIDE MATERIAL OD	FILLER OD	CAP OD	INSIDE MATERIAL	OUTSIDE MATERIAL	COATING DELAY (YRS)	FILLER
B1.21N	STAB	12.0	13.5	13.5	13.5	13.5	STEEL	STEEL	0.0	NONE
	CAN	13.5	14.0	14.0	14.5	14.5	STEEL	STEEL	0.0	SAND-B
	SLEEVE	14.5	21.5	22.0	48.0	48.0	IRON	ZIRC	0.0	SAND-B
B1.22N	STAB	12.0	13.5	13.5	13.5	13.5	STEEL	STEEL	0.0	NONE
	CAN	13.5	14.0	14.0	14.5	14.5	STEEL	STEEL	0.0	SAND-B
	SLEEVE	14.5	15.0	15.3	48.0	48.0	IRON	ZIRC	0.0	SAND-B
B1.23N	STAB	12.0	13.5	13.5	13.5	13.5	STEEL	STEEL	0.0	NONE
	CAN	13.5	14.0	14.0	14.5	14.5	STEEL	STEEL	0.0	SAND-B
	SLEEVE	14.5	26.5	26.8	48.0	48.0	IRON	ZIRC	0.0	SAND-B
B1.24N	STAB	12.0	12.0	12.0	12.0	13.5	HELIUM.	HELIUM	0.0	NONE
	CAN	13.5	14.0	14.0	14.5	14.5	STEEL	STEEL	0.0	SAND-B
	SLEEVE	14.5	21.5	21.5	48.0	48.0	IRON	IRON	0.0	SAND-B
B1.25N	STAB	12.0	12.0	12.0	12.0	13.5	AIR	AIR	0.0	NONE
	CAN	13.5	14.0	14.0	14.5	14.5	STEEL	STEEL	0.0	SAND-B
	SLEEVE	14.5	21.5	21.5	48.0	48.0	IRON	IRON	0.0	SAND-B
B1.26N	STAB	12.0	12.0	12.0	12.0	13.5	HELIUM.	HELIUM	0.0	NONE
	CAN	13.5	14.0	14.0	14.0	14.5	STEEL	STEEL	0.0	NONE
	SLEEVE	14.5	21.5	21.5	48.0	48.0	IRON	IRON	0.0	SAND-B
B1.27N	STAB	12.0	12.0	12.0	12.0	13.5	HELIUM.	HELIUM	0.0	NONE
	CAN	13.5	14.0	14.0	14.0	15.0	STEEL	STEEL	0.0	NONE
	SLEEVE	15.0	23.0	22.0	48.5	48.5	IRON	IRON	0.0	SAND-B
B1.28N	STAB	12.0	13.5	13.5	13.5	13.5	STEEL	STEEL	0.0	NONE
	CAN	13.5	14.0	14.0	14.0	16.0	STEEL	STEEL	0.0	NONE
	SLEEVE	16.0	23.0	23.0	49.5	49.5	IRON	IRON	0.0	SAND-B
B1.29N	STAB	12.0	13.5	13.5	13.5	13.5	STEEL	STEEL	0.0	NONE
	CAN	13.5	14.0	14.0	14.0	16.0	STEEL	STEEL	0.0	NONE
	SLEEVE	16.0	23.0	23.0	49.5	49.5	IRON	IRON	0.0	SAND-B

Table 4-4. (Continued)

CONCEPT	ELEMENT	INSIDE MATERIAL ID	INSIDE MATERIAL OD	OUTSIDE MATERIAL OD	FILLER OD	GAP OD	INSIDE MATERIAL	OUTSIDE MATERIAL	COATING DELAY (YRS)	FILLER
BE.1N	CA STAB	12.0	13.5	13.5	13.5	13.5	LEAD	LEAD	0.0	NONE
	CAN	13.5	14.0	14.0	14.5	14.5	304SST	304SST	0.0	SAND-B
	SLEEVE	14.5	15.0	15.0	48.0	48.0	IRON	IRON	0.0	SAND-B
BE.2N	CA STAB	12.0	13.5	13.5	13.5	13.5	LEAD	LEAD	0.0	NONE
	CAN	13.5	14.0	14.0	14.5	14.5	304SST	304SST	0.0	SAND-B
	SLEEVE	14.5	21.5	21.5	48.0	48.0	IRON	IRON	0.0	SAND-B
BE.3N	CA STAB	12.0	13.5	13.5	13.5	13.5	LEAD	LEAD	0.0	NONE
	CAN	13.5	14.0	14.0	14.5	14.5	304SST	304SST	0.0	SAND-B
	SLEEVE	14.5	26.5	26.5	48.0	48.0	IRON	IRON	0.0	SAND-B
BE.4N	CA STAB	12.0	13.5	13.5	13.5	13.5	LEAD	LEAD	0.0	NONE
	CAN	13.5	14.0	14.0	14.5	14.5	304SST	304SST	0.0	SAND-B
	SLEEVE	14.5	21.5	21.6	48.0	48.0	IRON	ZIRC	0.0	SAND-B
BE.5N	CA STAB	12.0	13.5	13.5	13.5	13.5	LEAD	LEAD	0.0	NONE
	CAN	13.5	14.0	14.0	14.5	14.5	304SST	304SST	0.0	SAND-B
	SLEEVE	14.5	21.5	22.0	48.0	48.0	IRON	ZIRC	0.0	SAND-B
BE.6N	CA STAB	12.0	13.5	13.5	13.5	13.5	LEAD	LEAD	0.0	NONE
	CAN	13.5	14.0	14.0	14.5	14.5	304SST	304SST	0.0	SAND-B
	SLEEVE	14.5	15.0	15.3	48.0	48.0	IRON	ZIRC	0.0	SAND-B
BE.7N	CA STAB	12.0	13.5	13.5	13.5	13.5	LEAD	LEAD	0.0	NONE
	CAN	13.5	14.0	14.0	14.5	14.5	304SST	304SST	0.0	SAND-B
	SLEEVE	14.5	26.5	26.5	48.0	48.0	IRON	ZIRC	0.0	SAND-B
BE.8N	CA STAB	12.0	13.5	13.5	13.5	13.5	LEAD	LEAD	0.0	NONE
	CAN	13.5	14.0	14.0	14.5	14.5	ZIRC	ZIRC	0.0	SAND-B
	SLEEVE	14.5	15.0	15.0	48.0	48.0	IRON	IRON	0.0	SAND-B
BE.9N	CA STAB	12.0	13.5	13.5	13.5	13.5	LEAD	LEAD	0.0	NONE
	CAN	13.5	14.0	14.0	14.5	14.5	ZIRC	ZIRC	0.0	SAND-B
	SLEEVE	14.5	21.5	21.5	48.0	48.0	IRON	IRON	0.0	SAND-B

Table 4-4. (Continued)

CONCEPT	ELEMENT	INSIDE MATERIAL ID	INSIDE MATERIAL OD	OUTSIDE MATERIAL OD	FILLER OD	CAP OD	INSIDE MATERIAL	OUTSIDE MATERIAL	COATING DELAY (YRS)	FILLER
BE.10N	CA STAB	12.0	13.5	13.5	13.5	13.5	LEAD	LEAD	0.0	NONE
	CAN	13.5	14.0	14.0	14.5	14.5	ZIRC	ZIRC	0.0	SAND-B
	SLEEVE	14.5	26.5	26.5	48.0	48.0	IRON	IRON	0.0	SAND-B
BE.11N	CA STAB	12.0	13.5	13.5	13.5	13.5	LEAD	LEAD	0.0	NONE
	CAN	13.5	14.0	14.0	14.5	14.5	ZIRC	ZIRC	0.0	SAND-B
	SLEEVE	14.5	21.5	21.6	48.0	48.0	IRON	ZIRC	0.0	SAND-B
BE.12N	CA STAB	12.0	13.5	13.5	13.5	13.5	LEAD	LEAD	0.0	NONE
	CAN	13.5	14.0	14.0	14.5	14.5	ZIRC	ZIRC	0.0	SAND-B
	SLEEVE	14.5	21.5	22.0	48.0	48.0	IRON	ZIRC	0.0	SAND-B
BE.13N	CA STAB	12.0	13.5	13.5	13.5	13.5	LEAD	LEAD	0.0	NONE
	CAN	13.5	14.0	14.0	14.5	14.5	ZIRC	ZIRC	0.0	SAND-B
	SLEEVE	14.5	15.0	15.3	48.0	48.0	IRON	ZIRC	0.0	SAND-B
BE.14N	CA STAB	12.0	13.5	13.5	13.5	13.5	LEAD	LEAD	0.0	NONE
	CAN	13.5	14.0	14.0	14.5	14.5	ZIRC	ZIRC	0.0	SAND-B
	SLEEVE	14.5	26.5	26.8	48.0	48.0	IRON	ZIRC	0.0	SAND-B
BE.15N	CA STAB	12.0	13.5	13.5	13.5	13.5	LEAD	LEAD	0.0	NONE
	CAN	13.5	14.0	14.0	14.5	14.5	INCONEL	INCONEL	0.0	SAND-B
	SLEEVE	14.5	15.0	15.0	48.0	48.0	IRON	IRON	0.0	SAND-B
BE.16N	CA STAB	12.0	13.5	13.5	13.5	13.5	LEAD	LEAD	0.0	NONE
	CAN	13.5	14.0	14.0	14.5	14.5	INCONEL	INCONEL	0.0	SAND-B
	SLEEVE	14.5	21.5	21.5	48.0	48.0	IRON	IRON	0.0	SAND-B
BE.17N	CA STAB	12.0	13.5	13.5	13.5	13.5	LEAD	LEAD	0.0	NONE
	CAN	13.5	14.0	14.0	14.5	14.5	INCONEL	INCONEL	0.0	SAND-B
	SLEEVE	14.5	26.5	26.5	48.0	48.0	IRON	IRON	0.0	SAND-B
BE.18N	CA STAB	12.0	13.5	13.5	13.5	13.5	LEAD	LEAD	0.0	NONE
	CAN	13.5	14.0	14.0	14.5	14.5	INCONEL	INCONEL	0.0	SAND-B
	SLEEVE	14.5	21.5	21.6	48.0	48.0	IRON	ZIRC	0.0	SAND-B

Table 4-4. (Continued)

CONCEPT	ELEMENT	INSIDE MATERIAL ID	INSIDE MATERIAL OD	OUTSIDE MATERIAL OD	FILLER OD	GAP OD	INSIDE MATERIAL	OUTSIDE MATERIAL	COATING DELAY (YRS)	FILLER
BE.19N	CA STAB	12.0	13.5	13.5	13.5	13.5	LEAD	LEAD	0.0	NONE
	CAN	13.5	14.0	14.0	14.5	14.5	INCONEL	INCONEL	0.0	SAND-B
	SLEEVE	14.5	21.5	22.0	48.0	48.0	IRON	ZIRC	0.0	SAND-B
BE.20N	CA STAB	12.0	13.5	13.5	13.5	13.5	LEAD	LEAD	0.0	NONE
	CAN	13.5	14.0	14.0	14.5	14.5	INCONEL	INCONEL	0.0	SAND-B
	SLEEVE	14.5	15.0	15.3	48.0	48.0	IRON	ZIRC	0.0	SAND-B
BE.21N	CA STAB	12.0	13.5	13.5	13.5	13.5	LEAD	LEAD	0.0	NONE
	CAN	13.5	14.0	14.0	14.5	14.5	INCONEL	INCONEL	0.0	SAND-B
	SLEEVE	14.5	26.5	26.8	48.0	48.0	IRON	ZIRC	0.0	SAND-B
BE.22N	CA STAB	12.0	13.5	13.5	13.5	13.5	LEAD	LEAD	0.0	NONE
	CAN	13.5	14.0	14.0	14.5	14.5	ZIRC	ZIRC	0.0	SAND-B
	SLEEVE	14.5	21.5	21.5	48.0	48.0	IRON	IRON	0.0	SAND-B
BE.23N	CA STAB	12.0	13.5	13.5	13.5	13.5	LEAD	LEAD	0.0	NONE
	CAN	13.5	14.0	14.0	14.5	14.5	ZIRC	ZIRC	0.0	SAND-B
	SLEEVE	14.5	26.5	26.5	48.0	48.0	IRON	IRON	0.0	SAND-B
BE.24N	CA STAB	12.0	13.5	13.5	13.5	13.5	LEAD	LEAD	0.0	NONE
	CAN	13.5	14.0	14.0	14.5	14.5	ZIRC	ZIRC	0.0	SAND-B
	SLEEVE	14.5	21.5	21.6	48.0	48.0	IRON	ZIRC	0.0	SAND-B
BE.25N	CA STAB	12.0	13.5	13.5	13.5	13.5	LEAD	LEAD	0.0	NONE
	CAN	13.5	14.0	14.0	14.5	14.5	ZIRC	ZIRC	0.0	SAND-B
	SLEEVE	14.5	21.5	22.0	48.0	48.0	IRON	ZIRC	0.0	SAND-B
BE.26N	CA STAB	12.0	13.5	13.5	13.5	13.5	LEAD	LEAD	0.0	NONE
	CAN	13.5	14.0	14.0	14.5	14.5	304SST	304SST	0.0	BENT
	SLEEVE	14.5	21.5	21.5	48.0	48.0	IRON	IRON	0.0	BENT
BE.27N	CA STAB	12.0	13.5	13.5	13.5	13.5	LEAD	LEAD	0.0	NONE
	CAN	13.5	14.0	14.0	14.5	14.5	304SST	304SST	0.0	BENT
	SLEEVE	14.5	21.5	21.6	48.0	48.0	IRON	ZIRC	0.0	BENT

Table 4-4. (Continued)

CONCEPT	ELEMENT	INSIDE MATERIAL ID	INSIDE MATERIAL OD	OUTSIDE MATERIAL OD	FILLER OD	GAP OD	INSIDE MATERIAL	OUTSIDE MATERIAL	COATING DELAY (YRS)	FILLER
BE.28N	CA STAB	12.0	13.5	13.5	13.5	13.5	LEAD	LEAD	0.0	NONE
	CAN	13.5	14.0	14.0	14.5	14.5	304SST	304SST	0.0	CLINO
	SLEEVE	14.5	21.5	21.5	48.0	48.0	IRON	IRON	0.0	CLINO
BE.29N	CA STAB	12.0	13.5	13.5	13.5	13.5	LEAD	LEAD	0.0	NONE
	CAN	13.5	14.0	14.0	14.5	14.5	304SST	304SST	0.0	CLINO
	SLEEVE	14.5	21.5	21.6	48.0	48.0	IRON	ZIRC	0.0	CLINO
BE.30N	CA STAB	12.0	13.5	13.5	13.5	13.5	LEAD	LEAD	0.0	NONE
	CAN	13.5	14.0	14.0	14.5	14.5	304SST	304SST	0.0	SAND-B
	SLEEVE	14.5	15.0	15.0	20.0	20.0	IRON	IRON	0.0	SAND-B
BE.31N	CA STAB	12.0	13.5	13.5	13.5	13.5	LEAD	LEAD	0.0	NONE
	CAN	13.5	14.0	14.0	14.5	14.5	304SST	304SST	0.0	SAND-B
	SLEEVE	14.5	15.0	15.0	36.0	36.0	IRON	IRON	0.0	SAND-B
BE.32N	CA STAB	12.0	13.5	13.5	13.5	13.5	LEAD	LEAD	0.0	NONE
	CAN	13.5	14.0	14.0	14.5	14.5	304SST	304SST	0.0	SAND-B
	SLEEVE	14.5	15.0	15.3	29.0	29.0	IRON	ZIRC	0.0	SAND-B
BE.33N	CA STAB	12.0	13.5	13.5	13.5	13.5	LEAD	LEAD	0.0	NONE
	CAN	13.5	14.0	14.0	14.5	14.5	304SST	304SST	0.0	SAND-B
	SLEEVE	14.5	15.0	15.3	36.0	36.0	IRON	ZIRC	0.0	SAND-B
BE.34N	CA STAB	12.0	13.5	13.5	13.5	13.5	LEAD	LEAD	0.0	NONE
	CAN	13.5	14.0	14.0	14.5	14.5	304SST	304SST	0.0	SAND-B
	SLEEVE	14.5	21.5	21.5	48.0	48.0	IRON	IRON	100.0	SAND-B
BE.35N	CA STAB	12.0	13.5	13.5	13.5	13.5	LEAD	LEAD	0.0	NONE
	CAN	13.5	14.0	14.0	14.5	14.5	304SST	304SST	0.0	SAND-B
	SLEEVE	14.5	21.5	21.6	48.0	48.0	IRON	ZIRC	100.0	SAND-B
BE.36N	CA STAB	12.0	13.5	13.5	13.5	13.5	LEAD	LEAD	0.0	NONE
	CAN	13.5	14.0	14.0	14.0	14.3	ZIRC	ZIRC	0.0	NONE
	SLEEVE	14.3	21.3	21.3	47.8	47.8	IRON	IRON	0.0	SAND-B

Table 4-4. (Continued)

CONCEPT	ELEMENT	INSIDE MATERIAL ID	INSIDE MATERIAL OD	OUTSIDE MATERIAL OD	FILLER OD	CAP OD	INSIDE MATERIAL	OUTSIDE MATERIAL	COATING DELAY (YRS)	FILLER
BE.37N	CA STAB	12.0	13.5	13.5	13.5	13.5	LEAD	LEAD	0.0	NONE
	CAN	13.5	14.0	14.0	14.0	14.5	ZIRC	ZIRC	0.0	NONE
	SLEEVE	14.5	21.5	21.5	48.0	48.0	IRON	IRON	0.0	SAND-B
BE.38N	CA STAB	12.0	13.5	13.5	13.5	13.5	LEAD	LEAD	0.0	NONE
	CAN	13.5	14.0	14.0	14.0	15.0	ZIRC	ZIRC	0.0	NONE
	SLEEVE	15.0	22.0	22.0	48.5	48.5	IRON	IRON	0.0	SAND-B
BE.39N	CA STAB	12.0	13.5	13.5	13.5	13.5	LEAD	LEAD	0.0	NONE
	CAN	13.5	14.0	14.0	14.0	16.0	ZIRC	ZIRC	0.0	NONE
	SLEEVE	16.0	23.0	23.0	49.5	49.5	IRON	IRON	0.0	SAND-B
C.7	STAB	12.0	12.0	12.0	12.0	13.5	HELIUM.	HELIUM	0.0	NONE
	CAN	13.5	15.5	15.5	16.0	16.0	ZIRC	ZIRC	0.0	SAND-B
	O PACK	16.0	18.0	18.0	40.0	40.0	ZIRC	ZIRC	0.0	SAND-B
C1.1	STAB	12.0	13.5	13.5	13.5	13.5	INCONEL	INCONEL	0.0	NONE
	CAN	13.5	14.0	14.0	14.5	14.5	INCONEL	INCONEL	0.0	SAND-B
	O PACK	14.5	15.0	15.0	15.5	15.5	304SST	304SST	0.0	SAND-B
	SLEEVE	15.5	22.5	22.5	45.0	45.0	IRON	IRON	0.0	SAND-B
C1.3	STAB	12.0	12.0	12.0	12.0	13.5	HELIUM.	HELIUM	0.0	NONE
	CAN	13.5	14.0	14.0	14.5	14.5	INCONEL	INCONEL	0.0	SAND-B
	O PACK	14.5	15.0	15.0	15.5	15.5	304SST	304SST	0.0	SAND-B
	SLEEVE	15.5	22.5	22.5	45.0	45.0	IRON	IRON	0.0	SAND-B
C1.6	STAB	12.0	13.5	13.5	13.5	13.5	ZIRC	ZIRC	0.0	NONE
	CAN	13.5	14.0	14.0	14.5	14.5	ZIRC	ZIRC	0.0	SAND-B
	O PACK	14.5	15.0	15.0	15.5	15.5	ZIRC	ZIRC	0.0	SAND-B
	SLEEVE	15.5	16.5	16.5	24.0	24.0	STEEL	STEEL	0.0	SAND-B
D.1	STAB	12.0	12.0	12.0	12.0	13.5	HELIUM	HELIUM	0.0	NONE
	CAN	13.5	14.0	14.0	14.5	14.5	STEEL	STEEL	0.0	SAND-B
	SLEEVE	14.5	21.5	21.5	48.0	48.0	IRON	IRON	10.0	SAND-B

Table 4-4. (Continued)

CONCEPT	ELEMENT	INSIDE MATERIAL ID	INSIDE MATERIAL OD	OUTSIDE MATERIAL OD	FILLER OD	GAP OD	INSIDE MATERIAL	OUTSIDE MATERIAL	COATING DELAY (YRS)	FILLER
D.3	STAB	12.0	13.5	13.5	13.5	13.5	STEEL	STEEL	0.0	NONE
	CAN	13.5	14.0	14.0	14.5	14.5	STEEL	STEEL	0.0	SAND-B
	SLEEVE	14.5	21.5	21.5	48.0	48.0	IRON	IRON	100.0	SAND-B
D.5	STAB	12.0	13.5	13.5	13.5	13.5	STEEL	STEEL	0.0	NONE
	CAN	13.5	14.0	14.0	14.5	14.5	STEEL	STEEL	0.0	SAND-B
	SLEEVE	14.5	16.5	16.5	48.0	48.0	ZIRC	ZIRC	100.0	SAND-B
D1.2	STAB	12.0	13.5	13.5	13.5	13.5	304SST	304SST	0.0	NONE
	CAN	13.5	14.0	14.0	14.5	14.5	304SST	304SST	0.0	SAND-B
	SLEEVE	14.5	22.5	22.5	48.0	48.0	IRON	IRON	100.0	SAND-B
D1.5	STAB	12.0	13.5	13.5	13.5	13.5	304SST	304SST	0.0	NONE
	CAN	13.5	14.0	14.0	14.5	14.5	304SST	304SST	0.0	SAND-B
	SLEEVE	14.5	15.0	15.0	20.0	20.0	304SST	304SST	100.0	SAND-B
D2.1	STAB	12.0	13.5	13.5	13.5	13.5	INCONEL	INCONEL	0.0	NONE
	CAN	13.5	14.0	14.0	14.5	14.5	INCONEL	INCONEL	0.0	SAND-B
	O PACK	14.5	15.0	15.0	15.5	15.5	INCONEL	INCONEL	0.0	SAND-B
	SLEEVE	15.5	23.5	23.5	48.0	48.0	IRON	IRON	100.0	SAND-B
D2.8	STAB	12.0	13.5	13.5	13.5	13.5	ZIRC	ZIRC	0.0	NONE
	CAN	13.5	14.0	14.0	14.5	14.5	ZIRC	ZIRC	0.0	SAND-B
	O PACK	14.5	15.0	27.0	27.5	27.5	ZIRC	LEAD	0.0	SAND-B
	SLEEVE	27.5	28.0	28.0	48.0	48.0	ZIRC	ZIRC	100.0	CLINO
E.3	CA STAB	12.0	13.5	13.5	13.5	13.5	LEAD	LEAD	0.0	NONE
	CAN	13.5	14.0	14.2	20.0	20.0	304SST	ZIRC	0.0	SAND-B
E.4	CA STAB	12.0	13.5	13.5	13.5	13.5	LEAD	LEAD	0.0	NONE
	CAN	13.5	14.0	14.0	20.0	20.0	ZIRC	ZIRC	0.0	SAND-B
E.24	CA STAB	12.0	13.5	13.5	13.5	13.5	LEAD	LEAD	0.0	NONE
	CAN	13.5	20.5	20.7	40.0	40.0	304SST	ZIRC	0.0	SAND-B

Table 4-4. (Continued)

CONCEPT	ELEMENT	INSIDE MATERIAL ID	INSIDE MATERIAL OD	OUTSIDE MATERIAL OD	FILLER OD	CAP OD	INSIDE MATERIAL	OUTSIDE MATERIAL	COATING DELAY (YRS)	FILLER
E.1N	CA STAB	12.0	13.5	13.5	13.5	13.5	LEAD	LEAD	0.0	NONE
	CAN	13.5	14.0	14.0	48.0	48.0	STEEL	STEEL	0.0	SAND-B
E.2N	CA STAB	12.0	13.5	13.5	13.5	13.5	LEAD	LEAD	0.0	NONE
	CAN	13.5	14.0	14.0	48.0	48.0	ZIRC	ZIRC	0.0	SAND-B
E.3N	CA STAB	12.0	13.5	13.5	13.5	13.5	LEAD	LEAD	0.0	NONE
	CAN	13.5	14.0	14.0	48.0	48.0	INCONEL	INCONEL	0.0	SAND-B
E.4N	CA STAB	12.0	13.5	13.5	13.5	13.5	LEAD	LEAD	0.0	NONE
	CAN	13.5	14.0	14.0	48.0	48.0	304SST	304SST	0.0	SAND-B
E.5N	CA STAB	12.0	13.5	13.5	13.5	13.5	LEAD	LEAD	0.0	NONE
	CAN	13.5	14.0	14.0	48.0	48.0	COPPER	COPPER	0.0	SAND-B
E.6N	CA STAB	12.0	13.5	13.5	13.5	13.5	LEAD	LEAD	0.0	NONE
	CAN	13.5	14.0	14.0	48.0	48.0	LEAD	LEAD	0.0	SAND-B
E.7N	CA STAB	12.0	13.5	13.5	13.5	13.5	LEAD	LEAD	0.0	NONE
	CAN	13.5	14.0	14.0	48.0	48.0	IRON	IRON	0.0	SAND-B
E.8N	CA STAB	12.0	13.5	13.5	13.5	13.5	LEAD	LEAD	0.0	NONE
	CAN	13.5	19.5	19.5	48.0	48.0	STEEL	STEEL	0.0	SAND-B
E.9N	CA STAB	12.0	13.5	13.5	13.5	13.5	LEAD	LEAD	0.0	NONE
	CAN	13.5	19.5	19.5	48.0	48.0	ZIRC	ZIRC	0.0	SAND-B
E.10N	CA STAB	12.0	13.5	13.5	13.5	13.5	LEAD	LEAD	0.0	NONE
	CAN	13.5	19.5	19.5	48.0	48.0	INCONEL	INCONEL	0.0	SAND-B
E.11N	CA STAB	12.0	13.5	13.5	13.5	13.5	LEAD	LEAD	0.0	NONE
	CAN	13.5	19.5	19.5	48.0	48.0	304SST	304SST	0.0	SAND-B

Table 4-4. (Continued)

CONCEPT	ELEMENT	INSIDE MATERIAL ID	INSIDE MATERIAL OD	OUTSIDE MATERIAL OD	FILLER OD	GAP OD	INSIDE MATERIAL	OUTSIDE MATERIAL	COATING DELAY (YRS)	FILLER
E.12N	CA STAB	12.0	13.5	13.5	13.5	13.5	LEAD	LEAD	0.0	NONE
	CAN	13.5	19.5	19.5	48.0	48.0	COPPER	COPPER	0.0	SAND-B
E.13N	CA STAB	12.0	13.5	13.5	13.5	13.5	LEAD	LEAD	0.0	NONE
	CAN	13.5	19.5	19.5	48.0	48.0	LEAD	LEAD	0.0	SAND-B
E.14N	CA STAB	12.0	13.5	13.5	13.5	13.5	LEAD	LEAD	0.0	NONE
	CAN	13.5	19.5	19.5	48.0	48.0	IRON	IRON	0.0	SAND-B
E.15N	CA STAB	12.0	13.5	13.5	13.5	13.5	LEAD	LEAD	0.0	NONE
	CAN	13.5	14.0	14.0	36.0	36.0	ZIRC	ZIRC	0.0	SAND-B
E.16N	CA STAB	12.0	13.5	13.5	13.5	13.5	LEAD	LEAD	0.0	NONE
	CAN	13.5	14.0	14.0	36.0	36.0	INCONEL	INCONEL	0.0	SAND-B
E.17N	CA STAB	12.0	13.5	13.5	13.5	13.5	LEAD	LEAD	0.0	NONE
	CAN	13.5	14.0	14.0	20.0	20.0	ZIRC	ZIRC	0.0	SAND-B
E.18N	CA STAB	12.0	13.5	13.5	13.5	13.5	LEAD	LEAD	0.0	NONE
	CAN	13.5	14.0	14.0	20.0	20.0	INCONEL	INCONEL	0.0	SAND-B
E.19N	CA STAB	12.0	13.5	13.5	13.5	13.5	LEAD	LEAD	0.0	NONE
	CAN	13.5	14.0	14.0	48.0	48.0	ZIRC	ZIRC	0.0	BENT
E.20N	CA STAB	12.0	13.5	13.5	13.5	13.5	LEAD	LEAD	0.0	NONE
	CAN	13.5	14.0	14.0	48.0	48.0	INCONEL	INCONEL	0.0	BENT
E.21N	CA STAB	12.0	13.5	13.5	13.5	13.5	LEAD	LEAD	0.0	NONE
	CAN	13.5	14.0	14.0	48.0	48.0	ZIRC	ZIRC	0.0	CLINO
E.22N	CA STAB	12.0	13.5	13.5	13.5	13.5	LEAD	LEAD	0.0	NONE
	CAN	13.5	14.0	14.0	48.0	48.0	INCONEL	INCONEL	0.0	CLINO

Table 4-4. (Continued)

CONCEPT	ELEMENT	INSIDE MATERIAL ID	INSIDE MATERIAL OD	OUTSIDE MATERIAL OD	FILLER OD	CAP OD	INSIDE MATERIAL	OUTSIDE MATERIAL	COATING DELAY (YRS)	FILLER
E.23N	CA STAB	12.0	13.5	13.5	13.5	13.5	LEAD	LEAD	0.0	NONE
	CAN	13.5	14.0	14.0	48.0	48.0	STEEL	STEEL	0.0	SAND-B
E.24N	CA STAB	12.0	13.5	13.5	13.5	13.5	LEAD	LEAD	0.0	NONE
	CAN	13.5	14.0	14.0	48.0	48.0	ZIRC	ZIRC	0.0	SAND-B
E.25N	CA STAB	12.0	13.5	13.5	13.5	13.5	LEAD	LEAD	0.0	NONE
	CAN	13.5	14.0	14.0	48.0	48.0	INCONEL	INCONEL	0.0	SAND-B
E.26N	CA STAB	12.0	13.5	13.5	13.5	13.5	LEAD	LEAD	0.0	NONE
	CAN	13.5	14.0	14.0	48.0	48.0	304SST	304SST	0.0	SAND-B
E.27N	CA STAB	12.0	13.5	13.5	13.5	13.5	LEAD	LEAD	0.0	NONE
	CAN	13.5	14.0	14.0	48.0	48.0	COPPER	COPPER	0.0	SAND-B
E.28N	CA STAB	12.0	13.5	13.5	13.5	13.5	LEAD	LEAD	0.0	NONE
	CAN	13.5	14.0	14.0	48.0	48.0	LEAD	LEAD	0.0	SAND-B
E.29N	CA STAB	12.0	13.5	13.5	13.5	13.5	LEAD	LEAD	0.0	NONE
	CAN	13.5	14.0	14.0	48.0	48.0	IRON	IRON	0.0	SAND-B
E.30N	CA STAB	12.0	13.5	13.5	13.5	13.5	LEAD	LEAD	0.0	NONE
	CAN	13.5	14.0	14.1	48.0	48.0	STEEL	ZIRC	0.0	SAND-B
E.31N	CA STAB	12.0	13.5	13.5	13.5	13.5	LEAD	LEAD	0.0	NONE
	CAN	13.5	14.0	14.5	48.0	48.0	STEEL	ZIRC	0.0	SAND-B

5. RESULTS

5.1 "BEST" PACKAGES FROM PREVIOUS WORK

In previous barrier performance studies (Lester, 1979)- (Stula, 1980a), various waste package designs were evaluated in four geologic media: salt, shale, basalt, and granite. In each package design category, the case resulting in the longest leach begin time was considered to be the "best" design case of that category. For comparison, performance of these "best" case designs was evaluated with the current version of the BARIER code. This comparison is presented in Table 5-1 for salt, shale and basalt geologies. A more detailed summary of calculations for these cases in the current study is presented in Table 5-2. The current model generally predicts leach begin times in basalt which are lower than in previous results. Current results compared to previous results in salt and shale give lower leach begin times for long-lived packages and higher leach begin times for relatively short-lived packages.

For completeness, Table 5-3 presents the best package designs in the current study for each geology. However, it should be noted that not every package design was evaluated in all of the geologies considered.

5.2 CAST STABILIZER CONCEPT (Concept E)

On the basis of previous work, a package design utilizing a solid cast stabilizer (Concept E) appeared to be one of the more promising package design candidates. As a result, a large part of the current study deals with Concept E and its design variations.

Results of calculations for the Concept E package design variations are tabulated in Table 5-4. Calculations were performed primarily in creeping geologic media with most of the cases evaluated in salt. Comparison of package designs varying only in canister material shows a large variance in leach begin time. Along with a significant dependence on canister thickness (E.1N - E.14N), this indicates that corrosion resistance is the life determining factor for the Concept E design. The use of different backfill materials and variable backfill

Table 5-1. Comparison of Previous Best Package Designs with Current Results.

Geology	Package Design	Leach Begin Time, (yrs)		Release Begin Time for Plutonium, (yrs) (Oxic Conditions)	Release End Time for Plutonium, (yrs) (Oxic Conditions)
		Previous	Current		
Salt	A.1	14	1	2.8×10^4	2.8×10^5
	A.5	14	5	5	4.0×10^5
	B1.11	1,900	1,000	2.9×10^4	2.8×10^5
	C1.1	13	20	2.8×10^4	2.8×10^5
	C1.3	13	20	2.8×10^4	2.8×10^5
	D.3	120	110	2.8×10^4	2.8×10^5
	D1.2	130	110	2.8×10^4	2.8×10^5
	D2.1	120	120	2.8×10^4	2.8×10^5
	E.4	6,300	2,500	2,500	3.9×10^5
Shale	A.1	30	1	2.8×10^4	2.8×10^5
	A.5	30	820	820	4.0×10^5
	B1.11	1,900	1,100	2.9×10^4	2.8×10^5
	C1.1	27	80	2.8×10^4	2.8×10^5
	C1.3	27	80	2.8×10^4	2.8×10^5
	D.1	37	80	2.8×10^4	2.8×10^5
	D1.2	140	190	2.8×10^4	2.8×10^5
	D2.1	140	200	2.8×10^4	2.8×10^5
	E.24	14,000	13,000	4.1×10^4	2.9×10^5
Basalt	A.10	25,000	10,000	2.9×10^4	2.9×10^5
	B.8	25,000	10,000	1.0×10^4	4.2×10^5
	B1.7	810	4,000	4,000	2.7×10^5
	C.7	49,000	20,000	4.6×10^4	2.9×10^5
	C1.6	12,000	4,900	4,900	3.5×10^5
	D.5	25,000	10,000	3.8×10^4	2.9×10^5
	D1.5	1,700	1,800	1,800	4.1×10^5
	D2.8	19,000	13,000	4.1×10^4	2.9×10^5

Table 5-2. Previous Best* Package Design Results with Current BARIER Model.

PACKAGE DESIGN	MEDIA	STABILIZER MATERIAL	CANISTER MATERIAL	CANISTER THICKNESS (INCHES)	SLEEVE MATERIAL	SLEEVE THICKNESS (INCHES)	BACKFILL MATERIAL	BACKFILL THICKNESS (INCHES)	MAX. WASTE TEMP., (°K)	LEACH BEGIN TIME (YRS) ANOXIC	LEACH BEGIN TIME (YRS) OXIC	Release Begin Time for Plutonium, (yrs) (Oxic Conditions)	Release End Time for Plutonium, (yr. (Oxic Conditions)
A.1	Salt	304SST	304SST	0.25	---	---	Sand-B	13.0	579	1	1	2.8×10^4	2.8×10^5
A.5		304SST	304SST (1.0" Thick)	1.0	---	---	Sand-B	2.25	494	100	5	5	4.0×10^5
A.10		Zircaloy	Zircaloy (1.0" Thick)	1.0	---	---	Sand-B	2.25	494	5,100	5,100	5,100	4.0×10^5
B.0		Steel	Steel	0.25	Zircaloy (overpack)	1.0	Sand-B	1.75	491	4,800	4,800	4,800	4.1×10^5
B1.7		Steel	Steel	0.25	Steel (+4.0" Lead)	0.25	Clino	3.5	520	2	2	2	2.6×10^5
B1.11		Steel	Steel	0.25	Iron (+0.1" Zircaloy)	4.0	Sand-B	12.65	551	1,100	1,000	2.9×10^4	2.8×10^5
C.7		Nalium	Zircaloy	1.0	Zircaloy (overpack)	1.0	Sand-B	11.0	559	9,100	9,100	3.6×10^4	2.8×10^5
C1.1		Inconel	Inconel	0.25	Iron (+0.25" 304SST overpack)	3.5	Sand-B	11.25	549	65	20	2.8×10^4	2.8×10^5
C1.3		Nalium	Inconel	0.25	Iron (+0.25" 304SST overpack)	3.5	Sand-B	11.25	551	65	20	2.8×10^4	2.8×10^5
C1.6		Zircaloy	Zircaloy	0.25	Steel (+0.25" Zircaloy overpack)	0.5	Sand-B	3.75	514	30	30	30	3.4×10^5
D.1		Nalium	Steel	0.25	Iron	3.5	Sand-B	13.25	559	65	19	2.8×10^4	2.8×10^5
D.3		Steel	Steel	0.25	Iron	3.5	Sand-B	13.25	557	160	110	2.8×10^4	2.8×10^5
D.5		Steel	Steel	0.25	Zircaloy	1.0	Sand-B	15.75	585	4,400	4,400	3.2×10^4	2.8×10^5
D1.2		304SST	304SST	0.25	Iron	4.0	Sand-B	12.75	562	170	110	2.8×10^4	2.8×10^5
D1.5		304SST	304SST	0.25	304SST	0.25	Sand-B	2.5	501	2	2	2	4.0×10^5
D2.1		Inconel	Inconel	0.25	Iron (+0.25" Inconel overpack)	4.0	Sand-B	12.25	551	180	120	2.8×10^4	2.8×10^5
D2.8		Zircaloy	Zircaloy	0.25	Zircaloy (+0.25" Zirc overpack with 4.0" lead cladding)	0.25	Clino	10.0	574	30	30	2.8×10^4	2.8×10^5
E.3		Lead	304SST (+0.1" Zirc)	0.25	---	---	Sand-B	2.9	503	1,700	1,000	1,000	3.9×10^5
E.4		Lead	Zircaloy	0.25	---	---	Sand-B	3.0	505	2,600	2,500	2,500	3.9×10^5
E.24		Lead	304SST (+0.1" Zirc)	3.5	---	---	Sand-B	9.65	530	9,800	1,200	3.0×10^4	2.9×10^5

*Best Package designs from (Lester, 1979) and (Stula, 1980a)

Table 5-2. Previous Best* Package Design Results with Current BARIER Model. (Continued)

PACKAGE DESIGN	MEDIA	SEAMLESS CAN MATERIAL	CANISTER MATERIAL	CANISTER THICKNESS (INCHES)	SLEEVE MATERIAL	SLEEVE THICKNESS (INCHES)	BACKFILL MATERIAL	BACKFILL THICKNESS (INCHES)	MAX. WASTE TEMP., (°K)	LEACH MEDIA TIME (YRS)		Release Begin Time for Plutonium, (yrs) (Basic Conditions)	Release End Time for Plutonium, (yrs) (Basic Conditions)
										Anoxic	Oxic		
A.1	Shale	304SS	304SS	0.25	---	---	Sand-B	13.0	568	1,000	350	2.9×10^4	2.9×10^5
A.5		304SS	304SS (1.0" thick)	1.0	---	---	Sand-B	2.25	483	8,000	2,900	2.9×10^4	4.1×10^5
A.10		Zircaloy	Zircaloy (1.0" thick)	1.0	---	---	Sand-B	2.25	483	9,600	9,600	9,600	4.1×10^5
B.8		Steel	Steel	0.25	Zircaloy (overpack)	1.0	Sand-B	1.75	480	9,600	9,600	9,600	4.2×10^5
B8.7		Steel	Steel	0.25	Steel (+4.0" Lead)	0.25	Clino	3.5	500	4	2	2	2.7×10^5
B8.11		Steel	Steel	0.25	Iron (+0.1" Zircaloy)	4.0	Sand-B	12.65	540	1,500	1,100	3.0×10^4	2.9×10^5
C.7		Nellum	Zircaloy	1.0	Zircaloy (overpack)	1.0	Sand-B	11.0	548	10,000	10,000	4.6×10^4	2.9×10^5
C8.1		Inconel	Inconel	0.25	Iron (+0.25" 304SS] over-pack)	3.5	Sand-B	11.25	538	1,000	820	2.9×10^4	2.9×10^5
C8.3		Nellum	Inconel	0.25	Iron (+0.25" 304SS] over-pack	3.5	Sand-B	11.25	540	1,000	820	2.9×10^4	2.9×10^5
C8.6		Zircaloy	Zircaloy	0.25	Steel (+0.25" Zirc overpack)	0.5	Sand-B	3.75	503	4,000	4,300	4,300	3.5×10^5
D.1		Nellum	Steel	0.25	Iron	3.5	Sand-B	13.25	549	420	110	2.9×10^4	3.5×10^5
D.3		Steel	Steel	0.25	Iron	3.5	Sand-B	13.25	546	510	200	2.9×10^4	3.5×10^5
D.5		Steel	Steel	0.25	Zircaloy	1.0	Sand-B	16.75	574	9,300	9,300	3.7×10^4	3.5×10^5
D8.2		304SS	304SS	0.25	Iron	4.0	Sand-B	12.75	541	2,000	670	2.9×10^4	3.5×10^5
D8.5		304SS	304SS	0.25	304SS	0.25	Sand-B	2.5	490	2,400	950	950	4.1×10^5
D2.1		Inconel	Inconel	0.25	Iron (+0.25" Inconel over-pack)	4.0	Sand-B	12.25	540	600	370	2.9×10^4	2.9×10^5
D2.8		Zircaloy	Zircaloy	0.25	Zircaloy (+0.25" Zirc overpack with 6.0" lead cladding)	0.25	Clino	10.0	563	12,000	12,000	3.0×10^4	2.9×10^5
E.3		Lead	304SS (+0.1" Zirc)	0.25	---	---	Sand-B	2.9	492	4,300	2,600	2,600	3.9×10^5
E.6		Lead	Zircaloy	0.25	---	---	Sand-B	3.0	494	3,300	3,300	3,300	3.9×10^5
E.10		Lead	304SS (+0.1" Zirc)	3.5	---	---	Sand-B	9.65	527	37,000	13,000	4.1×10^4	2.9×10^5

*Best Package designs from (Lester, 1979) and (Stula, 1980a)

Table 5-2. Previous Best* Package Design Results with Current BARIER Model. (Continued)

PACKAGE DESIGN	MEDIA	STABILIZER MATERIAL	CANISTER MATERIAL	CANISTER THICKNESS (INCHES)	SLEEVE MATERIAL	SLEEVE THICKNESS (INCHES)	BACKFILL MATERIAL	BACKFILL THICKNESS (INCHES)	MAX. WASTE TEMP., (°K)	LEACH BEGIN TIME (YRS) ANOXIC	LEACH BEGIN TIME (YRS) OXIC	Release Begin Time for Plutonium, (yrs) (Oxic Conditions)	Release End Time for Plutonium, (yrs) (Oxic Conditions)
A.1	Basalt	304SSI	304SSI	0.25	---	---	Sand-B	13.0	586	2,500	820	2.9×10^4	2.9×10^5
A.5		304SSI	304SSI (1.0" Thick)	1.0	---	---	Sand-B	2.25	581	10,000	3,300	3,300	4.1×10^5
A.10		Zircaloy	Zircaloy (1.0" Thick)	1.0	---	---	Sand-B	2.25	581	10,000	10,000	2.9×10^4	2.9×10^5
B.8		Steel	Steel	0.25	Zircaloy (overpack)	1.0	Sand-B	1.75	498	10,000	10,000	1.0×10^4	4.2×10^5
B1.7		Steel	Steel	0.25	Steel (+4.0" overpack)	0.25	Clino	3.5	527	4,300	4,000	4,000	2.7×10^5
C.7		Nelium	Zircaloy	1.0	Zircaloy (overpack)	1.0	Sand-B	11.0	566	20,000	20,000	4.6×10^4	2.9×10^5
C1.1		Inconel	Inconel	0.25	Iron (+0.25" 304SSI overpack)	3.5	Sand-B	11.25	556	3,000	1,400	3.0×10^4	2.9×10^5
C1.3		Nelium	Inconel	0.25	Iron (+0.25" 304SSI overpack)	3.5	Sand-B	11.25	556	3,000	1,400	3.0×10^4	2.9×10^5
C1.6		Zircaloy	Zircaloy	0.25	Steel (+0.25" Zirc overpack)	0.5	Sand-B	3.75	521	5,100	4,900	4,900	3.5×10^5
D.1		Nelium	Steel	0.25	Iron	3.5	Sand-B	13.25	566	570	220	2.9×10^4	2.9×10^5
D.3		Steel	Steel	0.25	Iron	3.5	Sand-B	13.25	564	660	210	2.9×10^4	2.9×10^5
D.5		Steel	Steel	0.25	Zircaloy	1.0	Sand-B	15.75	592	10,000	10,000	3.0×10^4	2.9×10^5
D1.2		Steel	304SSI	0.25	Iron	4.0	Sand-B	12.75	559	3,100	1,000	3.0×10^4	2.9×10^5
D1.5		304SSI	304SSI	0.25	304SSI	0.25	Sand-B	2.5	588	5,000	5,000	5,000	4.1×10^5
D2.1		Inconel	Inconel	0.25	Iron (+0.25" Inconel overpack)	4.0	Sand-B	12.25	558	800	1,200	3.0×10^4	2.9×10^5
D2.8		Zircaloy	Zircaloy	0.25	Zircaloy (+0.25" Zirc overpack with 4.0" Lead)	0.25	Clino	10.0	581	13,000	13,000	4.1×10^4	2.9×10^5
E.3		Lead	304SSI (+0.1" Zirc)	0.25	---	---	Sand-B	2.9	510	4,300	2,600	2,600	3.9×10^5
E.4		Lead	Zircaloy	0.25	---	---	Sand-B	3.0	512	3,300	3,300	3,300	3.9×10^5
E.26		Lead	304SSI (+0.1" Zirc)	3.5	---	---	Sand-B	9.65	545	37,000	13,000	4.1×10^4	2.9×10^5

Table 5-3. Best Package Designs in Current Study (Oxic Conditions).

Geology	Package Design	Leach Begin Time, (yrs)	Release Begin Time for Plutonium, (yrs) (Oxic Conditions)	Release End Time for Plutonium, (yrs) (Oxic Conditions)
Salt	BE.12N, BE.25N	5,000	3.3×10^4	2.9×10^5
	B1.18N	29,000	5.4×10^4	2.8×10^5
	E.9N	30,000	8.1×10^4	2.9×10^5
Shale	B1.21N	2,600	3.0×10^4	2.8×10^5
	BE.25N	5,900	3.4×10^4	2.9×10^5
	E.13N	3,800	3.2×10^4	2.9×10^5
Basalt	B1.9N	12,000	6.7×10^4	2.9×10^5
	BE.12N	5,900	3.4×10^4	2.9×10^5

Table 5-4. Concept E Results in Current Study.

PACKAGE DESIGN	MEDIA	STABILIZER MATERIAL	CANISTER MATERIAL	CANISTER THICKNESS (INCHES)	SLEEVE MATERIAL	SLEEVE THICKNESS (INCHES)	BACKFILL MATERIAL	BACKFILL THICKNESS (INCHES)	MAX. WASTE TEMP., (°F)	LEACH PLUG TIME (YRS)		Release Begin Time for Plutonium, (yrs) (Oxic Conditions)	Release End Time for Plutonium, (yrs) (Oxic Conditions)
										ANOXIC	OXIC		
E.1A	Salt	Lead	Steel	0.25	---	---	Sand-B	17.0	599	160	25	5.7×10^4	2.9×10^5
E.2A		Lead	Zircaloy	0.25	---	---	Sand-B	17.0	599	2,600	2,600	5.9×10^4	2.9×10^5
E.3A		Lead	Inconel	0.25	---	---	Sand-B	17.0	599	900	85	5.7×10^4	2.9×10^5
E.4A		Lead	304SST	0.25	---	---	Sand-B	17.0	599	690	30	5.7×10^4	2.9×10^5
E.5A		Lead	Copper	0.25	---	---	Sand-B	17.0	599	170	30	5.7×10^4	2.9×10^5
E.6A		Lead	Lead	0.25	---	---	Sand-B	17.0	599	90	30	5.7×10^4	2.9×10^5
E.7A		Lead	Iron	0.25	---	---	Sand-B	17.0	599	75	25	5.7×10^4	2.9×10^5
E.8A		Lead	Steel	3.0	---	---	Sand-B	14.25	563	1,100	35	2.9×10^4	2.9×10^5
E.9A		Lead	Zircaloy	3.0	---	---	Sand-B	14.25	564	30,000	30,000	8.1×10^4	2.9×10^5
E.10A		Lead	Inconel	3.0	---	---	Sand-B	14.25	564	30,000	700	2.9×10^4	2.9×10^5
E.11A		Lead	304SST	3.0	---	---	Sand-B	14.25	564	7,600	170	2.9×10^4	2.9×10^5
E.12A		Lead	Copper	3.0	---	---	Sand-B	14.25	563	1,300	90	2.9×10^4	2.9×10^5
E.13A		Lead	Lead	3.0	---	---	Sand-B	14.25	563	320	90	2.9×10^4	2.9×10^5
E.14A		Lead	Iron	3.0	---	---	Sand-B	14.25	563	150	30	2.9×10^4	2.9×10^5
E.15A		Lead	Zircaloy	0.25	---	---	Sand-B	11.0	568	2,600	2,600	3.1×10^4	2.9×10^5
E.16A		Lead	Inconel	0.25	---	---	Sand-B	11.0	568	900	85	2.9×10^4	2.9×10^5
E.17A		Lead	Zircaloy	0.25	---	---	Sand-B	3.0	505	2,600	2,600	2.5×10^4	3.9×10^5
E.18A		Lead	Inconel	0.25	---	---	Sand-B	3.0	506	900	85	84	3.9×10^5
E.19A		Lead	Zircaloy	0.25	---	---	Bent	17.0	698	---	---	---	---
E.20A		Lead	Inconel	0.25	---	---	Bent	17.0	698	---	---	---	---
E.21A		Lead	Zircaloy	0.25	---	---	Clino	17.0	698	---	---	---	---
E.22A		Lead	Inconel	0.25	---	---	Clino	17.0	698	---	---	---	---
E.23A		Lead	Steel	0.25	---	---	Sand-B	17.0	599	160	25	5.7×10^4	2.9×10^5
E.24A		Lead	Zircaloy	0.25	---	---	Sand-B	17.0	599	2,600	2,600	5.9×10^4	2.9×10^5
E.25A		Lead	Inconel	0.25	---	---	Sand-B	17.0	598	900	85	5.7×10^4	2.9×10^5
E.26A		Lead	304SST	0.25	---	---	Sand-B	17.0	599	690	30	5.7×10^4	2.9×10^5
E.27A		Lead	Copper	0.25	---	---	Sand-B	17.0	599	170	30	5.7×10^4	2.9×10^5
E.28A		Lead	Lead	0.25	---	---	Sand-B	17.0	599	90	30	5.7×10^4	2.9×10^5
E.29A		Lead	Iron	0.25	---	---	Sand-B	17.0	599	75	25	5.7×10^4	2.9×10^5
E.30A		Lead	Steel (0.05" liner)	0.25	---	---	Sand-B	17.0	598	670	640	5.75×10^4	2.85×10^5
E.31A		Lead	Steel (0.25" liner)	0.25	---	---	Sand-B	17.0	595	2,000	2,530	5.91×10^4	2.86×10^5

Table 5-4. Concept E Results in Current Study. (Continued)

PACKAGE MISSION	MEDIA	SHAFT LINER MATERIAL	CANISTER MATERIAL	CANISTER THICKNESS (INCHES)	SLEEVE MATERIAL	SLEEVE THICKNESS (INCHES)	BACKFILL MATERIAL	BACKFILL THICKNESS (INCHES)	MAX. WASTE TEMP., (°C)	LEACH BEGIN TIME (YRS)		Release Route Time for Plutonium, (yrs) (Basic Conditions)	Release End Time for Plutonium, (yrs) (Basic Conditions)
										Anoxic	Oxic		
0.12M	Shale	Lead	Copper	3.0	---	---	Sand-B	14.25	552	2,300	2,300	3.1×10^6	2.9×10^5
0.12M	Shale	Lead	Lead	3.0	---	---	Sand-B	14.25	552	3,000	3,000	3.2×10^6	2.9×10^5
0.12M	Shale	Lead	Iron	3.0	---	---	Sand-B	14.25	552	1,100	650	2.9×10^6	2.9×10^5
0.12M	Shale	Lead	Zircaloy	0.25	---	---	Sand-B	11.0	557	3,300	3,300	3.2×10^6	2.9×10^5
0.3	Salt	Lead	304SSI (+0.1" Zirc)	0.25	---	---	Sand-B	2.9	503	1,300	1,000	1,000	3.9×10^5
0.3	Shale	Lead	304SSI (+0.1" Zirc)	0.25	---	---	Sand-B	2.9	492	4,300	3,600	2,600	3.9×10^5
0.3	Basalt	Lead	304SSI (+0.1" Zirc)	0.25	---	---	Sand-B	2.9	510	4,300	2,600	2,600	3.9×10^5
0.6	Salt	Lead	Zircaloy	0.25	---	---	Sand-B	3.0	505	2,600	2,500	2,500	3.9×10^5
0.6	Shale	Lead	Zircaloy	0.25	---	---	Sand-B	3.0	484	3,300	3,300	3,300	3.9×10^5
0.6	Basalt	Lead	Zircaloy	0.25	---	---	Sand-B	3.0	512	3,300	3,300	3,300	3.9×10^5
0.24	Salt	Lead	304SSI (+0.10" Zirc)	0.25	---	---	Sand-B	9.65	530	9,600	1,200	3.0×10^6	2.9×10^5
0.24	Shale	Lead	304SSI (+0.10" Zirc)	0.25	---	---	Sand-B	9.65	527	37,000	33,000	4.1×10^6	2.9×10^5
0.24	Basalt	Lead	304SSI (+0.10" Zirc)	0.25	---	---	Sand-B	9.65	545	37,000	33,000	4.1×10^6	2.9×10^5

thickness was found to have a negligible effect on leach begin time. The use of the cast solid stabilizer provides sufficient package strength to make the effects of media crushing forces relatively small. Of the canister materials tested, Zircaloy canisters or canisters of other metals clad with Zircaloy were found to give the longest leach begin times. This is due primarily to the relatively small corrosion rates for Zircaloy.

As can be seen in Table 5-4, the radionuclide release breakthrough is delayed an enormous amount of time when appropriate backfill is used.

5.3 HEAVY SLEEVE CONCEPT (Concept B1)

Concept B1 originally consisted of a mild steel canister surrounded by a heavy sleeve designed to withstand high creep rate media crushing forces. In addition to the heavy sleeve, a backfill cushion was included for additional support. A protective sleeve cladding is also included in certain cases to increase the corrosion resistance of the sleeve. Previous work (Lester, 1979) had shown that backfill thickness had little or no effect on package performance but that sleeve design was significant in creeping media.

In addition, it was shown that of the materials considered for a sleeve cladding material, Zircaloy provided the best resistance. In the current study, sleeve material and thickness as well as sleeve cladding thickness are varied.

Results of the calculations for the Concept B1 package design variations are tabulated in Table 5-5. Conclusions that can be drawn from the calculations are consistent with those reported in (Stula, 1980a). That is, sleeve cladding thickness is significant only in those cases where sleeve thickness exceeds a minimum thickness. Corrosion resistance afforded by the cladding is inconsequential unless the sleeve is able to withstand media crushing forces. Of the materials tested, the best combinations consist of a Zircaloy cladding with a 304 SST sleeve. Calculated leach begin times in salt are generally less than corresponding times in shale which are, in turn, less than those in basalt. This is due to the high creep rate in salt and the negligible creep rate assumed in basalt.

As with the E concept, when a backfill is used, radionuclide release occurs at very long times after package failure, is attenuated by a large factor and is spread out over very long times.

Table 5-5. Concept B1 Results in Current Study.

PACKAGE DESIGN	MEDIA	STABILIZER MATERIAL	CANISTER MATERIAL	CANISTER THICKNESS (INCHES)	SLEEVE MATERIAL	SLEEVE THICKNESS (INCHES)	BACKFILL MATERIAL	BACKFILL THICKNESS (INCHES)	MAX. WASTE TEMP., (°K)	LEACH BEGIN TIME (YRS)		Release Begin Time for Plutonium, (yrs) (Anaerobic Conditions)	Release End Time for Plutonium, (yrs) (Anaerobic Conditions)
										ANAEROBIC	AEROBIC		
B1.1N	Salt	Steel	Steel	0.25	Iron	0.25	Sand-B	16.5	595	2	2	2.8×10^6	2.8×10^5
B1.2N		Steel	Steel	0.25	Iron	3.5	Sand-B	13.25	567	55	9	2.8×10^6	2.8×10^5
B1.3N		Steel	Steel	0.25	Iron	6.0	Sand-B	10.75	534	120	17	2.8×10^6	2.8×10^5
B1.4N		Steel	Steel	0.25	Iron (+0.05" Zirc)	3.5	Sand-B	13.2	566	560	520	2.8×10^6	2.8×10^5
B1.5N		Steel	Steel	0.25	Iron (+0.05" Zirc)	3.5	Sand-B	13.1	565	1,600	1,500	2.9×10^6	2.8×10^5
B1.6N		Steel	Steel	0.25	Iron (+0.25" Zirc)	3.5	Sand-B	13.0	554	2,600	2,500	3.0×10^6	2.8×10^5
B1.7N		Steel	Steel	0.25	Iron (+0.15" Zirc)	0.25	Sand-B	16.35	593	10	10	2.8×10^6	2.8×10^5
B1.8N		Steel	Steel	0.25	Iron (+0.15" Zirc)	6.0	Sand-B	10.6	533	1,600	1,500	2.9×10^6	2.8×10^5
B1.9N		Steel	Steel	0.25	304SST (+0.05" Zirc)	3.5	Sand-B	13.2	567	6,400	590	2.8×10^6	2.8×10^5
B1.10N		Steel	Steel	0.25	304SST (+0.05" Zirc)	3.5	Sand-B	13.0	555	8,500	2,600	3.0×10^6	2.8×10^5
B1.11N		Steel	Steel	0.25	Copper	0.25	Sand-B	16.5	595	2	2	2.8×10^6	2.8×10^5
B1.12N		Steel	Steel	0.25	Copper	3.5	Sand-B	13.25	556	2	2	2.8×10^6	2.8×10^5
B1.13N		Steel	Steel	0.25	Inconel	0.25	Sand-B	16.5	595	2	2	2.8×10^6	2.8×10^5
B1.14N		Steel	Steel	0.25	Inconel	3.5	Sand-B	13.25	557	8,100	600	2.8×10^6	2.8×10^5
B1.15N		Steel	Steel	0.25	304SST	0.25	Sand-B	16.5	595	2	2	2.8×10^6	2.8×10^5
B1.16N		Steel	Steel	0.25	304SST	3.5	Sand-B	13.25	557	5,900	81	2.8×10^6	2.8×10^5
B1.17N		Steel	Steel	0.25	Zircaloy	0.25	Sand-B	16.6	596	10	10	2.8×10^6	2.8×10^5
B1.18N		Steel	Steel	0.25	Zircaloy	3.5	Sand-B	13.25	567	29,000	29,000	5.4×10^6	2.8×10^5
B1.19N		Steel	Steel	0.25	Iron (+0.05" Zirc)	3.5	Sand-B	13.2	566	560	520	2.8×10^6	2.8×10^5
B1.20N		Steel	Steel	0.25	Iron (+0.15" Zirc)	3.5	Sand-B	13.1	555	1,600	1,500	2.9×10^6	2.8×10^5
B1.21N		Steel	Steel	0.25	Iron (+0.25" Zirc)	3.5	Sand-B	13.0	554	2,600	2,500	3.0×10^6	2.8×10^5

Table 5-5. Concept B1 Results in Current Study. (Continued)

PACKAGE DESIGN	MEDIA	STABILIZER MATERIAL	CANISTER MATERIAL	CANISTER THICKNESS (INCHES)	SLEEVE MATERIAL	SLEEVE THICKNESS (INCHES)	BACKFILL MATERIAL	BACKFILL THICKNESS (INCHES)	MAX. WASTE TEMP., (°K)	LEACH BEGIN TIME (yrs) ANOXIC	LEACH BEGIN TIME (yrs) OXIC	Release Begin Time for Plutonium, (yrs) (Oxic Conditions)	Release End Time for Plutonium, (yrs) (Oxic Conditions)
B1.22M	Salt	Steel	Steel	0.25	Iron (+0.15" Zirc)	0.25	Sand-B	16.35	593	2	2	2.8×10^4	2.8×10^5
B1.23M		Steel	Steel	0.25	Iron (+0.15" Zirc)	6.0	Sand-B	10.25	533	1,600	1,500	2.9×10^6	2.8×10^5
B1.24M		Helium	Steel	0.25	Iron	3.5	Sand-B	13.25	559	55	9	2.8×10^4	2.8×10^5
B1.25M		Air	Steel	0.25	Iron	3.5	Sand-B	13.25	560	55	9	2.8×10^6	2.8×10^5
B1.26M		Helium	Steel (+0.25" Air gap)	0.25	Iron	3.5	Sand-B	13.25	559	55	9	2.8×10^6	2.8×10^5
B1.27M		Helium	Steel (+0.5" Air gap)	0.25	Iron	3.5	Sand-B	13.25	558	54	9	2.8×10^6	2.8×10^5
B1.28M		Steel	Steel (+1.0" Air gap)	0.25	Iron	3.5	Sand-B	13.25	552	52	8	2.8×10^6	2.8×10^5
B1.29M		Steel	Steel (+2.0" Air gap)	0.25	Iron	3.5	Sand-B	13.25	548	48	8	2.8×10^6	2.8×10^5
B1.20M	Shale	Steel	Steel	0.25	Iron (+0.15" Zirc)	3.5	Sand-B	13.1	544	1,800	1,600	2.9×10^6	2.8×10^5
B1.21M		Steel	Steel	0.25	Iron (+0.25" Zirc)	3.5	Sand-B	13.0	543	2,000	2,000	3.0×10^6	2.8×10^5
B1.22M		Steel	Steel	0.25	Iron (+0.15" Zirc)	0.25	Sand-B	15.85	582	2	2	2.8×10^6	2.8×10^5
B1.23M		Steel	Steel	0.25	Iron (+0.15" Zirc)	6.0	Sand-B	10.6	522	2,100	1,700	2.9×10^6	2.8×10^5
B1.1M	Basalt	Steel	Steel	0.25	Iron	0.25	Sand-B	16.5	602	160	20	2.9×10^6	2.9×10^5
B1.7M		Steel	Steel	0.25	Iron (+0.15" Zirc)	0.25	Sand-B	16.35	600	1,700	1,500	3.0×10^6	2.9×10^5
B1.9M		Steel	Steel	0.25	304SST (+0.05" Zirc)	3.5	Sand-B	13.2	564	36,000	12,000	6.7×10^6	2.9×10^5
B1.11M		Steel	Steel	0.25	Copper	0.25	Sand-B	16.5	602	240	130	2.9×10^6	2.9×10^5
B1.12M		Steel	Steel	0.25	Copper	3.5	Sand-B	13.25	563	1,900	1,800	3.0×10^6	2.9×10^5
B1.13M		Steel	Steel	0.25	Inconel	0.25	Sand-B	16.5	602	220	510	2.9×10^6	2.9×10^5
B1.14M		Steel	Steel	0.25	Inconel	3.5	Sand-B	13.25	564	1,500	7,000	6.3×10^6	2.9×10^5
B1.15M		Steel	Steel	0.25	304SST	0.25	Sand-B	16.5	602	2,600	840	2.9×10^6	2.9×10^5
B1.17M		Steel	Steel	0.25	Zircaloy	0.25	Sand-B	16.5	602	2,600	2,500	5.9×10^6	2.9×10^5
B1.22M		Steel	Steel	0.25	Iron (+0.15" Zirc)	0.25	Sand-B	16.35	600	1,700	1,500	3.0×10^6	2.9×10^5

5.4 HEAVY SLEEVE/CAST STABILIZER CONCEPT (Concept BE)

A package design utilizing both a solid cast stabilizer and a heavy sleeve had been thought to be an attractive concept on the basis of results of previous work (Stula, 1980a). Therefore, variations of this design (Concept BE) are evaluated in the current study. Calculations are performed primarily in creeping geologic media with most of the cases evaluated in salt. Results of calculations for the Concept BE design variations are presented in Table 5-6.

Comparison of package designs varying only in canister material show a large variance in leach begin time which indicates a significant dependence on corrosion rate. As in the Concept B1 package design, sleeve thickness is sufficient to prevent immediate crushing of the package. With sufficient sleeve strength, corrosion resistance of the sleeve cladding is important in determining package lifetime. Backfill thickness was found to have no effect on leach begin time. Calculated leach begin times in salt are generally much less than corresponding times in shale and basalt.

As in all other designs the backfill greatly delays and attenuates radionuclide release.

5.5 PEAK WASTE TEMPERATURE

Use of design packages with many layers and/or low conductivity materials could result in very high waste temperatures. A maximum temperature criterion of 653°K (380°C) is used to reject package designs. Calculated peak waste temperatures for all package designs evaluated are included in Tables 5-2, 5-4, 5-5, and 5-6. Of the design cases evaluated, only four (E.19N - E.22N) exceed the maximum temperature criterion.

The package design characteristics having the most pronounced effect on peak waste temperature are type of backfill material and backfill thickness. The effect of type of backfill material is shown in Table 5-7 where use of backfill materials with relatively low thermal conductivities such as bentonite and clinoptilolite result in higher peak waste temperatures than in the case when sand-bentonite (10 percent) is used. The effect of backfill thickness is also shown in Table 5-7. Peak waste temperature increases significantly with increasing backfill thickness. Types of barrier wall materials (metals) and barrier wall thicknesses have little, if any, effect on peak waste temperature.

Table 5-6. Concept BE Results in Current Study.

PACKAGE DESIGN	MEDIA	STABILIZER MATERIAL	CANISTER MATERIAL	CANISTER THICKNESS (INCHES)	SLEEVE MATERIAL	SLEEVE THICKNESS (INCHES)	BACKFILL MATERIAL	BACKFILL THICKNESS (INCHES)	MAX. WASTE TEMP., (°F)	LEACH BEGIN TIME (YRS)		Release Begin Time for Plutonium, (yrs) (Oxic Conditions)	Release End Time for Plutonium, (yrs) (Oxic Conditions)
										Anoxic	Oxic		
84.1W	Salt	Lead	304SST	0.25	Iron	0.25	Sand-B	16.5	595	700	35	2.8×10^6	2.9×10^5
84.2W		Lead	304SST	0.25	Iron	3.5	Sand-B	13.25	557	790	50	2.8×10^6	2.9×10^5
84.3W		Lead	304SST	0.25	Iron	6.0	Sand-B	10.75	534	860	50	2.9×10^6	2.9×10^5
84.4W		Lead	304SST	0.25	Iron (+0.05" Zirc)	3.5	Sand-B	13.2	556	1,300	550	2.9×10^6	2.9×10^5
84.5W		Lead	304SST	0.25	Iron (+0.25" Zirc)	3.5	Sand-B	13.0	554	3,300	2,600	3.1×10^6	2.9×10^5
84.6W		Lead	304SST	0.25	Iron (+0.15" Zirc)	0.25	Sand-B	16.25	593	2,200	1,500	3.0×10^6	2.9×10^5
84.7W		Lead	304SST	0.25	Iron (+0.15" Zirc)	6.0	Sand-B	10.6	533	2,400	1,600	3.0×10^6	2.9×10^5
84.8W		Lead	Zircaloy	0.25	Iron	0.25	Sand-B	16.5	595	2,600	2,500	5.9×10^6	2.9×10^5
84.9W		Lead	Zircaloy	0.25	Iron	3.5	Sand-B	13.25	557	2,700	2,500	3.1×10^6	2.9×10^5
84.10W		Lead	Zircaloy	0.25	Iron	6.0	Sand-B	10.75	534	2,700	2,500	3.1×10^6	2.9×10^5
84.11W		Lead	Zircaloy	0.25	Iron (+0.05" Zirc)	3.5	Sand-B	13.2	556	3,200	3,000	3.1×10^6	2.9×10^5
84.12W		Lead	Zircaloy	0.25	Iron (+0.25" Zirc)	3.5	Sand-B	13.0	554	5,200	5,000	3.3×10^6	2.9×10^5
84.13W		Lead	Zircaloy	0.25	Iron (+0.15" Zirc)	0.25	Sand-B	16.25	593	4,100	4,000	3.2×10^6	2.9×10^5
84.14W		Lead	Zircaloy	0.25	Iron (+0.15" Zirc)	6.0	Sand-B	10.6	533	4,200	4,000	3.2×10^6	2.9×10^5
84.15W		Lead	Inconel	0.25	Iron	0.25	Sand-B	16.5	595	910	90	2.9×10^6	2.9×10^5
84.16W		Lead	Inconel	0.25	Iron	3.5	Sand-B	13.25	557	1,000	110	2.9×10^6	2.9×10^5
84.17W		Lead	Inconel	0.25	Iron	6.0	Sand-B	10.75	534	1,100	110	2.9×10^6	2.9×10^5
84.18W		Lead	Inconel	0.25	Iron (+0.05" Zirc)	3.5	Sand-B	13.2	556	1,500	610	2.9×10^6	2.9×10^5
84.19W		Lead	Inconel	0.25	Iron (+0.25" Zirc)	3.5	Sand-B	13.0	554	3,500	2,600	3.1×10^6	2.9×10^5
84.20W		Lead	Inconel	0.25	Iron (+0.15" Zirc)	0.25	Sand-B	16.25	593	2,400	1,600	3.0×10^6	2.9×10^5
84.21W		Lead	Inconel	0.25	Iron (+0.15" Zirc)	6.0	Sand-B	10.6	533	2,600	1,600	3.0×10^6	2.9×10^5

Table 5-6. Concept BE Results in Current Study. (Continued)

PACKAGE DESIGN	MEDIA	STABILIZER MATERIAL	CANISTER MATERIAL	CANISTER THICKNESS (INCHES)	SLEEVE MATERIAL	SLEEVE THICKNESS (INCHES)	BACKFILL MATERIAL	BACKFILL THICKNESS (INCHES)	MAX. MASTER TEMP., (°C)	LEACH BEGIN TIME (YRS) ANOXIC	LEACH BEGIN TIME (YRS) OXIC	Release begin time for Plutonium, (yrs) (Anoxic Conditions)	Release end time for Plutonium, (yrs) (Anoxic Conditions)
BE.22H	Salt	Lead	Zircaloy	0.25	Iron	3.5	Sand-B	13.25	557	2,300	2,500	3.1×10^4	2.9×10^5
BE.23H		Lead	Zircaloy	0.25	Iron	6.0	Sand-B	10.75	534	2,300	2,500	3.1×10^4	2.9×10^5
BE.24H		Lead	Zircaloy	0.25	Iron (+0.05" Zirc)	3.5	Sand-B	13.2	556	3,200	3,000	3.1×10^4	2.9×10^5
BE.25H		Lead	Zircaloy	0.25	Iron (+0.25" Zirc)	3.5	Sand-B	13.0	554	5,200	5,000	3.3×10^4	2.9×10^5
BE.26H		Lead	304SST	0.25	Iron	3.5	Bent	13.25	624	700	50	---	---
BE.27H		Lead	304SST	0.25	Iron (+0.05" Zirc)	3.5	Bent	13.2	623	1,300	550	---	---
BE.28H		Lead	304SST	0.25	Iron	3.5	Clean	13.25	624	600	50	2.9×10^4	2.9×10^5
BE.29H		Lead	304SST	0.25	Iron (+0.05" Zirc)	3.5	Clean	13.2	623	1,300	550	2.9×10^4	2.9×10^5
BE.30H		Lead	304SST	0.25	Iron	0.25	Sand-B	2.5	561	300	35	35	4.1×10^5
BE.31H		Lead	304SST	0.25	Iron	0.25	Sand-B	10.5	564	300	35	2.9×10^4	2.9×10^5
BE.32H		Lead	304SST	0.25	Iron (+0.15" Zirc)	0.25	Sand-B	2.35	489	2,200	1,400	1400	4.1×10^5
BE.33H		Lead	304SST	0.25	Iron (+0.15" Zirc)	0.25	Sand-B	10.35	562	2,200	1,400	3.0×10^4	2.9×10^5
BE.34H		Lead	304SST	0.25	Iron	3.5	Sand-B	13.25	557	800	150	2.9×10^4	2.9×10^5
BE.35H		Lead	304SST	0.25	Iron (+0.05" Zirc)	3.5	Sand-B	13.2	556	1,400	650	2.9×10^4	2.9×10^5
BE.36H		Lead	Zircaloy (+0.125" Air gap)	0.25	Iron	3.5	Sand-B	13.25	557	2,300	2,500	3.1×10^4	2.9×10^5
BE.37H		Lead	Zircaloy (+0.25" Air gap)	0.24	Iron	3.5	Sand-B	13.25	556	2,300	2,500	3.1×10^4	2.9×10^5
BE.38H		Lead	Zircaloy (+0.5" Air gap)	0.25	Iron	3.5	Sand-B	13.25	555	2,300	2,500	3.1×10^4	2.9×10^5
BE.39H		Lead	Zircaloy (+1.0" Air gap)	0.25	Iron	3.5	Sand-B	13.25	552	2,300	2,500	3.1×10^4	2.9×10^5

Table 5-6. Concept BE Results in Current Study. (Continued)

PACKAGE DESIGN	MEDIA	STABILIZER MATERIAL	CANISTER MATERIAL	CANISTER THICKNESS (INCHES)	SLEEVE MATERIAL	SLEEVE THICKNESS (INCHES)	BACKFILL MATERIAL	BACKFILL THICKNESS (INCHES)	MAX. WASTE TEMP., (°K)	LEACH BEGIN TIME (YRS)		Release Begin Time for Plutonium, (yrs) (Basic Conditions)	Release End Time for Plutonium, (yrs) (Basic Conditions)
										ANOXIC	OXIC		
BE.1H	Basalt	Lead	304SSI	0.25	Iron	0.25	Sand-B	16.5	602	3,200	1,600	3.0×10^4	2.9×10^5
BE.6H		Lead	304SSI	0.25	Iron (+0.1% Zirc)	0.25	Sand-B	16.25	600	4,000	3,100	3.1×10^4	2.9×10^5
BE.7H		Lead	304SSI	0.25	Iron (+0.1% Zirc)	6.0	Sand-B	10.5	540	5,500	3,200	3.2×10^4	2.9×10^5
BE.8H		Lead	Zircaloy	0.25	Iron	0.25	Sand-B	16.5	602	3,200	3,200	6.0×10^4	2.9×10^5
BE.12H		Lead	Zircaloy	0.25	Iron (+0.2% Zirc)	3.5	Sand-B	13.0	551	6,200	5,900	3.4×10^4	2.9×10^5
BE.13H		Lead	Zircaloy	0.25	Iron (+0.1% Zirc)	0.25	Sand-B	16.25	600	4,000	4,000	3.3×10^4	2.9×10^5
BE.14H		Lead	Zircaloy	0.25	Iron (+0.1% Zirc)	6.0	Sand-B	10.5	540	5,500	4,900	3.3×10^4	2.9×10^5
BE.19H		Lead	Inconel	0.25	Iron	0.25	Sand-B	16.5	602	890	1,300	3.0×10^4	2.9×10^5
BE.20H		Lead	Inconel	0.25	Iron (+0.1% Zirc)	0.25	Sand-B	16.25	600	2,000	2,000	3.1×10^4	2.9×10^5
BE.30H		Lead	304SSI	0.25	Iron	0.25	Sand-B	2.5	508	3,200	1,600	1,600	4.1×10^5
BE.31H		Lead	304SSI	0.25	Iron	0.25	Sand-B	10.5	571	3,200	1,600	3.0×10^4	2.9×10^5
BE.32H		Lead	304SSI	0.25	Iron (+0.1% Zirc)	0.25	Sand-B	2.25	506	4,000	3,100	3,100	4.1×10^5
BE.33H		Lead	304SSI	0.25	Iron (+0.1% Zirc)	0.25	Sand-B	10.25	569	4,000	3,100	3.1×10^4	2.9×10^5
BE.34H		Lead	304SSI	0.25	Iron	3.5	Sand-B	13.25	544	3,000	1,800	3.0×10^4	2.9×10^5
BE.25H	Shale	Lead	Zircaloy	0.25	Iron (+0.2% Zirc)	3.5	Sand-B	13.0	543	6,200	5,900	3.4×10^4	2.9×10^5
BE.26H		Lead	304SSI	0.25	Iron	3.5	Bent	13.25	613	3,700	1,700	---	---
BE.27H		Lead	304SSI	0.25	Iron (+0.0% Zirc)	3.5	Bent	13.2	612	4,200	2,200	---	---
BE.28H		Lead	304SSI	0.25	Iron	3.5	Clino	13.25	613	3,700	1,700	3.0×10^4	2.9×10^5

Table 5-7. Effect of Backfill Material and Thickness on Maximum Waste Temperature.

Package Design	Geology	Backfill Material	Backfill Thickness (Inches)	Peak Waste Temperature, (^{o}K)
BE.1N	Salt	Sand-Bentonite (10%)	16.5	595
BE.30N		Sand-Bentonite (10%)	2.5	501
BE.31N		Sand-Bentonite (10%)	10.5	564
BE.6N		Sand-Bentonite (10%)	16.35	593
BE.32N		Sand-Bentonite (10%)	2.35	499
BE.33N		Sand-Bentonite (10%)	10.35	562
BE.26N		Bentonite	13.25	624
BE.28N		Clinoptilolite	13.25	624
BE.34N		Sand-Bentonite (10%)	13.25	557
E.2N		Sand-Bentonite (10%)	17.0	599
E.15N		Sand-Bentonite (10%)	11.0	568
E.17N		Sand-Bentonite (10%)	3.0	505
E.19N		Bentonite	17.0	698
E.21N		Clinoptilolite	17.0	698

5.6 SENSITIVITY STUDIES

Sensitivity analyses were performed to determine the effects of certain package physical characteristics and geologic conditions on package performance. Previous sensitivity study results were reported in (Stula, 1980a) for evaluation of the list of best package concepts for salt and shale media as determined in FY'79 work (Lester, 1979). In the current study, the effects of variation of repository temperature and pressure, waste heat generation rate, gap thickness between package barriers, backfill thickness and compaction coefficients, and radionuclide solubility are evaluated.

The effects of variation of repository pressure on package performance are summarized in Table 5-8. Repository pressure was found to have no effect on designs utilizing a cast stabilizer. However, for non-cast stabilizer designs, canister thickness at failure and hence leach begin time are affected significantly. As repository pressure increases, canister thickness required to withstand media creep forces increases and leach begin time, or time of canister failure, decreases.

The effects of variation of repository temperature on package performance are summarized in Table 5-9. In all cases, peak waste temperature is affected only to the extent that repository temperature varies. That is, the ΔT between repository and waste is constant and dependent on waste heat generation rate. Repository temperature was found to have a small, but significant effect on canister thickness at failure for the non-cast stabilizer designs. The criteria used to determine minimum canister thickness required to withstand geologic creep forces are temperature dependent. Thus, leach begin time is inversely related to canister thickness at failure. For cast stabilizer designs, no effects on canister thickness at failure or leach begin time are evident. According to the BARIER corrosion model, temperature would affect corrosion rate to the extent that one of two corrosion rates corresponding to two temperature ranges would be utilized in any particular corrosion calculation.

The effect of waste heat generation rate on the calculated maximum waste temperature for several package designs is shown in Table 5-10. It can be seen that for package designs D2.1 and BE.27N, the maximum waste temperature increases linearly with increasing waste heat generation rate. This is to be expected from the nature of the heat transfer Equation (3.2.3) for heat transfer by conduction only. For heat transfer by conduction and radiation, use of Equations (3.2.3) - (3.2.5) with package design BE.39N shows essentially a linear

Table 5-8. Effect of Repository Pressure on Package Performance.

Package	Geology	Repository Pressure, (psi)	Repository Temperature, (^{o}K)	Can Thickness at Failure, (in)	Radiation Dose, (R/hr)	Leach Begin Time, (yrs)
A.10	Salt	1700	466	.321	.230	6790
A.10		2500	466	.491	.245	5090
A.10		3000	466	.603	.254	3970
E.24		1700	466	0	.089	2600
E.24		2500	466	0	.089	2600
E.24		3300	466	0	.089	2600

Table 5-9. Effect of Repository Temperature on Package Performance.

Package	Geology	Repository Temperature, (^{o}K)	Peak Waste Temperature, (^{o}K)	Can Thickness at Failure, (in)	Leach Begin Time, (yrs)
A.10	Salt	373	401	.464	5360
A.10		423	451	.478	5220
A.10		466	494	.491	5090
A.10		523	551	.509	4910
A.10		573	601	.526	4740
E.24N		373	506	0	2600
E.24N		423	556	0	2600
E.24N		466	599	0	2600
E.24N		523	656	0	2600
E.24N		573	706	0	2600

Table 5-10. Effect of Waste Heat Generation Rate on Maximum Waste Temperature.

Package	Geology	Waste Heat Generation Rate Q/L, (Watts/inch)	Air Gap Thickness Between Can and Sleeve (inches)	Repository Temperature, (^{o}K)	Maximum Waste Temperature, (^{o}K)
D2.1	Salt	0.5	0	466	475
D2.1		2.73	0	466	515
D2.1		4.73	0	466	551
D2.1		7.0	0	466	592
BE.27N		0.5	0	466	483
BE.27N		2.73	0	466	557
BE.27N		4.73	0	466	623
BE.27N		7.0	0	466	699
BE.39N		0.5	1.0	466	475
BE.39N		2.73	1.0	466	516
BE.39N		4.73	1.0	466	552
BE.39N		7.0	1.0	466	593

dependence of maximum waste temperature on waste heat generation rate. This indicates that for relatively small air gap thicknesses within a package, the radiation component of heat transfer is of minor importance in comparison to the conduction component. The effect of varying air gap thickness on maximum waste temperature is shown in Table 5-11 for small air gaps.

Variation of backfill compaction coefficients was found to have no effect on package life or any other performance characteristic with the exception of net pressure on a barrier at failure. However, this effect is relatively minor over the range of compaction coefficients considered. Net pressure of a barrier at failure with a "stiff" backfill is generally on the order of 5 psi higher than that for a barrier with a "soft" backfill in non-cast stabilizer package designs. This effect is shown in Table 5-12. For cast stabilizer designs, net pressure of a barrier at failure is independent of backfill compaction coefficients.

The effect of variation of backfill thickness on radionuclide transport resistance is shown in Table 5-13. It can be seen that most of the radionuclide transport resistance as calculated by the RELEAS subroutine is attributed to the backfill thickness except in the situation where the backfill thickness is extremely small (less than one inch). Radionuclide release rates reach steady state more quickly as the backfill thickness is decreased. Detailed results of these sensitivity calculations are included in Appendix F.

The effects of solubility of U-238 on radionuclide release rate are evident in the results of each package design evaluated. For the high solubility case, the release rate reaches steady state more quickly and is significantly higher than in the low solubility case.

Table 5-11. Effect of Air Gap Thickness on Maximum Waste Temperature.

Package	Geology	Waste Heat Generation Rate Q/L, (Watts/inch)	Air Gap Thickness Between Can and Sleeve (inches)	Repository Temperature, (^{o}K)	Maximum Waste Temperature, (^{o}K)
BE.39N	Salt	4.73	0.125	466	556.6
BE.39N		4.73	0.25	466	556.0
BE.39N		4.73	0.5	466	554.8
BE.39N		4.73	1.0	466	552.2
B1.26N		4.73	0.25	466	559.1
B1.27N		4.73	0.5	466	557.9
B1.28N		4.73	1.0	466	552.4
B1.29N		4.73	2.0	466	547.7

Table 5-12. Effect of Backfill Compaction Coefficients on Net Pressure on a Barrier at Failure.

Package	Medium	Barrier	Backfill Compaction Coefficients		Net Pressure on Barrier at Failure, (PSIA)
			A	K	
B1.4N	Salt	Canister	0.44	253	-2522.6
B1.19N		Canister	47.5	0	-2523.1
B1.4N		Sleeve	0.44	253	-2869.1
B1.19N		Sleeve	47.5	0	-2870.4
E.1N		Cast Stabilizer	0.44	253	-2500
E.23N		Cast Stabilizer	47.5	0	-2500
E.1N		Canister	0.44	253	-2500
E.23N		Canister	47.5	0	-2500

Table 5-13. Effect of Backfill Thickness on Radionuclide Transport Resistance.

Package Design	Backfill* Thickness, (Inches)	Radionuclide Transport Resistance Due to Backfill, (%)	Release Begin Time for Plutonium, (yrs) (Oxic Conditions)	Release End Time for Plutonium, (yrs) (Oxic Conditions)
BE.1N	16.5	97.6	2.9×10^4	2.9×10^5
	10.5	96.2	2.9×10^4	2.9×10^5
	2.5	85.8	40	4.1×10^5
	1.25	75.2	40	4.2×10^5
	0.5	54.8	40	4.2×10^5
E.2N	17.0	98.4	5.9×10^4	2.9×10^5
	11.0	97.6	3.1×10^4	2.9×10^5
	3.0	91.6	2500	3.9×10^5
	1.5	84.5	2500	4.3×10^5
	0.5	64.5	2500	4.2×10^5

*Sand-Bentonite (10%)

6. CONCLUSIONS AND RECOMMENDATIONS

The objective of the System Study on Engineered Barriers (SSEB) was to evaluate the efficacy of engineered waste packages in reducing the potential dose to the population due to releases after repository closure. The information from the study will be used to plan development work on engineered barriers and assess the technical incentives for use of multiple barrier packages.

Only a limited number of engineered barrier package designs have been analyzed in the SSEB since the work was limited to scoping studies to guide future work. Many engineering designs can be proposed which have not been considered but the tools have been developed to analyze additional designs. The emphasis on future programs should not be on the "best" package but rather a "sufficient" package to meet necessary criteria. The BARIER code provides a means to measure proposed packages against such criteria.

6.1 PACKAGE PERFORMANCE

On the basis of the post-closure, flooded repository scenario the preliminary analyses indicate that long-lived packages with low release rates can be designed. The performance model indicates that lifetimes of well over 1,000 years and in many cases over 10,000 years are reasonable to expect from packages constructed of common materials. Furthermore, judicious use of backfills to sorb radionuclides and/or exclude water can greatly reduce radionuclide releases after failure of canisters and overpacks as well as greatly delay the onset of radionuclide release.

The results indicate that a few inches of backfill thickness are sufficient to supply the necessary barrier to radionuclide release. Radionuclide retention times for U-238 as long as 10^7 years (e.g. Concept BE.26N) were calculated in many cases. Large backfill thicknesses are of little advantage as long as sufficient sleeve thicknesses and/or a cast stabilizer are used. Thus a well chosen chemical sorbent would be a good choice with only a small amount required. The stress defense contribution of the backfill is questionable as it

contributes very little and never contributes to stress application if a very "soft" material is used. The key question with regard to backfills remains whether the backfill material will retain its properties over long periods of time (more than 1,000 years). As was reported from previous studies (Lester, 1979) there is a serious question that a backfill would be intact in an environment capable of leaching material from a ceramic fuel material.

The new code version demonstrates, as did the previous version, that in creeping geologic media (salt or shale) the most important requirement is to withstand the media crushing pressure. This requires a heavy sleeve and/or a solid, "crush-proof" waste form (i.e., a cast stabilizer). Corrosion is important in that it steadily weakens a sleeve wall and eventually causes failure. In the case of the "crush-proof" stabilizer, corrosion results in a breakthrough which allows repository water to contact the waste.

In general, the results using the new BARIER model roughly correspond to those from the previous model. While corrosion rates in the new data base tend to be higher than the previous values, the stress calculations for crushing forces are based on real failure rather than ASME code criteria which tend to be very conservative.

6.2 AREAS OF UNCERTAINTY

The current performance calculation capability is quite comprehensive but still contains areas of uncertainty. Most of the concern is the lack of sufficient data in appropriate environments needed to support more sophisticated approaches. Generally, where such uncertainty exists, credit is not taken for possible lesser consequences. For instance, when a particular parameter value is not well known, bounding values are used and the limit yielding the worst consequences in the bounded range is chosen. Where the dependency of an effect on a certain parameter is not well understood the parameter is set constant at the limiting value yielding the worst consequences.

6.2.1 Corrosion Rate

Corrosion of package barriers is a dominating failure mechanism. To accurately assess the life of the package the corrosion rate as a function of key parameters and of time is needed. Extensive study of literature supported by hand and computer-assisted searches was performed to develop the best data base possible. The goal was to incorporate various modes of corrosion such as crack propagation, pitting, graphitization and bulk corrosion and to include other parameter effects such as temperature and radiaiton. Three deficiencies were encountered: (1) total lack of data in some categories for some materials, (2) data available but in chemical environments not corresponding to the repository condition of interest, and/or (3) ranges of parameters (temperature, pressure) not corresponding to those of interest. It was possible to divide corrosion rates into two temperature ranges and choose high values in known data ranges. One difficulty was encountered in choosing "highest values"; unreasonable rates sometimes result which lack common sense. In most of these instances the environment was too different from the repository. Such values were deleted.

The effect of radiation on corrosion is not well documented. Data that are available indicate a small effect for exposures of interest. A review of the detailed results shows that the radiation fields are generally very low at failure time compared to levels giving measureable effect. However, more information, especially in typical chemistry, is definitely needed or much overdesign will be required.

Another area of particular concern is local corrosion on joints, seams or other discontinuities in the bulk metal. Corrosion data is typically on base metal samples although some weldment testing has been done. Nevertheless, it is possible to introduce safety factors. For example, the literature gives guidance on corrosion allowances for non-base metals and one can design in conservation.

In general it is felt that package designs could proceed now if a large degree of overdesign is tolerable. To reduce cost and increase general confidence more pertinent corrosion data would be useful. Of special concern is the need to extrapolate over long periods of time. This is unavoidable and can be done with more confidence if based on comprehensive data.

6.2.2 Backfill Properties

Two basic categories of backfill properties are used in the current BARIER code: (1) Physico-mechanical and (2) chemical. The physico- mechanical properties are volume-pressure compaction characteristics (bulk modulus) and internal friction characteristics (shear modulus and Mohr slope) which determine the behavior of the backfill under external stress and how the repository stress is transmitted to the inner package components. The chemical charateristics are those parameters affecting radionuclide and water transport and include retardation factors (k_d), diffusivity, porosity and tortuosity.

Data are limited in both categories but reasonable bounding estimates can be made and are used in the current study. As with corrosion, increasing knowledge allows more precision in design. Confidence in the design is possible with current data but thick backfills may be needed to ensure sufficient performance. The greatest uncertainty is the ability of backfills to retain their properties over long periods in envrionments of interest. However, geologic data on montmorillonites and similar materials provide some insight in their stability thus allowing the bounding process. The most pessimistic conclusion leads to significant functional lifetimes (thousands of years) so that the problem is again one of design precision rather than of design integrity.

The vital importance of the backfill is evident in the results of this study. Therefore, it would be useful to expand understanding of these materials as a design support activity. Increased confidence and design precision in the backfill will yield many benefits.

6.2.3 Waste Leaching

This study has been restricted to disposal of unreprocessed, spent fuel. Nevertheless, all that is discussed here applies to any other waste form.

Consider the relationship of intrinsic (microscopic) data to global (physical system) data. The package is a global system the description of which is based on intrusion data. Data obtained to date is intrinsic (Katayama, 1976, 1980); that is, the measurements of leach rate are taken without the resistance due to contaminants present. If the intrusion leach rate is large compared to global system transport then the leachate around the waste form becomes saturated with a given species. In this case solubility data are needed. Solubility data

from Katayama were used because in all cases the transport rates were orders of magnitude below intrusion rates.

The release rates are sensitive to solubility so that more solubility data are needed depending on the desire to pinpoint release rates and breakthrough times. The extremely long times obtained raise some question as to whether one is concerned whether breakthrough times are 10^8 years or 10^{10} years. However, as more detailed precision package design is done and more refined risk analysis is carried out, increased confidence in the pertinent numbers will be needed. It is recommended that solubility numbers be emphasized in future testing. Leach rate measurements should be done in demonstration testing with deliberately failed packages so that global rate modeling can be validated.

6.2.4 Other Areas of Uncertainty

Some factors are not accounted for in the BARIER model. Of note are water exclusion effects and the role of protective coatings (not including metal cladding). These could be considered as delay times to be added to the package performance times reported. However, the magnitude of these times remains relatively uncertain. Much data are available on the behavior of swelling clays and protective coatings but not as a function of long periods of time. Work in this area would be beneficial in providing a measure of redundancy to design.

6.3 RISK MODEL DEVELOPMENT RECOMMENDATION

The BARIER code was not developed for the purpose of risk analysis but rather to provide scoping studies which could be used to make research and development decisions. However, in recognition of the amount of effort expended, the code was designed with ease of extention to a risk model in mind. Thus the code provides a baseline for development of a near-field risk model.

6.3.1 Applications of BARIER to Risk Analysis

The current BARIER code closely resembles the consequence part of a risk model concerned with long-term effects in the post-closure repository. It is based on one principal scenario but many sub-scenarios could be evaluated from the results (see discussions in Section-2). It carries this principal scenario to the consequence conclusion: release to the geology of specific radionuclides as a function of time. What it lacks is sufficient data base and in some cases analytical features required for full risk analysis. It is not a probabilistic model but is fast running and so could be driven by a probabilistic model. Some improvements can be made to BARIER now with additional work and some improvements must await further data acquistition.

The sections that follow give some suggestions on changes to convert the model to a near-field risk analysis. Many other changes will likely be identified as the actual job of incorporating this model into risk methodology is undertaken.

6.3.2 Near-Term Improvements

Further improvements in the release model could be made as discussed in Section 3.5. This includes adding the tail-off portion of the release curve. The benefits should be weighed against the added computational burden but can only be assessed by making the changes. Because of long delay times in the backfill, daughter product transport analysis capability would also be desirable. Analytical solutions can probably be developed for decay chains in the backfill with the flux boundary conditions. These would be similar to the GETOUT model but the boundary effects are different. More accurate representation of radiodecay in the backfill may be desirable for shorter-lived radionuclides.

The model for resistance effects of failed barriers could be coupled to corrosion mechanisms to allow a more accurate representation of the barrier resistance in radionuclide release. However, note that in many cases this represents less than 10 per cent of the total radionuclide release resistance.

Code function changes such as automatic variance of time increment to accommodate fast or slow rates of package degradation and to allow more efficient use of computational time would be desirable. In addition, further refinement of data manipulation and output format more appropriately tailored to interfacing in a risk model would be desirable.

Expansion of the data base will be needed to include more construction materials and backfill materials. Other waste forms will also be needed for future risk studies. The current data base was limited for scoping purposes and was not meant to cover all the design choices which will be considered as package development proceeds. Corrosion rates, material stress properties, retardation factors, porosities, tortuosities, thermal properties, heat generation rates, and many other such data are needed for additional materials.

The expansion to include many other radionuclides would also be desirable for risk studies. However, some parameters such as retardation factors will be very data-limited.

6.3.3 Long-Term Improvements

Changes in this category are those which require new data for support. The most significant improvement would be the use of more sophisticated corrosion rate models with more confidence in extrapolation of rates and consideration of non-linear effects. In addition, feedback between crack propagation/penetration and calculated stresses might be a desirable feature. Of particular importance is the improvement of the data base so that more applicable chemical-physical environments are represented and more accurate temperature dependency is available. It is not likely that this can be completed from existing literature but a start could be made. The effect of backfill corrosion should be included. Chemical adjustment, corrosion agent transport in a backfill and water transport are all factors not now considered. Intrusion corrosion rates are employed to assess the global system. This results in higher corrosion rates than might actually be observed.

As data on nuclear radiation effects become available the feedback loop between corrosion and radiation field calculations could be closed. When this is done the radiation field subroutine will require expansion to include photon sources other than spent fuel (such a change might be desirable now in the near-term).

The current model envisions a lithostatic pressure acting on the package. In most creeping media the effect of the slope of excavation, discontinuities in the geology and other asymmetric properties results in non-uniform stresses. Gross asymmetry may actually shorten package life. It would be desirable to do more sophisticated stress calculations. Furthermore,

the conservative assumption is now made that full overburden stress is applied at time = 0. At high temperature in salt this is quite reasonable as creep rates are high at low temperature. In other media (e.g., shale) consideration of rate of stress build-up could be a useful addition.

7. REFERENCES

American Society of Mechanical Engineers, 1977. Asme Boiler and Pressure Vessel Code, Section VIII, Division 1, July.

Ahlstrom, P. E., 1978. "Ceramic and Pure-Metal Canister in Buffer Material", Proceedings of the Conference on High-Level Radioactive Solid Waste Forms, NUREG/CP-0005, L. S. Casey, Ed., December.

Berry, W. E., 1971. Corrosion in Nuclear Applications, John Wiley & Sons.

Bird, R. B., et al, 1965. Transport Phenomena, John Wiley & Sons.

Blazer, R. V., and J. J. Owens, 1956. "Special Corrosion Study of Carbon and Low Alloy Steels", ASTM Symposium on High Purity Water Corrosion.

Braithwaite, J. W., and M. A. Molecke, 1979. Scientific Basis for Nuclear Waste Management and Technology, Vol. 1, G. J. McCarthy, ed., Plenum Press.

Bulischeck, T. S., and D. Van Rooyen, 1980. "Stress Corrosion Cracking of Alloy Goo Using Constant Strain Rate Test", NACE Corrosion/80, Preprint of Paper No. 183, March, 1980.

Butler, G., and H.C.K. Ison, 1966. Corrosion and Its Prevention in Water, Reinhold Publishing Co., New York.

Byerlee, J. D., 1967. "Frictional Characteristics of Granite Under High Confining Pressure", J. Geophys. Res., Vol. 72, No. 14, July 15.

Carslaw, H. W., and J. C. Jaeger, 1967. Conduction of Heat in Solids, Oxford University Press.

Cataldi, H. A., and C. F. Cheng, 1958. "Investigation of Erosion and Corrosion of Turbine Materials in Wet Oxygenated Steam", Trans. ASME, Vol. 80.

Cheng, C. F., 1980. "Canister Corrosion of a System Study on Engineered Barriers", Internal Letter, Science Applications, Inc.

Cooper, A. R. and L. E. Eaton, 1962. "Compaction Behavior of Several Ceramic Powders", J. Am. Ceram. Soc., Vol. 45, No. 3, March 1.

Copson, H. R., and W. E. Berry, 1960. "Qualifications of Inconel for Nuclear Power Plant Applications", Corrosion, Vol. 16, No. 1.

Danckwerts, P. V., 1951. Transactions of Faraday Society, Vol. 47, p. 1014.

Datsko, J., 1966. Material Properties and Manufacturing Processes, J. Wiley & Sons, Inc., New York.

Dennison, I. A., and M. Romanoff, 1946. "Soil Corrosion Studies: Ferrous Metal and Alloys", J. Research, NBS, Vol. 44.

Endell, et al, 1938. "Uber Zusammenhange Zwischen Wasserhaushalt der tomminerale and Boden physikalischen Eigenschaften bindiger Boden", Veroffentl. deut. Forsch. Bodenmech, 5.

Ford, F. P., and M. J. Povich, 1979. "The Effect of Oxygen Temperature Combinations of Stress Corrosion Crack Susceptibility of Sensitized Type 304 Stainless Steel in High Temperature Water", Corrosion, Vol. 35, No. 12.

Geel, J., et al, 1979. "Incorporation of Solid High Level Waste into Metal and Non-Metal Matrices", Proceedings of the Conference on High-Level Radioactive Solid Waste Forms, NUREG/CP-0005, L. A. Casey, ed., December.

Haggblom, H., 1977. Diffusion of Soluble Materials in a Fluid Filling a Porous Medium, KBS Technical Report 9, Stockholm, Sweden.

Hammer, N. E. Corrosion Data Survey, 5th ed., NACE, Houston, Texas.

International Nickel Co., Inc. General Seawater Corrosion, GM 3-785719 (2).

Katayama, Y. B., 1976. Leaching of Irradiated LWR Fuel Pellets in Deionized and Typical Ground Water, BNWL-2057, July.

Katayama, Y. B., 1980. Status Report on LWR Spent Fuel IAEA Leach Tests, PNL-3173, Battelle Pacific Northwest Laboratories, March.

LaQue, F. L., and H. R. Copson. Corrosion Resistance of Metals and Alloys, 2nd ed., Reinhold Publishing Co.

Lester, D. H., et al, 1979. System Study on Engineered Barriers Task 3 - Barrier Performance Analysis, Final Report, SAI01379-990LJ, Science Applications, Inc., prepared for Office of Nuclear Waste Isolation, September.

Low, P. F., and J. F. Margheim, 1979. "The Swelling of Clay. I. Basic Concepts and Empirical Equations", Soil Sci. Soc. Amer. Jour., Vol. 43, pp. 473-481.

Marks, L. S., 1952. Mechanical Engineers' Handbook, 5th ed., McGraw-Hill Publishing Co.

Mattson, E., and E. Fredrickson, 1968. "Pitting Corrosion in Copper Tubes: Causes of Corrosion and Countermeasures," British Con. J., Vol. 3, No. 5, September.

Nelson, G. A., 1967. Corrosion Data Survey, NACE, Houston, Texas.

Neretnieks, I., 1978. Transport of Oxidants and Radionuclides Through a Clay Barrier, KBS Teknisk Rapport, February 20.

Posey, F., and A. A. Palko, 1979. Corrosivity of Carbon Steel in Concentrated Chloride Solution", Corrosion, Vol. 35, No. 1, January.

Powell, B. E., and L. V. Lucey, 1966. Physical Studies of Water Formed Corrosion Products on Copper, Final Report to the International Copper Research Assoc., British Non-Ferrous Metals Tech. Center, London, England, March.

Pusch, R., 1978a. Highly Compacted Na Bentonite as Buffer Substance, KBS Report 174, Stockholm, Sweden.

Pusch, R., 1978b. Self-Ingestion of Highly Compacted Bentonite into Rock Joints, KBS Report 173, Stockholm, Sweden.

Rabald, E., 1968. Corrosion Guide, Elseview Publishing Co.

Rockwell, T., 1956. Reactor Shielding Design Manual, McGraw-Hill Publishing Co.

Schlichting, H., 1960. Boundary Layer Theory, J. Kestin, translator, 4th ed., McGraw-Hill Publishing Co., New York.

Schumacher, M., ed., 1979. Sea Water Corrosion Handbook, Noyes Data Corp., Park Ridge, New Jersey.

Smith, J. M., 1970. Chemical Engineering Kinetics, McGraw-Hill Publishing Co., New York.

Speidel, M. O., 1977. "Stress Corrosion Crack Growth in Austenitic Stainless Steel", Corrosion, Vol. 33, No. 6.

Stula, R. T., et al, 1980a. System Study on Engineered Barriers, Task 1 - Interim Report, SAI01379-1070LJ/F, Science Applications, Inc. prepared for Office of Nuclear Waste Isolation, March.

Stula, R. T., et al, 1980b. System Study on Engineered Barriers, Task 3.3 Interim Report, BARIER Code User Manual, SAI01380-437LJ, Science Applications, Inc., prepared for Office of Nuclear Waste Isolation, July.

Syrett, B. C., 1977. "Accreated Corrosion of Copper in Flow of Pure Water Contaminated with Oxygen and Sulfide", Corrosion, Vol. 33, No. 7.

Todd, B., and P. A. Lovett, 1956. "Selecting Materials for Sea Water Systems", in Marine Engineering Practice, Vol. I, Part 18, Institute of Marine Engineers, England.

Tuthill, A. H., and C. M. Schillmoller, 1965. "Guidelines for Selection of Marine Materials", Ocean Science and Engineering Conference, Marine Technology Society, June. International Nickel Co., Inc. Publication - 2M 11-76 (5M 2-76) 5303.

U.S. Department of Energy, 1979a. Draft Environmental Impact Statement - Management of Commercially Generated Radioactive Wastes, Vols. 1 and 2, DOE/EIS-0046-D, April.

U.S. Department of Energy, 1979b. Technology for Commercial Radioactive Waste Management, Vols. 1 through 5, DOE/ET-0028, May.

Westerman, R. E., et al, 1979. Preliminary Conceptual Designs for Advanced Packages for the Geologic Disposal of Spent Fuel, PNL-2990, Pacific Northwest Laboratories, April.

8. NOMENCLATURE

SYMBOL	PROGRAM VARIABLE	EQUATION	UNITS	EXPLANATION
A_1, A_2	---	3.6.3	Dimensionless	Coefficients used in caluculation of buildup factor in RADCLC subroutine
A_n	AN	3.5.19	gm/ml	Parameter in n-th term of Fourier series in RELEAS subroutine
A	A	3.4.4	Ksi	Empirical coefficient used in backfill pressure-vessel relationship in STRESS subroutine
B	B	3.6.1	Dimensionless	Buildup factor in flux calculation in RADCLC subroutine
B	BULK	3.4.13	Ksi	Bulk modulus of Barrier wall in STRESS subroutine
B'	BBULK	3.4.7	Ksi	Instantaneous bulk modulus of backfill in STRESS subroutine
B_n	---	3.5.28	gm/ml	Parameter in n-th term of Fourier series in RELEAS subroutine
B_1, B_2	B1,B2	3.4.13	Ksi	Coefficients in bulk modulus equation for barrier wall in STRESS subroutine
C_o	---	3.4.1	Ksi	Cohesion force in yield model of STRESS subroutine
D	DFL	3.5.6	cm^2/yr	Diffusion coefficient in species of interest in liquid in RELEAS subroutine
D_e	---	3.5.5	cm^2/yr	Effective diffusion coefficient for porous medium
E	E	3.4.44	Dimensionless	Joint efficiency for longitudinal seam in loop stress calculation in STRESS subroutine
$F(b_2)$	FFUNC	3.6.1	Dimensionless	Function used in flux calculation in RADCLC subroutine
G	SHEAR	3.4.14	Ksi	Shear modulus of barrier wall in STRESS subroutine
G_1, G_2	G1,G2	3.4.14	Ksi	Coefficients in shear modulus equation for barrier wall in STRESS subroutine
G'	BSHEAR	3.4.8	Ksi	Instantaneous shear modulus of backfill in STRESS subroutine
H_x	---	3.5.13	cm^3/yr	Mass conductance at x = ℓ in RELEAS subroutine

SYMBOL	PROGRAM VARIABLE	EQUATION	UNITS	EXPLANATION
H_{ℓ}^{o}	HLCA	3.5.28	cm^3/yr	Mass conductance at x=ℓ times area available for transport in RELEAS subroutine
I	I	---	Dimensionless	Barrier identification number for any package design case (I-1 for innermost barrier)
K	---	3.5.29	gm/yr	Parameter in Equation (3.5.29) of RELEAS subroutine
K	K	3.4.4	Ksi	Empirical coefficient used in backfill pressure-volume relationship in STRESS subroutine
K_{ℓ}	AKL	3.5.28	gm/yr	H_{ℓ}^{o} multiplied by concentration difference across the resistance at x=ℓ in RELEAS subroutine
L	---	3.2.2	Inches	Length of waste heat generation surface (cylindrical)
N_a	---	3.5.5	gm/cm^2-yr	Flux of species of interest due to diffusion in RELEAS subroutine
P	---	---	Ksi	Pressure on a transverse cylinder in Figure 2-3
P_o^o	---	3.4.31	Ksi	Initial internal pressure on a barrier in STRESS subroutine
P_1^o	---	3.4.32	Ksi	Initial pressure at R_1 in STRESS subroutine
P	P	3.2.6	Watts/in	Variable used in PKTEMP subroutine for maximum waste temperature calculation
P_R	REPRES	3.4.1	Ksi	Absolute value of mean stress in yield model of STRESS subroutine (repository pressure)
P_1	EPRESS	3.4.29	Ksi	Pressure at R_1 in STRESS subroutine
P_2	---	3.4.36	Ksi	Pressure at R_2 in STRESS subroutine
P_3	REPRES	3.4.36	Ksi	Pressure at R_3 in STRESS subroutine
P_o	---	3.4.29	psi	Internal pressure on a barrier
P_{pore}	---	3.4.1	Ksi	Pore water pressure in yield model of STRESS subroutine
Q	HEAT(Q/L)	3.2.3	Watts	Radial waste heat generation of packaged waste
Q_i	---	---	gm	Initial radionuclide quantities

SYMBOL	PROGRAM VARIABLE	EQUATION	UNITS	EXPLANATION
R	---	3.4.23	Inches	Outside radium of cylinder in STRESS subroutine
R_e	---	---	Dimensionless	Reynolds number
R_f	---	3.5.43	Dimensionless	Retard factor in RELEAS subroutine
R_o	IDIAM	3.4.29	Inches	Radius of inner surface of innermost barrier layer in STRESS subroutine
R_1	ODIAM	3.4.29	Inches	Radius of outer surface of innermost barrier layer in STRESS subroutine
R_2	ODIAM2	3.4.36	Inches	Radius of outer surface of second innermost barrier layer
R_3	FDIAM	3.4.36	Inches	Radius of outer surface of filler or backfill
R_o	RO	3.6.1	cm	Radius of waste assemble
R_c	CORRAT	3.3.1	in/yr	Corrosion rate
$\ddot{R}$	---	3.4.23	in/sec^2	d^2R/dt^2
S	PMAXW	3.4.44	psi	Allowable stress for material in hoop stress calculation in STRESS subroutine
S1,S4	S1,S4	3.4.45	psi	Constants in equations to calculate allowable stress in STRESS subroutine
S2	S2	3.4.45	psi/^oC	Same as above
S3	S3	3.4.45	^oC	Same as above
S_v	SV	3.6.1	Photons/cm^3/sec	Source intensity (cylindrical) in flux calculation in RADCLC subroutine
T_o	---	3.5.65	yr	Time at which zero inventory is obtained in the waste
T	TCENT	3.4.12	^oC	Temperature of barrier wall in STRESS subroutine
T_A	MAXTMP (for innermost barrier layer only)	3.2.3	^oK	Temperature at inner surface of barrier layer (= MAXTMP for innermost barrier)
T_B	TOUTER	3.2.4	^oK	Temperature at outer surface of outermost (gas gap) barrier layer (= temperature of geology for outermost barrier)

SYMBOL	PROGRAM VARIABLE	EQUATION	UNITS	EXPLANATION
T_3	TINNER	3.2.3	^oK	Temperature at outer surface of filler or backfill
T_R	REPTEM	3.2.1	^oK	Temperature at repository surface
T1,T4	T1,T4	3.2.1	^oC	Constants used in repository temperture calculation
T2	T2	3.2.1	$^oC/yr$	Same as above
T3	T3	3.2.1	yr	Same as above
T_c	TEMP	3.2.7	^oK	Temperature at outer surface of barrier layer (TEMPER subroutine)
U'	---	3.4.36	Inches	Radial displacement at R_2 in STRESS subroutine
U	---	3.4.25	Inches	Radial displacement - STRESS subroutine
V	---	---	in/sec	Fluid velocity around a transverse cylinder in Figure 2-3
V	---	3.4.3	cm^3	Backfill volume after compression by pressure P_2
V_o	---	3.4.3	cm^3	Original backfill volume
V*	VSTAR	3.4.3	Dimensionless	Indication of pressure-volume relationship of backfill
X_n	---	3.5.19	Dimensionless	Parameter in n-th term of Fourier series in RELEAS subroutine
Y	Yield	3.4.12	Ksi	Yield strength in yield model of STRESS subroutine
Y_1,Y_2	Y1,Y2	3.4.12	Ksi	Coefficients in yield stress equation for barrier wall in STRESS subroutine
a	---	3.4.27	Dimensionless	Constant in strain equations in STRESS subroutine
a	---	3.6.1	cm	Distance to the point of interest from the edge of the waste cylinder in the RADCLC subroutine
a_1,a_2	---	3.6.3	Dimensionless	Coefficients used in calculation of buildup factor in RADCLC subroutine
b	---	3.4.27	Dimensionless	Constant in strain equations in STRESS subroutine
b_2	---	3.6.1	Dimensionless	Number of mean free paths to point of interest in the RACLC subroutine

SYMBOL	PROGRAM VARIABLE	EQUATION	UNITS	EXPLANATION
b	---	3.5.33	Dimensionless	Radio-diffusion parameter in RELEAS subroutine
c_∞	---	3.5.27	gm/ml	Concentration of species of interest in liquid at infinite distance in a slab in RELEAS subroutine
c_ℓ	---	3.5.2	gm/ml	Concentration at ℓ of species of interest in liquid in RELEAS subroutine
c	CONC	3.5.1	gm/ml	Concentration of species of interest in liquid in RELEAS subroutine
c_s	---	3.5.9	gm/gm	Grams of species of interest absorbed on one gram of solid
e	EM	3.2.4	Dimensionless	Effective emmisivity across gas gap of a barrier layer
e_B	EOUTER	3.2.5	Dimensionless	Emissivity at outer surface of barrier gas gap
e_3	EINNER	3.2.5	Dimensionless	Emissivity at inner surface of barrier gas gap
f(x)	---	3.5.52	gm/ml	Concentration profile in the backfill at zero inventory in the waste package
f	---	3.4.26	Dimensionless	Constant in radial displacement equation in STRESS subroutine
f(t)	---	3.5.27	gm/yr	Rate of transport of species of interest out of waste canister
g	---	3.4.26	in^2	Constant in radial displacement equation in STRESS subroutine
h_o	HZ	3.5.3	cm^{-1}	Mass conductance at x=0 divided by diffusion coefficient for species of interest in the backfill
h_ℓ	HL	3.5.2	cm^{-1}	Mass conductance at x=ℓ divided by diffusion coefficient for species of interest in the backfill
h_{BR}	COEFF	3.2.7	Watts/in^2-^oK	Estimated overall heat transfer coefficient between repository and failed barrier surface
k	---	3.5.1	cm/yr	Constant in Equation (3.5.1) in RELEAS subroutine
k_c	---	3.5.44	cm/yr	Constant in Equation (3.5.44) in RELEAS subroutine

SYMBOL	PROGRAM VARIABLE	EQUATION	UNITS	EXPLANATION
k_p	---	---	cm/min	Permeability of porous media
k	K	3.5.12	cm^2/yr	Constant in exponential terms which generate transient response of series in RELEAS subroutine
k_d	KD	3.5.9	ml/gm	Equilibrium constant relating concentration of species of interest in liquid to that absorbed on solid in RELEAS
k^{A1}	MCOND(MAT)	3.2.3	Watt/in-^oK	Thermal conductivity of innermost barrier layer
k^{12}	MCOND(MAT2)	3.2.3	Watt/in-^oK	Thermal conductivity of second innermost barrier layer
k^{23}	FCOND(BAK)	3.2.3	Watt/in-^oK	Thermal conductivity of filler or backfill
k^{3B}	MCOND(MATGAP)	3.2.4	Watt/in-^oK	Thermal conductivity of barrier gas gap
ℓ	L	3.5.1	cm	Thickness of Backfill in RELEAS subroutine
q	---	3.5.15	gm/yr-cm^2	Transport flux through a slab in RELEAS subroutine
r	---	---	inches	Radius of barrier package layer relative to waste centerline (r=0)
r_A	IDIAM	3.2.3	inches	Radius of inner surface of innermost barrier layer
r_B	GDIAM	3.2.3	inches	Radius of outer surface of barrier gas gap
r_1	ODIAM	3.2.3	inches	Radius of outer surface of innermost barrier layer
r_2	ODIAM2	3.2.3	inches	Radius of outer surface of second innermost barrier layer
r_3	FDIAM	3.2.3	inches	Radius of outer surface of filler or backfill
r_{tr}	---	3.5.30	gm/yr	Constant rate of transport of species of interest out or waste canister
t	TIME	3.2.1	yr	Time elapsed since package emplacement
t_f	TFINAL	3.5.31	yr	Time when quantity of radionuclides in waste is zero
t_s	TS	3.5.25	yr	Time at which constant transport conditions prevail (steady state time) in RELEAS subroutine
t'	---	3.5.35	yr	Time elapsed since package emplacement
$u(x)$	EXACT	3.5.17	gm/ml	Concentration profile in backfill at constant transport conditions (steady state profile)

SYMBOL	PROGRAM VARIABLE	EQUATION	UNITS	EXPLANATION
$v(x,o)$	---	3.5.52	gm/ml	Concentration profile in the backfill for the insulated condition
$w(x,t)$	SERIES	3.5.17	gm/ml	Time-dependent concentration profile in the backfill
x	X	3.5.1	cm	Distance from arbitrary reference point
x_0	THICK,THICK2	3.3.1	inches	Previous barrier layer thickness
x_1	THICK,THICK2	3.3.1	inches	New barrier layer thickness after corrosion over an increment of time
y_0	---	3.5.28	gm	Initial quantity of waste in RELEAS subroutine
y	Y	3.5.27	gm	Quantity of species of interest remaining in waste before constant transport prevails in RELEAS subroutine
z_s	---	3.5.48	cm	Location of soluble substance-solution interface in a solid in RELEAS subroutine
z	---	3.5.30	gm	Quantity of species of interest remaining in waste after constant transport conditions prevail in RELEAS subroutine
z	--	3.6.1	cm	Self-shielding distance factor in RADCLC subroutine
z_0	Y	3.5.31	gm	Quantity of species of interest in waste at time when constant transport conditions prevail in RELEAS subroutine
$\ddot{z}$	---	3.4.24	in/sec^2	d^2L/dt^2
α	---	3.5.21	cm^{-1}	Parameter in Fourier series in RELEAS subroutine
α_1	---	3.5.25	cm^{-1}	Parameter in Fourier series in RELEAS subroutine
α_n	R(N)	3.5.19	cm^{-1}	Parameter in n-th term of Fourier series in RELEAS subroutine
β_j	---	3.5.53	cm^{-1}	N-th positive root of Equation (3.5.54)
β	BETA	3.4.1	Dimensionless	Constant slope of Mohr envelope in yield model of STRESS
ν	POISS	3.4.8	Dimensionless	Poisson's ratio in STRESS subroutine
Δr	THICK	3.2.7	inches	Thickness of inner barrier layer (wall) at time of failure

SYMBOL	PROGRAM VARIABLE	EQUATION	UNITS	EXPLANATION
Δt	DELTA	3.31	yr	Time increment
$\Delta\sigma_R$	---	3.4.16	Ksi	Change in radial stress - STRESS subroutine
$\Delta\sigma_Z$	---	3.4.18	Ksi	Change in axial stress - STRESS subroutine
$\Delta\sigma_\theta$	---	3.4.17	Ksi	Change in angular stress - STRESS subroutine
δ	TORTUR	3.5.6	Dimensionless	Tortuosity of porous medium with respect to diffusion in RELEAS subroutine
δ	THICK	3.4.44	inches	Wall thickness used in hoop stress calculation in STRESS subroutine
ϵ_z	---	3.4.36	in/in	Change in axial strain at R_2 in STRESS subroutine
ϵ	EP	3.4.16	Dimensionless	Void volume of porous medium in RELEAS subroutine
ϵ_R	---	3.5.16	in/in	Change in radial strain - STRESS subroutine
ϵ_z	---	3.4.16	in/in	Change in axial strain - STRESS subroutine
ϵ_θ	---	3.4.16	in/in	Change in angular strain - STRESS subroutine
η	ETA	3.4.38	Dimensionless	Constant defined by Equation (3.4.39) in STRESS subroutine
λ_n	---	3.5.40	Dimensionless	Parameter in RELEAS subroutine, $\lambda_n = n\Pi$
λ_m	---	3.5.65	Dimensionless	Parameter in RELEAS subroutine, $\lambda_m = m\Pi$
λ	LAMBDA	3.4.16	Ksi	Lamé constant for barrier wall in STRESS subroutine
λ	DECAYC	3.5.27	yr^{-1}	Radiodecay constant of species of interest in RELEAS subroutine
λ	BLAMB	3.4.10	Ksi	Lamé constant for backfill in STRESS subroutine
ρ	CLAYD	3.5.11	gm/ml	Bulk density of porous medium in RELEAS subroutine
ρ	---	3.4.23	lb/in^3	Density
σ	---	3.2.4	$watt/in^2\text{-}^oK^4$	Boltzman constant
θ	---	3.5.66	Dimensionless	Parameter in RELEAS subroutine, $\theta = kt/\ell^2$
∞	---	3.5.44	cm	Infinite transport distance in a slab in RELEAS subroutine

SYMBOL	PROGRAM VARIABLE	EQUATION	UNITS	EXPLANATION
ϑ	---	3.4.23	Inches	Outside radius of cylinder in STRESS subroutine
σ_R	---	3.4.16	Ksi	Radial stress in STRESS subroutine
σ_z	---	3.4.18	Ksi	Axial stress in STRESS subroutine
σ_θ	---	3.4.17	Ksi	Angular stress in STRESS subroutine
σ_R^o	---	3.4.19	Ksi	Initial radial stress in STRESS subroutine
σ_z^o	---	3.4.20	Ksi	Initial axial stress in STRESS subroutine
σ_θ^o	---	3.4.19	Ksi	Initial angular stress in STRESS subroutine
BAK	BAK	---	Dimensionless	Identification code for backfill material type
BFAIL	BFAIL	---	Dimensionless	Designates backfill integrity in STRESS subroutine (= 0 indicates failure)
CLPRES	CLPRES	---	psi	Internal pressure on barrier at time of repository sealing
CLTEMP	CLTEMP	---	^oK	Internal temperature on barrier at time of repository sealing
COAT	COAT	---	yr	Coating delay time in CORODE subroutine
FLUX	FLUX	3.6.1	photons/cm^2/sec	Gamma ray flux at a particular package location
IB	IB	---	Dimensionless	Number of barriers in a package design case (I=IB for outermost barrier)
IGE	IGE	---	Dimensionless	Identification code for geology
IL	IL	---	Dimensionless	Identification code for type of barrier
IWATER	IWATER	---	Dimensionless	Identification code for type of repository water
MAT	MAT	---	Dimensionless	Identification code for type of material in inner barrier layer
MAT2	MAT2	---	Dimensionless	Identification code for type of material in second innermost barrier layer

SYMBOL	PROGRAM VARIABLE	EQUATION	UNITS	EXPLANATION
MATGAP	MATGAP	---	Dimensionless	Identification code for barrier gas gap material type
WFAIL	WFAIL	---	Dimensionless	Designates barrier wall integrity in STRESS subroutine (= 0 indicates failure)

APPENDIX A

BARIER PROGRAM LISTING

The program listing of BARIER and all of its subroutines is provided in this Appendix.

```
C             PROGRAM BARIER
C
C
C             CALCULATION OF ENGINEERED BARRIER PERFORMANCE
C                MAIN PROGRAM SETS DIMENSIONS AND READS INPUT
C                ALL MATRIXES ARE AVAILABLE TO SUBROUTINES BY
C                THE COMMON MATRIX...
C
      INCLUDE 'COMMON.NEW'
      DOUBLE PRECISION BARFIL,DATSET
      DOUBLE PRECISION CTITLE,MATLAB,BKLAB,ILLAB
      DIMENSION CTITLE(CEO),WLAB(3,IBAR),MATLAB(IMTR),ILLAB(5)
     1          ,BKLAB(IBAK)
      INTEGER FLAG
C             HEAT GENERATION RATE    WATTS/IN
      DATA HEAT/4.73/
C
C     LABEL INPUT
C
      DATA CTITLE/     10HSALT       ,
     2                 10HBASALT     ,
     3                 10HGRANIT     ,
     4                 10HSHALE     /
      DATA WLAB/5HBRINE,5H,ANOX,5HIC    ,
     1          5HBRINE,5H,OXIC,5H      ,
     2          5HLOW 1,5HON,AN,5HOXIC  ,
     3          5HLOW 1,5HON,OX,5HIC    ,
     4          5HNONE ,5H      ,5H     /
     DATA MATLAB/10HSTEEL.
     2              10HZINC       ,
     3              10HINCONL     ,
     4              10H304SST     ,
     5              10HCOPPER     ,
     6              10HLEAD       ,
     7              10HIRON       ,
A                   10HBELIUM     ,
B                   10HAIR        ,
C                     10HNONE      /
      DATA ILLAB/      10HCAST STAB ,
     1                 10HSTAB      ,
     2                 10HCAN       ,
     3                 10HOPACK     ,
     4                 10HSLEEVE   /
      DATA BKLAB/      10HONE       ,
     2                 10HBENT      ,
     3                 10HSAND-B    ,
     4                 10HCLINO    /
C     THERMAL CONDUCTIVITIES FOR METALS AND CASES (WATTS/IN-C)
C
      DATA MCOND/1.1,.40,.35,.41,9.4,.70,1.2,.003,.0005,.0005/
C
C     THERMAL CONDUCTIVITIES OF FILLERS (WATTS/IN-C)
C
      DATA FCOND/.0005 ,.004,.007,.004/
C
C
C           EMMISSIVITIES OF ' TALS
C
      DATA EMAT/.8,.9,.07,.85,.78,.63,.66,.9,.9,.9/
C
C           EMMISSIVITIES OF   ACKFILLS
C
      DATA EBAK/.9,.9,.9,.9/
C
C           OPEN OUTPUT FILES
      OPEN(UNIT=25,DEVICE='DSK',FILE='PERFOR.DAT')
```

```
C
C       ENTRY OF RUN PARAMETERS AND INPUT FILE NAME
C
2        TYPE 200
200      FORMAT(' ENTER INPUT F' E NAME FOR CASES.. ',$)
         ACCEPT 201,DATSET
201      FORMAT(A10)
         IF(DATSET.EQ.'STOP') GO TO 600
         TYPE 1200
1200     FORMAT(' ENTER DELTA TIME ????(YEARS)  ',$)
         ACCEPT *,DELTA
         TYPE 1007
1007     FORMAT(' NOW SET A ICE .... ',$)
         ACCEPT *,ICE
         TYPE 202
202      FORMAT(' ENTER IWATER .... ',$)
         ACCEPT *,IWATER
         ICOUNT=IWATER
         OPEN (UNIT=20,DEVICE='DSK',ACCESS='SEQIN',FILE=DATSET)
         OPEN (UNIT=22,DEVICE='DSK',ACCESS='SEQIN',FILE='GEOMAT.DAT')
         OPEN (UNIT=23,DEVICE='DSK',ACCESS='SEQIN',FILE='MATMAT.DAT')
         OPEN (UNIT=24,DEVICE='DSK',ACCESS='SEQIN',FILE='CORMAT.DAT')
C
C                NOW READ INPUT FROM FILES
         READ(22,1002,END=9999,ERR=9999)(LABEL(I),REPRES(I),
        1        CREEP(I),ECEO(I),
        1        T1(I),T2(I),T3(I),T4(I),COEFF(I)),I=1,ICEO)
1002     FORMAT(A5,F10.0,A5,6F10.0)
       REPRES(ICE)=REPRES(ICE)/1000.
       READ(23,1003,END=99999,ERR=99999)((Y1(I),Y2(I),
        1        B1(I),B2(I),C1(I),C2(I),S1(I),S2(I),S3(I),S4(I)
        2        ),I=1,IMTR-3)
1003     FORMAT(10F10.0)
         READ(24,1005,ERR=99950,END=99950)((CORRAT(I,J),I=1,8),J=1,IMTR-3)
1005     FORMAT(8F10.0)
4        READ(20,250,END=2)BARFIL,IB
250      FORMAT(A10,I2)
         OPEN (UNIT=21,DEVICE='DSK',ACCESS='SEQIN',FILE=BARFIL)
         READ(21,1001,END=999,ERR=999)(ILC(I),IDIAM(I),ODIAM(I),
        1        ODIAM2(I),FDIAM(I),CDIAM(I),
        1        A(I),K(I),MAT(I),MAT2(I),E(I),COAT(I),BAK(I),MATCAP(I)
        2        ,CLPRES(I),CLTEMP(I),BETA(I),POISS(I)
        1        ),I=1,IB)
         FLAG=ILC(1)
1001     FORMAT(5X,I5,7F10.0,/,2I5,2F10.0,2I5,2F10.0,2F5.0)
C
C                HERE WE PRINT OUT SOME INPUT INFORMATION
         100=25
         WRITE(100,299),BARFIL
299      FORMAT('1',50X,'CONCEPT  ',A10,/)
       BALL(ICE)=REPRES(ICE)*1000.
         WRITE(100,300)CTITLE(ICE),BALL(ICE)  ,CREEP(ICE)
300      FORMAT(/,' GEOLOGY:    ',A10,/,' REPOSITORY PRESSURE (PSI):',
        1        F10.4,/,' CREEPING MEDIUM ?  ',A5)
C
C                CALCULATE PEAK WASTE TEMPERATURE
         CALL PKTEMP
         WRITE(100,1201),MAXTMP
1201     FORMAT(' MAXIMUM WASTE TEMP.:  ',F5.1,'(K)')
         IF(MAXTMP .GT.653.)GO TO 10
         WRITE(100,1000)
1000     FORMAT(' WASTE TEMPERATURE EXCEEDED ')
         GO TO 568
10       CONTINUE
C
C       PRINT HEADINGS
```

```
      WRITE(IOU,302)
302   FORMAT(' ELEMENT  I.D.   O.D.   O.D.   O.D.   O.D.    ',
     1'BACKFILL   INNER  OUTER  JOINT  COAT  FILLER    ',
     2'CAP       SEAL   SEAL  BACKFILL BACKFILL'
     1,/,9X,'INNER  INNER  OUTER  FILLER',
     3'  CAP   COEFFICIENTS SOLID  SOLID   EFF  DELAY',
     4' MATERIAL MATERIAL  PRESS   TEMP'
     4,'     MOHR   POISSON',/
     4,9X,'SOLID  SOLID ',
     5' SOLID   (IN)   (IN)   A        K',23X,'(YRS)',20X,
     6'(PSI)    (K)    SLOPE   RATIO'
     6,/,10X,'(IN)   (IN)   (IN)')
C     PRINT  MORE INPUT INFORMATION
      DO 303 I=IB,1,-1
      WRITE(IOU,304),ILLAB(ILC(I)+1),IDIAM(I),
     1ODIAM(I),ODIAM2(I),FDIAM(I),CDIAM(I)
     1              ,A(I),K(I),MATLAB(MAT(I))
     2     ,MATLAB(MAT2(I))   ,E(I),COAT(I),BKLAB(BAK(I)+1)
     3     ,MATLAB(MATCAP(I))
     3              ,CLPRES(I),CLTEMP(I)
     4              ,BETA(I),POISS(I)
303   CONTINUE
304   FORMAT(1X,A7,5F7.3,1X,F5.2,F7.2,1X,2A7,
     1      F5.2,1X,F5.1,2(2X,A7),F7.2,F8.2,
     1F7.2,F9.2)
      WRITE(IOU,305)
305   FORMAT(/,' BARRIER PERFORMANCE',/,'___________________',/)
6     IF(IWATER.EQ.ICOUNT) GO TO 2000
      WRITE(IOU,307)MLAB(1,IWATER),MLAB(2,IWATER),MLAB(3,IWATER)
307   FORMAT('1',' WATER:   ',3A5)
      GO TO 308
2000  WRITE(IOU,306)MLAB(1,IWATER),MLAB(2,IWATER),MLAB(3,IWATER)
306   FORMAT(' WATER:   ',3A5)
308   WRITE(IOU,309)
309   FORMAT(' ELEMENT          FAILURE        NET          ',
     1'THICKNESS      ELEMENT      REPOSITORY     RAD FLUX',/,16X,
     2'TIME(YRS)    PRESS(PSIA)       (IN)          ',
     3'TEMP(K)       TEMP(K)       (N/HR)')
      ILIM=IB
C              ILIM IS THE NO. OF BARRIERS
      TIME=0.0
      IDONE=2
      IF(FLAG.EQ.0)IDONE=1
      DO 100 I=ILIM,IDONE,-1
C           CALCULATE THICK HERE
     THICK=(ODIAM(I)-IDIAM(I))/2.
     THICK2=(ODIAM2(I)-ODIAM(I))/2.
1299  CONTINUE
     NFAIL=1
      INDX=I
      M=MAT(I)
      TIMBAR=0.0
7     CONTINUE
      TIMBAR=TIMBAR+DELTA
      TIME=TIME+DELTA
      CALL TEMPER
     CALL RADCLC
      CALL CORODE
      IF(FLAG.EQ.0.AND.(...EEP(ICE).EQ.'YES')GO TO 8
      IF(FLAG.EQ.0.AND.CREEP(ICE).EQ.'NO' )GO TO 9
      CALL STRESS
     IF(THICK.LE.0.0) NFAIL=0
      GO TO 1099
8     NFAIL=1
      IF(THICK.LE.0)NFAIL=0
      RIPRS=-REPRES(ICE)*1000.
```

```
      GO TO 1099
9     WFAIL=1
      IF(THICK.LE.0)WFAIL=0
      NTPRS=(CLPRES(INDX)*TEMP/CLTEMP(INDX)-15.)
1099  IF(WFAIL.EQ.0) GO TO 12
      GO TO 7
12    CONTINUE
     IF(THICK.LE.0.0)THICK=0.0
C               HERE WRITE INFO ABOUT INDIVIDUAL BARIERS..
      WRITE(100,310),ILABC(IL(I)+1),TIMBAR,NTPRS,THICK,
     1                TEMP,REPTEM,FLUX
310   FORMAT(1X,A10,2F13.2,F14.3,3X,F12.2,F13.2,1PE15.3)
100   CONTINUE
C               SET I TO 1
C               FOR THE REST OF THE MAIN PROGRAM..
      I=1
C
C               PRINT TIME ...
      WRITE(100,456),TIME
456   FORMAT(/' LEACH BEGIN TIME (YEARS) =  ',F9.2)
C               LEACH BEGIN
C
                        CALL RELEAS
      IWATER=IWATER+1
      IF(IWATER.LE.ICOUNT+1)GO TO 6
560   CLOSE (UNIT=21,DEVICE='DSK',ACCESS='SEQIN',FILE=BARFIL)
      IWATER=ICOUNT
      GO TO 4
600   STOP
999   TYPE 990
990   FORMAT(' TROUBLE WITH UNIT 21  ')
      STOP
9999  TYPE 9990
9990  FORMAT(' TROUBLE WITH UNIT 22  ')
      STOP
99999 TYPE 99990
99990 FORMAT(' TROUBLE WITH UNIT 23  ')
      STOP
99950 TYPE 99940
99940 FORMAT(' TROUBLE WITH UNIT 24 ')
     STOP
      END
      SUBROUTINE CORODE
C               ALL MATRIXES ARE AVAILABLE TO SUBROUTINES BY
C               THE COMMON MATRIX...
C
      INCLUDE 'COMMON.NEW'
C               ALLOW FOR COATING DELAY TIME
      IF(TIMBAR .LE. COAT(INDX)) RETURN
     IF(TEMP.GT.373.) GO TO 13
     KKK=2*IWATER-1
     GO TO 15
  13 KKK=2*IWATER
  15 IF(THICK2.LE.0.0)GO TO 14
      THICK2=THICK2-CORRAT(KKK,    MAT2(INDX))*DELTA
      RETURN
14    THICK = THICK - CORRAT(KKK,    MD)*DELTA
      RETURN
      END
```

```
      SUBROUTINE PKTEMP
C             ALL MATRICES ARE AVAILABLE TO SUBROUTINES BY
C             THE COMMON MATRIX. . .
C
        INCLUDE 'COMMON.NEW'
      TOUTER=T4(ICE)+273.0
      DO 100 I=IB,1,-1
      IF(FDIAM(I).EQ.CDIAM(I)) GO TO 90
      XY=0.0
      DT=2.0
      ICONT=0
      TINNER=TOUTER
      IF(FDIAM(I).EQ.ODIAM2(I)) EINNER=EMAT(MAT2(I))
      IF(FDIAM(I).GT.ODIAM2(I)) EINNER=EBAK(BAK(I)+1)
      IF(I.EQ.IB) EOUTER=EGEO(ICE)
      IF(I.LT.IB) EOUTER=EMAT(MAT(I+1))
      EM=1.0/(1.0/EINNER+(FDIAM(I)/CDIAM(I))*(1.0/EOUTER-1.0))
10    P=2.0*3.14159*(FDIAM(I)*EM*3.60*10.0**(-11.0)*(TINNER**4.0-
     1TOUTER**4.0)+(TINNER-TOUTER)*HCOND(MATCAP(I))/ALOG(CDIAM(I)/
     2FDIAM(I)))-HEAT
      IF(ABS(P).LT.ABS(.01)) GO TO 50
      ICONT=ICONT+1
      IF(ICONT.GT.100) GO TO 48
      IF(P.LT.0.0) GO TO 30
      IF(P.GT.0.0) GO TO 40
30    IF(ABS(P+XY).LT.ABS(P-XY)) GO TO 35
      GO TO 37
35    DT=DT/2.0
37    TINNER=TINNER+DT
      XY=P
      GO TO 10
40    IF(ABS(P+XY).LT.ABS(P-XY)) GO TO 45
      GO TO 47
45    DT=DT/2.0
47    TINNER=TINNER-DT
      XY=P
      GO TO 10
48    WRITE(IOU,49),I
49    FORMAT(' ITERATIONS EXCEED 100 FOR BARRIER =',I3)
50    CONTINUE
      GO TO 95
90    TINNER=TOUTER
95    SUM=ALOG(FDIAM(I)/ODIAM2(I))/FCOND(BAK(I)+1)
      SUM=SUM+ALOG(ODIAM2(I)/ODIAM(I))/MCOND(MAT2(I))
      SUM=SUM+ALOG(ODIAM(I)/IDIAM(I))/MCOND(MAT(I))
      MAXTMP=TINNER+HEAT*SUM/(2.0*3.14159)
      TOUTER=MAXTMP
100   CONTINUE
      RETURN
      END
```

```
      SUBROUTINE TEMPER
C               ALL MATRICES ARE AVAILABLE TO SUBROUTINES BY
C               THE COMMON MATRIX...
C
      INCLUDE 'COMMON.NEW'
      IF (TIME.LT.T3(ICE)) GO TO 10
      REPTEM=T4(ICE)
      GO TO 11
   10 CONTINUE
      REPTEM=T1(ICE)+T2(ICE)*ALOG(TIME)
   11 CONTINUE
      REPTEM=273.0+REPTEM
C               NOW CALCULATE TEMP...
      TEMP=HEAT/(3.14159*(DIAM(INDX)+2.*THICK)*COEFF(ICE))+REPTEM
      RETURN
      END
```

```
      SUBROUTINE STRESS
        INCLUDE 'COMMON.NEW'
      R0=IDIAM(INDX)/2.
      IF THICK.LE.0.0000001) GO TO 100
      R1=R0+THICK
      R2=ODIAM2(INDX)/2.
      R3=FDIAM(INDX)/2.
      TCENT=TEMP-273.
      IF(CREEP(ICE).EQ.'NO') GO TO 200
      YIELD=Y1(M)+Y2(M)*TCENT
      BULK=B1(M)+B2(M)*TCENT
      SHEAR=G1(M)+G2(M)*TCENT
      IF((FDIAM(INDX)-ODIAM2(INDX)).LT..01) GO TO 140
      IF(BFAIL.EQ.0.0) GO TO 80
      IF(K(INDX).LT.0.01) GO TO 50
      VSTAR=-A(INDX)+SQRT(A(INDX)*2.   +4. *K(INDX)*REPRES(ICE))
      VSTAR=VSTAR/2./K(INDX)
      GO TO 60
   50 VSTAR=REPRES(ICE)/A(INDX)
   60 BBULK=A(INDX)*(VSTAR+1.)+2.*K(INDX)*VSTAR*(VSTAR+1.)
      BSHEAR=1.5*BBULK*(1.-2.*POISS(INDX))/(1.+POISS(INDX))
      LAMBDA=BULK-2.*SHEAR/3.
      BLAMB=BBULK-2.*BSHEAR/3.
      DENOM=R1*(R1**2.  /(LAMBDA+SHEAR)+R0**2./SHEAR)/2./(R1**2.-R0**2.)
      DENOM=DENOM+R2*(R2**2./(BLAMB+BSHEAR)+R3**2./BSHEAR)/2.
     1       /(R3**2.-R2**2.)
      DENOM=DENOM*2.*(R3**2.-R2**2.)
      EPRESS=REPRES(ICE)*R2*R3**2.*(1./(BLAMB+BSHEAR)+1./BSHEAR)
      EPRESS=EPRESS/DENOM
      ETA=SQRT(0.148148*BETA(INDX)**2.*(1.-POISS(INDX))**2.
     1     -(1.-2.*POISS(INDX))**2./3.)
      PMINB=REPRES(ICE)*(1.-ETA)/(1.-ETA*R2**2./R3**2.)
      IF(EPRESS.LT.PMINB) GO TO 150
      BFAIL=1
   80 NU=(3.*BULK-2.*SHEAR)/(3.*BULK+SHEAR)/2.
      PMAXW=(YIELD/2.)*(1.-R0**2./R1**2.)/SQRT(1.-NU+NU**2.)
      NTPRS=-PRESS*1000.
      IF(EPRESS.GT.PMAXW) GO TO 100
   90 WFAIL=1
      RETURN
  100 WFAIL=0
      RETURN
  140 EPRESS=REPRES(ICE)
      NTPRS=-EPRESS*1000
      GO TO 80
  150 BFAIL=0
      EPRESS=REPRES(ICE)
      NTPRS=-EPRESS*1000
      GO TO 80
C
C       INTERNAL PRESSURE DOMINATES - NO CREEP
C
  200 IF(TCENT.GE.S3(M)) S=S1(M)-S2(M)*TCENT
      IF(TCENT.LT.S3(M)) S=S4(M)
      PMAXW=THICK*S*E(INDX)/(R0+.6*THICK)/1000.
      FORCE=(CLPRES(INDX)*TEMP/CLTEMP(INDX)-15.)/1000.
      NTFRS=FORCE*1000.
      IF(PMAXW-FORCE) 100,100,90
      END
```

```
      SUBROUTINE RADCLC
      INCLUDE 'COMMON.NEW(4073,4073)'
      DIMENSION XMUBF(4),XMUBR(9),TPRR(9),PRR(9)
      DIMENSION T(50),MID(50),B(50)
      DIMENSION A1(4),A2(4),ALPH1(4),ALPH2(4),MXBF(4),MXBR(9)
C
C  DEFINITION OF VARIABLES
C
C    B     = BUILDUP FACTOR, B(JMAX+1)=TOTAL BUILDUP FACTOR
C    SV    = SOURCE INTENSITY
C    RO    =RADIUS OF FUEL ASSEMBLY
C    FLUX  = PHOTON FLUX
C    XMUBF       = ARRAY OF ATTENUATION COEFFICIENTS FOR BACKFILL MATERIALS
C    XMUBR       = ARRAY OF ATTENUATION COEFFICIENTS FOR BARRIER MATERIALS
C    PRR   = ARRAY OF PHOTON RELEASE RATE VS TIME
C    TPRR  = ARRAY OF TIMES CORRESPONDING TO PRR
C    XMU   = TEMPORARY ATTENUATION COEFFICIENT
C    T     = TEMPORARY MATERIAL THICKNESS, THEN XMU*T
C    ARG   = TEMPORARY SUM OF XMU*T THROUGH MATERIALS
C    MID   = ARRAY FOR MATERIAL ID'S
C    JMAX  = NUMBER OF THICKNESSES OUT TO DOSE POINT
C    A1,A2,ALPH1,ALPH2 = BUILDUP FACTOR COEFFICIENTS
C    MXBF        = BACKFILL MATERIAL CROSS REF TO BUILDUP FACTOR
C    MXBR        = BARRIER MATERIAL CROSS REFERENCE TO BUILDUP FACTOR
C
C    STOP CODES
C    1111 NEED TO INCREASE DIMENSION ON T, MID, AND B
C    2222 TIME RANGE FOR SOURCE INTENSITY EXCEEDED
C
      DATA MXBF/0,3,3,3/
      DATA MXBR/1,1,1,1,2,2,1,0,0/
      DATA A1/9,2.3,10.11/
      DATA A2/-0,-1.3,-9,-10/
      DATA ALPH1/-.081,-.04,-.083,-.104/
      DATA ALPH2/.0255,.17,.03,.03/
C
      DATA XMUBF/0.,0.130,0.140,0.130/
      DATA XMUBR/0.470,0.367,0.472,0.462,0.50 ,0.797,
     *.470,0.0,0.0,0.0/
      DATA TPRR/0,1,10,30,100,300,1000,3000,1 000/
      DATA PRR/5.51E+15,4.70E+15,2.43E+15,1.4 E+15,2.95E+14,
     *2.05E+12,2.56E+10,2.30E+10,1.86E+10/
C
C  GET MATERIAL THICKNESSES
C
      J=0
      DO 10 I=1,INDX
      J=J+1
      IF (J.GT.50) STOP 1111
      T(J)=ODIAM(I)-IDIAM(I)
      MID(J)=MAT(I)
      J=J+1
      IF (J.GT.50) STOP 1 11
      T(J)=ODIAM2(I)-ODIA (I)
      MID(J)=MAT2(I)
      IF (I.EQ.INDX) GOTO 10
      J=J+1
      IF (J.GT.50) STOP 1111
      T(J)=IDIAM(I)-ODIAM2(I)
      MID(J)=-BAK(I)
      J=J+1
      IF (J.GT.50) STOP 1111
      T(J)=CDIAM(I)-IDIAM(I)
      MID(J)=MATCAP(I)
 10   CONTINUE
      JMAX=J
```

```
C       TYPE 2000,(J,T(J),MID(J),J=1,JMAX)
 2000 FORMAT(I5,F10.3,I5)
C
C   CALCULATE ARC
C
        ARC=0
        DO 20 J=1,JMAX
        IF(MID(J).GE.10) GOTO 12
        IF(MID(J)) 11,12,13
  11    XMU=XMUBF(ABS(MID(J)))
        GOTO 15
  12    XMU=0.
        GOTO 15
  13    XMU=XMUBR(MID(J))
  15    T(J)=T(J)*XMU/2.54
  20    ARC=ARC+T(J)
C       TYPE 2001,(J,T(J),J=1,JMAX)
 2001 FORMAT(I5,1PE10.3)
C
C   CALCULATE BUILDUP FACTORS
C
        DO 21 J=1,50
  21    B(J)=1.
        JJ=JMAX+1
        DO 50 J=1,JMAX
        IF (MID(J).GE.10) GOTO 23
        IF(MID(J))22 23,24
  22    MB=MXBBF(-MID(J))
        GOTO 25
  23    MB=0
        GOTO 25
  24    MB=MXBBR(MID(J))
  25    IF(MB.NE.0) GOTO 30
        B(J)=1.
        GOTO 50
  30    B(J)=A1(MB)*EXP(-ALPH1(MB)*T(J))+A2(MB)*EXP(-ALPH2(MB)*T(J))
  50    B(JJ)=B(JJ)*B(J)
C       TYPE 2001,(J,B(J),J=1,JJ)
C
C   GET SOURCE INTENSITY
C
        DO 70 I=1,9
        IF (TIME-TPRR(I)) 55,65,70
  70    CONTINUE
C   INTERPOLATE SEMILOG
  55    IM1=I-1
        SONE=PRR(IM1)
        STWO=PRR(I)
        TONE=TPRR(IM1)
        TTWO=TPRR(I)
        SV=SONE*(STWO/SONE)**((TIME-TONE)/(TTWO-TONE))
        GOTO 75
  65    SV=PRR(I)
        GOTO 75
        STOP 2222
C
C   NORMALIZATION FACTOR
C
  75    SV=3.50E-09*SV
C
C   CALCULATE FLUX - UNITS ARE ROENTGENS/HR.
        FLUX B(JJ)*SV*FFUNC(ARC)/ODIAN2(INDX)
C       FF=FFUNC(ARC)
C       TYPE 2002,B(JJ),SV,FF,ODIAN(INDX)
 2002 FORMAT(1P4E10.3)
        RETURN
```

```
      END
      FUNCTION FFUNC(B)
      DATA N/5/,THETA/90/
      T=.01745329*THETA
      FF=0
      DT=T/N
      DO 10 I=1,N
      X1=(I-1)*DT
      X2=I*DT
      F1=F(X1,B)
      F2=F(X2,B)
      FF=FF+(F1+F2)*DT/2
10    CONTINUE
      FFUNC=FF
      RETURN
      END
      FUNCTION F(X,B)
      F=COS(X)
      IF(F.GT.0.001) GOTO 1
      F=0
      RETURN
1     F=-B/F
      F=EXP(F)
      RETURN
      END
```

```
      SUBROUTINE RELEAS
      INCLUDE 'COMMON.NEW'
      REAL*8 CLAYOD,CLAYID,CANID,EP,CLAYD,NUCLID
      REAL*4 AV,FDATA,TFINAL
      COMMON /AJAX/ CLAYOD,CLAYID,CANID,EP,CLAYD,NDEX
      COMMON /DATIN/ NUCLID(10,10)
      COMMON /PTA/ IUU,IBXK
      COMMON /SCUBA/ FDATA(2,10),TFINAL,AV,IS,IT
      DIMENSION ANAME(10,5)
      DATA CM,NC/2.54,4/
      DATA (ANAME(1,J),J=1,5)/'U-238',' (HIG','H SOL','UBILI'
     1,'TY)  '/
      DATA (ANAME(2,J),J=1,5)/'U-238',' (LOW',' SOLU','BILIT'
     1,'Y)   '/
      DATA (ANAME(3,J),J=1,5)/'PLUTO','NIUM ','240  ',' -  '
     1,'     '/
      DATA (ANAME(4,J),J=1,5)/'AMERI','CIUM ','241  ','     '
     1,'     '/
      DATA (NUCLID(1,J),J=1,10)/471420.,3.3E-07,1.07E-03,1.53E-10,31.5
     1,50.,4*0./
      DATA (NUCLID(2,J),J=1,10)/471420.,3.3E-07,3.8E-11,1.53E-10
     1,31.5,1800.,4*0./
      DATA (NUCLID(3,J),J=1,10)/2933.,0.061,3.8E-11,2.8E-03,31.5
     1,1200.,4*0./
      DATA (NUCLID(4,J),J=1,10)/539.,3.22,3.8E-11,1.5E-03,31.5
     1,4000.,4*0./
      IUU=100
      IBXK=2
      ICODE=1
      CLAYOD=CM*CDIAM(ID)
      CLAYID=CM*CDIAM2(ID)
      CANID=CM*IDIAM(IDONE)
      TEST1=CLAYOD-CLAYID
      TEST2=CLAYID-CANID
      IF(TEST1.LT.0.1) ICODE=2
      IF(TEST2.LT.0.1) ICODE=3
      IF(ICODE.GT.1) GO TO 999
      DO 500 NDEX=1,NC
      ARG=NUCLID(NDEX,4)*TIME
      NUCLID(NDEX,10)=NUCLID(NDEX,1)*EXP(-ARG)
500   CONTINUE
      MI=BAK(ID)+1
      GO TO (10,20,30,40), MI
10    EP=1.
      CLAYD=1.
      GO TO 50
20    EP=0.01
      CLAYD=2.
      GO TO 50
30    EP=0.1
      CLAYD=2.
      GO TO 50
40    EP=0.1
      CLAYD=2.
50    WRITE (100,49)
49    FORMAT(/,1X,'NUCLIDE GEOLOGY RELEASE RATE INFORMATION',/)
      DO 100 NDEX=1,NC
      IF(IBXK.EQ.2) GO TO 82
      WRITE (100,98) CLAYOD,CLAYID
98    FORMAT(2X,'BACKFILL OD = ',1PE10.3,', ID = ',1PE10.3,' CM')
      WRITE (100,97) CANID
97    FORMAT(2X,'CAN ID = ',1PE10.3,' CM')
      WRITE (100,96) EP,CLAYD
96    FORMAT(2X,'CLAY VOID FRACTION = ',F4.2,', DENSITY = ',
     1F4.2,' GM/CC')
82    IF(NUCLID(NDEX,10).LT.1.) GO TO 99
```

```
      CALL RELCAL
      GO TO (201,301), IS
201   AV=AV*100.
      WRITE (100,202) (ANAME(NDEX,J),J=1,5),TIME,AV
202   FORMAT(1X,5A5,'RELEASE TO GEOLOGY BEGINS AT',1PE10.3,' YEARS, B
     1ACKFILL IS',0PF5.1,'% OF TRANSPORT RESISTANCE, RELEASE
     2 RATES ARE:')
      DO 501 KA=1,10
      FDATA(2,KA)=FDATA(2,KA)*NUCLID(NDEX,2)
      FDATA(1,KA)=FDATA(1,KA)+TIME
501   CONTINUE
      WRITE (100,203) (FDATA(1,J),J=1,10)
203   FORMAT(1X,'TIME(YR)    ',10(1X,1PE10.3))
      WRITE (100,204) (FDATA(2,J),J=1,10)
204   FORMAT(1X,'RATE(CI/YR)',10(1X,1PE10.3))
      TFINAL=TFINAL+TIME
      WRITE (100,205) FDATA(2,10),FDATA(1,10),TFINAL
205   FORMAT(1X,'CONSTANT GEOLOGICAL RELEASE RATE OF',1PE10.3,' CI
     1/YR OCCURS FROM',1PE10.3,' YEARS TO',1PE10.3,' YEARS',/)
      GO TO 100
301   AV=AV*100.
      GO TO (401,402),  IT
401   DO 502 KA=1,10
      IF(FDATA(2,KA).LT.0.) FDATA(2,KA)=0.
      FDATA(2,KA)=FDATA(2,KA)*NUCLID(NDEX,2)
      FDATA(1,KA)=FDATA(1,KA)+TIME
502   CONTINUE
      DO 503 KA=1,10
      TSS=FDATA(1,KA)
      IF(FDATA(2,KA).GT.0.) GO TO 504
503   CONTINUE
504   WRITE (100,202) (ANAME(NDEX,J),J=1,5),TSS,AV
      WRITE (100,203) (FDATA(1,J),J=1,10)
      WRITE (100,214) (FDATA(2,J),J=1,10)
214   FORMAT(1X,'RATE(CI/YR)',10(1X,1PE10.3))
      WRITE (100,302) FDATA(1,10),FDATA(2,10)
302   FORMAT(1X,'CONSTANT GEOLOGICAL RELEASE RATE DOES NOT OCCUR
     1, RELEASE ENDS AT',1PE10.3,' YEARS AT A RELEASE RATE OF'
     2,1PE10.3,' CI/YR',/)
      GO TO 100
402   WRITE (100,403) (ANAME(NDEX,J),J=1,5)
403   FORMAT(1X,5A5,'DOES NOT REACH 10 PERCENT OF CONSTANT GEO
     1LOGICAL RELEASE RATE')
      WRITE (100,413)
413   FORMAT(1X,'TRANSIENT RELEASE RATE TOO SMALL TO CALCULATE',/)
      GO TO 100
99    WRITE (100,95) (ANAME(NDEX,J),J=1,5)
95    FORMAT(1X,5A5,'RELEASE CALCULATION NOT PERFORMED BECAUSE')
      WRITE (100,94) NUCLID(NDEX,10)
94    FORMAT(1X,'INITIAL INVENTORY OF ',1PE10.3,' GRAMS IS TOO SMALL'
     1,/)
100   CONTINUE
999   CONTINUE
      END
```

```
      SUBROUTINE RELCAL
      IMPLICIT REAL*8 (A-H,O-Z)
      REAL*8 K,L,KD,NUCLID
      REAL*4 AV,FDATA,TFINAL
      COMMON /AJAX/ CLAYOD,CLAYID,CANID,EP,CLAYD,NDEX
      COMMON /TOAD/ R(100),XNL(100),K,UXL,HLCA,CONC,DECAYC
      COMMON /DATIN/ NUCLID(10,10)
      COMMON /PTA/ IUU,IBXK
      COMMON /SCUBA/ FDATA(2,10),TFINAL,AV,IS,IT
      DIMENSION AN(100)
      DATA TORTUR,HEIGHT,DELTA,NTERM/4.,360.3,3.1416926,30/
      IP=0
      IOU=IUU
      CRANS=NUCLID(NDEX,10)
      DFL=NUCLID(NDEX,5)
      CONC=NUCLID(NDEX,3)
      KD=NUCLID(NDEX,6)
      DECAYC=NUCLID(NDEX,4)
      E=EP
      L=(CLAYOD-CLAYID)/2.
      DELX=(CLAYID-CANID)/2.
      HLC=DFL/DELX/10.
      HZC=10.*HLC
      K=DFL/(1.+KD*CLAYD/E)/TORTUR
      DC=E*DFL/TORTUR
      AREA=3.14*HEIGHT*CLAYID
      HLCA=HLC*AREA
      HZCA=HZC*AREA
      HL=HLC/DC
      HZ=10.*HL
      HZ2=HZ*HZ
      HL2=HL*HL
      HLHZ=HL*HZ
      A=L*L*HLHZ
      B=L*(HZ+HL)
      H=1.+HL*(L+1./HZ)
      AV=L*HL/H
      IF(AV.LT.0.8) GO TO 599
      CONC=CONC*AV
      CALL CLAMP(K,L,DECAYC,DC,CRANS,CONC,AREA)
      GO TO 666
599   IF(IBXK.EQ.2) GO TO 170
      WRITE (IOU,600) HLC
600   FORMAT(2X,'CONDUCTANCE AT X=L = ',1PE10.2,' CM/SEC')
      WRITE (IOU,601) HL
601   FORMAT(2X,'SMALL HL = ',1PE10.3,' 1/CM')
      WRITE (IOU,602) DECAYC,DC
602   FORMAT(2X,'RADIO DECAY CONSTANT = ',1PE10.3,' 1/YEAR,
     1 DIFF COEFF = ',1PE10.3,' CM*CM/YEAR')
      WRITE (IOU,603) K,L
603   FORMAT(2X,'K = ',1PE10.3,' CM*CM/YEAR, L = ',1PE10.3,
     1' CM')
      WRITE (IOU,604) H,CONC
604   FORMAT(2X,'H = ',1PE10.3,' UNITLESS, CONC = ',1PE10.3,
     1' CM/CC')
      WRITE (IOU,614) AREA
614   FORMAT(2X,'INSIDE AREA = ',1PE10.3,' CM*CM')
      WRITE (IOU,605) AV
605   FORMAT(2X,'A VALUE = ',1PE10.3,' UNITLESS')
      IF(IP.EQ.0) GO TO 170
      WRITE (IOU,169)
169   FORMAT(13X,'ROOT',10X,'F(ROOT)',9X,'A(N)')
170   DO 200 J=1,NTERM
      XL=(J-1)*DELTA
      XR=XL+DELTA
      FX=1.
```

```
      CALL BROOT(XL,XR,FX,X,A,B)
      R(J)=X/L
      ALPHA=R(J)
      AL=ALPHA*L
      A2=ALPHA*ALPHA
      TEMP=H*((A2+HZ2)*L+(A2+HZ2)/(A2+HL2)*HL+HZ)
      AN(J)=HZ*L*DCOS(AL)/ALPHA-(L+HZ/A2+1./HZ)*DSIN(AL)
      AN(J)=2.*ALPHA*HL*AN(J)/TEMP
      AN(J)=CONC*AN(J)
      XNL(J)=((A2+HZ2)/(A2-HLHZ))*DCOS(AL)
      XNL(J)=XNL(J)*AN(J)
      IF(IP.EQ.0.OR.IBXK.EQ.2) GO TO 200
      WRITE (IOU,199) J,R(J),FX,AN(J)
199   FORMAT(5X,I2,3(2X,1PE13.6))
200   CONTINUE
      TS=4.605/(R(1)*R(1)*K)
      IF(IBXK.EQ.2) GO TO 202
      WRITE (IOU,201) TS
201   FORMAT(2X,'STEADY STATE TIME= ',1PE10.3,' YEARS')
      WRITE (IOU,171)
171   FORMAT(11X,'X',12X,'SERIES',10X,'EXACT')
202   STEP=1./10.
      HLEAD=CONC*HL/H
      X=0.
      DO 400 I=1,11
      SERIES=0.
      DO 350 J=1,NTERM
      ALPHA=R(J)
      AX=ALPHA*X
      XN=DCOS(AX)+HZ*DSIN(AX)/ALPHA
      SERIES=SERIES+AN(J)*XN
350   CONTINUE
      EXACT=HLEAD*(X+1./HZ)
      IF(IBXK.EQ.2) GO TO 399
      WRITE (IOU,351) I,X,SERIES,EXACT
351   FORMAT(2X,I2,4(2X,1PE13.6))
399   X=X+STEP
400   CONTINUE
      IF(IBXK.EQ.2) GO TO 203
      WRITE (IOU,721) GRAMS
721   FORMAT(2X,'QUANTITY OF NUCLIDE AT T=0 = ',1PE10.3,' GMS').
203   UXL=CONC*HL*(L+1./HZ)/H
      UXZ=CONC*HL/H/HZ
      IS=1
      XL=0.
      XR=TS
      FX=1.
      DO 100 KK=1,25
      XT=(XR+XL)/2.
      GMS=GRAMS
      CALL REMAIN(XT,FT,GMS)
      TEST=FT*FX
      IF(TEST.LT.0.) GO TO 80
      XL=XT
      FX=FT
      GO TO 100
80    XR=XT
      IS=2
100   CONTINUE
      IT=1
      GO TO (101,103), IS
101   IF(IBXK.EQ.2) GO TO 204
      WRITE (IOU,102) GMS
102   FORMAT(2X,'GRAMS AT STEADY STATE = ',1PE10.3)
204   STEP=TS/10.
      GO TO 105
```

```
103     IF(IBXK.EQ.2) GO TO 205
        WRITE (100,104) XL
104     FORMAT(2X,'TIME WHEN INVENTORY HIT ZERO = ',1PE10.3)
205     TEST=XL/TS
        IF(TEST.LT.0.1) IT=3
        STEP=XL/10.
105     TIME=0.
        IF(IBXK.EQ.2) GO TO 206
        WRITE (100,120)
120     FORMAT(3X,'TIME',3X,'GRAMS LEFT',2X,'DECAY RATE',3X,
     1'DIFF RATE',3X,'GEOL. RATE, CM/YEAR')
206     AKL=BLCA*(UXL-CONC)
        DO 109 KK=1,10
        TIME=TIME+STEP
        SUM1=0.
        SUM2=0.
        SUM3=0.
        SUM4=0.
        SUM5=0.
        CAZ=0.
        DO 107 J=1,NTERM
        EX=0.
        ARG1=K*R(J)*R(J)
        ARG=ARG1*TIME
        IF(ARG.LT.23.) EX=DEXP(-ARG)
        SUM1=SUM1+XNL(J)*EX/(DECAYC-ARG1)
        SUM2=SUM2+XNL(J)/(DECAYC-ARG1)
        SUM3=SUM3+(AN(J)/(-ARG1))*EX
        SUM4=SUM4+AN(J)/(-ARG1)
        CAZ=CAZ+AN(J)*EX
        SUM5=SUM5+XNL(J)*EX
107     CONTINUE
        CAZ=CAZ+UXZ
        T1=BLCA*SUM1+AKL/DECAYC
        T2=GRAMS-BLCA*SUM2-AKL/DECAYC
        EX=0.
        ARG=DECAYC*TIME
        IF(ARG.LT.23.) EX=DEXP(-ARG)
        Y=T1+T2*EX
        DECAY=DECAYC*Y
        GRATE=BZCA*CAZ
        IF(IT.EQ.2) GRATE=0.
        DRATE=BLCA*(CONC-SUM5-UXL)
        FDATA(1,KK)=TIME
        FDATA(2,KK)=GRATE
        IF(IBXK.EQ.2) GO TO 109
        WRITE (100,108) TIME,Y,DECAY,DRATE,GRATE
108     FORMAT(5(2X,1PE10.3))
109     CONTINUE
        TOTALG=BZCA*(SUM3+UXZ*TIME-SUM4)
        IF(IT.EQ.2) TOTALG=0.
        IF(IBXK.EQ.2) GO TO 207
        WRITE (100,141) TOTALG
141     FORMAT(2X,'TOTAL FLUXED TO GEOLOGY = ',1PE10.3,' GRAMS')
207     GO TO (130,132), IS
130     IF(IBXK.EQ.2) GO TO 208
        WRITE (100,131)
131     FORMAT(2X,'PROFILE IN CLAY IS STEADY STATE LISTED ABOVE')
208     TFINAL=(DLOG((DECAYC*Y+DRATE)/DRATE))/DECAYC
        CXTRA=TFINAL*GRATE
        IF(IBXK.EQ.2) GO TO 666
        WRITE (100,146) TFINAL
146     FORMAT(2X,'INVENTORY GOES TO ZERO AFTER STEADY STATE
     1 IN ',1PE10.3,' YEARS')
        WRITE (100,147) CXTRA
147     FORMAT(2X,'GEOLOGY GETS ',1PE10.3,' MORE GRAMS AFTER
```

```
     1 STEADY STATE')
       GO TO 666
132    IF(IBXK.EQ.2) GO TO 209
       WRITE (100,133)
133    FORMAT(2X,'PROFILE WHEN INVENTORY HIT ZERO FOLLOWS')
209    GO TO (174,175),IT
175    IF(IBXK.EQ.2) GO TO 666
       WRITE (100,173)
173    FORMAT(2X,'NOT FAR ENOUGH FROM TIME=0 TO CALCULATE')
       GO TO 666
174    IF(IBXK.EQ.2) GO TO 211
       WRITE (100,134)
134    FORMAT(9X,'X',7X,'CONCENTRATION')
211    TIME=XL
       X=0.
       STEP=L/10.
       DO 139 I=1,11
       SERIES=0.
       DO 138 J=1,NTERM
       ALPHA=R(J)
       AX=ALPHA*X
       XN=DCOS(AX)+HZ*DSIN(AX)/ALPHA
       EX=0.
       ARG=K*R(J)*R(J)*TIME
       IF(ARG.LT.23.) EX=DEXP(-ARG)
       SERIES=SERIES+AN(J)*XN*EX
138    CONTINUE
       SERIES=SERIES+HLEAD*(X+1./HZ)
       IF(IBXK.EQ.2) GO TO 212
       WRITE (100,137) X,SERIES
137    FORMAT(2(4X,1PE10.3))
212    X=X+STEP
139    CONTINUE
666    IF(IBXK.EQ.2) GO TO 668
       WRITE (100,667)
667    FORMAT(2X,'END')
668    CONTINUE
       END
       SUBROUTINE REMAIN(XT,FT,CMS)
       IMPLICIT REAL*8 (A-H,O-Z)
       REAL*8 K
       COMMON /TOAD/ R(100),XNL(100),K,UXL,HLCA,CONC,DECAYC
       NTERM=99
       FT=1.
       AKL=HLCA*(UXL-CONC)
       TIME=XT
       SUM1=0.
       SUM2=0.
       DO 610 J=1,NTERM
       EX=0.
       ARG1=K*R(J)*R(J)
       ARG=ARG1*TIME
       IF(ARG.LT.23.) EX=DEXP(-ARG)
       SUM1=SUM1+XNL(J)*EX/(DECAYC-ARG1)
       SUM2=SUM2+XNL(J)/(DECAYC-ARG1)
610    CONTINUE
       T1=HLCA*SUM1+AKL/DECAYC
       T2=CMS-HLCA*SUM2-AKL/DECAYC
       EX=0.
       ARG=DECAYC*TIME
       IF(ARG.LT.23.) EX=DEXP(-ARG)
       Y=T1+T2*EX
       IF(Y.LT.1.) GO TO 622
       GO TO 613
622    FT=-1.
613    CMS=Y
```

```
      RETURN
      END
      SUBROUTINE DBROOT(XL,XR,FX,X,A,B)
      IMPLICIT REAL*8 (A-H,O-Z)
      COT(ARG)=DCOS(ARG)/DSIN(ARG)
      DO 100 K=1,30
      XT=(XR+XL)/2.
      FT=XT*COT(XT)+(A-XT*XT)/B
      TEST=FT*FX
      IF(TEST.LT.0.) GO TO 80
      XL=XT
      FX=FT
      GO TO 100
   80 XR=XT
  100 CONTINUE
      X=XT
      FX=FT
      RETURN
      END
```

```
      SUBROUTINE CLAMP(K,L,DECAYC,DC,GRAMS,CONC,AREA)
      IMPLICIT REAL*8 (A-H,O-Z)
      REAL*8 K,L
      REAL*4 AV,FDATA,TFINAL
      COMMON /PTA/ IUU,IBXK
      COMMON /SCUBA/ FDATA(2,10),TFINAL,AV,IS,IT
      DATA PIE,NTERM/3.1415926D0,99/
      AK=K*(PIE/L)**2
      DA=DC*AREA
      TS=4.605/AK
      PL=PIE/L
      STEP=L/10.
      X=0.
      IOU=IUU
      IF(IBXK.EQ.2) GO TO 201
      WRITE (IOU,159)
159   FORMAT(2X,'IN THE CLAMPED ROUTINE')
      WRITE (IOU,160) K,L
160   FORMAT(2X,'K = ',1PE10.3,' CM*CM/YEAR, L = ',1PE10.3,
     1' CM')
      WRITE (IOU,161) DECAYC,DC
161   FORMAT(2X,'RADIO DECAY CONSTANT = ',1PE10.3,' 1/YEAR,
     1 DIFF COEFF = ',1PE10.3,' CM*CM/YEAR')
      WRITE (IOU,162) CONC
162   FORMAT(2X,'CONCENTRATION AT X=L = ',1PE10.3,' GM/CC')
      WRITE (IOU,169) GRAMS
169   FORMAT(2X,'GRAMS AT START = ',1PE10.3)
      WRITE (IOU,170)
170   FORMAT(2X,'A CHECK OF THE SERIES')
      WRITE (IOU,171)
171   FORMAT(11X,'X',12X,'SERIES',10X,'EXACT')
201   DO 400 I=1,11
      SERIES=0.
      DO 350 J=1,NTERM
      A=J
      SERIES=SERIES+(-1.)**J*DSIN(A*PL*X)/A
350   CONTINUE
      SERIES=2.*CONC*SERIES/PIE
      EXACT=CONC*X/L
      IF(IBXK.EQ.2) GO TO 202
      WRITE (IOU,351) I,X,SERIES,EXACT
351   FORMAT(2X,I2,4(2X,1PE13.6))
202   X=X+STEP
400   CONTINUE
      IF(IBXK.EQ.2) GO TO 203
      WRITE (IOU,401) TS
401   FORMAT(2X,'STEADY STATE TIME = ',1PE10.3,' YEARS')
203   IS=1
      XL=0.
      XR=TS
      FX=1.
      DO 100 KK=1,25
      XT=(XR+XL)/2.
      GMS=GRAMS
      CALL RLEFT(FT,XT,AK,CONC,L,DA,DECAYC,GMS,NTERM)
      TEST=FT*FX
      IF(TEST.LT.0.) GO TO 80
      XL=XT
      FX=FT
      GO TO 100
80    XR=XT
      IS=2
100   CONTINUE
      IT=1
      GO TO (101,103),IS
101   IF(IBXK.EQ.2) GO TO 135
```

```
      WRITE (100,102) CRS
102   FORMAT(2X,'GRAMS AT STEADY STATE = ',1PE10.3)
135   STEP=TS/10.
      GO TO 105
103   IF(IBXK.EQ.2) GO TO 204
      WRITE (100,104) XL
104   FORMAT(2X,'TIME WHEN INVENTORY HIT ZERO = ',1PE10.3)
204   TEST=XL/TS
      IF(TEST.LT.0.1) IT=3
      STEP=XL/10.
105   TIME=0.
      IF(IBXK.EQ.2) GO TO 205
      WRITE (100,120)
120   FORMAT(3X,'TIME',5X,'GRAMS LEFT',2X,'DECAY RATE',3X,
     1'DIFF RATE',3X,'GEOL RATE, CM/YEAR')
205   AK1=CONC*DA/L
      DO 109 KK=1,10
      TIME=TIME+STEP
      SUM1=0.
      SUM2=0.
      SUM3=0.
      SUM4=0.
      SUM5=0.
      SUM6=0.
      DO 107 J=1,NTERM
      EX=0.
      A=J
      ARG1=AK*A*A
      ARG=ARG1*TIME
      IF(ARG.LT.23.) EX=DEXP(-ARG)
      SUM1=SUM1+EX/(DECAYC-ARG1)
      SUM2=SUM2+1./(DECAYC-ARG1)
      SIGN=(-1.)**J
      SUM3=SUM3+SIGN*EX
      SUM4=SUM4+SIGN*EX/(-ARG)
      SUM5=SUM5+SIGN/(-ARG)
      SUM6=SUM6+EX
107   CONTINUE
      T1=-AK1*(2.*SUM1+1./DECAYC)
      T2=GRAMS+AK1*(2.*SUM2+1./DECAYC)
      EX=0.
      ARG=DECAYC*TIME
      IF(ARG.LT.23.) EX=DEXP(-ARG)
      Y=T1+T2*EX
      CRATE=AK1*(2.*SUM3+1.)
      IF(IT.EQ.2) CRATE=0.
      DECAY=DECAYC*Y
      DRATE=AK1*(2.*SUM6+1.)
      FDATA(1,KK)=TIME
      FDATA(2,KK)=CRATE
      IF(IBXK.EQ.2) GO TO 109
      WRITE (100,108) TIME,Y,DECAY,DRATE,CRATE
108   FORMAT(5(2X,1PE10.3))
109   CONTINUE
      TOTALG=AK1*(2.*SUM4+TIME-2.*SUM5)
      IF(IT.EQ.2) TOTALG=0.
      IF(IBXK.EQ.2) GO TO 206
      WRITE (100,141) TOTALG
141   FORMAT(2X,'TOTAL FLUXED TO GEOLOGY = ',1PE10.3,' GRAMS')
206   GO TO (130,132), IS
130   TFINAL=(DLOG((DECAYC*Y+DRATE)/DRATE))/DECAYC
      CXTRA=TFINAL*CRATE
      IF(IBXK.EQ.2) GO TO 666
      WRITE (100,131)
131   FORMAT(2X,'PROFILE IN CLAY IS STEADY STATE LISTED ABOVE')
      WRITE (100,146) TFINAL
```

```
146     FORMAT(2X,'INVENTORY GOES TO ZERO AFTER STEADY STATE
     1 IN ',1PE10.3,' YEARS')
        WRITE (100,147) EXTRA
147     FORMAT(2X,'GEOLOGY GETS ',1PE10.3,' MORE GRAMS AFTER
     1 STEADY STATE')
        GO TO 666
132     IF(IBXK.EQ.2) GO TO 208
        WRITE (100,133)
133     FORMAT(2X,'PROFILE WHEN INVENTORY HIT ZERO FOLLOWS')
208     GO TO (174,175), IT
175     IF(IBXK.EQ.2) GO TO 666
        WRITE (100,176)
176     FORMAT(2X,'NOT FAR ENOUGH FROM TIME=0 TO CALCULATE')
        GO TO 666
174     IF(IBXK.EQ.2) GO TO 209
        WRITE (100,134)
134     FORMAT(9X,'X',7X,'CONCENTRATION')
209     TIME=XL
        X=0.
        STEP=L/10.
        DO 139 I=1,11
        SERIES=0.
        DO 138 J=1,NTERM
        EX=0.
        A=J
        ARG=TIME*AK*A*A
        IF(ARG.LT.23.) EX=DEXP(-ARG)
        SERIES=SERIES+(-1.)**J*DSIN(A*PL*X)*EX/A
138     CONTINUE
        SERIES=2.*CONC*SERIES/PIE+CONC*X/L
        IF(IBXK.EQ.2) GO TO 210
        WRITE (100,137) X,SERIES
137     FORMAT(2(4X,1PE10.3))
210     X=X+STEP
139     CONTINUE
666     RETURN
        END
        SUBROUTINE RLEFT(FT,XT,AK,CONC,L,DA,DECAYC,CHS,NTERM)
        IMPLICIT REAL*8 (A-H,O-Z)
        REAL*8 L
        AK1=CONC*DA/L
        FT=1.
        TIME=XT
        SUM1=0.
        SUM2=0.
        DO 610 J=1,NTERM
        EX=0.
        A=J
        ARG1=AK*A*A
        ARG=ARG1*TIME
        IF(ARG.LT.23.) EX=DEXP(-ARG)
        SUM1=SUM1+EX/(DECAYC-ARG1)
        SUM2=SUM2+1./(DECAYC-ARG1)
610     CONTINUE
        T1=-AK1*(2.*SUM1+1./DECAYC)
        T2=CHS+AK1*(2.*SUM2+1./DECAYC)
        EX=0.
        ARG=DECAYC*TIME
        IF(ARG.LT.23.) EX=DEXP(-ARG)
        Y=T1+T2*EX
        IF(Y.LT.1.) GO TO 622
        GO TO 613
622     FT=-1.
613     CHS=Y
        RETURN
        END
```

APPENDIX B
DATA BASE FOR CORROSION MODEL (CORODE)

Corrosion rates were determined on the basis of the following

(1) materials considered included only mild steel, Zircaloy-2, Inconel-600, 304SST, copper, lead and cast iron

(2) the barrier package was assumed to be filled with medium "Brine B" or ground water of "low ionic strength" at one of two temperature ranges ($25^{o}C$-$100^{o}C$ and $100^{o}C$-$250^{o}C$)

(3) corrosion rates (mils/yr) were selected from open literature (Cheng, 1980)

(4) effects of irradiation and migration of chemical species were excluded

Tables B-1 and B-2 summarize the corrosion rates in mils/yr of metals under anoxic and oxic conditions immersed in Brine B and ground water. Two types of corrosion rates were evaluated

(1) metal loss - steady corrosion rate calculated from descaled metal loss

(2) crack propagation - maximum crack penetration rate associated with pitting corrosion, stress corrosion or graphitization

The rationale of data selection for corrosion rates of package materials in Brine B and ground water are discussed herein.

It was noted in (Braithwaite and Molecke, 1979) that solution corrosivity increases in the order: BRINE B <Sea Water <Brine A for the barrier materials. Thus, the corrosion rates in Table B-1 taken from data in sea water

Table B-1. Corrosion Rates of Barrier Materials in Brine B.

Material	Temp. Range, °C	Metal Loss (mils/yr)			Crack Propagation[a] (mils/yr)		
		Anoxic	Oxic	Reference	Anoxic	Oxic	Reference
Mild Steel	25-100	1	-	Posey & Palko Braithwaite & Molecke	<½P	-	Braithwaite & Molecke
		-	3	Schumacher	-	27P	Schumacher
	100-250	2.8	276	Braithwaite & Molecke	<½P	<½P	Braithwaite & Molecke
Zircaloy-2	25-100	<½	-	Braithwaite & Molecke	<½P	<½P	International Nickel Co.
		-	<½	International Nickel Co.	-	-	
	100-250	<½	-	Braithwaite & Molecke	<½P	-	International Nickel Co.
		-	<½	International Nickel Co.	-	<½P	Braithwaite & Molecke
Inconel-600	25-100	1	4	Reinhart	6P	<½P	International Nickel Co. Schumacher
	100-250	<½	4	Braithwaite & Molecke	<½P	<½P	Braithwaite & Molecke
304 SST	25-100	<½	-	Todd & Lovett	20P	-	Todd & Lovett
		-	5	Tuthill & Schillmoler	-	30P	Schumacher
	100-250	<½	3.9	Braithwaite & Molecke	<½P	-	Braithwaite & Molecke
		-	-		-	3.7×10^{4}S	Speidel
Copper	25-100	<½	<½	Schumacher	5P	5P	Tuthill & Schillmoler
	100-250	3	47	Braithwaite & Molecke	<½P	<½P	Braithwaite & Molecke
Lead	25-100	<½	0.6	Geel, et al.	<½P	<½P	Geel, et al.
	100-250	12	47	Braithwaite & Molecke	<½P	<½P	Braithwaite & Molecke
Cast Iron	25-100	3	-	Schumacher	12P	-	Hamner
		-	54	Hamner	-	100G	Tuthill & Schillmoler
	100-250	36	-	Rabald	40G	-	Tuthill & Schillmoler
		-	50	Nelson	-	300G	Tuthill & Schillmoler

(a) estimated from maximum crack penetration associated with P (pitting corrosion), S(stress corrosion) or G (graphitization) data.

Table B-2. Corrosion Rates of Barrier Materials in Ground Water

Material	Temp. Range, °C	Metal Loss (mils/yr)			Crack Propagation[a] (mils/yr)		
		Anoxic	Oxic	Reference	Anoxic	Oxic	Reference
Mild Steel	25-100	0.5	0.5	Denison & Romanoff	2P	2P	Denison & Romanoff
	100-250	1	2	Blazer & Owens	2P	19P	Cataldi & Cheng
Zircaloy-2	25-100	<½	<½	Berry	<½P	<½P	Berry
	100-250	<½	<½	Berry	<½P	<½P	Berry
Inconel-600	25-100	<½	<½	Copson & Berry	<½P	<½P	Copson & Berry
	100-250	<½	<½	Copson & Berry	2½S	-	Bulischeck & Van Rooyen
		-	-		-	<½P	Copson & Berry
304 SST	25-100	<½	-	Denison & Romanoff	<½P	-	Denison & Romanoff
		-	<½	Reinhart	-	1.2×10^{5}S	Ford & Povich
	100-250	<½	-	Copson & Berry	<½P	-	Berry
		-	<½	Cataldi & Cheng	-	3.8×10^{6}S	Ford & Povich
Copper	25-100	<½	12	Syrett	<½P	-	Denison & Romanoff
		-	-		-	<½P	Mattson & Fredrickson
	100-250	2	-	Hammer	<½P	-	Hammer
		-	2	LaQue & Copson	-	<½	LaQue & Copson
Lead	25-100	<½	<½	Denison & Romanoff	<½P	0.6P	Denison & Romanoff
	100-250	<½	<½	Butler & Ison	1P	1P	Ahlstrom
Cast Iron	25-100	4	<½	Denison & Romanoff	35P	6P	Denison & Romanoff
	100-250	2	-	Hammer	8P	-	Hammer
		-	2	Cataldi & Cheng	-	35P	Cataldi & Cheng

(a) estimated from maximum crack penetration associated with P (pitting corrosion), S(stress corrosion), or G (graphitization) data.

or Brine A for use in Brine B can be considered to be conservatively high. For Brine B

(1) Mild Steel - Hot brines are very corrosive with corrosion rates increasing with brine velocity, oxygen concentration, temperature and other oxidation (Braithwaite and Molecke, 1979). In addition, mild steel does not usually pit severely or stress crack in hot solution. However, at low temperature oxygen tends to promote pitting. A corrosion rate equation (Posey and Palko, 1979) for metal loss in anoxic 4M NaCl is in good agreement with (Braithwaite and Molecke, 1979).

(2) Zircaloy-2 - The corrosion rates in brine solutions are insignificantly low and the rates are not affected by the oxygen concentration and temperature range considered (Braithwaite and Molecke, 1979).

(3) Inconel-600 - The corrosion rates for metal loss are low and not affected by the oxygen concentration and temperature range considered (Braithwaite and Molecke, 1979). In addition, Inconel-600 is very resistant to chloride stress corrosion cracking (Schumacher, 1979). In anoxic solution at low temperature ($25^{o}C$-100^{o}), some pitting does occur (International Nickel Co.).

(4) Type 304 Stainless Steel - The corrosion rates for metal loss are much lower than for mild steel, but austenitic types are susceptible to pitting and stress corrosion. At low temperature ($25^{o}C$-$100^{o}C$), oxygen concentration increases pitting rate while at high temperature ($100^{o}C$-$250^{o}C$) oxygen concentration promotes stress corrosion cracking (Schumacher, 1979)(Todd and Lovett, 1956). (Speidel, 1977) reported a crack propagation rate of $3.7x10^{4}$ mils/yr for sensitized type 304L stainless steel in 42 percent MgCl at $130^{o}C$. In view of the chloride concentration mechanism, the same order of magnitude of crack propagation rate might be expected in oxic Brine B.

(5) Copper - At low temperature, corrosion rates are small and relatively insensitive to oxygen concentration in slowly moving sea water (Schumacher, 1979). Highly oxygenated brines are corrosive with oxygen discharge usually the controlling factor (Braithwaite and Molecke, 1979).

(6) Lead - The corrosion rates for metal loss increase with temperature and oxygen concentration (Braithwaite and Molecke, 1979).

(7) Cast Iron - The corrosion rates in crack propagation associated with graphitization mask the rates for metal loss. Oxygen significantly increases graphitization and leads to very high corrosion rates (Tuthill and Schillmoler, 1965).

Corrosion data taken from inorganic reducing acid (pH 5.6) or oxidizing alkaline (pH 8.0) ground waters as well as hydrogen or oxygenated waters were used to estimate corrosion rates for metal loss and crack propagation associated with pitting corrosion and stress corrosion.

(1) Mild Steel - The corrosion rates for metal loss are small in anoxic and oxic water. At high temperature (100°C-250°C) corrosion rate for crack propagation associated with pitting may be significant (Cataldi and Cheng, 1958).

(2) Zircaloy-2 - The corrosion rates are negligible in anoxic or oxic waters. No stress corrosion or pitting occurs (Berry, 1971).

(3) Inconel-600 - The corrosion rates are negligible in anoxic or oxic waters. No pitting or stress corrosion normally occurs (Copson and Berry, 1960). Under certain sensitized conditions, stress corrosion cracking has been reported in pure deaerated water at high temperatures (Bulischeck and Van Rooyen, 1980).

(4) Type 304 Stainless Steel - The corrosion rates for metal loss are negligible in anoxic or oxic waters with no pitting or stress corrosion (Denison and Romanoff, 1946)(Copson and Berry, 1960). Under certain

BWR water conditions, severe stress corrosion cracking of sensitized type 304 stainless steel can occur (Ford and Povich, 1979).

(5) Copper - The corrosion rates in anoxic or oxic water are insignificant. However, studies (Syrett, 1977) on the corrosion of copper in 30°C water contaminated with sulfide, oxygen, or both have shown that the presence of either sulfide plus low oxygen or oxygen alone causes low corrosions rates. If sulfide and oxygen are both present in certain concentration ranges, a dramatic increase in corrosion rate for metal loss may result. Pitting corrosion or stress corrosion is not likely in anoxic or oxic waters. Pitting of copper is usually a cold water phenomenon (Mattson and Fredrickson, 1968). Cold water pitting is associated with the formation of a protective mat of cuprous oxide on the copper surface (Powell and Lucey, 1966).

(6) Lead - Corrosion rates for metal loss or pitting in anoxic or oxic waters are negligible (Denison and Romanoff, 1946)(Butler and Ison, 1966).

(7) Cast Iron - The corrosion rates for metal loss are small in anoxic or oxic waters. However, high pitting corrosion rates have been reported both in reducing alkaline ground water (pH 7.1) and low sulfide (Denison and Romanoff, 1946) and in high purity water with oxygen at 285°C (Cataldi and Cheng, 1958).

APPENDIX C
DATA BASE FOR BARRIER FAILURE MODEL (STRESS) CRITERIA

In the STRESS subroutine a number of material properties are used in the calculations. Properties were obtained from various sources and in some cases were estimated where no values could be obtained.

Wall Materials - Compressive Yield

Compressive yield strength is fitted as a linear function of temperature. Most values were obtained from the ASME Code Division 2, Section VIII (1977). These were usually available as a function of temperature. Some temperature functions were obtained by extrapolating data to a zero yield at the melting point. Because of the small temperature range of interest such approximations have only a minor effect on the end results.

Values for carbon steel specification SA-285 are given in Table C-1 and were taken from Table ACS-1 of the ASME Code. A linear fit with intercept = 15.7 KSI and slope -0.011 KSI/^{o}C was obtained from these data.

Only one value for copper was available in Table ANF-2.2 of the code. For specification SB-11 copper the value reported is 10 KSI at 20^{o}C. Extrapolation to zero yield at the melting point of 1083^{o}C gave an intercept of 10.2 KSI and slopes of - 0.0094 KSI/^{o}C.

Inconel (Ni-Fe-Cr alloy 800H spec SB-409) data were then taken from the ASME Code and are given in Table C-2. A linear fit gave an intercept of 25.2 KSI and slope of -0.022 KSI/^{o}C.

Values for Stainless Steel type 304 spec SA-240 taken from the ASME Code are reported in Table C-3. A linear correlation gave an intercept of 30.7 KSI and slope of -0.053 KSI/^{o}C.

The compressive yield strength used for cast iron was 20 KSI at 20^{o}C and was from the Mechanical Engineers Handbook (Marx, 1952). Extrapolation to zero at the melting point (1538^{o}C) gave an intercept of 20.3 KSI and slope of -0.013 KSI/^{o}C.

Table C-1. Compressive Yield for Carbon Steel

(from ASME Div. 2, Section VIII, Table ACS-1)

Temperature (°C)	Yield Strength (KSI)
38	15.0
93	14.6
149	14.2
204	13.7

Table C-2. Compressive Yield for Inconel Alloy 800 H

(from ASME Div. 2, Section VIII, Table ANF-2.3)

Temperature (°C)	Yield Strength (KSI)
38	25.0
93	23.1
149	21.7
204	20.3

Table C-3. Compressive Yield for Stainless Steel Type 304

(from ASME Div. 2, Section VIII, Table AHA-2)

Temperature (°C)	Yield Strength (KSI)
38	30.0
93	25.1
149	22.5
204	20.8

Table C-4. Material Properties (x 10^3 KSI)

(from Mechanical Engineers Handbook, by (Marks, 1952))

Material	Shear Modulus (G)	Bulk Modulus (B)	Poisson Ratio (ν)
Carbon Steel (rolled)	11.3	20.2	0.265
Cast Iron	6.7	12.0	0.255
Copper (annealed)	5.8	17.9	0.355
Inconel	11.0	-	-
Zircaloy	4.8	3.9	0.44

Similarly, the yield strength for Zircaloy was extrapolated from 43 KSI at 20°C (Marks, 1952) to zero at 1760°C for an intercept of 43.5 KSI and slope of -0.0247 KSI/°C.

Wall Materials - Bulk and Shear Modulus

Table C-4 gives values of bulk and shear moduli for various materials (Marks, 1952). Assuming a Poisson ratio, ν, of 0.3 for Inconel the bulk modulus, B, was estimated from the shear modulus, G, by

$$B = \frac{2}{3} G\left(\frac{1+\nu}{1-2\nu}\right) = \frac{2}{3}(11)\left(\frac{1.3}{.4}\right) = 23.8 \times 10^3 \text{ KSI} \qquad (C.1)$$

Extrapolation to zero at melting points shown in Table C-5 gave results shown in Table C-6 for the temperature fits of shear moduli.

Detailed data for stainless steel moduli were available (Datsko, 1966). The temperature fits developed for shear modulus had a slope of - 3.77 KSI/°C and an intercept of 10,000 KSI.

Bulk moduli are relatively insensitive to temperature and no reasonable basis for extrapolation was available. Stainless Steel data were available (Datsko, 1966). Table C-7 shows the temperature fits used for bulk modulus.

Wall Materials - Tensile Yield

The ASME code criteria for tensile yield were used in the STRESS subroutine. Wall thickness required is related to the allowable stress, S. The values of S are obtained versus temperature from ASME, Division 1, Section VIII. Four coefficients are used to describe S as a function of temperature that is

Table C-5. Melting Points Used for Shear Modulus Extrapolation

Material	Temperature (°C)
Carbon Steel	1538
Cast Iron	1538
Copper	1083
Inconel	1455
Zircaloy	1760

Table C-6. Temperature Fits for Shear Modulus

Material	Intercept (KSI)	Slope (KSI/°C)
Carbon Steel	5.84×10^3	-3.8
Cast Iron	6.78×10^3	-4.4
Copper	5.9×10^3	-5.5
Inconel	11.2×10^3	-7.67
Zircaloy	4.88×10^3	-2.77

Table C-7. Temperature Fits for Bulk Modulus

Material	Intercept (KSI)	Slope (KSI/°C)
Carbon Steel	17,900	0
Cast Iron	12,000	0
Copper	17,900	0
Inconel	23,800	0
Zircaloy	3,861	0
Stainless Steel	19,310	1.05

Table C-8. Allowable Stresses for Internal Pressure

Material	S1 (PSI)	S2 (PSI/°C)	S3 (°C)	S4 (PSI)
Carbon Steel	12500	0	50	12500
Zircaloy	13451	26.7	38	12436
Inconel	21200	0	50	21200
304SST	19316	16.3	38	18700
Copper	7399	19.5	38	6660
Cast Iron	6000	0	50	6000

$$S = S1 - S2\,(T) \qquad T > S3 \qquad (C.2)$$

$$S = S4 \qquad T \leq S3 \qquad (C.3)$$

where T = ^{o}C and S = PSI.

The values are summarized in Table C-8.

Note that for materials for which S is independent of T, an artificial temperature break was introduced to satisfy the logic in the code.

Backfill Materials - Bulk Modulus

The pressure-volume relationship of a packed granular material was represented by

$$P_R = A\left(\frac{V_o}{V} - 1\right) + K\left(\frac{V_o}{V} - 1\right)^2 \qquad (C.4)$$

where V_o = original volume, (cm^3)

V = volume after compression by P_R, (cm^3)

P_R = external pressure, (KSI)

A, K = empirical constants, (KSI)

The bulk modulus was obtained by

$$B = A(V^* + 1) + 2KV^*(V^* + 1) \qquad (C.5)$$

where

$$V^* = \left(\frac{V_o}{V} - 1\right) = \frac{-A + \sqrt{A^2 + 4KP_R}}{2K} \text{ or } \frac{P_R}{A} \text{ if } K = 0 \qquad (C.6)$$

APPENDIX D
INPUT/OUTPUT DESCRIPTION

This appendix is designed to guide the user through the steps necessary to operate the BARIER code. First, a description of the input data required to operate the code is presented. Then, the input techniques and requirements for execution are discussed including operator-machine interactions and procedures. Finally, a description of output data and format is presented.

D.1 INPUT DATA

All non-internal physical data required to execute BARIER are contained in five external data files:

(1) CORRAT - contains corrosion rate data for use in the CORODE subroutine for each possible package material (metal) as a function of temperature and water type (corrosive environment)

(2) GEOMAT - contains repository physical data for each of the four geologies of concern (salt, shale, granite, basalt)

(3) MATMAT - contains all material stress and other related constants utilized in the STRESS subroutine

(4) BARFIL - a dummy variable for a file containing all necessary package design data or specifications for an individual case to be evaluated - each individual case has its own separate file name

(5) DATSET - dummy variable representing a file listing all "BARFIL" files to be run

The corrosion rate data contained in CORODE is comprised of eight separate values for each package material (metals). Four corrosive environments are considered:

(1) Anoxic brine B

(2) Oxic brine B

(3) Anoxic water

(4) Oxic water

over two temperature ranges (25^{o}-100^{o}C, 100^{o}-250^{o}C). Each corrosion rate is assumed constant over its temperature range and is taken from the maximum of rates corresponding to specific corrosion mechanisms. A listing of CORRAT with current data is provided in Appendix E.

The repository physical data for the four geologies is contained in GEOMAT and includes the variables shown in Table D-1. The format of GEOMAT is (A5, F10.0, A5, 6F10.0) and a listing with current data is provided in Appendix E.

Physical constants utilized in the STRESS subroutine are contained in MATMAT and include the variables shown in Table D-2. The format of MATMAT is (10F10.0) and a listing with current data is provided in Appendix E.

For each specific package design case to be evaluated by BARIER, a BARFIL data file must be provided. BARFIL is actually a dummy variable name equivalent to a specific file name corresponding to a specific package design. A complete physical description of the specific package design is supplied to BARIER by this file. The variables included in BARFIL are shown in Table D-3. A value for each of the variables in Table D-3 is supplied for each barrier of a particular package design. The format of BARFIL is (5X, I5, 7F10.0, /, 2I5, 2F10.0, 2I5, 2F10.0, 2F5.0) and a sample listing is provided in Appendix E.

For each radionuclide of concern, input data to the RELEAS subroutine are stored in an array NUCLID (I,J). The i-th radionuclide is

Table D-1. GEOMAT Variables

Variable		Definition
LABEL	-	Geology
REPRES	-	Repository pressure, psia
CREEP	-	Signifies creeping geology (yes or no)
EGEO	-	Emissivity of repository surface
T1	-	Constants used in repository temperature correlations
T2	-	
T3	-	
T4	-	
COEFF	-	Overall heat transfer coefficient between repository and barrier, $w/in^2\text{-}^oK$

Table D-2. MATMAT Variables

Variable		Definition
Y1	-	Coefficient for yield strength temperature correlation, Ksi
Y2	-	Coefficient for yield strength temperature correlation, Ksi/^{o}C
B1	-	Coefficient for bulk modulus temperature correlation, Ksi
B2	-	Coefficient for bulk modulus temperature correlation, Ksi/^{o}C
G1	-	Coefficient for shear modulus temperature correlation, Ksi
G2	-	Correlation for shear modulus temperature correlation, Ksi/^{o}C
S1	-	Hoop stress yield temperature correlation constant, psi
S2	-	Hoop stress yield temperature correlation constant, psi/^{o}C
S3	-	Hoop stress yield temperature correlation constant, ^{o}C
S4	-	Hoop stress yield temperature correlation constant, psi

Table D-3. BARFIL Variables

Variable	Definition
IL	- Type of barrier (stabilizer, can, overpack, sleeve)
IDIAM	- Inside diameter of inner barrier layer, in.
ODIAM	- Outside diameter of inner barrier layer, in.
ODIAM2	- Outside diameter of second innermost barrier layer, in.
FDIAM	- Outside diameter of third barrier layer (backfill), in.
GDIAM	- Outside diameter of outer barrier layer (gap), in.
A	- Backfill pressure-volume coefficient, psi
K	- Backfill pressure-volume coefficient, psi
MAT	- Type of material in inner barrier layer
MAT2	- Type of material in second innermost barrier layer
E	- Joint efficiency in stress calculation, dimensionless
COAT	- Coating delay time (for corrosion), yr
BAK	- Backfill material type
MATGAP	- Gap material type
CLPRES	- Internal pressure on barrier at time of repository sealing, psi
CLTEMP	- Internal temperature on barrier at time of repository sealing, ^{o}K
BETA	- Backfill Mohr circle slope, dimensionless
POISS	- Backfill Poisson ratio, dimensionless

i = 1 : Uranium-238 (high solubility)
2 : Uranium-238 (low solubility)
3 : Plutonium-239
4 : Americium-241

The columns of NUCLID (I,J) contain the following radionuclide specific information:

j = 1 : grams at t = 0
2 : conversion factor for grams to curies
3 : concentration, gm/ml
4 : λ in, yr^{-1}
5 : diffusion coefficient (liquid), cm^2/year
6 : k_d, ml/gm

Columns 7 - 10 are zeroed out but available for use. Use is made of column 10 where the radionuclide quantity at some time t > 0 is stored.

The value of D used in the RELEAS calculations is that for a substance in water and is conservatively estimated to be 10^{-6} cm/sec or 31.5 cm^2/year (Smith, 1970). However, the value of D used to calculate H is 0.1 D to account for the fact that the corroded barrier has a decreased diffusivity due to void volume and tortuosity. The other input data for all radionuclides are

ε = 0.01 to 0.1
δ = 4
ρ = 1 to 2 gm/ml

The radionuclide specific data are the initial radionuclide quantities, Q_i, tne equilibrium constants, k_d, and the concentrations, c. These data are

	Q_i	λ	k_d	c
i = 1	471420	1.5×10^{-10}	50	1.07×10^{-3}
2	471420	1.5×10^{-10}	1800	3.3×10^{-11}
3	2953	2.8×10^{-5}	1200	3.8×10^{-11}
4	539	1.5×10^{-3}	4000	3.8×10^{-11}

The concentration estimates were obtained from the experimental value for plutonium (Katayama, 1976), except for the uranium-high concentration value which approximates that of the uranyl carbonate complex (Neretnieks, 1978). The k_d values were obtained from the same reference for the uranyl carbonate complex solubility, except for the case of uranium-high solubility which was conservatively set at 50. Since americium-241 is a decay product, an initial quantity for it was calculated so that the quantity at large time (i.e., after the parent has decayed) would be correct if the parent were not transported out of the fuel bundle. This results in a conservative initial quantity for americium-241 because the parent (plutonium) does transport out of the fuel bundle.

D.2 INPUT TECHNIQUES AND REQUIREMENTS

The BARIER code as written is tailored for a time-shared terminal but only minor modifications would be required to allow batch processing. Input is made through a series of input files and some control parameters obtained by interrogation on the terminal. A driver file must be prepared listing the BARFIL files by name for each package design case to be evaluated. This driver file has the dummy variable name DATSET in the program and can be given any valid name which is entered on the terminal when requested. The general form of DATSET is shown in Table D-4 where each BARFIL file is identified (e.g., A.1) along with the corresponding number of barriers in that particular package design case. The format for DATSET is (A10, I2). Thus, an unlimited number of independent and consecutive package design cases may be evaluated with one input message.

Upon execution of BARIER, the input information shown in Table D-5 is requested by the terminal (in order) and typed in by the user. Execution of the program may be terminated by entering "STOP" when the program requests a new driver file.

Table D-4. General Form of DATSET.

FILE	NUMBER OF BARRIERS
A.1	2
A.2	3
A.3	2
B.1	3
B.2	3
C1.1	4
E.1	2

Table D-5. Input Information Required for BARIER Execution

(1) Name of the driver file containing the list of BARFIL files
(2) Time increment (DELTA) by which time will be varied when performing successive calculations leading to barrier failure, yrs
(3) Geology code (IGE), (1-salt, 2-basalt, 3-granite, 4-shale)
(4) Water code (IWATER), (1-anoxic brine, 3-anoxic water)
NOTE: The code increments IWATER so that both anoxic and oxic cases are automatically run.

D.3 OUTPUT DESCRIPTION

All output from BARIER is stored in a data file called PERFOR.DAT. Output for all cases listed in DATSET is maintained in this file until a subsequent execution of BARIER with a different DATSET file. Each time a DATSET file is evaluated by BARIER, output from the previous program execution is overwritten in PERFOR.DAT. Output printouts may be obtained by writing PERFOR.DAT following termination of BARIER execution.

Output from a sample problem is provided in Appendix E. For each design case, pertinent input data is printed first and is followed by specific performance data for each type of environment (water) to be analyzed. Starting with the outermost package barrier, data at the time of failure of each barrier is printed. This includes barrier failure time, net pressure on the barrier at time of failure, barrier thickness and temperature, repository temperature, and radiation dose. Leach begin time, or the time of failure of the innermost barrier, is printed next and is followed by nuclide geology release rate information from the RELEAS subroutine. For each package design case and water environment (brine or water) specified, BARIER analyses are performed for both the anoxic and oxic environments and are printed separately in the output on successive pages.

The output data from the RELEAS subroutine are the radionuclide release rates as a function of time at the backfill-geology interface as defined in Equations (3.5.1) - (3.5.4). There are three types of release output data possible:

(1) When there is a sufficient quantity of a radionuclide at the beginning of the leach time tor each steady state transport, the output will be ten release values for $0.1t_s$, $0.2t_s$, etc., where t_s is the time to reach steady state. The release rate at steady state is the value reported at t_s. The time is then printed for the initial quantity of radionuclide to decay and diffuse away until none remains.

(2) When there is <u>not</u> a sufficient quantity of the radionuclide at the beginning of the leach time to reach steady state, the time when the quantity goes to zero is divided by ten and release rates are reported for 0.1t, 0.2t, etc.

(3a) When there is not a sufficient quantity of the radionuclide at the beginning of the leach time to transport to $0.1t_s$, no release rates are reported because the concentration profile at the backfill-geology interface is too flat for all times.

(3b) When there is less than one gram of radionuclide at the start of the release calculation, the calculation is not performed.

In order to write only the data described above, the write switch IBYK must be set to 2. Setting IBYK = 1 will result in the writing of intermediate results. This option is available to aid in determining which radionuclide quantities are important in the transport rates. In order to obtain a printout of the Fourier series coefficients and roots as defined in Equation (3.5.20), the write switch IP must be set to 1 and IBYK = 1. These two switches are not external input and must be set through a statement or DATA block.

APPENDIX E
SAMPLE PROBLEMS

Examples of sample problems and BARIER input data are provided in this Appendix. Files GEOMAT.DAT, CORRAT.DAT, and MATMAT.DAT contain input data required to run any and all package design cases. File COMMON.NEW is included throughout BARIER and is shown here for completeness. Files D2.1, BE.27N, and E.11N represent particular barrier package designs (BARFIL file) which are evaluated by BARIER.

In these sample problems, a time increment of 1.0 year, a salt geology, and an anoxic and oxic brine will be the remaining input control variables. This information is entered on a remote terminal upon request. Output for these cases is also presented.

CONCEPT DE.27N

	012.000	13.500	13.500	13.500	13.500	0.0		0.0	
6	6 1.0	0.0	0	10 0.0	325.0	0.6	0.4		
	213.500	14.000	14.000	14.500	14.500	0.44		253.0	
4	4 1.0	0.0	1	10 0.0	325.0	0.6	0.4		
	414.500	21.500	21.500	40.000	40.000	0.44		253.0	
7	2 1.0	0.0	1	10 0.0	325.0	0.6	0.4		

CONCEPT E.11N

	012.000	13.500	13.500	13.500	13.500	0.0		0.0	
6	6 1.0	0.0	0	10 0.0	325.0	0.6	0.4		
	213.500	19.500	19.500	40.000	40.000	0.44		253.0	
4	4 1.0	0.0	2	10 0.0	325.0	0.6	0.4		

GEOMAT.DAT

```
SALT  2500.00  YES   0.75   122.66   23.60   20.00   193.00   5.00
BASAL 4500.00  NO    0.90   128.80   31.15   10.00   200.00   5.00
CHANI 5000.00  NO    0.80   129.24   29.97   10.00   198.00   5.00
SHALE 3100.00  YES   0.73   100.45   30.00   15.00   182.00   5.00
```

CONMAT.DAT

```
0.00100   0.00280   0.02700   0.27600   0.00200   0.00200   0.00200   0.01900
0.00010   0.00010   0.00010   0.00010   0.00010   0.00010   0.00010   0.00010
0.00600   0.00030   0.00400   0.00400   0.00030   0.00230   0.00030   0.00030
0.02000   0.00040   0.03000   0.03000   0.00010   0.00010   0.00030   0.00030
0.00500   0.00250   0.00500   0.04700   0.00050   0.00200   0.01200   0.00200
0.00030   0.01200   0.00060   0.04700   0.00030   0.00100   0.00060   0.00100
0.01200   0.04000   0.10000   0.30000   0.03500   0.00000   0.00600   0.03500
```

MATMAT.DAT

```
13.7     -.011   17900.   0.00    5840.   -3.8    12500.   0.0    30.   12500.
43.5     -.025    3861.   0.00    4881.   -2.8    13431.  26.7    38.   12436.
25.2     -.022   23800.   0.00   11200.   -7.67   21200.   0.0    30.   21200.
30.7     -.033   19310.   1.05   10900.   -3.77   19316.  16.3    38.   10700.
10.2     -.009   17900.   0.00    5900.   -3.5     7399.  19.3    38.    6640.
 0.0      0.0        0.   0.00       0.    0.0        0.   0.0     0.      0.
20.3     -.013   12000.   0.0     6700.   -4.4     6000.   0.0    30.    6000.
```

COMMON.NEW

```
      PARAMETER (IBAR=3, ICEO=4, IMTR=10, IBAK=4
     REAL, MAXTHP, LRATE, NU, LAMBDA, IDIAM, LABEL, K, MCOND, NTPRS
     COMMON /MATRIX/  IDIAM(IBAR),ODIAM(IBAR),FDIAM(IBAR),A(IBAR),HEAT,
     1         X(IBAR),MAT(IBAR),E(IBAR),COAT(IBAR),FORCE,MCOND(IMTR),
     2         BAK(IBAR),ODIAM2(IBAR),MAT2(IBAR),ILC(IBAR),WFAIL,BETA(IBAR)
     3         ,CORMAT(8,7),       TIMBAR,                FCOND(IBAK),MATCAP
     4         (IBAR),LABEL(ICEO),REPRES(ICEO),CREEP(ICEO),POISS(IBAR),
     5         T1(ICEO),T2(ICEO),T3(ICEO),T4(ICEO),NTPRS,KMAT(IMTR),
     6                  TIME,INDX,M,ICE,DIAM,REPTEM,IB,DELTA,THICK2,
     7         CLPRES(IBAR),CLTEMP(IBAR),TEMP,IDONE,  IWATER,EPRESS,
     8         THICK,LRATE(ICEO),RELTIM,DELTIM,TCENT,IOU,WFAIL,ECEO(ICEO),
     9         ODIAM(IBAR),Y1(IMTR),Y2(IMTR),  S1(IMTR),S2(IMTR),
     1         C1(IMTR),C2(IMTR),S1(IMTR),S2(IMTR),S3(IMTR),S4(IMTR),
     2         FBAK(IBAK),MAXTHP,COEFF(ICEO),BAILA(ICEO),KKK,FLUX
      INTEGER BAK
```

CONCEPT D2.1

```
      112.000    13.500    13.500    13.500    13.500    0.0       0.0
3  3     1.0        0.0       0  10     15.0     325.0     0.6   0.4
      213.500    14.000    14.000    14.500    14.500    0.44          253.0
3  3     1.0        0.0       2  10     15.0     325.0     0.6   0.4
      314.500    15.000    15.000    15.500    15.500    0.44          253.0
3  3     1.0        0.0       3  10     15.0     325.0     0.6   0.4
      415.500    23.500    23.500    48.000    48.000    0.44          253.0
7  7     1.0      100.0       2  10     15.0     325.0     0.6   0.4
```

WATER: BRINE,OXIC

ELEMENT	FAILURE TIME(YRS)	NET PRESS(PSIA)	THICKNESS (IN)	ELEMENT TEMP(K)	REPOSITORY TEMP(K)	RAD DOSE (R/HR)
SLEEVE	113.00	-2730.33	0.100	468.80	466.00	1.152E+09
OPACK	20.00	-2823.01	0.170	469.07	466.00	2.140E+03
CAN	33.00	-2823.53	0.158	469.30	466.00	1.720E+03

LEACH BEGIN TIME (YEARS) = 156.00

NUCLIDE GEOLOGY RELEASE RATE INFORMATION

U-238 (HIGH SOLUBILITY) RELEASE TO GEOLOGY BEGINS AT 1.560E+02 YEARS, BACKFILL IS 89.9% OF TRANSPORT RESISTANCE, RELEASE RATES ARE:

TIME(YR)	6.098E+03	1.164E+04	1.730E+04	2.312E+04	2.897E+04	3.461E+04	4.035E+04	4.609E+04	5.183E+04	5.767E+04
RATE(CI/YR)	1.365E-08	1.407E-07	3.804E-07	5.797E-07	4.441E-07	4.849E-07	5.100E-07	5.271E-07	5.373E-07	5.430E-07

CONSTANT GEOLOGICAL RELEASE RATE OF 5.430E-07 CI/YR OCCURS FROM 5.767E+04 YEARS TO 1.790E+05 YEARS

U-238 (LOW SOLUBILITY) RELEASE TO GEOLOGY BEGINS AT 1.560E+02 YEARS, BACKFILL IS 89.9% OF TRANSPORT RESISTANCE, RELEASE RATES ARE:

TIME(YR)	3.067E+03	4.132E+03	6.197E+03	8.262E+03	1.033E+04	1.239E+04	1.446E+04	1.653E+04	1.859E+04	2.066E+04
RATE(CI/YR)	4.849E-16	4.996E-15	9.964E-15	1.349E-14	1.677E-14	1.722E-14	1.814E-14	1.872E-14	1.909E-14	1.931E-14

CONSTANT GEOLOGICAL RELEASE RATE OF 1.931E-14 CI/YR OCCURS FROM 2.066E+04 YEARS TO 4.626E+10 YEARS

PLUTONIUM 239 RELEASE TO GEOLOGY BEGINS AT 2.066E+04 YEARS, BACKFILL IS 89.9% OF TRANSPORT RESISTANCE, RELEASE RATES ARE:

TIME(YR)	2.066E+04	5.717E+04	8.568E+04	1.142E+05	1.427E+05	1.712E+05	1.997E+05	2.282E+05	2.567E+05	2.852E+05
RATE(CI/YR)	6.691E-20	7.111E-14	4.334E-12	3.242E-11	1.050E-10	2.207E-10	3.921E-10	5.722E-10	7.858E-10	9.946E-10

CONSTANT GEOLOGICAL RELEASE RATE DOES NOT OCCUR, RELEASE ENDS AT 3.052E+05 YEARS AT A RELEASE RATE OF 9.946E-10 CI/YR

AMERICIUM 241 DOES NOT REACH 10 PERCENT OF CONSTANT GEOLOGICAL RELEASE RATE
TRANSIENT RELEASE RATE TOO SMALL TO CALCULATE

GEOLOGY: SALT
REPOSITORY PRESSURE (PSI): 2500.0000
CREEPING MEDIUM ? YES
MAXIMUM WASTE TEMP.: 623.3(K)

ELEMENT	I.D. INNER SOL.ID (IN)	O.D. INNER SOL.ID (IN)	O.D. OUTER SOL.ID (IN)	O.D. FILLER (IN)	O.D. CAP (IN)	BACKFILL COEFFICIENTS A	BACKFILL COEFFICIENTS K	INNER SOL.ID	OUTER SOL.ID	JOINT EFF	COAT DELAY (YRS)	FILLER MATERIAL	CAP MATERIAL	SEAL PRESS (PSI)	SEAL TEMP (K)	BACKFILL SPUR SLOPE	BACKFILL POISSON RATIO
SLEEVE	14.500	21.500	21.600	40.000	40.000	0.44	253.00	IRON	ZINC	1.00	0.0	BENT	NONE	0.00	325.00	0.60	0.40
CAN	13.500	14.000	14.000	14.500	14.500	0.44	253.00	304SST	304SST	1.00	0.0	BENT	NONE	0.00	325.00	0.60	0.40
CAST ST	12.000	13.500	13.500	13.500	13.500	0.00	0.00	LEAD	LEAD	1.00	0.0	NONE	NONE	0.00	325.00	0.60	0.40

BARRIER PERFORMANCE

WATER: BRINE,ANOXIC

ELEMENT	FAILURE TIME(YRS)	NET PRESS(PSIA)	THICKNESS (IN)	ELEMENT TEMP(K)	REPOSITORY TEMP(K)	RAD DOSE (R/HR)
SLEEVE	500.00	-2500.00	0.000	469.14	466.00	1.470E-03
CAN	626.00	-2500.00	0.000	469.38	466.00	8.016E-02
CAST STAB	63.00	-2500.00	0.000	469.80	466.00	1.120E-01

LEACH BEGIN TIME (YEARS) = 1277.00

NUCLIDE GEOLOGY RELEASE RATE INFORMATION

U-238 (HIGH SOLUBILITY) RELEASE TO GEOLOGY BEGINS AT 1.277E+03 YEARS, BACKFILL IS 99.0% OF TRANSPORT RESISTANCE, RELEASE RATES ARE:

TIME(YR)	6.709E+04	1.343E+05	2.011E+05	2.677E+05	3.343E+05	4.009E+05	4.675E+05	5.342E+05	6.008E+05	6.674E+05
RATE(CI/YR)	1.283E-09	1.321E-08	2.633E-08	3.947E-08	4.171E-08	4.883E-08	4.799E-08	4.931E-08	5.043E-08	5.109E-08

CONSTANT GEOLOGICAL RELEASE RATE OF 5.109E-08 CI/YR OCCURS FROM 6.674E+05 YEARS TO 1.013E+06 YEARS

U-238 (LOW SOLUBILITY) RELEASE TO GEOLOGY BEGINS AT 1.277E+03 YEARS, BACKFILL IS 99.0% OF TRANSPORT RESISTANCE, RELEASE RATES ARE:

TIME(YR)	3.999E+06	4.797E+06	7.194E+06	9.592E+06	1.199E+07	1.439E+07	1.679E+07	1.918E+07	2.158E+07	3.358E+07
RATE(CI/YR)	4.855E-17	4.693E-16	9.359E-16	1.267E-15	1.481E-15	1.610E-15	1.704E-15	1.766E-15	1.793E-15	1.814E-15

CONSTANT GEOLOGICAL RELEASE RATE OF 1.814E-15 CI/YR OCCURS FROM 3.358E+07 YEARS TO 4.169E+10 YEARS

PLUTONIUM 239 DOES NOT REACH 10 PERCENT OF CONSTANT GEOLOGICAL RELEASE RATE
TRANSIENT RELEASE RATE TOO SMALL TO CALCULATE

AMERICIUM 241 DOES NOT REACH 10 PERCENT OF CONSTANT GEOLOGICAL RELEASE RATE
TRANSIENT RELEASE RATE TOO SMALL TO CALCULATE

Concept BE.27A (Continued)

WATER: BRINE,OXIC

ELEMENT	FAILURE TIME(YRS)	NET PRESS(PSIA)	THICKNESS (IN)	ELEMENT TEMP(K)	REPOSITORY TEMP(K)	RAD DOSE (R/HR)
SLEEVE	513.00	-2500.00	0.000	469.06	466.00	3.361E-03
CAN	9.00	-2500.00	0.000	469.37	466.00	3.287E+00
CAST STAB	16.00	-2500.00	0.000	469.77	466.00	3.632E+00

LEACH BEGIN TIME (YEARS) = 537.00

NUCLIDE GEOLOGY RELEASE RATE INFORMATION

U-238 (HIGH SOLUBILITY) RELEASE TO GEOLOGY BEGINS AT 5.370E+02 YEARS, BACKFILL IS 99.0% OF TRANSPORT RESISTANCE, RELEASE RATES ARE:

TIME(YR)	6.716E+04	1.338E+05	2.004E+05	2.670E+05	3.336E+05	4.002E+05	4.668E+05	5.334E+05	6.000E+05	6.666E+05
RATE(CI/YR)	1.283E-09	1.331E-08	2.635E-08	3.867E-08	4.171E-08	4.853E-08	4.798E-08	4.951E-08	5.043E-08	5.102E-08

CONSTANT GEOLOGICAL RELEASE RATE OF 5.109E-08 CI/YR OCCURS FROM 6.666E+05 YEARS TO 1.812E+06 YEARS

U-236 (LOW SOLUBILITY) RELEASE TO GEOLOGY BEGINS AT 5.370E+02 YEARS, BACKFILL IS 99.0% OF TRANSPORT RESISTANCE, RELEASE RATES ARE:

TIME(YR)	3.398E+06	4.796E+06	7.194E+06	9.591E+06	1.199E+07	1.439E+07	1.678E+07	1.918E+07	2.158E+07	2.398E+07
RATE(CI/YR)	4.855E-17	4.693E-16	9.359E-16	1.267E-15	1.481E-15	1.618E-15	1.704E-15	1.758E-15	1.792E-15	1.814E-15

CONSTANT GEOLOGICAL RELEASE RATE OF 1.814E-15 CI/YR OCCURS FROM 3.398E+07 YEARS TO 6.169E+10 YEARS

PLUTONIUM 239 DOES NOT REACH 10 PERCENT OF CONSTANT GEOLOGICAL RELEASE RATE
TRANSIENT RELEASE RATE TOO SMALL TO CALCULATE

AMERICIUM 241 DOES NOT REACH 10 PERCENT OF CONSTANT GEOLOGICAL RELEASE RATE
TRANSIENT RELEASE RATE TOO SMALL TO CALCULATE

GEOLOGY: SALT
REPOSITORY PRESSURE (PSI): 2000.0000
CREEPING MEDIUM ? YES
MAXIMUM WASTE TEMP.: 563.7(K)

ELEMENT	I.D. INNER SOL.ID (IN)	O.D. INNER SOL.ID (IN)	O.D. OUTER SOL.ID (IN)	O.D. FILLER (IN)	O.D. CAP (IN)	BACKFILL COEFFICIENTS: A	K	INNER SOL.ID	OUTER SOL.ID	JOINT EFF	COAT DELAY (YRS)	FILLER MATERIAL	CAP MATERIAL	SEAL PRESS (PSI)	SEAL TEMP (K)	BACKFILL SOIL SLOPE	BACKFILL POISSON RATIO
CAN	13.500	13.500	13.500	48.000	48.000	0.44	253.00	304SST	304SST	1.00	0.0	SAND-B	NONE	0.00	328.00	0.60	0.40
CAST ST	12.000	13.500	13.500	13.500	13.500	0.00	0.00	LEAD	LEAD	1.00	0.0	NONE	NONE	0.00	328.00	0.60	0.40

BARRIER PERFORMANCE

WATER: BRINE,ANOXIC

ELEMENT	FAILURE TIME(YRS)	NET PRESS(PSIA)	THICKNESS (IN)	ELEMENT TEMP(K)	REPOSITORY TEMP(K)	RAD DOSE (R/HR)
CAN	7500.00	-2500.00	0.000	469.38	466.00	3.063E-04
CAST STAB	63.00	-2500.00	0.000	469.00	466.00	9.020E-02

LEACH BEGIN TIME (YEARS) = 7563.00

NUCLIDE GEOLOGY RELEASE RATE INFORMATION

U-238 (HIGH SOLUBILITY) RELEASE TO GEOLOGY BEGINS AT 7.563E+03 YEARS, BACKFILL IS 93.3% OF TRANSPORT RESISTANCE, RELEASE RATES ARE:

TIME(YR)	1.533E+04	2.310E+04	3.037E+04	3.864E+04	4.641E+04	5.418E+04	6.195E+04	6.972E+04	7.749E+04	8.526E+04
RATE(CI/YR)	1.010E-08	1.041E-07	2.076E-07	2.809E-07	3.205E-07	3.588E-07	3.779E-07	3.899E-07	3.976E-07	4.024E-07

CONSTANT GEOLOGICAL RELEASE RATE OF 4.024E-07 CI/YR OCCURS FROM 8.526E+04 YEARS TO 2.491E+05 YEARS

U-238 (LOW SOLUBILITY) RELEASE TO GEOLOGY BEGINS AT 7.563E+03 YEARS, BACKFILL IS 93.3% OF TRANSPORT RESISTANCE, RELEASE RATES ARE:

TIME(YR)	2.070E+05	5.644E+05	8.459E+05	1.125E+06	1.403E+06	1.684E+06	1.964E+06	2.243E+06	2.523E+06	2.802E+06
RATE(CI/YR)	3.507E-16	3.696E-15	7.572E-15	9.977E-15	1.167E-14	1.274E-14	1.342E-14	1.385E-14	1.413E-14	1.429E-14

CONSTANT GEOLOGICAL RELEASE RATE OF 1.429E-14 CI/YR OCCURS FROM 2.802E+06 YEARS TO 4.022E+10 YEARS

PLUTONIUM 239 RELEASE TO GEOLOGY BEGINS AT 3.533E+04 YEARS, BACKFILL IS 93.3% OF TRANSPORT RESISTANCE, RELEASE RATES ARE:

TIME(YR)	3.533E+04	6.310E+04	9.087E+04	1.186E+05	1.464E+05	1.742E+05	2.019E+05	2.297E+05	2.575E+05	2.852E+05
RATE(CI/YR)	8.734E-20	4.037E-16	1.317E-13	2.280E-12	1.231E-11	3.723E-11	8.112E-11	1.442E-10	2.240E-10	3.168E-10

CONSTANT GEOLOGICAL RELEASE RATE DOES NOT OCCUR, RELEASE ENDS AT 2.852E+05 YEARS AT A RELEASE RATE OF 3.168E-10 CI/YR

AMERICIUM 241 RELEASE CALCULATION NOT PERFORMED BECAUSE
INITIAL INVENTORY OF 6.379E-03 CURIE IS TOO SMALL

Concept E.11B (Continued)

```
 WATER: BRINE,OXIC
ELEMENT          FAILURE      NET          THICKNESS     ELEMENT      REPOSITORY    RAD DOSE
                 TIME(YRS)    PRESS(PSIA)  (IN)          TEMP(K)      TEMP(K)       (R/HR)
CAN              100.00       2500.00      0.000         469.36       466.00        4.448E+00
CAST STAR        10.00        2500.00      0.000         469.77       466.00        9.003E+02

LEACH BEGIN TIME (YEARS) =      116.00

NUCLIDE GEOLOGY RELEASE RATE INFORMATION

U-238 (HIGH SOLUBILITY)  RELEASE TO GEOLOGY BEGINS AT 1.160E+02 YEARS, BACKFILL IN 93.3% OF TRANSPORT RESISTANCE, RELEASE RATES ARE:
TIME(YR)      7.806E+03  1.564E+04  2.343E+04  3.120E+04  3.897E+04  4.673E+04  5.450E+04  6.227E+04  7.004E+04  7.781E+04
RATE(CI/YR)   1.010E 08  1.041E-07  2.076E 07  2.099E-07  3.205E 07  3.600E-07  3.779E-07  3.899E 07  3.976E-07  4.024E-07
CONSTANT GEOLOGICAL RELEASE RATE OF 4.024E-07 CI/YR OCCURS FROM 7.781E+04 YEARS TO 2.417E+06 YEARS

U-238 (LOW SOLUBILITY)   RELEASE TO GEOLOGY BEGINS AT 1.160E+02 YEARS, BACKFILL IN 93.3% OF TRANSPORT RESISTANCE, RELEASE RATES ARE:
TIME(YR)      2.796E+05  5.590E+05  8.384E+05  1.118E+06  1.397E+06  1.677E+06  1.956E+06  2.236E+06  2.515E+06  2.795E+06
RATE(CI/YR)   3.587E 16  3.696E-15  7.372E-15  9.977E 15  1.167E-14  1.274E-14  1.342E-14  1.385E-14  1.412E-14  1.429E-14
CONSTANT GEOLOGICAL RELEASE RATE OF 1.429E-14 CI/YR OCCURS FROM 2.795E+06 YEARS TO 4.822E+10 YEARS

PLUTONIUM 239            RELEASE TO GEOLOGY BEGINS AT 2.063E+04 YEARS, BACKFILL IN 93.3% OF TRANSPORT RESISTANCE, RELEASE RATES ARE:
TIME(YR)      2.063E+04  5.714E+04  8.566E+04  1.142E+05  1.427E+05  1.712E+05  1.997E+05  2.282E+05  2.567E+05  2.852E+05
RATE(CI/YR)   4.515E-20  6.367E-16  1.777E-13  2.046E-12  1.468E-11  4.297E-11  9.185E-11  1.600E-10  3.403E-10  3.434E-10
CONSTANT GEOLOGICAL RELEASE RATE DOES NOT OCCUR, RELEASE ENDS AT 2.852E+05 YEARS AT A RELEASE RATE OF 3.434E-10 CI/YR

AMERICIUM 241            DOES NOT REACH 10 PERCENT OF CONSTANT GEOLOGICAL RELEASE RATE
TRANSIENT RELEASE RATE TOO SMALL TO CALCULATE
```

DISTRIBUTION LIST

ACRES AMERICAN INC
A. S. BURGESS
R. STRUBLE
ALLIED GENERAL NUCLEAR SERVICES
P.F. HIGHBERGER
M. A. KOLB
ALLIS-CHALMERS
GARRICK J. SOLOVEY
AMERICAN NUCLEAR INSURERS
DOTTIE SHERMAN
ANALYSIS & TECHNOLOGY INC
T. MAZOUR
ANALYTIC & COMPUTATIONAL RESEARCH INC
B. SAGAR
APPLIED MECHANICS INC
JOHN R. WILLIAMS
ARGONNE NATIONAL LABORATORY
J. HOWARD KITTEL
W. J. MECHAM
MARTIN SEITZ
MARTIN J. STEINDLER
ARINC RESEARCH CORP
H. P. HIMPLER
ARTHUR D. LITTLE INC
CHARLES R. HADLOCK
ATOMIC ENERGY CONTROL BOARD
J. L. WALLACH
ATOMIC ENERGY OF CANADA LTD
M.O. LUKE
ANN QUINN
F. P. SARGENT
ATOMIC ENERGY RESEARCH ESTABLISHMENT
D. P. HODGKINSON
JOHN RAE
ATOMIC INDUSTRIAL FORUM INC
AUSTRALIAN ATOMIC ENERGY COMMISSION
BABCOCK & WILCOX
INFORMATION SERVICES
BATTELLE COLUMBUS DIVISION
SANFORD G. BLOOM
JOHN T. MCGINNIS
JEFFREY L. MEANS
NEIL E. MILLER
STEPHEN NICOLOSI
THOMAS M. TRAINER
KENNETH R. YATES
BECHTEL GROUP INC
THOMAS S. BAER
DON B. CRANDALL
LESLIE J. JARDINE
N. A. NORMAN
RICHARD J. TOSETTI
BENDIX FIELD ENGINEERING CORP
JOHN C. PACER
BHABHA ATOMIC RESEARCH CENTRE
V. SUKUMORAN
K. T. THOMAS
BLACK & VEATCH
M. JOHN ROBINSON
BRITISH NUCLEAR FUELS LTD
R. S. WILKS
BROOKHAVEN NATIONAL LABORATORY
GERALD BIDA
DONALD E. CLARK
M. S. DAVIS
SANDRA G. LANE
PETER SOO
HELEN TODOSOW (2)
BUNDESMINISTERIUM FUR FORSCHUNG
ROLF-PETER RANDL
BURNS AND ROE INDUSTRIAL SERVICES CORP
JOHN PIRRO
C.F.H.F.
BILL DUESING
C.R. WATTS ASSOCIATES
CURTIS WATTS
CALIFORNIA DEPT OF CONSERVATION
PERRY AMIMITO
CALIFORNIA DEPT OF HEALTH SERVICES
BEVERLEE MYERS
CALIFORNIA INSTITUTE OF TECHNOLOGY
LEON T. SILVER
CAMP, DRESSER, AND MCKEE INC
DAVID A. WOODRUFF
CAPITAL AREA GROUND WATER CONSERVATION COMMISSION
A. N. TURCAN JR.
CASTUS VALLEY ORCHARDS
CARL ANDERSON
CAYUGA LAKE CONSERVATION ASSOCIATION INC
D. S. KIEFER
CENTRAL WASHINGTON UNIVERSITY
J.R. HINTHORNE
CENTRE D ETUDE DE L ENERGIE NUCLEAIRE
RENE HEREMANS
CENTRE D'INFORMATIQUE GEOLOGIQUE
GHISLAIN DE MARSILY
CITIZENS ASSOCIATION FOR SOUND ENERGY
JUANITA ELLIS
COLUMBIA UNIVERSITY
HUBERT STAUDIGEL
CONVERSE WARD
A. M. HALE
CORNELL UNIVERSITY
JOHN BIRD
COUNCIL ON ECONOMIC PRIORITIES
MARVIN RESNIKOFF
CYGNA ENERGY SERVICES
DONALD GARDNER
DAMES & MOORE
RON KEAR
O. L. OZTUNOLI
DAPPOLONIA CONSULTING ENGINEERS INC
LISA K. DONOHUE
ABBY FORREST
AMIRA HAMDY
PETER C. KELSALL
CARL E. SCHUBERT
DAWCON MANAGEMENT CONSULTING SERVICE
DAVID A. WEBSTER
DELAWARE CUSTOM MATERIEL INC
HOWARD NOVITCH
DEPT OF THE ENVIRONMENT
F. S. FEATES
DIVISION OF ENVIRONMENTAL SAFETY RESEARCH
HARUTO NAKAMURA
DRAVO ENGINEERS AND CONSTRUCTORS
KEN BEALL
DUKE UNIVERSITY
THOMAS DAVIS
DYNATECH R/D COMPANY
STEPHEN E. SMITH
E.I. DU PONT DE NEMOURS & COMPANY
DONALD E. GORDON
E.R. JOHNSON ASSOCIATES INC
E. R. JOHNSON
G.L. JOHNSON
EARTH SCIENCES CONSULTANTS INC
HARRY L. CROUSE
EBASCO SERVICES INC
ZUBAIR SALEEM
EDS NUCLEAR INC
C. SUNDARARAJAN
EG & G IDAHO INC
GEORGE B. LEVIN
M. D. MCCORMACK
T. H. SMITH
RICHARD TALLMAN
ELECTROWATT ENGINEERING SERVICE
H. N. PATAK
ELSAM
A. V. JOSHI
EMBASSY OF THE UNITED STATES
MAUD LI HAIJLEN-RYLANDER
ENERCOR INC
JOHN RODOSEVICH
ENERGY FUELS NUCLEAR INC
DON M. PILLMORE
ENERGY RESEARCH GROUP INC
MARC GOLDSMITH
ENERGY RESEARCH LABORATORY HITACHI INC
MAKOTO KIKUCHI
ENVIRONMENT CANADA
CLAUDE BARRAUD
ENVIRONMENTAL POLICY INSTITUTE
DAVID M. BERICK
FRED MILLAR
ENVIRONMENTAL RESEARCH GROUP INC
PETER G. COLLINS
ENVIROSPHERE COMPANY
BOB HAINES
EXXON NUCLEAR IDAHO COMPANY INC
D. L. CONDOTTA
W. B. KERR
EXXON PRODUCTION RESEARCH
GARY WAYMIRE
FENIX & SCISSON INC
JOSE A. MACHADO
CHARLENE SPARKMAN
FLORIDA INSTITUTE OF TECHNOLOGY
JOSEPH A. ANGELO, JR.
FLUOR ADVANCED TECHNOLOGY DIVISION
JOAN V. MCCURRY
FLUOR ENGINEERS & CONSTRUCTORS INC
RAYMOND J. DUGAL
FORD, BACON & DAVIS UTAH INC
PRESTON H. HUNTER
ROBERT F. OVERMYER
BURTON J. THAMER
FOSTER-MILLER ASSOCIATES INC
NORBERT PAAS
FREIE UNIVERSITAET BERLIN
HANSKARL BRUEHL
GENERAL ATOMIC COMPANY
ROBERT M. BURGOYNE
ROBERT J. CAMPANA
GENERAL COURT OF MASSACHUSETTS
TIMOTHY J. BURKE
GEOLOGICAL SURVEY OF CANADA
ROOM 350
GEORGIA INSTITUTE OF TECHNOLOGY
GEOFFREY G. EICHHOLZ
ALFRED SCHNEIDER
GEOTRONS
JAMES MERCER
GERMANTOWN FRIENDS SCHOOL
HERB BASSOW

GIBBS & HILL INC
ROBERT PRIETO
GILBERT/COMMONWEALTH
JERRY L. ELLIS
GOLDER ASSOCIATES
ELIZABETH EISENHOOD
CLEMENT M. K. YUEN
GTC GEOLOGIC TESTING CONSULTANTS LTD
JOHN F. PICKENS
H & R TECHNICAL ASSOCIATES INC
WILLIAM R. RHYNE
HAHN-MEITNER-INSTITUT FUR KERNFORSCHUNG BERLIN
KLAUS ECKART MAASS
HANFORD ENGINEERING DEVELOPMENT LABORATORY
ALBERT G. BLASEWITZ
ROBERT EINZIGER
R. L. KNECHT
W. E. ROAKE
HARDING LAWSON ASSOCIATES
FRANK C. KRESSE
HARVARD UNIVERSITY
RAYMOND SIEVER
IDAHO BUREAU OF MINES AND GEOLOGY
EARL H. BENNETT
IMPERIAL COLLEGE OF SCIENCE AND TECHNOLOGY
B. K. ATKINSON
INSTITUT FUR TIEFLAGERUNG
WERNT BREWITZ
KLAUS KUHN
E. R. SOLTER
PETER UERPMANN
INSTITUTE FOR CHEMICAL TECHNOLOGY
REINHARD ODOJ
INSTITUTE OF GEOLOGICAL SCIENCES
NEIL A. CHAPMAN
INSTITUTE OF RADIATION PROTECTION
KAI JAKOBSSON
INTERA ENVIRONMENTAL CONSULTANTS INC
F. J. PEARSON, JR.
ROBERT WILEMS
INTERNATIONAL ENERGY SYSTEMS CORP
JOHN A. BOWLES
INTERNATIONAL ENGINEERING COMPANY INC
TERRY L. STEINBORN
MAX ZASLAWSKY
INTERNATIONAL RESEARCH AND EVALUATION
R. DANFORD
IRT CORP
J. STOKES
ISTITUTO SPERIMENTALE MODELLI E STRUTTURE S.P.A.
F. GERA
J.F.T. AGAPITO & ASSOCIATES INC
MICHAEL P. HARDY
JACKSON STATE UNIVERSITY
ESTUS SMITH
JAPAN ATOMIC ENERGY RESEARCH INSTITUTE
TARO ITO
JGC CORPORATION
MASAHIKO MAKINO
JOINT RESEARCH CENTRE
GIRARDI FRANCESCO
JORDAN GORRILL ASSOCIATES
JOHN D. TEWHEY
KAISER ENGINEERS INC
W. J. DODSON
J. S. RITCHIE
KANSAS DEPT OF HEALTH AND ENVIRONMENT
GERALD W. ALLEN
KBS
LARS B. NILSSON
KELLER WREATH ASSOCIATES
FRANK WREATH
KERNFORSCHUNGSZENTRUM KARLSRUHE GMBH
K. D. CLOSS
R. KOSTER
HORST PENTINGHAUS
KIHN ASSOCIATES
HARRY KIHN
KLM ENGINEERING INC
B. GEORGE KNIAZEWYCZ
KYOTO UNIVERSITY
YORITERU INOUE
LAWRENCE BERKELEY LABORATORY
JOHN A. APPS
THOMAS DOE
NORMAN M. EDELSTEIN
BRIAN KANEHIRO
S. KLAINER
ROBIN SPENCER
J. WANG
LAWRENCE LIVERMORE NATIONAL LABORATORY
LYNDEN B. BALLOU
JOHN H. CAMPBELL
D. D. JACKSON
R. CARROLL MANINGER
LAWRENCE D. RAMSPOTT (2)
W. G. SUTCLIFFE
TECHNICAL INFORMATION DEPARTMENT L-53
RICHARD VAN KONYNENBURG
LEHIGH UNIVERSITY
D. R. SIMPSON
LOS ALAMOS NATIONAL LABORATORY
ERNEST A. BRYANT
GEORGE A. COWAN
BRUCE R. ERDAL
CLAUDE HERRICK
K. K. S. PILLAY
KURT WOLFSBERG
LOS ALAMOS TECHNICAL ASSOCIATES INC
R. J. KINGSBURY
LOUISIANA TECH UNIVERSITY
LIBRARY
NORMAN WITRIAL
MACLAREN PLANSEARCH INC
ALEX BUCHNEA
MASSACHUSETTS INSTITUTE OF TECHNOLOGY
JOHN DEUTCH
RICHARD K. LESTER
MARSHA LEVINE
MCDERMOTT INC
KAREN L. FURLOW
MCMASTER UNIVERSITY
L. W. SHEMILT
MECHANICAL TECHNOLOGY INC
WARREN BESSLER
STANLEY W. DOROFF
MEMBERS OF THE GENERAL PUBLIC
DAVID H. BOLTZ
JAMES BOYD
WILLIAM E. CONAWAY
WILLIAM V. CONN
D.P. DAUTOVICH
DANNELLE D. DUDEK
FRANCES FARLEY
SHIRLEY M. GIFFORD
DOUGLAS H. GREENLEE
C. F. HAJEK
D. C. LANGSTAFF
DAVID LYLE
MAX MCDOWELL
ALAN D. PASTERNAK
SHAILER S. PHILBRICK
ROGER E. POWERS
PAUL SHEWMON
M. J. SZULINSKI
JIMMY L. WHITE
MICHAEL BAKER, JR INC
C. J. TOUHILL
MICHIGAN DEPT OF PUBLIC HEALTH
DON VANFAROWE
MICHIGAN DISTRICT HEALTH DEPT NO 4
EDGAR KREFT
MICHIGAN LEGISLATIVE OFFICE OF SCIENCE ADVISOR
MICHIGAN TECHNOLOGICAL UNIVERSITY
GARY L. DOWNEY
MINNESOTA GEOLOGICAL SURVEY
MATT S. WALTON
MISSISSIPPI ATTORNEY GENERALS OFFICE
MACK CAMERON
MISSISSIPPI CITIZENS AGAINST NUCLEAR DISPOSAL
STANLEY DEAN FLINT
MISSISSIPPI DEPT OF ENERGY AND TRANSPORTATION
JOHN W. GREEN (3)
MISSISSIPPI DEPT OF NATURAL RESOURCES
CHARLES L. BLALOCK
MISSISSIPPI DEPT OF WILDLIFE CONSERVATION
JOSEPH W. JACOB, JR.
MISSISSIPPI STATE BOARD OF HEALTH
EDDIE S. FUENTE
J. WARREN GREEN
MISSISSIPPI STATE HOUSE OF REPRESENTATIVES
JERRY OKEEFE
MITRE CORP
LESTER A. ETTLINGER
MITSUBISHI METAL CORP
TATSUO ARIMA
NASA JOHNSON SPACE CENTER
MICHAEL R. HELFERT
NATIONAL ACADEMY OF SCIENCES
JOHN T. HOLLOWAY
PETER B. MYERS
NATIONAL BOARD FOR SPENT NUCLEAR FUEL, KARNBRANSLENAMDEN
NILS RYDELL
NATIONAL BUREAU OF STANDARDS
RILEY M. CHUNG
WILLIAM P. REED
NATIONALE GENOSSENSCHAFT FUR DIE LAGERUNG RADIOAKTIVER ABFALLE
MARLIES KUHN
NATURAL RESOURCES DEFENSE COUNCIL
THOMAS B. COCHRAN
NEVADA DEPT OF ENERGY
ROBERT R. LOUX
NEW ENGLAND NUCLEAR CORP
KERRY BENNERT
NEW JERSEY DEPT OF ENVIRONMENTAL PROTECTION
JEANETTE ENG
NEW MEXICO ENVIRONMENTAL EVALUATION GROUP
ROBERT H. NEILL

NEW YORK DEPT OF HEALTH
DAVID AXELROD,M.D.
NEW YORK STATE ELECTRIC & GAS CORP
LEWIS L. STALEY
NEW YORK STATE ENVIRONMENTAL FACILITIES CORP
PICKETT T. SIMPSON
NEW YORK STATE ERDA
JOHN C. DEMPSEY
NEW YORK STATE GEOLOGICAL SURVEY
ROBERT H. FAKUNDINY
NEW YORK STATE PUBLIC SERVICE COMMISSION
FRED HAAG
NEW YORK UNIVERSITY MEDICAL CENTER
MERRIL EISENBUD
NORTH DAKOTA GEOLOGICAL SURVEY
DON L. HALVORSON
NTR GOVERNMENT SERVICES
THOMAS V. REYNOLDS
NUCLEAR ASSURANCE CORP
JOHN V. HOUSTON
RHONNIE L. SMITH
DAVID A. WEBSTER
NUCLEAR SAFETY ASSOCIATES INC
JOSEPH A. LIEBERMAN
NUCLEAR SAFETY RESEARCH ASSOCIATION
KAZUMORI MATSUO
NUCLEAR SYSTEMS ASSOCIATES INC
CHARLES J. DIVONA
NUCLEAR WASTE WATCHERS
HELEN LETARTE
NUS CORP
W. G. BELTER
JOSEPH J. DINUNNO
BARRY N. NAFT
DOUGLAS D. ORVIS
DOUGLAS W. TONKAY
NWT CORP
W. L. PEARL
OAK RIDGE NATIONAL LABORATORY
H. C. CLAIBORNE
ALLEN G. CROFF
LESLIE R. DOLE
JOHN T. ENSMINGER
CATHY S. FORE
DAVID C. KOCHER
ELLEN D. SMITH
OFFICE OF NWTS INTEGRATION
ROBERT E. HEINEMAN
OHIO ENVIRONMENTAL COUNCIL
STEPHEN H. SEDAM
OHIO STATE UNIVERSITY
R. N. CHRISTENSEN
M. A. CORNWELL
OKLAHOMA STATE DEPT OF HEALTH
R. L. CRAIG
ONTARIO HYDRO
C. F. LEE
CRAIG J. SIMPSON
ONTARIO RESEARCH FOUNDATION
LYDIA M. LUCKEVICH
OREGON DEPT OF ENERGY
DONALD W. GODARD
ORGANIZATION FOR ECONOMIC COOPERATION AND DEVELOPMENT
J. P. OLIVIER
PACIFIC NORTHWEST LABORATORY
W. F. BONNER
DON J. BRADLEY
H. C. BURKHOLDER
L. L. CLARK
HARVEY DOVE
ORVILLE F. HILL
FLOYD N. HODGES
J. H. JARRETT
MAX R. KREITER
DONALD E. LARSON
R. D. NELSON
R. WILLIAM NELSON
R. E. NIGHTINGALE
R. JEFF SERNE
R. E. WESTERMAN
J. H. WESTSIK, JR.
PARSONS, BRINCKERHOFF, QUADE, & DOUGLAS, INC.
T. C. CHEN
T. R. KUESEL
PB-KBB INC
DILIP K. PAUL
MARK E. STEINER
PENBERTHY ELECTROMELT INTERNATIONAL INC.
LARRY PENBERTHY
PENNSYLVANIA OFFICE OF VOCATIONAL REHABILITATION
ANDREW CHOPAK
PENNSYLVANIA STATE UNIVERSITY
MICHAEL GRUTZECK
WILLIAM A. JESTER
WILLIAM B. WHITE
MICHAEL ZOLENSKY
PERRY COUNTY SCHOOLS
MANIEL A. COCHRAN
PHYSIKALISCH-TECHNISCHE BUNDESANSTALT
PETER BRENNECKE
POINT BEACH NUCLEAR POWER PLANT
GLENN A. REED
PORTLAND GENERAL ELECTRIC
J. W. LENTSCH
POWER AUTHORITY OF THE STATE OF NEW YORK
MYRON M. KACZMARSKY
POWER REACTOR AND NUCLEAR FUEL DEVELOPMENT CORPORATION
PRESQUE ISLE COURTHOUSE
PRINCETON UNIVERSITY
PETER MONTAGUE
G. F. PINDER
PROCESS AND ENGINEERING DEVELOPMENT
GERALD L. RITTER
PUBLIC SERVICE INDIANA
ROBERT S. WEGENG
QUADREX CORP
FRANCIS J. KENESHEA
RADIAN CORP
BARBARA MAXEY
RE/SPEC INC
GARY D. CALLAHAN
PAUL F. GNIRK
RENSSELAER POLYTECHNIC INSTITUTE
JAMES WU
RIDIHALGH, EGGERS & ASSOCIATES INC
PHILIP E. EGGERS
ROCKWELL HANFORD OPERATIONS
RONALD C. ARNETT
HARRY BABAD
G. S. BARNEY
R. A. DEJU
R. J. GIMERA
KARL M. LA RUE
MICHAEL J. SMITH
K. THIRUMALAI
DAVE A. TURNER
ROCKWELL INTERNATIONAL ENERGY SYSTEMS GROUP
W. S. BENNETT
HARRY PEARLMAN
LAWRENCE J. SMITH
ROGERS & ASSOCIATES ENGINEERING CORP
ARTHUR SUTHERLAND
ROYAL INSTITUTE OF TECHNOLOGY
IVARS NERETNIEKS
ROGER THUNVIK
S.E. LOGAN & ASSOCIATES INC
STANLEY E. LOGAN
S.M. STOLLER CORP
ROBERT W. KUPP
SAN DIEGO GAS & ELECTRIC COMPANY
LOUIS BERNATH
SAN JOSE STATE UNIVERSITY SCHOOL OF ENGINEERING
R. N. ANDERSON
SANDIA NATIONAL LABORATORIES
G. C. ALLEN
R. L. HUNTER
THOMAS O. HUNTER
J. KEITH JOHNSTONE
O. E. JONES
R. W. LYNCH
MARTIN A. MOLECKE
ANTHONY MULLER
E. J. NOWAK
RICHARD E. PEPPING
G. F. RUDOLFO
SCOTT SINNOCK
A. W. SNYDER
A. E. STEPHENSON
DANIEL M. TALBERT
LYNN D. TYLER
WENDELL D. WEART
WIPP CENTRAL FILES
SAVANNAH RIVER LABORATORY
CAROL JANTZEN
WILLIAM R. MCDONELL
S. W. OREAR SR
JOHN A. STONE
SCIENCE APPLICATIONS INC
JEFFREY ARBITAL
JERRY J. COHEN
J. DONALD DIXON
RALPH FULLWOOD
JAMES E. HAMMELMAN
RONALD HOFMANN
J. ROBERT LARIVIERE
DAVID H. LESTER
PETER E. MCGRATH
JOHN E. MOSIER
KRISHAN K. WAHI
ROBERT A. YODER
SIERRA GEOPHYSICS INC
STEPHEN L. GILLETT
SIX-COUNTY COMMISSIONERS ORGANIZATION
G. ALLEN FAWCETT
SNAKE RIVER ALLIANCE
TIM MCNEIL
SOUTH DAKOTA OFFICE OF ENERGY POLICY
STEVEN M. WEGMAN
SOUTHWEST RESEARCH AND INFORMATION CENTER
DON HANCOCK
ST BONAVENTURE UNIVERSITY
CARL J. TWAROG
ST MARTIN HIGH SCHOOL
RAYMOND J. WERTHNER

STANFORD UNIVERSITY
KONRAD B. KRAUSKOPF
GEORGE A. PARKS
IRWIN REMSON
STEARNS-ROGER SERVICES INC
VERYL ESCHEN
STONE & WEBSTER ENGINEERING CORP
PATRICIA ANN OCONNELL
A. PORT
EVERETT N. WASHER
STUBBS OVERBECK & ASSOCIATES INC
TED E. KOLBOHM
STUDSVIK ENERGITEKNIK AB
ROLF SJOBLOM
SWISS FEDERAL OFFICE OF ENERGY
U. NIEDERER
SYSTEMS SCIENCE AND SOFTWARE
PETER LAGUS
T.M. GATES INC
TODD M. GATES
T.T.I. ENGINEERING CORP
DONALD C. TONIKA
TECHNICAL INFORMATION PROJECT
DONALD PAY
TECHNICAL RESEARCH CENTRE OF FINLAND
OLLI J. HEINONEN
SILJA RUMMUKAINEN
KARI SAARI
SEPPO VUORI
TEKNEKRON RESEARCH INC
ANTHONY F. MOSCATI
TEXAS A&M UNIVERSITY
GARY ROBBINS
TEXAS BUREAU OF RADIATION CONTROL
DONALD G. ANDERSON
TEXAS DEPT OF HEALTH
DAVID K. LACKER
TEXAS ENERGY & NATURAL RESOURCES ADVISORY COUNCIL
TERRY BARRON
CAROL KING
TEXAS STATE REPRESENTATIVE
PETE LANEY
THE ANALYTIC SCIENCES CORP
JOHN W. BARTLETT
CHARLES M. KOPLIK
THE CLARION-LEDGER
MARK SCHLEIFSTEIN
TRW INC
PETER ALEXANDER
E. R. CHRISTIE
TUN ISMAIL ATOMIC RESEARCH CENTRE
PUSPATI LIBRARY
TUSKEGEE INSTITUTE
IRA G. DILLON
TVO POWER COMPANY
VEIJO RYHANEN
U.H.D.E.
FRANK STEINBRUNN
U.K. DEPT. OF THE ENVIRONMENT
RADIOACTIVE WASTE MANAGEMENT DIVISION
U.S. ARMY CORPS OF ENGINEERS
ALAN BUCK
U.S. BUREAU OF LAND MANAGEMENT
EDWARD R. SCHERICK
GREGORY F. THAYN
U.S. BUREAU OF MINES
GEORGE E. NIEWIADOMSKI
U.S. BUREAU OF RECLAMATION
REGE LEACH
U.S. DEPT OF ENERGY - ALBUQUERQUE OPERATIONS OFFICE
R. LOWERY
JOSEPH M. MCGOUGH
DORNER T. SCHUELER
U.S. DEPT OF ENERGY - ASSISTANT GENERAL COUNSEL FOR ENVIRONMENT
S. H. GREENLEIGH
U.S. DEPT OF ENERGY - CHICAGO OPERATIONS OFFICE
R. SELBY
U.S. DEPT OF ENERGY - DALLAS SUPPORT OFFICE
CURTIS E. CARLSON, JR.
U.S. DEPT OF ENERGY - DIVISION OF WASTE REPOSITORY DEPLOYMENT
W. WADE BALLARD, JR.
J. W. BENNETT
C. R. COOLEY (2)
WARREN EISTER
THOMAS P. LONGO
HARRY W. SMEDES
RALPH STEIN
U.S. DEPT OF ENERGY - IDAHO OPERATIONS OFFICE
JAMES F. LEONARD
J. H. SAKO
JOHN B. WHITSETT
U.S. DEPT OF ENERGY - MATERIALS SCIENCE DIVISION
R. J. GOTTSCHALL
U.S. DEPT OF ENERGY - NEVADA OPERATIONS OFFICE
M.P. KUNICH
U.S. DEPT OF ENERGY - NWTS PROGRAM OFFICE
T. BAILLIEUL
M. BLANCHARD
L. A. CASEY
R. LAHOTI
L. K. MCCLAIN
J. O. NEFF
K. K. WU
R. C. WUNDERLICH
U.S. DEPT OF ENERGY - OFFICE OF WASTE ISOLATION
JOSEPH A. LEARY
JANIE SHAHEEN
U.S. DEPT OF ENERGY - OFFICE OF WASTE PRODUCTS
G. K. OERTEL
U.S. DEPT OF ENERGY - RICHLAND OPERATIONS OFFICE
R. B. GORANSON
D. J. SQUIRES
U.S. DEPT OF ENERGY - SAVANNAH RIVER OPERATIONS OFFICE
REGINA T. HARRIS
T. B. HINDMAN
U.S. DEPT OF ENERGY - WIPP PROGRAM
LAWRENCE H. HARMON
U.S. ENVIRONMENTAL PROTECTION AGENCY
DIVISION OF CRITERIA & STANDARDS
DONALD HUNTER
JAMES NEIHEISEL
U.S. GEOLOGICAL SURVEY - COLUMBUS
A. M. LA SALA, JR.
U.S. GEOLOGICAL SURVEY - DENVER
RICHARD WADDELL
U.S. GEOLOGICAL SURVEY - MENLO PARK
JOHN BREDEHOEFT
JACOB RUBIN
U.S. GEOLOGICAL SURVEY - RESTON
I-MING CHOU
JOHN ROBERTSON
EDWIN ROEDDER
EUGENE H. ROSEBOOM JR
PETER R. STEVENS
DAVID B. STEWART
U.S. HOUSE SUBCOMMITTEE ON ENERGY AND THE ENVIRONMENT
MORRIS K. UDALL
U.S. NUCLEAR REGULATORY COMMISSION
J. CALVIN BELOTE
R. BOYLE
ENRICO F. CONTI
MICHAEL C. CULLINGFORD
J. J. DAVIS
JOSEPH F. DONOGHUE
F. L. DOYLE
PAUL F. GOLDBERG
HIGH-LEVEL WASTE LICENSING BRANCH
HIGH-LEVEL WASTE TECHNICAL
LINDA L. LEHMAN
LIBRARY
JAMES C. MALARO
JOHN B. MARTIN (3)
JOHN C. MCKINLEY
HUBERT MILLER
R. JOHN STARMER
EVERETT A. WICK
U.S. SENATE COMMITTEE ON ENERGY AND NATURAL RESOURCES
WILLIS D. SMITH
UHDE GMBH
OLINGER
UNC NUCLEAR INDUSTRIES
ED POWERS
UNION OF CONCERNED SCIENTISTS
MICHAEL FADEN
UNIVERSITY OF ALABAMA AT BIRMINGHAM
J. WALTER MASON
UNIVERSITY OF ALBERTA
F.W. SCHWARTZ
UNIVERSITY OF ARIZONA
JAAK DAEMEN
JAMES G. MCCRAY
ROY G. POST
UNIVERSITY OF CALIFORNIA AT BERKELEY
TODD LAPORTE
THOMAS H. PIGFORD
UNIVERSITY OF CALIFORNIA AT LOS ANGELES
D. OKRENT
UNIVERSITY OF CALIFORNIA AT SAN DIEGO
RICHARD J. WILLIS
UNIVERSITY OF DELAWARE
FRANK A. KULACKI
UNIVERSITY OF FLORIDA
DAVID E. CLARK
DOLORES C. JENKINS
UNIVERSITY OF ILLINOIS AT URBANA - CHAMPAIGN
ALBERT J. MACHIELS
UNIVERSITY OF LOWELL
JAMES R. SHEFF
UNIVERSITY OF LULEA
JAN NILSSON
UNIVERSITY OF MISSOURI AT KANSAS CITY
EDWIN D. GOEBEL
UNIVERSITY OF MISSOURI AT ROLLA
ARVIND KUMAR
UNIVERSITY OF MODERA
M. ANTONINI
UNIVERSITY OF NEVADA AT RENO
BECKY WEIMER

UNIVERSITY OF NEW MEXICO
RODNEY C. EWING
UNIVERSITY OF OKLAHOMA
DANIEL T. BOATRIGHT
UNIVERSITY OF OTTAWA
TUNCER OREN
UNIVERSITY OF PITTSBURGH
B. L. COHEN
UNIVERSITY OF SOUTHERN MISSISSIPPI
CHARLES R. BRENT
JAMES W. PINSON
UNIVERSITY OF TENNESSEE AT KNOXVILLE
J.B. FUSSELL
UNIVERSITY OF TEXAS AT AUSTIN
THOMAS C. GUSTAVSON
JOE D. LEDBETTER
UNIVERSITY OF TEXAS AT SAN ANTONIO
DONALD R. LEWIS
UNIVERSITY OF TOKYO
RYOMEI KIYOSE
UNIVERSITY OF UTAH RESEARCH INSTITUTE
LIBRARY
UNIVERSITY OF WASHINGTON
M. A. ROBKIN
UNIVERSITY OF WESTERN ONTARIO
WILLIAM S. FYLE
UNIVERSITY OF WISCONSIN
B. C. HAIMSON
UNIVERSITY OF WISCONSIN AT FOND DU LAC
JOHN B. HEIL
UNIVERSITY OF WISCONSIN AT MILWAUKEE
HOWARD PINCUS
UTAH BUREAU OF RADIATION CONTROL
DARRELL M. WARREN
UTAH GEOLOGICAL AND MINERAL SURVEY
MAGE YONETANI
UTAH SOUTHEASTERN DISTRICT HEALTH DEPARTMENT
ROBERT L. FURLOW
VANDERBILT UNIVERSITY
FRANK L. PARKER
VERMONT STATE NUCLEAR ADVISORY PANEL
VIRGINIA CALLAN
VIRGINIA DEPT OF HEALTH
ROBERT G. WICKLINE
VIRGINIA MILITARY INSTITUTE
HENRY D. SCHREIBER
VIRGINIA POLYTECHNIC INSTITUTE AND STATE UNIVERSITY
WALTER HIBBARD
DAVID R. WONES
WASHINGTON DEPT OF SOCIAL AND HEALTH SERVICES
T. STRONG
WASHINGTON HOUSE OF REPRESENTATIVES
RAY ISAACSON
WASHINGTON STATE SENATE
DONN CHARNLEY
WAYNE STATE UNIVERSITY
JAMES A. WOODYARD
WBAI-FM
WARREN LIEBOLD
WEST DADE REGIONAL LIBRARY
LOURDES BLANCO LOPEZ
WEST VALLEY NUCLEAR SERVICES COMPANY INC
RICHARD M. WINAR
WEST VIRGINIA GEOLOGICAL AND ECONOMIC SURVEY
ROBERT B. ERWIN
WESTINGHOUSE ELECTRIC CORP
GEORGE V. B. HALL
CAROL A. KIZIS
D. NEWBY
GEORGE P. SABOL
WESTINGHOUSE WIPP PROJECT
WESTINGHOUSE ELECTRIC CORPORATION
WISCONSIN GEOLOGICAL AND NATURAL HISTORY SURVEY
MICHAEL G. MUDREY, JR.
WISCONSIN PUBLIC SERVICE CORP
PAUL WOZNIAK
WOODWARD-CLYDE CONSULTANTS
ASHOK PATWARDHAN
WP-SYSTEM AB
IVAR SAGEFORS
WYOMING GEOLOGICAL SURVEY
DANIEL N. MILLER

☆U. S. GOVERNMENT PRINTING OFFICE: 1982/659-102/1336

BATTELLE Project Management Division
505 King Avenue
Columbus, Ohio 43201